

April 29, 2008 (8:00am)

OFFICE OF SECRETARY
RULEMAKINGS AND
ADJUDICATIONS STAFF

UNITED STATES
NUCLEAR REGULATORY COMMISSION
ATOMIC SAFETY AND LICENSING BOARD

Before Administrative Judges:

Alex S. Karlin, Chairman
Dr. Richard E. Wardwell
Dr. William H. Reed

In the Matter of)

ENTERGY NUCLEAR VERMONT YANKEE, LLC)
and ENTERGY NUCLEAR OPERATIONS, INC.)

(Vermont Yankee Nuclear Power Station))

Docket No. 50-271-LR
ASLBP No. 06-849-03-LR

NEW ENGLAND COALITION, INC.

CONTENTIONS 2A and 2B

PREFILED EXHIBITS

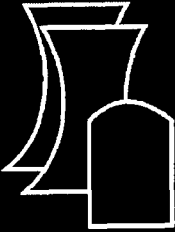
NEC-JH_26 – NEC-JH_35
NEC-JH_62

April 28, 2008

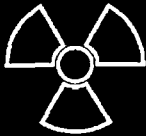
Volume 3

Complete by -055

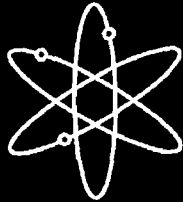
DS-03



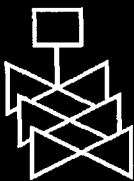
Effect of LWR Coolant Environments on the Fatigue Life of Reactor Materials



Final Report



Argonne National Laboratory



U.S. Nuclear Regulatory Commission
Office of Nuclear Regulatory Research
Washington, DC 20555-0001



NUREG/CR-6909
ANL-06/08

Effect of LWR Coolant Environments on the Fatigue Life of Reactor Materials

Final Report

Manuscript Completed: November 2006
Date Published: February 2007

Prepared by
O. K. Chopra and W. J. Shack

Argonne National Laboratory
9700 South Cass Avenue
Argonne, IL 60439

H. J. Gonzalez, NRC Project Manager

Prepared for
Division of Fuel, Engineering and Radiological Research
Office of Nuclear Regulatory Research
U.S. Nuclear Regulatory Commission
Washington, DC 20555-0001
NRC Job Code N6187



Abstract

The ASME Boiler and Pressure Vessel Code provides rules for the design of Class 1 components of nuclear power plants. Figures I-9.1 through I-9.6 of Appendix I to Section III of the Code specify design curves for applicable structural materials. However, the effects of light water reactor (LWR) coolant environments are not explicitly addressed by the Code design curves. The existing fatigue strain-vs.-life (ϵ - N) data illustrate potentially significant effects of LWR coolant environments on the fatigue resistance of pressure vessel and piping steels. Under certain environmental and loading conditions, fatigue lives in water relative to those in air can be a factor of ≈ 12 lower for austenitic stainless steels, ≈ 3 lower for Ni-Cr-Fe alloys, and ≈ 17 lower for carbon and low-alloy steels. This report summarizes the work performed at Argonne National Laboratory on the fatigue of piping and pressure vessel steels in LWR environments. The existing fatigue ϵ - N data have been evaluated to identify the various material, environmental, and loading parameters that influence fatigue crack initiation, and to establish the effects of key parameters on the fatigue life of these steels. Fatigue life models are presented for estimating fatigue life as a function of material, loading, and environmental conditions. The environmental fatigue correction factor for incorporating the effects of LWR environments into ASME Section III fatigue evaluations is described. The report also presents a critical review of the ASME Code fatigue design margins of 2 on stress (or strain) and 20 on life and assesses the possible conservatism in the current choice of design margins.

This page is intentionally left blank.

Foreword

This report summarizes, reviews, and quantifies the effects of the light-water reactor (LWR) environment on the fatigue life of reactor materials, including carbon steels, low-alloy steels, nickel-chromium-iron (Ni-Cr-Fe) alloys, and austenitic stainless steels. The primary purpose of this report is to provide the background and technical bases to support Regulatory Guide 1.207, "Guidelines for Evaluating Fatigue Analyses Incorporating the Life Reduction of Metal Components Due to the Effects of the Light-Water Reactor Environment for New Reactors."

Previously published related reports include NUREG/CR-5704, "Effects of LWR Coolant Environments on Fatigue Design Curves of Austenitic Stainless Steels," issued April 1999; NUREG/CR-6717, "Environmental Effects on Fatigue Crack Initiation in Piping and Pressure Vessel Steels," issued May 2001; NUREG/CR-6787, "Mechanism and Estimation of Fatigue Crack Initiation in Austenitic Stainless Steels in LWR Environments," issued August 2002; NUREG/CR-6815, "Review of the Margins for ASME Code Fatigue Design Curve – Effects of Surface Roughness and Material Variability," issued September 2003; and NUREG/CR-6583, "Effects of LWR Coolant Environments on Fatigue Design Curves of Carbon and Low-Alloy Steels," issued February 1998. This report provides a review of the existing fatigue ϵ -N data for carbon steels, low-alloy steels, Ni-Cr-Fe alloys, and austenitic stainless steels to define the potential effects of key material, loading, and environmental parameters on the fatigue life of the steels. By drawing upon a larger database than was used in earlier published reports, the U.S. Nuclear Regulatory Commission (NRC) has been able to update the Argonne National Laboratory (ANL) fatigue life models used to estimate the fatigue curves as a function of those parameters. In addition, this report presents a procedure for incorporating environmental effects into fatigue evaluations. The database described in this report (and its predecessors) reinforces the position espoused by the NRC that a guideline for incorporating the LWR environmental effects in the fatigue life evaluations should be developed and that the design curves for the fatigue life of pressure boundary and internal components fabricated from stainless steel should be revised. Toward that end, this report proposes a method for establishing reference curves and environmental correction factors for use in evaluating the fatigue life of reactor components exposed to LWR coolants and operational experience.

Data described in this review have been used to define fatigue design curves in air that are consistent with the existing fatigue data. Specifically, the published data indicate that the existing code curves are nonconservative for austenitic stainless steels (e.g., Types 304, 316, and 316NG). Regulatory Guide 1.207 endorses the new stainless steel fatigue design curves presented herein for incorporation in fatigue analyses for new reactors. However, because of significant conservatism in quantifying other plant-related variables (such as cyclic behavior, including stress and loading rates) involved in cumulative fatigue life calculations, the design of the current fleet of reactors is satisfactory.

Brian W. Sheron, Director
Office of Nuclear Regulatory Research
U.S. Nuclear Regulatory Commission

This page is intentionally left blank.

Contents

Abstract	iii
Foreword	v
Executive Summary	xv
Abbreviations	xvii
Acknowledgments	xix
1. Fatigue Analysis	1
2. Fatigue Life	7
3. Fatigue Strain vs. Life Data	9
4 Carbon and Low-Alloy Steels	11
4.1 Air Environment	11
4.1.1 Experimental Data	11
4.1.2 Temperature	12
4.1.3 Strain Rate	12
4.1.4 Sulfide Morphology	13
4.1.5 Cyclic Strain Hardening Behavior	13
4.1.6 Surface Finish	14
4.1.7 Heat-to-Heat Variability	15
4.1.8 Fatigue Life Model	17
4.1.9 Extension of the Best-Fit Mean Curve from 10^6 to 10^{11} Cycles	18
4.1.10 Fatigue Design Curve	19
4.2 LWR Environment	21
4.2.1 Experimental Data	21
4.2.2 Strain Rate	22
4.2.3 Strain Amplitude	23

4.2.4	Temperature	26
4.2.5	Dissolved Oxygen.....	29
4.2.6	Water Conductivity.....	30
4.2.7	Sulfur Content in Steel	30
4.2.8	Tensile Hold Period	31
4.2.9	Flow Rate	33
4.2.10	Surface Finish	34
4.2.11	Heat-to-Heat Variability.....	35
4.2.12	Fatigue Life Model	36
4.2.13	Environmental Fatigue Correction Factor.....	38
4.2.14	Modified Rate Approach.....	38
5	Austenitic Stainless Steels.....	41
5.1	Air Environment	41
5.1.1	Experimental Data	41
5.1.2	Specimen Geometry.....	43
5.1.3	Temperature	43
5.1.4	Cyclic Strain Hardening Behavior.....	44
5.1.5	Surface Finish	45
5.1.6	Heat-to-Heat Variability.....	45
5.1.7	Fatigue Life Model	46
5.1.8	New Fatigue Design Curve	48
5.2	LWR Environment	49
5.2.1	Experimental Data	49
5.2.2	Strain Amplitude.....	51
5.2.3	Hold-Time Effects	52

5.2.4	Strain Rate	53
5.2.5	Dissolved Oxygen.....	54
5.2.6	Water Conductivity.....	54
5.2.7	Temperature	55
5.2.8	Material Heat Treatment	56
5.2.9	Flow Rate	57
5.2.10	Surface Finish	58
5.2.11	Heat-to-Heat Variability.....	58
5.2.12	Cast Stainless Steels	60
5.2.13	Fatigue Life Model	61
5.2.14	Environmental Correction Factor	63
6	Ni-Cr-Fe Alloys and Welds.....	65
6.1	Air Environment	65
6.1.1	Experimental Data	65
6.1.2	Fatigue Life Model	66
6.2	LWR Environment	67
6.2.1	Experimental Data	67
6.2.2	Effects of Key Parameters.....	68
6.2.3	Environmental Correction Factor	68
7	Margins in ASME Code Fatigue Design Curves	71
7.1	Material Variability and Data Scatter.....	73
7.2	Size and Geometry.....	73
7.3	Surface Finish	74
7.4	Loading Sequence.....	74
7.5	Fatigue Design Curve Margins Summarized	75

8 Summary.....	79
References.....	83
APPENDIX A.....	A.1

Figures

1.	Schematic illustration of growth of short cracks in smooth specimens as a function of fatigue life fraction and crack velocity as a function of crack depth.....	7
2.	Crack growth rates plotted as a function of crack depth for A533-Gr B low-alloy steel and Type 304 SS in air and LWR environments.....	8
3.	Fatigue strain vs. life data for carbon and low-alloy steels in air at room temperature.	11
4.	Fatigue strain vs. life data for carbon and low-alloy steels in air at 288°C.	12
5.	Effect of strain rate and temperature on cyclic stress of carbon and low-alloy steels.	13
6.	Effect of surface finish on the fatigue life of A106-Gr B carbon steel in air at 289°C.....	14
7.	Estimated cumulative distribution of constant A in the ANL models for fatigue life for heats of carbon steels and low-alloy steels in air.	16
8.	Experimental and predicted fatigue lives of carbon steels and low-alloy steels in air.	18
9.	Fatigue design curve for carbon steels in air.	20
10.	Fatigue design curve for low-alloy steels in air.....	20
11.	Strain amplitude vs. fatigue life data for A533-Gr B and A106-Gr B steels in air and high-dissolved-oxygen water at 288°C.....	21
12.	Dependence of fatigue life of carbon and low-alloy steels on strain rate.	23
13.	Fatigue life of A106-Gr B carbon steel at 288°C and 0.75% strain range in air and water environments under different loading waveforms.	24
14.	Fatigue life of carbon and low-alloy steels tested with loading waveforms where slow strain rate is applied during a fraction of tensile loading cycle.	25
15.	Experimental values of fatigue life and those predicted from the modified rate approach without consideration of a threshold strain.....	26
16.	Change in fatigue life of A333-Gr 6 carbon steel with temperature and DO.....	26
17.	Dependence of fatigue life on temperature for carbon and low-alloy steels in water.	27
18.	Waveforms for change in temperature during exploratory fatigue tests.....	28
19.	Fatigue life of A333-Gr 6 carbon steel tube specimens under varying temperature, indicated by horizontal bars.	28
20.	Dependence on DO of fatigue life of carbon steel in high-purity water.....	29

21.	Effect of strain rate on fatigue life of low-alloy steels with different S contents.....	30
22.	Effect of strain rate on the fatigue life of A333-Gr 6 carbon steels with different S contents. ...	31
23.	Fatigue life of A106-Gr B steel in air and water environments at 288°C, 0.78% strain range, and hold period at peak tensile strain.....	32
24.	Effect of water flow rate on fatigue life of A333-Gr 6 carbon steel at 289°C and strain amplitude and strain rates of 0.3% and 0.01%/s and 0.6% and 0.001%/s.....	33
25.	Effect of flow rate on low-cycle fatigue of carbon steel tube bends in high-purity water at 240°C.	34
26.	Effect of surface roughness on fatigue life of A106-Gr B carbon steel and A533 low-alloy steel in air and high-purity water at 289°C.	34
27.	Estimated cumulative distribution of parameter A in the ANL models for fatigue life for heats of carbon and low-alloy steels in LWR environments.	35
28.	Experimental and predicted fatigue lives of carbon steels and low-alloy steels in LWR environments.	37
29.	Application of the modified rate approach to determine the environmental fatigue correction factor F_{en} during a transient.....	39
30.	Fatigue ϵ -N behavior for Types 304, 316, and 316NG austenitic stainless steels in air at various temperatures.	41
31.	Influence of specimen geometry on fatigue life of Types 304 and 316 stainless steel.....	43
32.	Influence of temperature on fatigue life of Types 304 and 316 stainless steel in air.....	43
33.	Effect of strain amplitude, temperature, and strain rate on cyclic strain-hardening behavior of Types 304 and 316NG SS in air.....	44
34.	Effect of surface roughness on fatigue life of Type 316NG and Type 304 SSs in air.....	45
35.	Estimated cumulative distribution of constant A in the ANL model for fatigue life for heats of austenitic SS in air.	46
36.	Experimental and predicted fatigue lives of austenitic SSs in air.....	47
37.	Fatigue design curve for austenitic stainless steels in air.	48
38.	Strain amplitude vs. fatigue life data for Type 304 and Type 316NG SS in water at 288°C.....	49
39.	Higher-magnification photomicrographs of oxide films that formed on Type 316NG stainless steel in simulated PWR water and high-DO water.....	50

40.	Schematic of the corrosion oxide film formed on austenitic stainless steels in LWR environments.	50
41.	Effects of environment on formation of fatigue cracks in Type 316NG SS in air and low-DO water at 288°C.	51
42.	Results of strain rate change tests on Type 316 SS in low-DO water at 325°C.	52
43.	Fatigue life of Type 304 stainless steel tested in high-DO water at 260–288°C with trapezoidal or triangular waveform.	52
44.	Dependence of fatigue lives of austenitic stainless steels on strain rate in low-DO water.	53
45.	Dependence of fatigue life of Types 304 and 316NG stainless steel on strain rate in high- and low-DO water at 288°C.	53
46.	Effects of conductivity of water and soaking period on fatigue life of Type 304 SS in high-DO water.	55
47.	Change in fatigue lives of austenitic stainless steels in low-DO water with temperature.	55
48.	Fatigue life of Type 316 stainless steel under constant and varying test temperature.	56
49.	The effect of material heat treatment on fatigue life of Type 304 stainless steel in air, BWR and PWR environments at 289°C, $\approx 0.38\%$ strain amplitude, sawtooth waveform, and 0.004%/s tensile strain rate.	57
50.	Effect of water flow rate on the fatigue life of austenitic SSs in high-purity water at 289°C	57
51.	Effect of surface roughness on fatigue life of Type 316NG and Type 304 stainless steels in air and high-purity water at 289°C.	58
52.	Estimated cumulative distribution of constant A in the ANL model for fatigue life for heats of austenitic SSs in water.	59
53.	Dependence of fatigue lives of CF-8M cast SSs on strain rate in low-DO water at various strain amplitudes.	60
54.	Estimated cumulative distribution of constant A in the ANL model for fatigue life of wrought and cast austenitic stainless steels in air and water environments.	61
55.	Experimental and predicted values of fatigue lives of austenitic SSs in LWR environments. ...	63
56.	Fatigue ϵ -N behavior for Alloys 600 and 690 in air at temperatures between room temperature and 315°C.	65
57.	Fatigue ϵ -N behavior for Alloys 82, 182, 132, and 152 welds in air at various temperatures. ..	66
58.	Fatigue ϵ -N behavior for Alloy 600 and its weld alloys in simulated BWR water at $\approx 289^\circ\text{C}$...	67

59.	Fatigue ϵ -N behavior for Alloys 600 and 690 and their weld alloys in simulated PWR water at 315 or 325°C.....	67
60.	Dependence of fatigue lives of Alloys 690 and 600 and their weld alloys in PWR water at 325°C and Alloy 600 in BWR water at 289°C.....	68
61.	The experimental and estimated fatigue lives of various Ni alloys in BWR and PWR environments.	69
62.	Fatigue data for carbon and low-alloy steel and Type 304 stainless steel components.	72
63.	Estimated cumulative distribution of parameter A in the ANL models that represent the fatigue life of test specimens and actual components in air.	77

Tables

1.	Sources of the fatigue ϵ -N data on reactor structural materials in air and water environments.	9
2.	Values of parameter A in the ANL fatigue life model for carbon steels in air and the margins on life as a function of confidence level and percentage of population bounded.	16
3.	Values of parameter A in the ANL fatigue life model for low-alloy steels in air and the margins on life as a function of confidence level and percentage of population bounded.....	17
4.	Fatigue design curves for carbon and low-alloy steels and proposed extension to 10^{11} cycles.	20
5.	Fatigue data for STS410 steel at 289°C in water with 1 ppm DO and trapezoidal waveform....	33
6.	Values of parameter A in the ANL fatigue life model for carbon steels in water and the margins on life as a function of confidence level and percentage of population bounded.....	36
7.	Values of parameter A in the ANL fatigue life model for low-alloy steels in water and the margins on life as a function of confidence level and percentage of population bounded.....	36
8.	Values of parameter A in the ANL fatigue life model and the margins on life for austenitic SSs in air as a function of confidence level and percentage of population bounded.....	46
9.	The new and current Code fatigue design curves for austenitic stainless steels in air.	48
10.	Values of parameter A in the ANL fatigue life model and the margins on life for austenitic SSs in water as a function of confidence level and percentage of population bounded.	59
11.	The median value of A and standard deviation for the various fatigue ϵ -N data sets used to evaluate material variability and data scatter.	73
12.	Factors on life applied to mean fatigue ϵ -N curve to account for the effects of various material, loading, and environmental parameters.	76
13.	Margin applied to the mean values of fatigue life to bound 95% of the population.....	77

Executive Summary

Section III, Subsection NB, of the ASME Boiler and Pressure Vessel Code contains rules for the design of Class 1 components of nuclear power plants. Figures I-9.1 through I-9.6 of Appendix I to Section III specify the Code design fatigue curves for applicable structural materials. However, Section III, Subsection NB-3121 of the Code states that the effects of the coolant environment on fatigue resistance of a material were not intended to be addressed in these design curves. Therefore, the effects of environment on the fatigue resistance of materials used in operating pressurized water reactor (PWR) and boiling water reactor (BWR) plants, whose primary-coolant pressure boundary components were designed in accordance with the Code, are uncertain.

The current Section-III design fatigue curves of the ASME Code were based primarily on strain-controlled fatigue tests of small polished specimens at room temperature in air. Best-fit curves to the experimental test data were first adjusted to account for the effects of mean stress and then lowered by a factor of 2 on stress and 20 on cycles (whichever was more conservative) to obtain the design fatigue curves. These factors are not safety margins but rather adjustment factors that must be applied to experimental data to obtain estimates of the lives of components. Recent fatigue-strain-vs.-life (ϵ -N) data obtained in the U.S. and Japan demonstrate that light water reactor (LWR) environments can have potentially significant effects on the fatigue resistance of materials. Specimen lives obtained from tests in simulated LWR environments can be much shorter than those obtained from corresponding tests in air.

This report reviews the existing fatigue ϵ -N data for carbon and low-alloy steels, wrought and cast austenitic stainless steels (SSs), and nickel-chromium-iron (Ni-Cr-Fe) alloys in air and LWR environments. The effects of various material, loading, and environmental parameters on the fatigue lives of these steels are summarized. The results indicate that in air, the ASME mean curve for low-alloy steels is in good agreement with the available experimental data, and the curve for carbon steels is somewhat conservative. However, in air, the ASME mean curve for SSs is not consistent with the experimental data at strain amplitudes $<0.5\%$ or stress amplitudes <975 MPa (<141 ksi); the ASME mean curve is nonconservative. The results also indicate that the fatigue data for Ni-Cr-Fe alloys are not consistent with the current ASME Code mean curve for austenitic SSs.

The fatigue lives of carbon and low-alloy steels, austenitic SSs, and Ni-Cr-Fe alloys are decreased in LWR environments. The reduction depends on some key material, loading, and environmental parameters. The fatigue data are consistent with the much larger database on enhancement of crack growth rates in these materials in LWR environments. The key parameters that influence fatigue life in these environments, e.g., temperature, dissolved-oxygen (DO) level in water, strain rate, strain (or stress) amplitude, and, for carbon and low-alloy steels, S content of the steel, have been identified. Also, the range of the values of these parameters within which environmental effects are significant has been clearly defined. If these critical loading and environmental conditions exist during reactor operation, then environmental effects will be significant and need to be included in the ASME Code fatigue evaluations.

Fatigue life models developed earlier to predict fatigue lives of small smooth specimens of carbon and low-alloy steels, wrought and cast austenitic SSs, and Ni-Cr-Fe alloys as a function of material, loading, and environmental parameters have been updated/revised by drawing upon a larger fatigue ϵ -N database. The functional form and bounding values of these parameters were based on experimental observations and data trends. An approach that can be used to incorporate the effects of LWR coolant environments into the ASME Code fatigue evaluations, based on the environmental fatigue correction factor, F_{en} , is discussed. The fatigue usage for a specific stress cycle of load set pair based on the Code fatigue design curves is multiplied by the correction factor to account for environmental effects.

The report also presents a critical review of the ASME Code fatigue design margins of 2 on stress and 20 on life and assesses the possible conservatism in the current choice of design margins. Although these factors were intended to be somewhat conservative, they should not be considered safety margins. These factors cover the effects of variables that can influence fatigue life but were not investigated in the experimental data that were used to obtain the fatigue design curves. Data available in the literature have been reviewed to evaluate the margins on cycles and stress that are needed to account for such differences and uncertainties. Monte Carlo simulations were performed to determine the margin on cycles needed to obtain a fatigue design curve that would provide a somewhat conservative estimate of the number of cycles to initiate a fatigue crack in reactor components. The results suggest that for both carbon and low-alloy steels and austenitic SSs, the current ASME Code requirements of a factor of 20 on cycle to account for the effects of material variability and data scatter, as well as size, surface finish, and loading history in low cycle fatigue, contain at least a factor of 1.7 conservatism. Thus, to reduce this conservatism, fatigue design curves have been developed from the ANL fatigue life model by first correcting for mean stress effects, and then reducing the mean-stress adjusted curve by a factor of 2 on stress or 12 on cycles, whichever is more conservative. These design curves are consistent with the existing fatigue ϵ -N data. A detailed procedure for incorporating environmental effects into fatigue evaluations is presented.

Abbreviations

ANL	Argonne National Laboratory
ANN	Artificial Neural Network
ASME	American Society of Mechanical Engineers
BWR	Boiling Water Reactor
CGR	Crack Growth Rate
CUF	Cumulative Usage Factor
DO	Dissolved Oxygen
EAC	Environmentally Assisted Cracking
ECP	Electrochemical Potential
EPR	Electrochemical Potentiodynamic Reactivation
EPRI	Electric Power Research Institute
GE	General Electric Co.
IHI	Ishikawajima-Harima Heavy Industries
KWU	Kraftwerk Union Laboratories
LWR	Light Water Reactor
MA	Mill Annealed
MEA	Materials Engineering Associates
MHI	Mitsubishi Heavy Industries
MPA	Materialprüfungsanstalt
MSC	Microstructurally Small Crack
NRC	Nuclear Regulatory Commission
ORNL	Oak Ridge National Laboratory
PVRC	Pressure Vessel Research Council
PWR	Pressurized Water Reactor
RCS	Reactor Coolant System
RT	Room Temperature
SCC	Stress Corrosion Cracking
SICC	Strain Induced Corrosion Cracking
SS	Stainless Steel
UTS	Ultimate Tensile Strength
WRC	Welding Research Council

This page is intentionally left blank.

Acknowledgments

The authors thank W. H. Cullen, Jr., and J. Fair for their helpful comments. This work is sponsored by the Office of Nuclear Regulatory Research, U.S. Nuclear Regulatory Commission, under NRC Job Code N6187; Project Manager: H. J. Gonzalez.

This page is intentionally left blank.

1. Fatigue Analysis

The American Society of Mechanical Engineers (ASME) Boiler and Pressure Vessel Code Section III, Subsection NB, which contains rules for the design of Class I components for nuclear power plants, recognizes fatigue as a possible mode of failure in pressure vessel steels and piping materials. Fatigue has been a major consideration in the design of rotating machinery and aircraft, where the components are subjected to a very large number of cycles (e.g., high-cycle fatigue) and the primary concern is the endurance limit, i.e., the stress that can be applied an infinite number of times without failure. However, cyclic loadings on a reactor pressure boundary component occur because of changes in mechanical and thermal loadings as the system goes from one load set (e.g., pressure, temperature, moment, and force loading) to another. The number of cycles applied during the design life of the component seldom exceeds 10^5 and is typically less than a few thousand (e.g., low-cycle fatigue). The main difference between high-cycle and low-cycle fatigue is that the former involves little or no plastic strain, whereas the latter involves strains in excess of the yield strain. Therefore, design curves for low-cycle fatigue are based on tests in which strain rather than stress is the controlled variable.

The ASME Code fatigue evaluation procedures are described in NB-3200, "Design by Analysis," and NB-3600, "Piping Design." For each stress cycle or load set pair, an individual fatigue usage factor is determined by the ratio of the number of cycles anticipated during the lifetime of the component to the allowable cycles. Figures I-9.1 through I-9.6 of the mandatory Appendix I to Section III of the ASME Boiler and Pressure Vessel Code specify fatigue design curves that define the allowable number of cycles as a function of applied stress amplitude. The cumulative usage factor (CUF) is the sum of the individual usage factors, and ASME Code Section III requires that at each location the CUF, calculated on the basis of Miner's rule, must not exceed 1.

The ASME Code fatigue design curves, given in Appendix I of Section III, are based on strain-controlled tests of small polished specimens at room temperature in air. The design curves have been developed from the best-fit curves to the experimental fatigue-strain-vs.-life (ϵ - N) data, which are expressed in terms of the Langer equation¹ of the form

$$\epsilon_a = A1(N)^{-n1} + A2, \quad (1)$$

where ϵ_a is the applied strain amplitude, N is the fatigue life, and $A1$, $A2$, and $n1$ are coefficients of the model. Equation 1 may be written in terms of stress amplitude S_a instead of ϵ_a . The stress amplitude is the product of ϵ_a and elastic modulus E , i.e., $S_a = E \cdot \epsilon_a$ (stress amplitude is one-half the applied stress range). The current ASME Code best-fit or mean curve described in the Section III criteria document² for various steels is given by

$$S_a = \frac{E}{4\sqrt{N_f}} \ln\left(\frac{100}{100 - A_f}\right) + B_f, \quad (2)$$

where E is the elastic modulus, N_f is the number of cycles to failure, and A_f and B_f are constants related to reduction in area in a tensile test and endurance limit of the material at 10^7 cycles, respectively. The current Code mean curve for carbon steel is expressed as

$$S_a = 59,734 (N_f)^{-0.5} + 149.2, \quad (3)$$

for low-alloy steel, as

$$S_a = 49,222 (N_f)^{-0.5} + 265.4; \quad (4)$$

and for austenitic SSs, as

$$S_a = 58,020 (N_f)^{-0.5} + 299.9. \quad (5)$$

Note that because most of the data used to develop the Code mean curve were obtained on specimens that were tested to failure, in the Section III criteria document, fatigue life is defined as cycles to failure. Accordingly, the ASME Code fatigue design curves are generally considered to represent allowable number of cycles to failure. However, in Appendix I to Section III of the Code the design curves are simply described as stress amplitude (S_a) vs. number of cycles (N).

In the fatigue tests performed during the last three decades, fatigue life is defined in terms of the number of cycles for tensile stress to decrease 25% from its peak or steady-state value. For typical cylindrical specimens used in these studies, this corresponds to the number of cycles needed to produce an ≈ 3 -mm-deep crack in the test specimen. Thus, the fatigue life of a material is actually being described in terms of three parameters, viz., strain or stress, cycles, and crack depth. The best-fit curve to the existing fatigue ϵ - N data describes, for given strain or stress amplitude, the number of cycles needed to develop a 3-mm deep crack. The fatigue ϵ - N data are typically expressed by rewriting Eq. 1 as

$$\ln(N) = A - B \ln(\epsilon_a - C), \quad (6)$$

where A , B , and C are constants; C represents the fatigue limit of the material; and B is the slope of the log-log plot of fatigue ϵ - N data. The ASME Code mean-data curves (i.e., Eqs. 3-5) may be expressed in terms of Eq. 6 as follows. The fatigue life of carbon steels is given by

$$\ln(N) = 6.726 - 2.0 \ln(\epsilon_a - 0.072), \quad (7)$$

for low-alloy steels, by

$$\ln(N) = 6.339 - 2.0 \ln(\epsilon_a - 0.128), \quad (8)$$

and, for austenitic SSs, by

$$\ln(N) = 6.954 - 2.0 \ln(\epsilon_a - 0.167). \quad (9)$$

The Code fatigue design curves have been obtained from the best-fit (or mean-data) curves by first adjusting for the effects of mean stress using the modified Goodman relationship given by

$$S'_a = S_a \left(\frac{\sigma_u - \sigma_y}{\sigma_u - S_a} \right) \quad \text{for } S_a < \sigma_y, \quad (10)$$

and

$$S'_a = S_a \quad \text{for } S_a > \sigma_y, \quad (11)$$

where S'_a is the adjusted value of stress amplitude, and σ_y and σ_u are yield and ultimate strengths of the material, respectively. Equations 10 and 11 assume the maximum possible mean stress and typically give a conservative adjustment for mean stress. The fatigue design curves are then obtained by reducing the fatigue life at each point on the adjusted best-fit curve by a factor of 2 on strain (or stress) or 20 on cycles, whichever is more conservative.

The factors of 2 and 20 are not safety margins but rather adjustment factors that should be applied to the small-specimen data to obtain reasonable estimates of the lives of actual reactor components. As described in the Section III criteria document,² these factors were intended to account for data scatter (including material variability) and differences in surface condition and size between the test specimens and actual components. In comments about the initial scope and intent of the Section III fatigue design procedures Cooper³ states that the factor of 20 on life was regarded as the product of three subfactors:

Scatter of data (minimum to mean)	2.0
Size effect	2.5
Surface finish, atmosphere, etc.	4.0

Although the Section III criteria document² states that these factors were intended to cover such effects as environment, Cooper³ further states that the term "atmosphere" was intended to reflect the effects of an industrial atmosphere in comparison with an air-conditioned laboratory, not the effects of a specific coolant environment. Subsection NB-3121 of Section III of the Code explicitly notes that the data used to develop the fatigue design curves (Figs. I-9.1 through I-9.6 of Appendix I to Section III) did not include tests in the presence of corrosive environments that might accelerate fatigue failure. Article B-2131 in Appendix B to Section III states that the owner's design specifications should provide information about any reduction to fatigue design curves that is necessitated by environmental conditions.

Existing fatigue ϵ - N data illustrate potentially significant effects of light water reactor (LWR) coolant environments on the fatigue resistance of carbon and low-alloy steels and wrought and cast austenitic SSs.⁴⁻⁴⁵ Laboratory data indicate that under certain reactor operating conditions, fatigue lives of carbon and low-alloy steels can be a factor of 17 lower in the coolant environment than in air. Therefore, the margins in the ASME Code may be less conservative than originally intended.

The fatigue ϵ - N data are consistent with the much larger database on enhancement of crack growth rates (CGRs) in these materials in simulated LWR environments. The key parameters that influence fatigue life in these environments, e.g., temperature, dissolved-oxygen (DO) level in water, strain rate, strain (or stress) amplitude, and, for carbon and low-alloy steels, S content of the steel, have been identified. Also, the range of the values of these parameters within which environmental effects are significant has been clearly defined. If these critical parameters and environmental conditions exist during reactor operation, then environmental effects will be significant and need to be included in the ASME Code fatigue evaluations. Experience with nuclear power plants worldwide indicates that the critical range of loading and environmental conditions that leads to environmental effects on fatigue crack initiation can occur during plant operation.⁴⁵⁻⁶¹

Many failures of reactor components have been attributed to fatigue; examples include piping, nozzles, valves, and pumps.⁴⁶⁻⁵³ The mechanism of cracking in feedwater nozzles and piping has been attributed to corrosion fatigue or strain-induced corrosion cracking (SICC).⁵⁴⁻⁵⁶ A review of significant occurrences of corrosion fatigue damage and failures in various nuclear power plant systems, has been presented in an Electric Power Research Institute (EPRI) report.⁴⁵ In piping components, several failures were associated with thermal loading due to thermal stratification and striping. Thermal stratification is

caused by the injection of low-flow, relatively cold feedwater during plant startup, hot standby, or variations below 20% of full power, whereas thermal striping is caused by rapid, localized fluctuations of the interface between hot and cold feedwater. Significant cracking has also occurred in nonisolable piping connected to a PWR reactor coolant system (RCS). In most cases, thermal cycling was caused by interaction of hot RCS fluid from turbulent penetration at the top of the pipe, and cold valve leakage fluid that had stratified at the bottom of the pipe. Lenz et al.⁵⁵ have shown that in feedwater lines, strain rates are 10^{-3} – 10^{-5} %/s due to thermal stratification and 10^{-1} %/s due to thermal shock. They also have reported that thermal stratification is the primary cause of crack initiation due to SICC. Full-scale mock-up tests to generate thermal stratification in a pipe in a laboratory have confirmed the applicability of laboratory data to component behavior.^{44,62} A study conducted on SS pipe bend specimens in simulated PWR primary water at 240°C concluded that reactor coolant environment can have a significant effect on the fatigue life of SSs.⁶³ Relative to the fatigue life in an inert environment, life in the PWR environment at a strain amplitude of 0.52% was decreased by factor of 5.8 and 2.8 at strain rates of 0.0005%/s and 0.01%/s, respectively. These values show excellent agreement with the values predicted from the correlations presented in Section 5.2.14 of this report.

Thermal loading due to flow stratification or mixing was not included in the original design basis analyses. Regulatory evaluation has indicated that thermal-stratification cycling can occur in all PWR surge lines.⁶⁴ In PWRs, the pressurizer water is heated to $\approx 227^\circ\text{C}$. The hot water, flowing at a very low rate from the pressurizer through the surge line to the hot-leg piping, rides on a cooler water layer. The thermal gradients between the upper and lower parts of the pipe can be as high as 149°C .

Two approaches have been proposed for incorporating the environmental effects into ASME Section III fatigue evaluations for primary pressure boundary components in operating nuclear power plants: (a) develop new fatigue design curves for LWR applications, or (b) use an environmental fatigue correction factor to account for the effects of the coolant environment.

In the first approach, following the same procedures used to develop the current fatigue design curves of the ASME Code, environmentally adjusted fatigue design curves are developed from fits to experimental data obtained in LWR environments. Interim fatigue design curves that address environmental effects on the fatigue life of carbon and low-alloy steels and austenitic SSs were first proposed by Majumdar et al.⁶⁵ Fatigue design curves based on a more rigorous statistical analysis of experimental data were developed by Keisler et al.⁶⁶ These design curves have subsequently been revised on the basis of updated ANL models.^{4,6,38,39} However, because, in LWR environments, the fatigue life of carbon and low-alloy steels, nickel-chromium-iron (Ni-Cr-Fe) alloys, and austenitic SSs depends on several loading and environmental parameters, such an approach would require developing several design curves to cover all possible conditions encountered during plant operation. Defining the number of these design curves or the loading and environmental conditions for the curves is not easy.

The second approach, proposed by Higuchi and Iida,¹³ considers the effects of reactor coolant environments on fatigue life in terms of an environmental fatigue correction factor, F_{en} , which is the ratio of fatigue life in air at room temperature to that in water under reactor operating conditions. To incorporate environmental effects into fatigue evaluations, the fatigue usage factor for a specific stress cycle or load set pair, based on the ASME Code design curves, is multiplied by the environmental fatigue correction factor. Specific expressions for F_{en} , based on the Argonne National Laboratory (ANL) fatigue life models, have been developed.³⁹ Such an approach is relatively simple and is recommended in this report.

This report presents an overview of the existing fatigue ϵ - N data for carbon and low-alloy steels, Ni-Cr-Fe alloys, and wrought and cast austenitic SSs in air and LWR environments. The data are evaluated to (a) identify the various material, environmental, and loading parameters that influence fatigue crack initiation and (b) establish the effects of key parameters on the fatigue life of these steels. Fatigue life models, presented in earlier reports, for estimating fatigue life as a function of material, loading, and environmental conditions have been updated using a larger database. The F_{en} approach for incorporating effects of LWR environments into ASME Section III fatigue evaluations is described. The report also presents a critical review of the ASME Code fatigue design margins of 2 on stress (or strain) and 20 on life and assesses the possible conservatism in the current choice of design margins.

This page is intentionally left blank.

2. Fatigue Life

The formation of surface cracks and their growth to an engineering size (3-mm deep) constitute the fatigue life of a material, which is represented by the fatigue ϵ - N curves. Fatigue life has conventionally been divided into two stages: initiation, expressed as the number of cycles required to form microcracks on the surface; and propagation, expressed as cycles required to propagate the surface cracks to engineering size. During cyclic loading of smooth test specimens, surface cracks 10 μm or longer form early in life (i.e., <10% of life) at surface irregularities either already in existence or produced by slip bands, grain boundaries, second-phase particles, etc.^{4,5} Thus, fatigue life may be considered to constitute propagation of cracks from 10 to 3000 μm long.

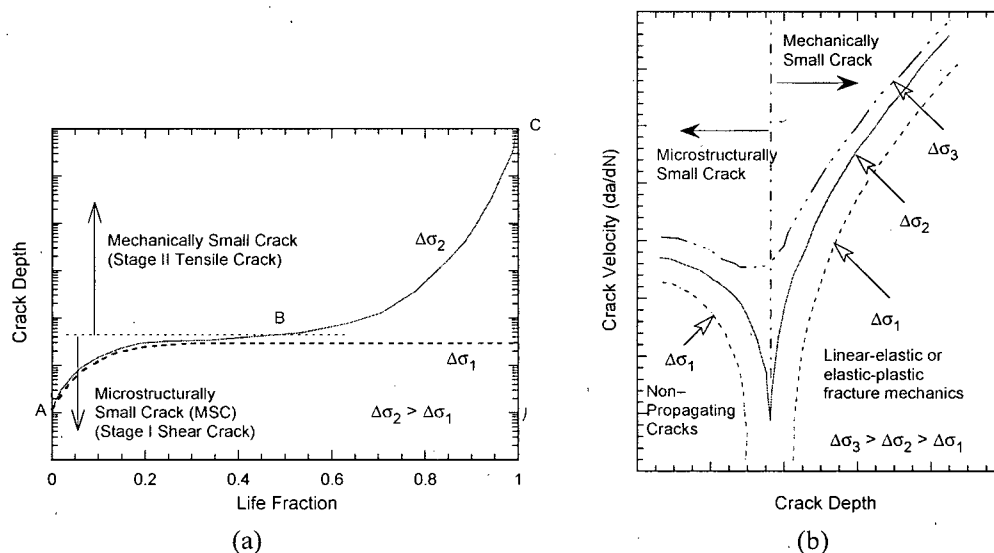


Figure 1. Schematic illustration of (a) growth of short cracks in smooth specimens as a function of fatigue life fraction and (b) crack velocity as a function of crack depth.

A schematic illustration of the initiation and propagation stages of fatigue life is shown in Fig. 1. The initiation stage involves growth of “microstructurally small cracks” (MSCs), characterized by decelerating crack growth (Region AB in Fig. 1a). The propagation stage involves growth of “mechanically small cracks,” characterized by accelerating crack growth (Region BC in Fig. 1a). The growth of the MSCs is very sensitive to microstructure.⁵ Fatigue cracks greater than a critical depth show little or no influence of microstructure and are considered mechanically small cracks. Mechanically small cracks correspond to Stage II (tensile) cracks, which are characterized by striated crack growth, with the fracture surface normal to the maximum principal stress. Various criteria, summarized in Section 5.4.1 of Ref. 6, have been used to define the crack depth for transition from microstructurally to mechanically small crack. The transition crack depth is a function of applied stress (σ) and microstructure of the material; actual values may range from 150 to 250 μm . At low enough stress levels ($\Delta\sigma_1$), the transition from MSC growth to accelerating crack growth does not occur. This circumstance represents the fatigue limit for the smooth specimen. Although cracks can form below the fatigue limit, they can grow to engineering size only at stresses greater than the fatigue limit. The fatigue limit for a material is applicable only for constant loading conditions. Under variable loading conditions, MSCs can grow at high stresses ($\Delta\sigma_3$) to depths larger than the transition crack depth and then can continue to grow at stress levels below the fatigue limit ($\Delta\sigma_1$).

Studies on the formation and growth characteristics of short cracks in smooth fatigue specimens in LWR environments indicate that the decrease in fatigue life in LWR environments is caused primarily by the effects of the environment on the growth of MSCs (i.e., cracks <200 μm deep) and, to a lesser extent, on the growth of mechanically small cracks.^{4,7} Crack growth rates measured in smooth cylindrical fatigue specimens of A533-Gr B low-alloy steel and austenitic Type 304 SSs in LWR environments and air are shown in Fig. 2. The results indicate that in LWR environments, the period spent in the growth of MSCs (region ABC in Fig. 1a) is decreased. For the A533-Gr B steel, only 30–50 cycles are needed to form a 100- μm crack in high-DO water, whereas ≈ 450 cycles are required to form a 100- μm crack in low-DO water and more than 3000 cycles in air. These values correspond to average growth rates of ≈ 2.5 , 0.22, and 0.033 $\mu\text{m}/\text{cycle}$ in high-DO water, low-DO water, and air, respectively. Relative to air, CGRs for A533-Gr B steel in high-DO water are nearly two orders of magnitude higher for crack sizes <100 μm , and one order of magnitude higher for crack sizes >100 μm .

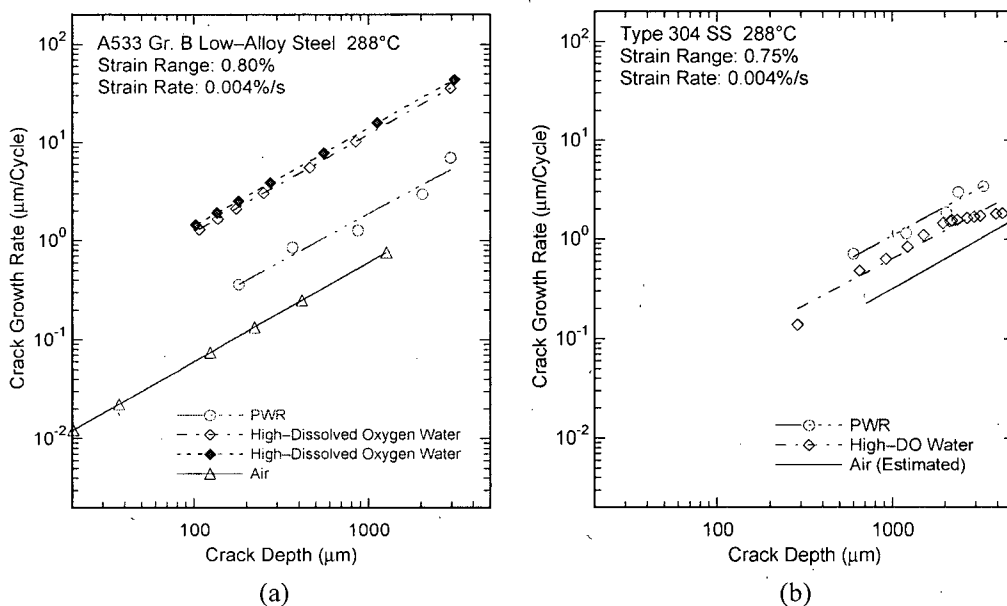


Figure 2. Crack growth rates plotted as a function of crack depth for (a) A533-Gr B low-alloy steel and (b) Type 304 SS in air and LWR environments.

The fatigue ϵ -N data for carbon and low-alloy steels in air and LWR environments have been examined from the standpoint of fracture mechanics and CGR data.^{67,68} Fatigue life is considered to consist of an initiation stage, composed of the growth of microstructurally small cracks, and a propagation stage, composed of the growth of mechanically small cracks. The growth of the latter has been characterized in terms of the J-integral range ΔJ and crack growth rate data in air and LWR environments. The estimated values show good agreement with the experimental ϵ -N data for test specimens in air and water environments.

3. Fatigue Strain vs. Life Data

The existing fatigue ϵ -N data developed at various establishments and research laboratories worldwide have been compiled by the Pressure Vessel Research Council (PVRC), Working Group on ϵ -N Curve and Data Analysis. The database used in the ANL studies is an updated version of the PVRC database. A summary of the sources included in the updated PVRC database, as categorized by material type and test environment, is presented in Table 1.

Unless otherwise mentioned, smooth cylindrical gauge specimens were tested under strain control with a fully reversed loading, i.e., strain ratio of -1 . Tests on notched specimens or at values of strain ratio other than -1 were excluded from the fatigue ϵ -N data analysis. For the tests performed at ANL, the estimated uncertainty in the strain measurements is about 4% of the reported value. For the data obtained in other laboratories, the uncertainty in the reported values of strain is unlikely to be large enough to significantly affect the results.

In nearly all tests, fatigue life is defined as the number of cycles, N_{25} , necessary for tensile stress to drop 25% from its peak or steady-state value. For the specimen size used in these studies, e.g., 5.1–9.5 mm (0.2–0.375 in.) diameter cylindrical specimens, this corresponds to a ≈ 3 -mm-deep crack. Some of the earlier tests in air were carried out to complete failure of the specimen, and life in some tests is defined as the number of cycles for peak tensile stress to decrease by 1–5%. Also, in fatigue tests that were performed using tube specimens, life was represented by the number of cycles to develop a leak.

Table 1. Sources of the fatigue ϵ -N data on reactor structural materials in air and water environments.

Source	Material	Environment	Reference
General Electric Co.	Carbon steel, Type 304 SS	Air and BWR water	8–11
Japan; including Ishikawajima-Harima Heavy Industries (IHI) Co., Mitsubishi Heavy Industries (MHI) Ltd., Hitachi Research Laboratory	Carbon and low-alloy steel, wrought and cast austenitic SS, Ni-Cr-Fe alloys	Air, BWR, and PWR water	JNUFAD* database, 12–33
Argonne National Laboratory	Carbon and low-alloy steel, wrought and cast austenitic SS	Air, BWR, and PWR water	4–7, 34–40
Materials Engineering Associates (MEA) Inc.	Carbon steel, austenitic SS	Air and PWR water	41–43
Germany; including MPA	Carbon steel		44–45
France; including studies sponsored by Electricite de France (EdF)	Austenitic SS	Air and PWR water	69–71
Jaske and O'Donnell	Austenitic SS, Ni-Cr-Fe alloys	Air	72
Others	Austenitic SS, Ni-Cr-Fe alloys	Air	73–78

* Private communication from M. Higuchi, Ishikawajima-Harima Heavy Industries Co. Japan, to M. Prager of the Pressure Vessel Research Council, 1992. The old database "Fadal" has been revised and renamed "JNUFAD."

For the tests where fatigue life was defined by a criterion other than 25% drop in peak tensile stress (e.g., 5% decrease in peak tensile stress or complete failure), fatigue lives were normalized to the 25% drop values before performing the fatigue data analysis.⁴ The estimated uncertainty in fatigue life determined by this procedure is about 2%.

An analysis of the existing fatigue ϵ - N data and the procedures for incorporating environmental effects into the Code fatigue evaluations has been presented in several review articles⁷⁹⁻⁹⁰ and ANL topical reports.^{4,6,7,38-40} The key material, loading, and environmental parameters that influence the fatigue lives of carbon and low-alloy steels and austenitic stainless steels have been identified, and the range of these key parameters where environmental effects are significant has been defined.

How various material, loading, and environmental parameters affect fatigue life and how these effects are incorporated into the ASME Code fatigue evaluations are discussed in detail for carbon and low-alloy steels, wrought and cast SSs, and Ni-Cr-Fe alloys in Sections 4, 5, and 6, respectively.

4 Carbon and Low-Alloy Steels

The primary sources of relevant ϵ - N data for carbon and low-alloy steels are the tests performed by General Electric Co. (GE) in a test loop at the Dresden 1 reactor;^{8,9} work sponsored by EPRI at GE;^{10,11} the work of Terrell at Mechanical Engineering Associates (MEA);⁴¹⁻⁴³ the work at ANL on fatigue of pressure vessel and piping steels;^{4-7,34-40} the large JNUFAD database for "Fatigue Strength of Nuclear Plant Component" and studies at Ishikawajima-Harima Heavy Industries (IHI), Hitachi, and Mitsubishi Heavy Industries (MHI) in Japan;¹²⁻³⁰ and the studies at Kraftwerk Union Laboratories (KWU) and Materialprüfungsanstalt (MPA) in Germany.⁴⁴⁻⁴⁵ The database is composed of ≈ 1400 tests; $\approx 60\%$ were obtained in the water environment and the remaining in air. Carbon steels include ≈ 12 heats of A333-Grade 6, A106-Grade B, A516-Grade 70, and A508-Class 1 steel, while the low-alloy steels include ≈ 16 heats of A533-Grade B, A302-Gr B, and A508-Class 2 and 3 steels.

4.1 Air Environment

4.1.1 Experimental Data

In air, the fatigue lives of carbon and low-alloy steels depend on steel type, temperature, and for some compositions, applied strain rate and sulfide morphology. Fatigue ϵ - N data from various investigations on carbon and low-alloy steels are shown in Fig. 3. The best-fit curves based on the ANL models (Eqs. 15 and 16 from Section 4.1.8) and the ASME Section III mean-data curves (at room temperature) are also included in the figures. The results indicate that, although significant scatter is apparent due to material variability, the fatigue lives of these steels are comparable at less than 5×10^5 cycles, and those of low-alloy steels are greater than carbon steels for $> 5 \times 10^5$ cycles. Also, the fatigue limit of low-alloy steels is higher than that of carbon steels.

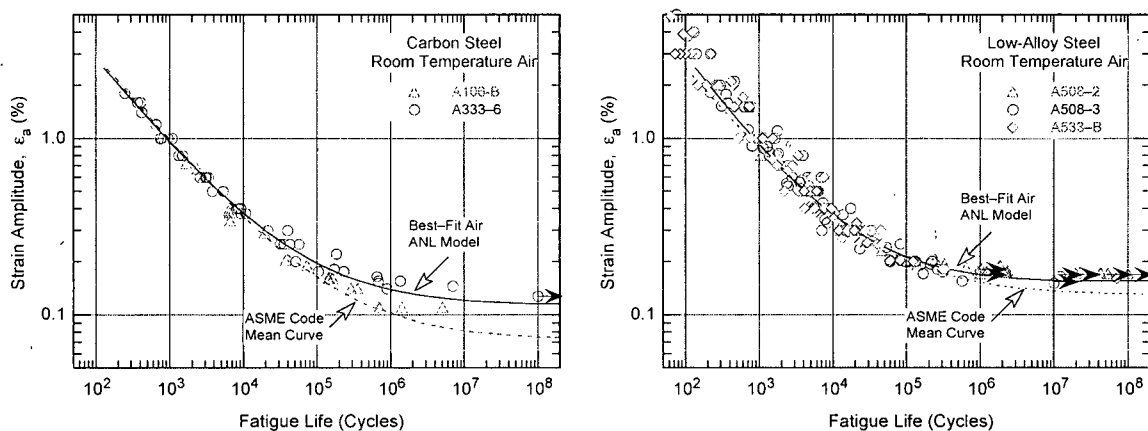


Figure 3. Fatigue strain vs. life data for carbon and low-alloy steels in air at room temperature (JNUFAD database and Refs. 4,12,13,41).

The existing fatigue ϵ - N data for low-alloy steels are in good agreement with the ASME mean data curve. The existing data for carbon steels are consistent with the ASME mean data curve for fatigue life $\leq 5 \times 10^5$ cycles and are above the mean curve at longer lives. Thus, above 5×10^5 cycles, the Code mean curve is conservative with respect to the existing fatigue ϵ - N data.

- The current Code mean data curves are either consistent with the existing fatigue ϵ - N data or are somewhat conservative under some conditions.

4.1.2 Temperature

In air, the fatigue life of both carbon and low-alloy steels decreases with increasing temperature; however, the effect is relatively small (less than a factor of 1.5). Fatigue ϵ - N data from the JNUFAD database and other investigations in air at 286–300°C are shown in Fig. 4. For each grade of steel, the data represent several heats of material. The best-fit curves for carbon and low-alloy steels at room temperature (Eqs. 15 and 16 from Section 4.1.8) and at 289°C (Eqs. 13 and 14 from Section 4.1.8) are also included in the figures. The results indicate a factor of ≈ 1.5 decrease in fatigue life of both carbon and low-alloy steels as the temperature is increased from room temperature to 300°C. As discussed later in Section 4.1.7, the greater-than-predicted difference between the best-fit air curve at room temperature and the data for A106-Gr B steel at 289°C is due to heat-to-heat variability and not temperature effects.

- The effect of temperature is not explicitly considered in the mean data curve used for obtaining the fatigue design curves; variations in fatigue life due to temperature are accounted for in the subfactor for “data scatter and material variability.”

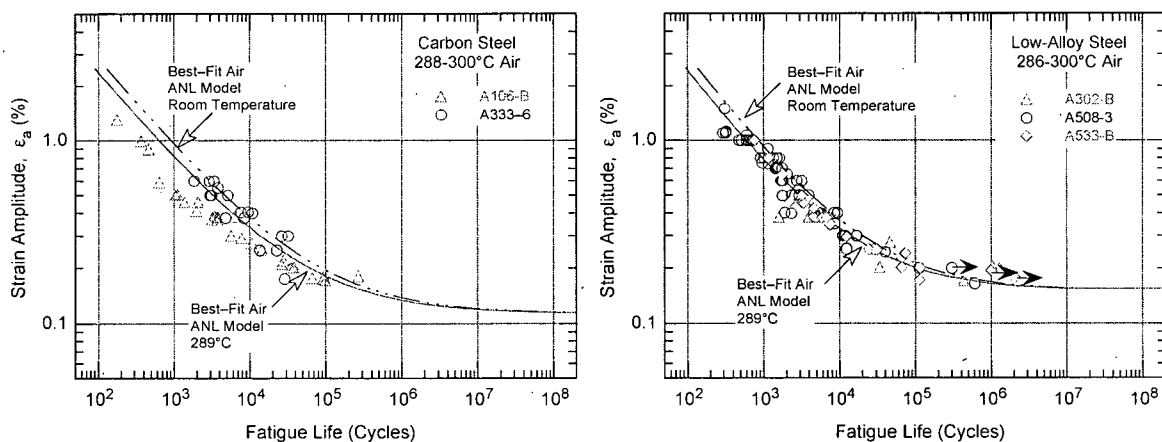


Figure 4. Fatigue strain vs. life data for carbon and low-alloy steels in air at 288°C (JNUFAD database, and Refs. 4,12,13,42,43).

4.1.3 Strain Rate

The effect of strain rate on the fatigue life of carbon and low-alloy steels in air appears to depend on the material composition. The existing data indicate that in the temperature range of dynamic strain aging (200–370°C), some heats of carbon and low-alloy steel are sensitive to strain rate; with decreasing strain rate, the fatigue life in air may be either unaffected,⁴ decrease for some heats,⁹¹ or increase for others.⁹² The C and N contents in the steel are considered to be important. Inhomogeneous plastic deformation can result in localized plastic strains. This localization retards blunting of propagating cracks that is usually expected when plastic deformation occurs and can result in higher crack growth rates.⁹¹ The increases in fatigue life have been attributed to retardation of CGRs due to crack branching and suppression of the plastic zone. Formation of cracks is easy in the presence of dynamic strain aging.⁹²

- Variations in fatigue life due to the effects of strain rate are not explicitly considered in the fatigue design curves, they are accounted for in the subfactor for “data scatter and material variability.”

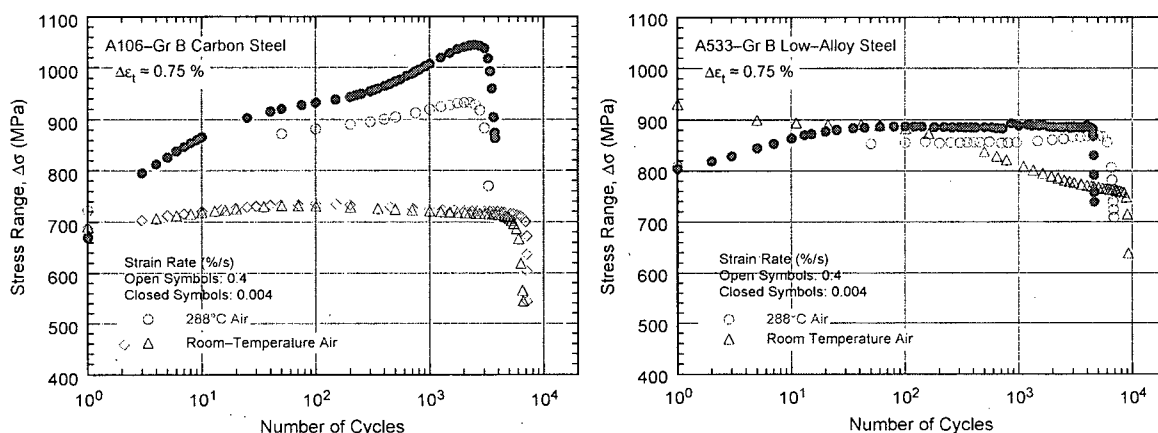


Figure 5. Effect of strain rate and temperature on cyclic stress of carbon and low-alloy steels.

4.1.4 Sulfide Morphology

Some high-S steels exhibit very poor fatigue properties in certain orientations because of structural factors such as the distribution and morphology of sulfides in the steel. For example, fatigue tests on a high-S heat of A302-Gr. B steel in three orientations* in air at 288°C indicate that the fatigue life and fatigue limit in the T2 orientation are lower than those in the R and T1 orientations.⁴ At low strain rates, fatigue life in the T2 orientation is nearly one order of magnitude lower than in the R orientation. In the orientation with poor fatigue resistance, crack propagation is preferentially along the sulfide stringers and is facilitated by sulfide cracking.

- *Variations in fatigue life due to differences in sulfide morphology are accounted for in the subfactor for "data scatter and material variability."*

4.1.5 Cyclic Strain Hardening Behavior

The cyclic stress-strain response of carbon and low-alloy steels varies with steel type, temperature, and strain rate. In general, these steels show initial cyclic hardening, followed by cyclic softening or a saturation stage at all strain rates. The carbon steels, with a pearlite and ferrite structure and low yield stress, exhibit significant initial hardening. The low-alloy steels, with a tempered bainite and ferrite structure and a relatively high yield stress, show little or no initial hardening and may exhibit cyclic softening with continued cycling. For both steels, maximum stress increases as applied strain increases and generally decreases as temperature increases. However, at 200–370°C, these steels exhibit dynamic strain aging, which results in enhanced cyclic hardening, a secondary hardening stage, and negative strain rate sensitivity.^{91,92} The temperature range and extent of dynamic strain aging vary with composition and structure.

The effect of strain rate and temperature on the cyclic stress response of A106-Gr B carbon steel and A533-Gr B low-alloy steel is shown in Fig. 5. For both steels, cyclic stresses are higher at 288°C than at room temperature. At 288°C, all steels exhibit greater cyclic and secondary hardening because of dynamic strain aging. The extent of hardening increases as the applied strain rate decreases.

* Both transverse (T) and radial (R) directions are perpendicular to the rolling direction, but the fracture plane is across the thickness of the plate in the transverse orientation and parallel to the plate surface in the radial orientation.

- The cyclic strain hardening behavior is likely to influence the fatigue limit of the material; variations in fatigue life due to the effects of strain hardening are not explicitly considered in the fatigue design curves, they are accounted for in the subfactor for "data scatter and material variability."

4.1.6 Surface Finish

The effect of surface finish must be considered to account for the difference in fatigue life expected in an actual component with industrial-grade surface finish, compared with the smooth polished surface of a test specimen. Fatigue life is sensitive to surface finish; cracks can initiate at surface irregularities that are normal to the stress axis. The height, spacing, shape, and distribution of surface irregularities are important for crack initiation. The most common measure of roughness is average surface roughness R_a , which is a measure of the height of the irregularities. Investigations of the effects of surface roughness on the low-cycle fatigue of Type 304 SS in air at 593°C indicate that fatigue life decreases as surface roughness increases.^{93,94} The effect of roughness on crack initiation $N_i(R)$ is given by

$$N_i(R_q) = 1012 R_q^{-0.21}, \quad (12)$$

where the root-mean-square (RMS) value of surface roughness R_q is in μm . Typical values of R_a for surfaces finished by different metalworking processes in the automotive industry⁹⁵ indicate that an R_a of 3 μm (or an R_q of 4 μm) represents the maximum surface roughness for drawing/extrusion, grinding, honing, and polishing processes and a mean value for the roughness range for milling or turning processes. For carbon steel or low-alloy steel, an R_q of 4 μm in Eq. 12 (the R_q of a smooth polished specimen is $\approx 0.0075 \mu\text{m}$) would decrease fatigue life by a factor of ≈ 3 .⁹³

Fatigue test has been conducted on a A106-Gr B carbon steel specimen that was intentionally roughened in a lathe, under controlled conditions, with 50-grit sandpaper to produce circumferential scratches with an average roughness of 1.2 μm and an R_q of 1.6 μm (≈ 62 micro in.).³⁹ The results for smooth and roughened specimens are shown in Fig. 6. In air, the fatigue life of a roughened A106-Gr B specimen is a factor of ≈ 3 lower than that of smooth specimens. Another study of the effect of surface finish on the fatigue life of carbon steel in room-temperature air showed a factor of 2 decrease in life when R_a was increased from 0.3 to 5.3 μm .⁹⁶ These results are consistent with Eq. 12. Thus, a factor of 2–3 on cycles may be used to account for the effects of surface finish on the fatigue life of carbon and low-alloy steels.

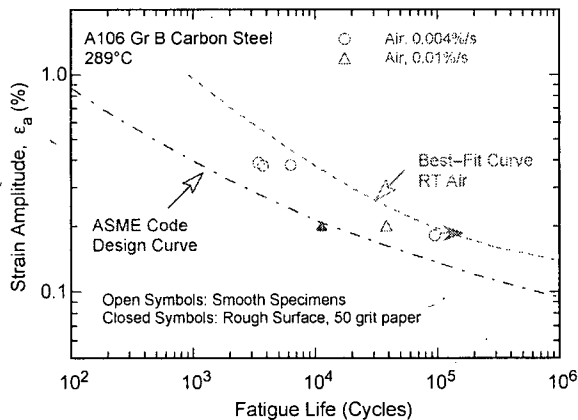


Figure 6. Effect of surface finish on the fatigue life of A106-Gr B carbon steel in air at 289°C.

- *The effect of surface finish was not investigated in the mean data curve used to develop the Code fatigue design curves; it is included as part of the subfactor that is applied to the mean data curve to account for "surface finish and environment."*

4.1.7 Heat-to-Heat Variability

Several factors, such as small differences in the material composition and structure, can change the tensile and fatigue properties of the material. The effect of interstitial element content on dynamic strain aging and the effect of sulfide morphology on fatigue life have been discussed in Sections 4.1.3 and 4.1.4, respectively. The effect of tensile strength on the fatigue life has been included in the expression for the mean data curve described in the Section III criteria document, i.e., constant A_f in Eq. 2. Also, the fatigue limit of a material has been correlated with its tensile strength, e.g., the fatigue limit increases with increasing tensile yield stress.⁹⁷

The effects of material variability and data scatter must be included to ensure that the design curves not only describe the available test data well, but also adequately describe the fatigue lives of the much larger number of heats of material that are found in the field. The effects of material variability and data scatter are often evaluated by comparing the experimental data to a specific model for fatigue crack initiation, e.g., the best-fit (in some sense) to the data. The adequacy of the evaluation will then depend on the sample of data used in the analysis. For example, if most of the data have been obtained from a heat of material that has poor resistance to fatigue damage or under loading conditions that show significant environmental effects, the results may be conservative for most of the materials or service conditions of interest. Conversely, if most data are from a heat of material with a high resistance to fatigue damage, the results could be nonconservative for many heats in service.

Another method to assess the effect of material variability and data scatter is by considering the best-fit curves determined from tests on individual heats of materials or loading conditions as samples of the much larger population of heats of materials and service conditions of interest. The fatigue behavior of each of the heats or loading conditions is characterized by the value of the constant A in Eq. 6. The values of A for the various data sets are ordered, and median ranks are used to estimate the cumulative distribution of A for the population.^{98,99} The distributions were fit to lognormal curves. No rigorous statistical evaluation was performed, but the fits seem reasonable and describe the observed variability adequately. Results for carbon and low-alloy steels in air are shown in Fig. 7. The data were normalized to room-temperature values using Eqs. 13 and 14 (section 4.1.8). The median value of the constant A is 6.583 and 6.449, respectively, for the fatigue life of carbon steels and low-alloy steels in room-temperature air. Note that the two heats of A106-Gr B carbon steel are in the 10-25 percentile of the data, i.e., the fatigue lives of these heats are much lower than the average value for carbon steels.

The A values that describe the 5th percentile of these distributions give fatigue ϵ - N curves that are expected to bound the fatigue lives of 95% of the heats of the material. The cumulative distributions in Fig. 7 contain two potential sources of error. The mean and standard deviation of the population must be estimated from the mean and standard deviation of the sample,¹⁰⁰ and confidence bounds can then be obtained on the population mean and standard deviation in terms of the sample mean and standard deviation. Secondly, even this condition does not fully address the uncertainty in the distribution because of the large uncertainties in the sample values themselves, i.e., the "horizontal" uncertainty in the actual value of A for a heat of material, as indicated by the error bars in Fig. 7. A Monte Carlo analysis was performed to address both sources of uncertainty. The results for the median value and standard deviation of the constant A from the Monte Carlo analysis did not differ significantly from those determined directly from the experimental values.

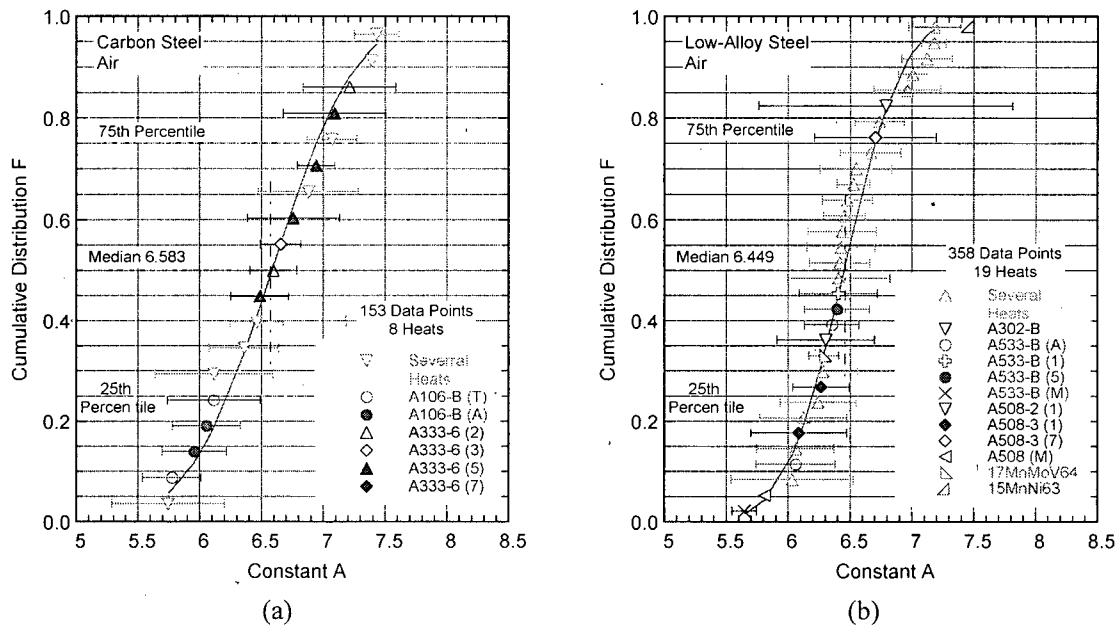


Figure 7. Estimated cumulative distribution of constant A in the ANL models for fatigue life for heats of (a) carbon steels and (b) low-alloy steels in air.

The results for carbon and low-alloy steels are summarized in Tables 2 and 3, respectively, in terms of values for A that provide bounds for the portion of the population and the confidence that is desired in the estimates of the bounds. In air, the 5th percentile value of Parameter A at a 95% confidence level is 5.559 for carbon steels and 5.689 for low-alloy steels. From Fig. 7, the median value of A for the sample is 6.583 for carbon steels and 6.449 for low-alloy steels. Thus, the 95/95 value of the margin to account for material variability and data scatter is 2.8 and 2.1 on life for carbon steels and low-alloy steels, respectively. These margins are needed to provide 95% confidence that the resultant life will be greater than that observed for 95% of the materials of interest. The margin is higher for carbon steels because the analysis is based on a smaller number of data sets, i.e., 19 for carbon steels and 32 for low-alloy steels.

- *The mean data curve used to develop the Code fatigue design curves represents the average behavior; heat-to-heat variability is included in the subfactor that is applied to the mean data curve to account for "data scatter and material variability."*

Table 2. Values of parameter A in the ANL fatigue life model for carbon steels in air and the margins on life as a function of confidence level and percentage of population bounded.

Confidence Level	Percentage of Population Bounded (Percentile Distribution of A)				
	95 (5)	90 (10)	75 (25)	67 (33)	50 (50)
<u>Values of Parameter A</u>					
50	5.798	5.971	6.261	6.373	6.583
75	5.700	5.883	6.183	6.295	6.500
95	5.559	5.756	6.069	6.183	6.381
<u>Margins on Life</u>					
50	2.2	1.8	1.4	1.2	1.0
75	2.4	2.0	1.5	1.3	1.1
95	2.8	2.3	1.7	1.5	1.2

Table 3. Values of parameter A in the ANL fatigue life model for low-alloy steels in air and the margins on life as a function of confidence level and percentage of population bounded.

Confidence Level	Percentage of Population Bounded (Percentile Distribution of A)				
	95 (5)	90 (10)	75 (25)	67 (33)	50 (50)
	<u>Values of Parameter A</u>				
50	5.832	5.968	6.196	6.284	6.449
75	5.774	5.916	6.150	6.239	6.403
95	5.689	5.840	6.085	6.175	6.337
	<u>Margins on Life</u>				
50	1.9	1.6	1.3	1.2	1.0
75	2.0	1.7	1.3	1.2	1.0
95	2.1	1.8	1.4	1.3	1.1

4.1.8 Fatigue Life Model

Fatigue life models for estimating the fatigue lives of these steels in air based on the existing fatigue ϵ - N data have been developed at ANL as best-fits of a Langer curve to the data.^{4,39} The fatigue life, N , of carbon steels is represented by

$$\ln(N) = 6.614 - 0.00124 T - 1.975 \ln(\epsilon_a - 0.113), \quad (13)$$

and that of low-alloy steels, by

$$\ln(N) = 6.480 - 0.00124 T - 1.808 \ln(\epsilon_a - 0.151), \quad (14)$$

where ϵ_a is applied strain amplitude (%), and T is the test temperature ($^{\circ}\text{C}$). Thus, in room-temperature air, the fatigue life of carbon steels is expressed as

$$\ln(N) = 6.583 - 1.975 \ln(\epsilon_a - 0.113), \quad (15)$$

and that of low-alloy steels, by

$$\ln(N) = 6.449 - 1.808 \ln(\epsilon_a - 0.151). \quad (16)$$

Note that these equations have been updated based on the analysis presented in Section 4.1.7; constant A in the equations is different from the value reported earlier in NUREG/CR-6583 and 6815. Relative to the earlier model, the fatigue lives predicted by the updated model are $\approx 2\%$ higher for carbon steel and $\approx 16\%$ lower for low-alloy steels. The experimental values of fatigue life and those predicted by Eqs. 15 and 16 for carbon and low-alloy steels in air are plotted in Fig. 8. The predicted fatigue lives show good agreement with the experimental values; the experimental and predicted values are within a factor of 3.

- *The fatigue life models represent mean values of fatigue life of specimens tested under fully reversed strain-controlled loading. The effects of parameters (such as mean stress, surface finish, size and geometry, and loading history) that are known to influence fatigue life are not explicitly considered in the model; such effects are accounted for in the several subfactors that are applied to the mean data curve to obtain the Code fatigue design curve.*

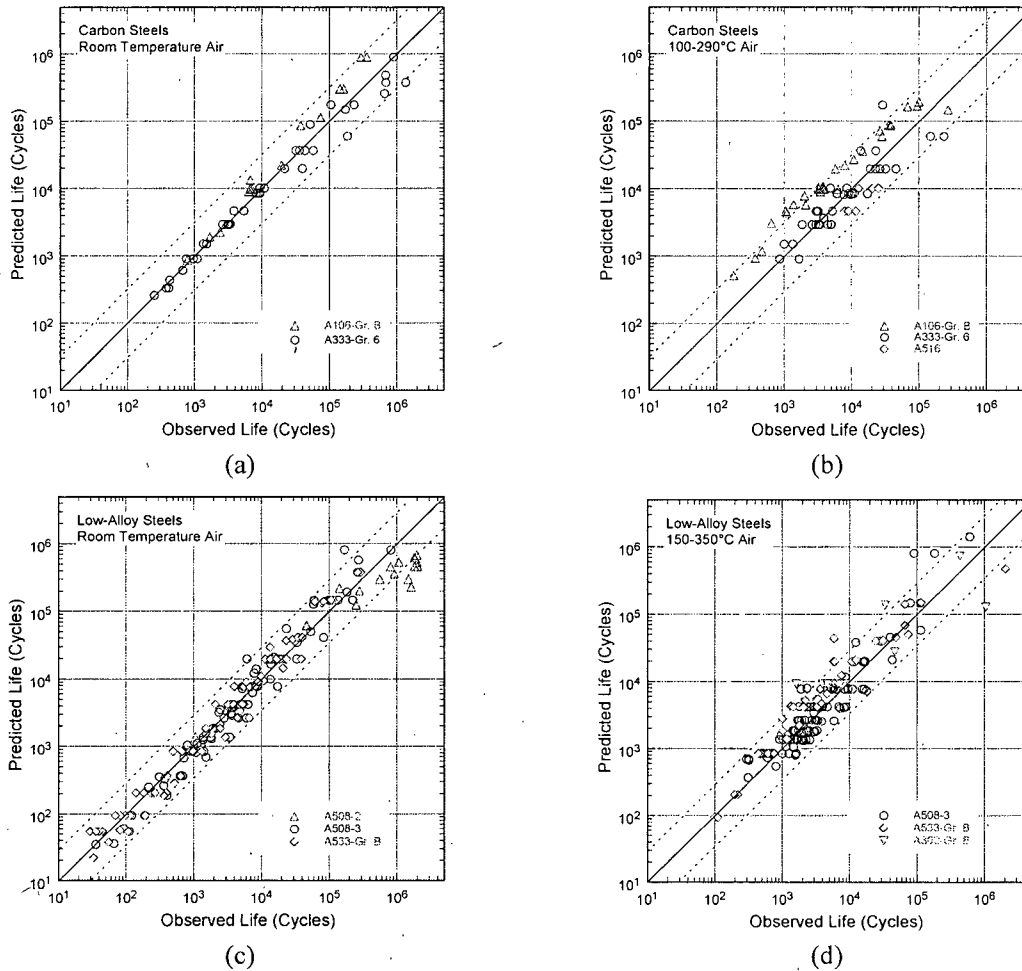


Figure 8. Experimental and predicted fatigue lives of (a, b) carbon steels and (c, d) low-alloy steels in air.

4.1.9 Extension of the Best-Fit Mean Curve from 10^6 to 10^{11} Cycles

The experimental fatigue ϵ - N curves that were used to develop the current Code fatigue design curve for carbon and low-alloy steels were based on low-cycle fatigue data (less than 2×10^5 cycles). The design curves proposed in this report are developed from a larger database that includes fatigue lives up to 10^8 cycles. Both the ASME mean curves and the ANL models in this report use the modified Langer equation to express the best-fit mean curves and are not recommended for estimating lives beyond the range of the experimental data, i.e., in the high-cycle fatigue regime.

An extension of the current high-cycle fatigue design curves in Section III and Section VIII, Division 2, of the ASME Code for carbon and low-alloy steels from 10^6 to 10^{11} cycles has been proposed by W. J. O'Donnell for the ASME Subgroup on Fatigue Strength.* In the high-cycle regime, at temperatures not exceeding 371°C (700°F), the stress amplitude vs. life relationship is expressed as

$$S_a = E\epsilon_a = C_1 N^{-0.05}, \quad (17)$$

*W. J. O'Donnell, "Proposed Extension of ASME Code Fatigue Design Curves for Carbon and Low-Alloy Steels from 10^6 to 10^{11} Cycles for Temperatures not Exceeding 700°F ," presented to ASME Subgroup on Fatigue Strength December 4, 1996.

where ϵ_a is applied strain amplitude, E is the elastic modulus, N is the fatigue life, and C_1 is a constant. A fatigue life exponent of -0.05 was selected based on the fatigue stress range vs. fatigue life data on plain plates, notched plates, and typical welded structures given in Welding Research Council (WRC) Bulletin 398.¹⁰¹ Because these data were obtained from load-controlled tests with a load ratio $R = 0$, they take into account the effect of maximum mean stresses and, may over estimate the effect of mean stress under strain-controlled loading conditions. Also, the fatigue data presented in Bulletin 398 extend only up to 5×10^6 cycles; extrapolation of the results to 10^{11} cycles using a fatigue life exponent of -0.05 may yield conservative estimates of fatigue life.

Manjoine and Johnson⁹⁷ have developed fatigue design curves up to 10^{11} cycles for carbon steels and austenitic SSs from inelastic and elastic strain relationships, which can be correlated with ultimate tensile strength. The log-log plots of the elastic strain amplitudes vs. fatigue life data are represented by a bilinear curve. In the high-cycle regime, the elastic-strain-vs.-life curve has a small negative slope instead of a fatigue limit.⁹⁷ For carbon steel data at room temperature and 371°C and fatigue lives extending up to 4×10^7 cycles, Manjoine and Johnson obtained an exponent of -0.01. The fatigue ϵ - N data from the present study at room temperature and with fatigue lives up to 10^8 cycles yield a fatigue life exponent of approximately -0.007 for both carbon and low-alloy steels. Because the data are limited, the more conservative value obtained by Manjoine and Johnson⁹⁷ is used. Thus, in the high-cycle regime, the applied stress amplitude is given by the relationship

$$S_a = E\epsilon_a = C_2 N^{-0.01}. \quad (18)$$

The high-cycle curve (i.e., Eq. 18) can be used to extend the best-fit mean curves beyond 10^6 cycles; the mean curves will exhibit a small negative slope instead of the fatigue limit predicted in the modified Langer equation. The constant C_2 is determined from the value of strain amplitude at 10^8 cycles obtained from Eq. 15 for carbon steels and from Eq. 16 for low-alloy steels.

4.1.10 Fatigue Design Curve

Although the two mean curves for carbon and low-alloy steels (i.e., Eqs. 7 and 9) are significantly different, because the mean stress correction is much larger for the low-alloy steels, the differences between the curves is much smaller when mean stress corrections are considered. Thus, the ASME Code provides a common curve for both carbon and low-alloy steels. Fatigue design curves for carbon steels and low-alloy steels based on the ANL fatigue life models can be obtained from Eqs. 15 and 18, and Eqs. 16 and 18, respectively.

The best-fit curves are first corrected for mean stress effects by using the modified Goodman relationship, and the mean-stress adjusted curve is reduced by a factor of 2 on stress or 12 on cycles, whichever is more conservative. The discussions presented later in Section 7.5 indicate that the current Code requirement of a factor of 20 on cycles, to account for the effects of material variability and data scatter, specimen size, surface finish, and loading history, is conservative by at least a factor of 1.7. Thus, to reduce this conservatism, fatigue design curves based on the ANL model for carbon and low-alloy steels have been developed using factors of 12 on life and 2 on stress. These design curves are shown in Figs. 9 and 10, respectively. The current Code design curve for carbon and low-alloy steels with ultimate tensile strength (UTS) ≤ 552 MPa (≤ 80 ksi) and the extension of the design curve to 10^{11} cycles proposed by W. J. O'Donnell are also included in the figures. The values of stress amplitude (S_a) vs. cycles for the ASME Code curve with O'Donnell's extension, and the design curve based on the updated ANL fatigue life model (i.e., Eqs. 15 and 18 for carbon steel and, 16 and 18 for low-alloy steel) are listed in Table 4.

- For low-alloy steels, the current Code fatigue design curve for carbon and low-alloy steels with ultimate tensile strength $<552 \text{ MPa}$ ($<80 \text{ ksi}$) is either consistent or conservative with respect to the existing fatigue ϵ - N data. Also, discussions presented in Section 7.5 indicate that the current Code requirement of a factor of 20 on life is conservative by at least a factor of 1.7. Fatigue design curves have been developed from the ANL model using factors of 12 on life and 2 on stress.

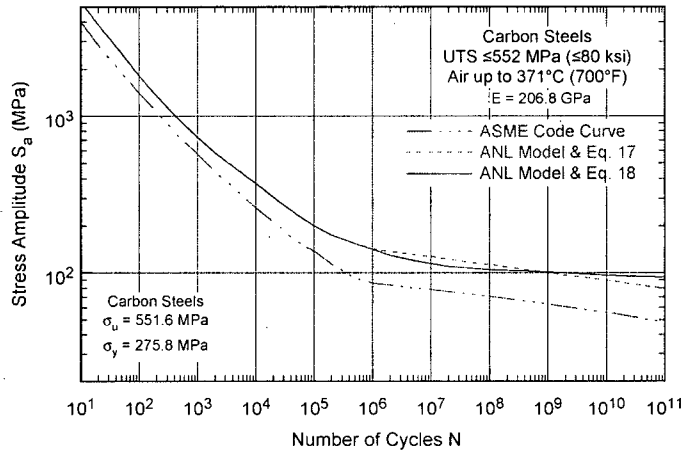


Figure 9. Fatigue design curve for carbon steels in air. The curve developed from the ANL model is based on factors of 12 on life and 2 on stress.

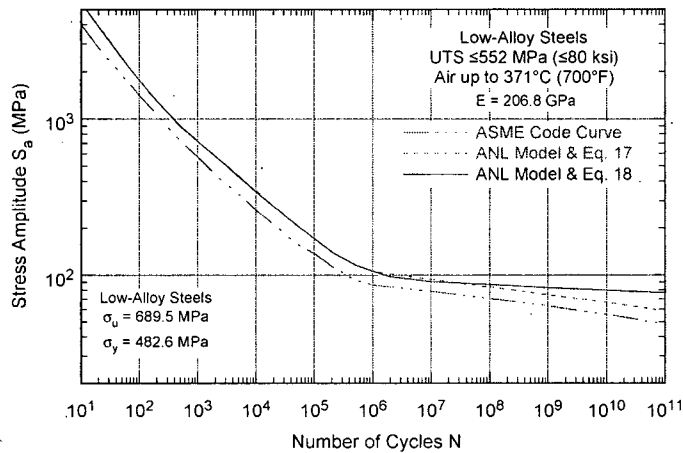


Figure 10. Fatigue design curve for low-alloy steels in air. The curve developed from the ANL model is based on factors of 12 on life and 2 on stress.

Table 4. Fatigue design curves for carbon and low-alloy steels and proposed extension to 10^{11} cycles.

Cycles	Stress Amplitude (MPa/ksi)			Cycles	Stress Amplitude (MPa/ksi)		
	ASME Code Curve	Eqs. 15 & 18 Carbon Steel	Eqs. 16 & 18 Low-Alloy Steel		ASME Code Curve	Eqs. 15 & 18 Carbon Steel	Eqs. 16 & 18 Low-Alloy Steel
1 E+01	3999 (580)	5355 (777)	5467 (793)	2 E+05	114 (16.5)	176 (25.5)	141 (20.5)
2 E+01	2827 (410)	3830 (556)	3880 (563)	5 E+05	93 (13.5)	154 (22.3)	116 (16.8)
5 E+01	1896 (275)	2510 (364)	2438 (354)	1 E+06	86 (12.5)	142 (20.6)	106 (15.4)
1 E+02	1413 (205)	1820 (264)	1760 (255)	2 E+06		130 (18.9)	98 (14.2)
2 E+02	1069 (155)	1355 (197)	1300 (189)	5 E+06		120 (17.4)	94 (13.6)
5 E+02	724 (105)	935 (136)	900 (131)	1 E+07	76.5 (11.1)	115 (16.7)	91 (13.2)
1 E+03	572 (83)	733 (106)	720 (104)	2 E+07		110 (16.0)	90 (13.1)
2 E+03	441 (64)	584 (84.7)	576 (83.5)	5 E+07		107 (15.5)	88 (12.8)
5 E+03	331 (48)	451 (65.4)	432 (62.7)	1 E+08	68.3 (9.9)	105 (15.2)	87 (12.6)
1 E+04	262 (38)	373 (54.1)	342 (49.6)	1 E+09	60.7 (8.8)	102 (14.8)	83 (12.0)
2 E+04	214 (31)	305 (44.2)	276 (40.0)	1 E+010	54.5 (7.9)	97 (14.1)	80 (11.6)
5 E+04	159 (23)	238 (34.5)	210 (30.5)	1 E+011	48.3 (7.0)	94 (13.6)	77 (11.2)
1 E+05	138 (20.0)	201 (29.2)	172 (24.9)				

4.2 LWR Environments

4.2.1 Experimental Data

Fatigue ϵ - N data on carbon and low-alloy steels in air and high-DO water at 288°C are shown in Fig. 11. The curves based on the ANL models (Eqs. 20 and 21 in Section 4.2.12) are also included in the figures. The fatigue data in LWR environments indicate a significant decrease in fatigue life of carbon and low-alloy steels when four key threshold conditions are satisfied simultaneously, viz., applied strain range, service temperature, and DO in the water are above a minimum threshold level, and the loading strain rate is below a threshold value. The S content of the steel is also an important parameter for environmental effects on fatigue life. Although the microstructures and cyclic-hardening behavior of carbon steels and low-alloy steels are significantly different, environmental degradation of fatigue life of these steels is identical. For both steels, environmental effects on fatigue life are moderate (i.e., it is a factor of ≈ 2 lower) if any one of the key threshold conditions is not satisfied.

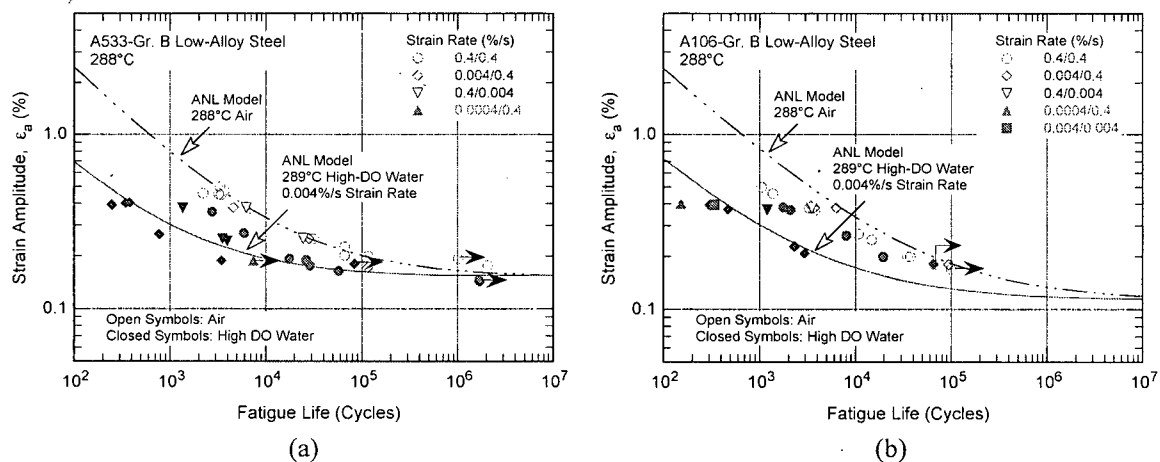


Figure 11. Strain amplitude vs. fatigue life data for (a) A533-Gr B and (b) A106-Gr B steels in air and high-dissolved-oxygen water at 288°C (Ref. 4).

The existing fatigue data indicate that a slow strain rate applied during the tensile-loading cycle is primarily responsible for environmentally assisted reduction in fatigue life of these steels.⁴ The mechanism of environmentally assisted reduction in fatigue life of carbon and low-alloy steels has been termed strain-induced corrosion cracking (SICC).^{48,55,56} A slow strain rate applied during both the tensile-load and compressive-load portion of the cycle (i.e., slow/slow strain rate test) does not further decrease the fatigue life, e.g., see solid diamonds and square in Fig. 11b for A106-Gr B carbon steel. Limited data from fast/slow tests indicate that a slow strain rate during the compressive load cycle also decreases fatigue life. However, the decrease in life is relatively small; for fast/slow strain rate tests, the major contribution of environment most likely occurs during slow compressive loading near peak tensile load. For example, the fatigue life of A533-Gr B low-alloy steel at 288°C, 0.7 ppm DO, and $\approx 0.5\%$ strain range decreased by factors of 5, 8, and 35 for the fast/fast, fast/slow, and slow/fast tests, respectively, i.e., see solid circles, diamonds, and inverted triangles in Fig. 11a. Similar results have been observed for A333-Gr 6 carbon steel;¹⁷ relative to the fast/fast test, fatigue life for slow/fast and fast/slow tests at 288°C, 8 ppm DO, and 1.2% strain range decreased by factors of 7.4 and 3.4, respectively.

The environmental effects on the fatigue life of carbon and low-alloy steels are consistent with the slip oxidation/dissolution mechanism for crack propagation.^{102,103} A critical concentration of sulfide

(S²⁻) or hydrosulfide (HS⁻) ions, which is produced by the dissolution of sulfide inclusions in the steel, is required at the crack tip for environmental effects to occur. The requirements of this mechanism are that a protective oxide film is thermodynamically stable to ensure that the crack will propagate with a high aspect ratio without degrading into a blunt pit, and that a strain increment occurs to rupture that oxide film and thereby expose the underlying matrix to the environment. Once the passive oxide film is ruptured, crack extension is controlled by dissolution of freshly exposed surface and by the oxidation characteristics. The effect of the environment increases with decreasing strain rate. The mechanism assumes that environmental effects do not occur during the compressive load cycle, because during that period water does not have access to the crack tip.

A model for the initiation or cessation of environmentally assisted cracking (EAC) of these steels in low-DO PWR environments has also been proposed.¹⁰⁴ Initiation of EAC requires a critical concentration of sulfide ions at the crack tip, which is supplied with the sulfide ions as the advancing crack intersects the sulfide inclusions, and the inclusions dissolve in the high-temperature water. Sulfide ions are removed from the crack tip by one or more of the following processes: (a) diffusion due to the concentration gradient, (b) ion transport due to differences in the electrochemical potential (ECP), and (c) fluid flow induced within the crack due to flow of coolant outside the crack. Thus, environmentally enhanced CGRs are controlled by the synergistic effects of S content, environmental conditions, and flow rate. The EAC initiation/cessation model has been used to determine the minimum crack extension and CGRs that are required to maintain the critical sulfide ion concentration at the crack tip and sustained environmental enhancement of growth rates.

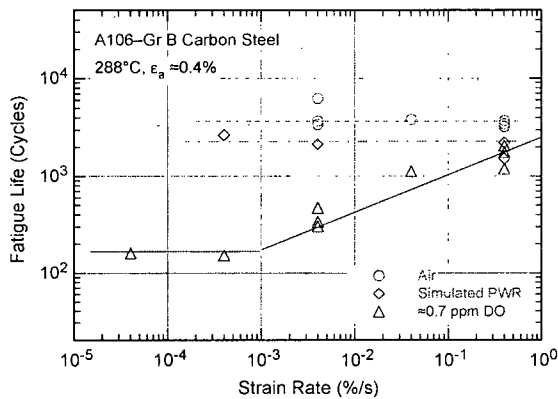
- *A LWR environment has a significant effect on the fatigue life of carbon and low-alloy steels; such effects are not considered in the current Code design curve. Environmental effects may be incorporated into the Code fatigue evaluation using the F_{en} approach described in Section 4.2.13.*

4.2.2 Strain Rate

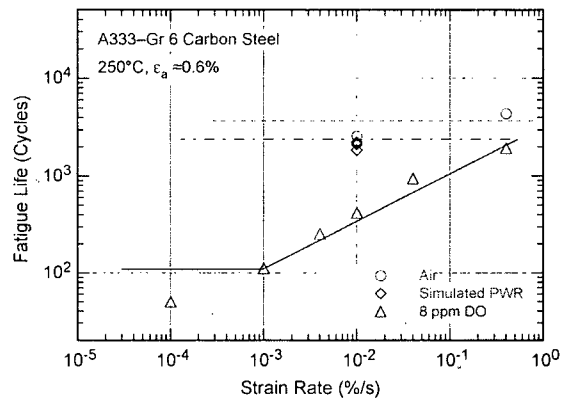
The effects of strain rate on fatigue life of carbon and low-alloy steels in LWR environments are significant when other key threshold conditions, e.g., strain amplitude, temperature, and DO content, are satisfied. When any one of the threshold conditions is not satisfied, e.g., low-DO PWR environment or temperature <150°C, the effects of strain rate are consistent with those observed in air:

When all threshold conditions are satisfied, the fatigue life of carbon and low-alloy steels decreases logarithmically with decreasing strain rate below 1%/s. The fatigue lives of A106-Gr B and A333-Gr 6 carbon steels and A533-Gr B low-alloy steel^{4,17} are plotted as a function of strain rate in Fig. 12. Only a moderate decrease in fatigue life is observed in simulated (low-DO) PWR water, e.g., at DO levels of ≤0.05 ppm. For the heats of A106-Gr B carbon steel and A533-Gr B low-alloy steel, the effect of strain rate on fatigue life saturates at ≈0.001%/s strain rate. Although the data for A333-Gr 6 carbon steel at 250°C and 8 ppm DO do not show an apparent saturation at ≈0.001%/s strain rate, the results are comparable to those for the other two steels.

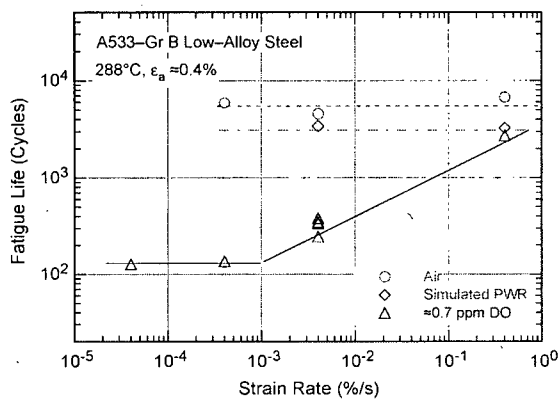
- *In LWR environments, the effect of strain rate on the fatigue life of carbon and low-alloy steels is explicitly considered in F_{en} given in Eqs. 27 and 28 (Section 4.2.13). Also, guidance is provided for defining the strain rate for a specific stress cycle or load set pair.*



(a)



(b)



(c)

Figure 12.
Dependence of fatigue life of carbon and low-alloy steels on strain rate (Refs. 4, 17).

4.2.3 Strain Amplitude

A minimum threshold strain range is required for environmentally assisted decrease in fatigue life, i.e., the LWR coolant environments have no effect on the fatigue life of these steels at strain ranges below the threshold value. The fatigue lives of A533-Gr B and A106-Gr B steels in high-DO water at 288°C and various strain rates⁴ are shown in Fig. 11. Fatigue tests at low strain amplitudes are rather limited. Because environmental effects on fatigue life increase with decreasing strain rate, fatigue tests at low strain amplitudes and strain rates that would result in significant environmental effects are restrictively time consuming. For the limited data that are available, the threshold strain amplitude (one-half the threshold strain range) appears to be slightly above the fatigue limit of these steels.

Exploratory fatigue tests with changing strain rate have been conducted to determine the threshold strain range beyond which environmental effects are significant during a fatigue cycle. The tests are performed with waveforms in which the slow strain rate is applied during only a fraction of the tensile loading cycle.^{4,18} The results for A106-Gr B steel tested in air and low- and high-DO environments at 288°C and $\approx 0.78\%$ strain range are summarized in Fig. 13. The waveforms consist of segments of loading and unloading at fast and slow strain rates. The variation in fatigue life of two heats of carbon steel and one heat of low-alloy steel^{4,18} is plotted as a function of the fraction of loading strain at slow strain rate in Fig. 14. Open symbols indicate tests where the slow portions occurred near the maximum tensile strain, and closed symbols indicate tests where the slow portions occurred near the maximum compressive strain. In Fig. 14, if the relative damage was the same at all strain levels, fatigue life should decrease linearly from A to C along the chain-dot line. Instead, the results indicate that during a strain

cycle, the relative damage due to slow strain rate occurs only after the strain level exceeds a threshold value. The threshold strain range for these steels is 0.32–0.36%.

Loading histories with slow strain rate applied near the maximum tensile strain (i.e., waveforms C, D, E, or F in Fig. 13) show continuous decreases in life (line AB in Fig. 14) and then saturation when a portion of the slow strain rate occurs at strain levels below the threshold value (line BC in Fig. 14). In contrast, loading histories with slow strain rate applied near maximum compressive strain (i.e., waveforms G, H, or I in Fig. 13) produce no damage (line AD in Fig. 14a) until the fraction of the strain is sufficiently large that slow strain rates are occurring for strain levels greater than the threshold value. However, tests with such loading histories often show lower fatigue lives than the predicted values, e.g., solid inverted triangle or solid diamond in Fig. 14a.

Similar strain–rate–change tests on austenitic SSs in PWR environments have also showed the existence of a strain threshold below which the material is insensitive to environmental effects.²⁹ The threshold strain range $\Delta\epsilon_{th}$ appears to be independent of material type (weld metal or base metal) and temperature in the range of 250–325°C, but it tends to decrease as the strain range is decreased. The threshold strain range has been expressed in terms of the applied strain range $\Delta\epsilon$ by the equation

$$\Delta\epsilon_{th}/\Delta\epsilon = -0.22 \Delta\epsilon + 0.65. \quad (19)$$

This expression may also be used for carbon and low-alloy steels.

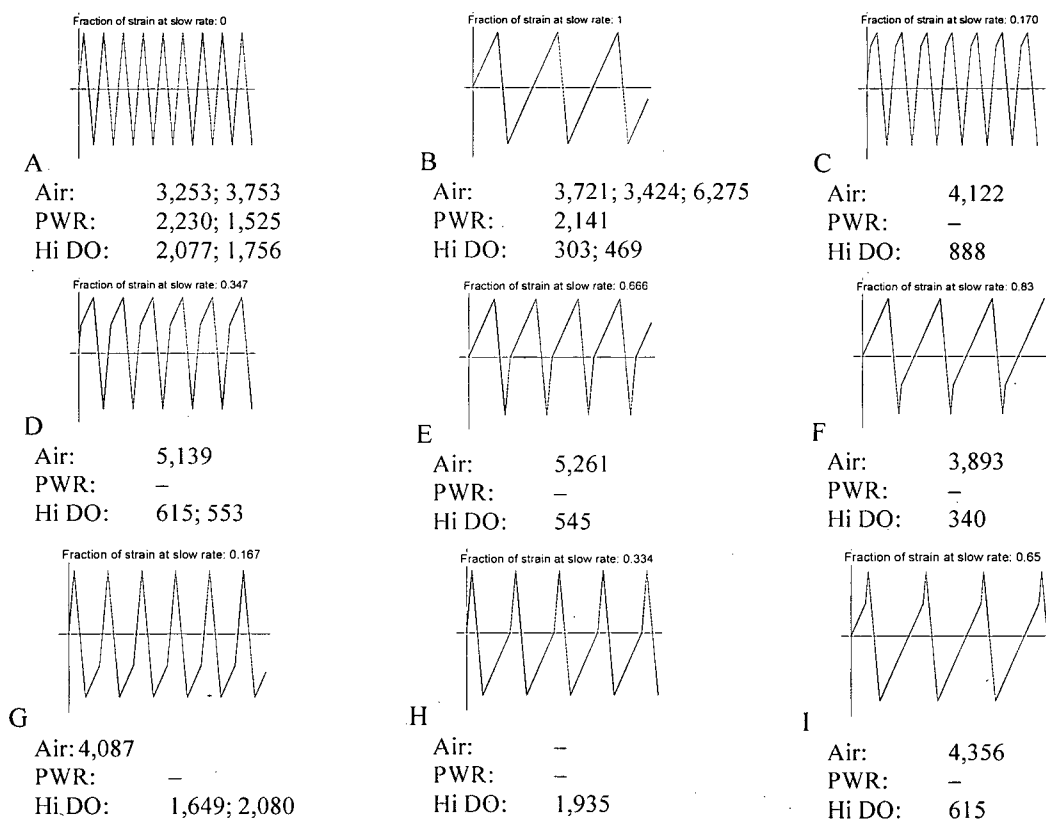
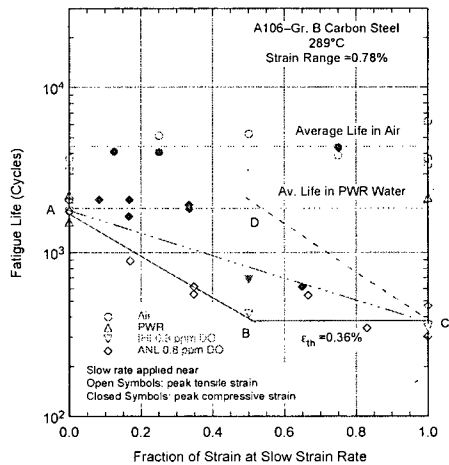
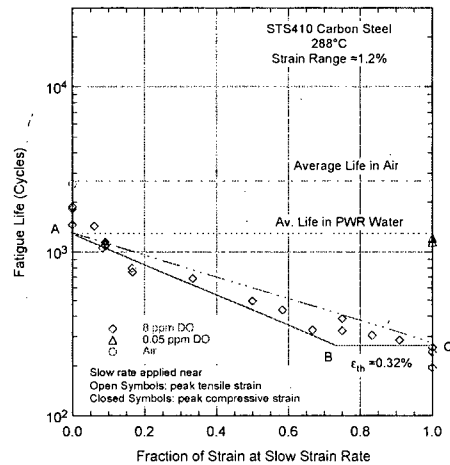


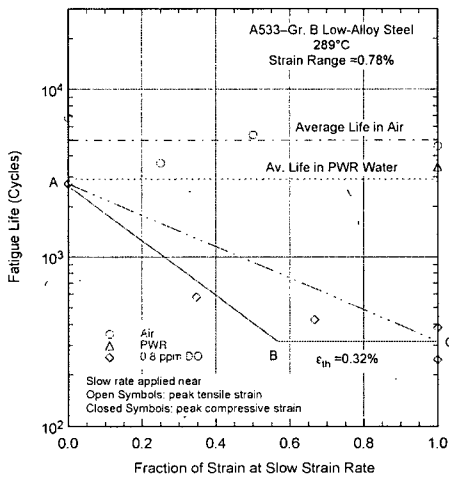
Figure 13. Fatigue life of A106-Gr B carbon steel at 288°C and 0.75% strain range in air and water environments under different loading waveforms (Ref. 4).



(a)



(b)



(c)

Figure 14.

Fatigue life of carbon and low-alloy steels tested with loading waveforms where slow strain rate is applied during a fraction of tensile loading cycle (Refs. 4, 18).

The modified rate approach, described in Section 4.2.14, has been used to predict the results from tests on four heats of carbon and low-alloy steels conducted with changing strain rate in low- and high-DO water at 289°C.¹⁸ The results indicate that the modified rate approach, without the consideration of a strain threshold, gives the best estimates of life (Fig. 15). Most of the scatter in the data is due to heat-to-heat variation rather than any inaccuracy in estimation of fatigue life; for the same loading conditions, the fatigue lives of Heat #2 of STS410 steel are a factor of ≈ 5 lower than those of Heat #1. The estimated fatigue lives are within a factor of 3 of the experimental values.

- In LWR coolant environments, the procedure for calculating F_{en} , defined in Eqs. 27 and 28 (Section 4.2.13), includes a threshold strain range below which environment has no effect on fatigue life, i.e., $F_{en} = 1$. However, while using the damage rate approach to determine F_{en} for a stress cycle or load set pair, including a threshold strain (Eq. 31 in Section 4.2.14) may yield nonconservative estimates of life.

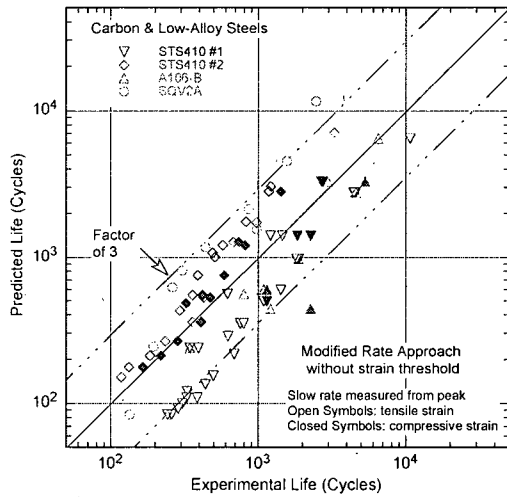


Figure 15. Experimental values of fatigue life and those predicted from the modified rate approach without consideration of a threshold strain (Ref. 18).

4.2.4 Temperature

The change in fatigue life of two heats of A333-Gr 6 carbon steel^{12,13,16} with test temperature at different levels of DO is shown in Fig. 16. Other parameters, e.g., strain amplitude and strain rate, were kept constant; the applied strain amplitude was above and strain rate was below the critical threshold. In air, the two heats have a fatigue life of ≈ 3300 cycles. The results indicate a threshold temperature of 150°C , above which environment decreases fatigue life if DO in water is also above the critical level. In the temperature range of $150\text{--}320^\circ\text{C}$, the logarithm of fatigue life decreases linearly with temperature; the decrease in life is greater at high temperatures and DO levels. Only a moderate decrease in fatigue life is observed in water at temperatures below the threshold value of 150°C or at DO levels ≤ 0.05 ppm. Under these conditions, fatigue life in water is a factor of ≈ 2 lower than in air; Fig. 16 shows an average life of ≈ 2000 cycles for the heat with 0.015 wt.% S, and ≈ 1200 cycles for the 0.012 wt.% S steel.

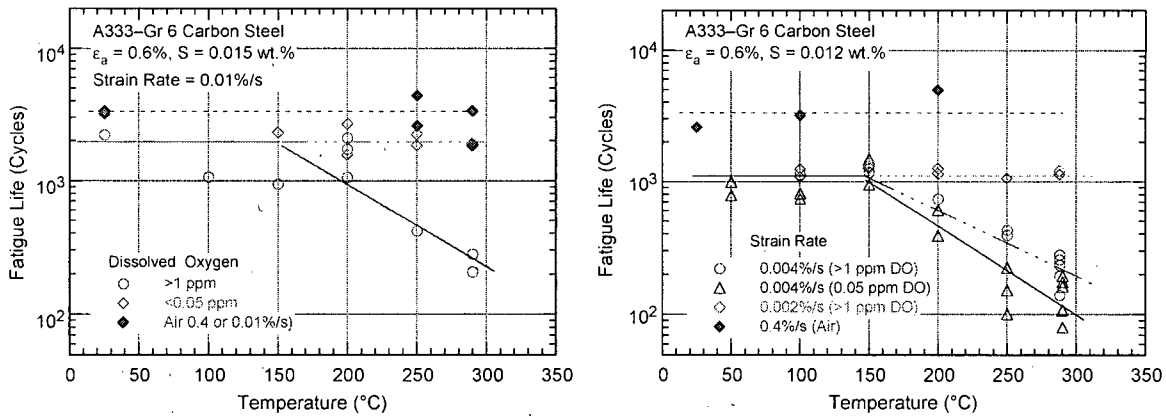


Figure 16. Change in fatigue life of A333-Gr 6 carbon steel with temperature and DO.

An artificial neural network (ANN) has also been used to find patterns and identify the threshold temperature below which environmental effects are moderate.¹⁰⁵ The main benefits of the ANN approach are that estimates of life are based purely on the data and not on preconceptions, and by learning trends, the network can interpolate effects where data are not present. The factors that affect fatigue life can have synergistic effects on one another. A neural network can detect and utilize these effects in its predictions. A neural network, consisting of two hidden layers with the first containing ten nodes and the second containing six nodes, was trained six times; each training was based on the same data set, but the order in which the data were presented to the ANN for training was varied, and the initial ANN weights were randomized to guard against overtraining and to ensure that the network did not arrive at a solution that was a local minimum. The effect of temperature on the fatigue life of carbon steels and low-alloy steels estimated from ANN is shown in Fig. 17 as dashed or dotted lines. The solid line represents estimates based on the ANL model, and the open circles represent the experimental data. The results indicate that at high strain rate (0.4%/s), fatigue life is relatively insensitive to temperature. At low strain rate (0.004%/s), fatigue life decreases with an increase in temperature beyond a threshold value of $\approx 150^\circ\text{C}$. The precision of the data indicates that this trend is present in the data used to train the ANN.

Nearly all of the fatigue ϵ -N data have been obtained under loading histories with constant strain rate, temperature, and strain amplitude. The actual loading histories encountered during service of nuclear power plants involve variable loading and environmental conditions. Fatigue tests have been conducted in Japan on tube specimens (1- or 3-mm wall thickness) of A333-Gr 6 carbon steel in oxygenated water under combined mechanical and thermal cycling.¹⁵ Triangular waveforms were used for both strain and temperature cycling. Two sequences were selected for temperature cycling (Fig. 18):

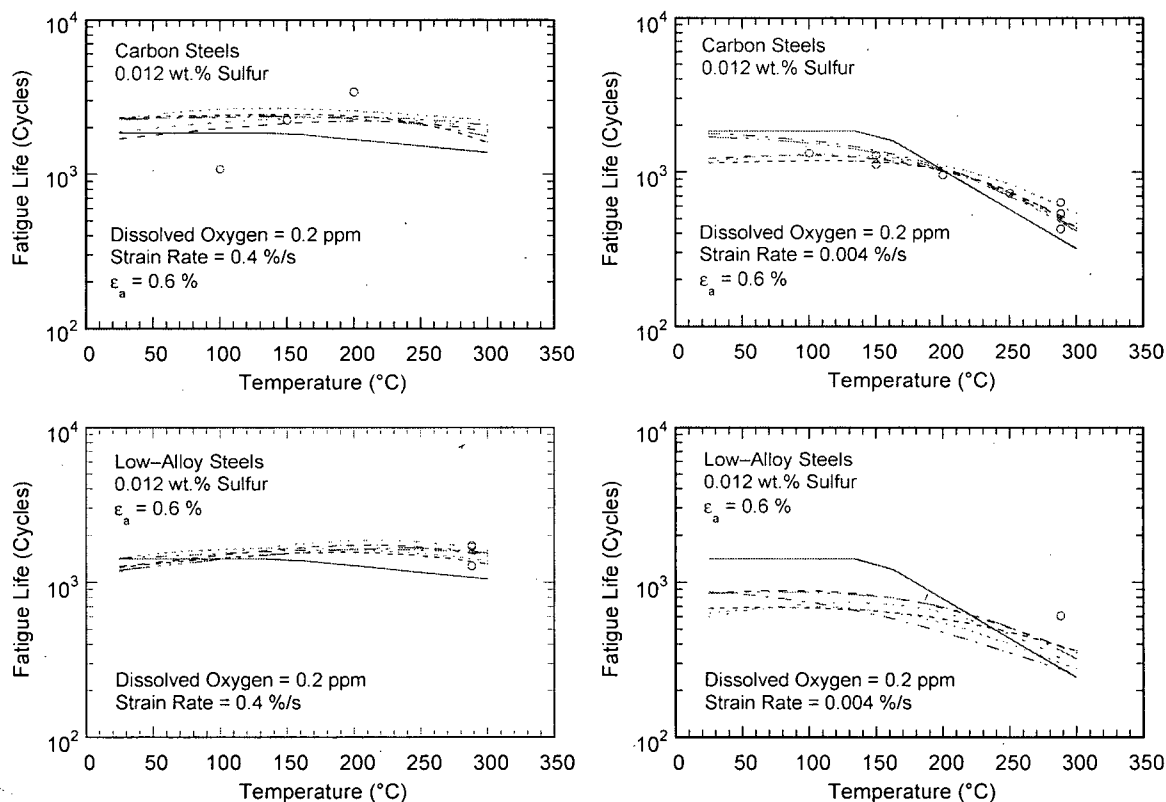


Figure 17. Dependence of fatigue life on temperature for carbon and low-alloy steels in water.

an in-phase sequence in which temperature cycling was synchronized with mechanical strain cycling, and another sequence in which temperature and strain were out of phase, i.e., maximum temperature occurred at minimum strain level and vice versa. Three temperature ranges, 50–290°C, 50–200°C, and 200–290°C, were selected for the tests. The results are shown in Fig. 19; an average temperature is used to plot the thermal cycling tests. Because environmental effects on fatigue life are moderate and independent of temperature below 150°C, the temperature for tests cycled in the range of 50–290°C or 50–200°C was determined from the average of 150°C and the maximum temperature. The results in Fig. 19 indicate that load cycles involving variable temperature conditions may be represented by an average temperature, e.g., the fatigue lives from variable-temperature tests are comparable with those from constant-temperature tests.

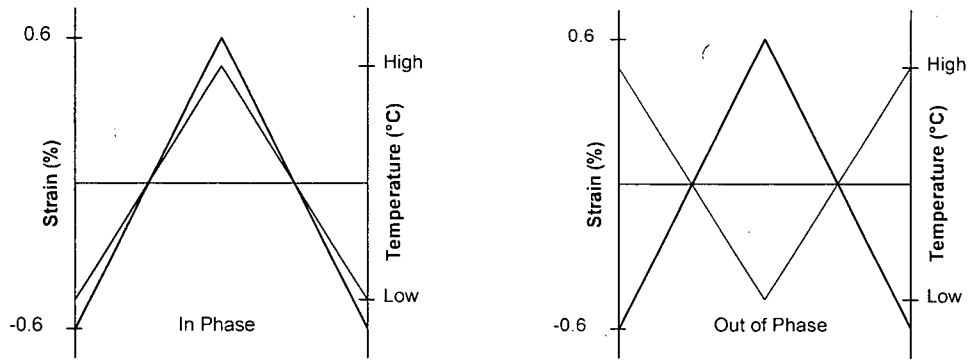


Figure 18. Waveforms for change in temperature during exploratory fatigue tests.

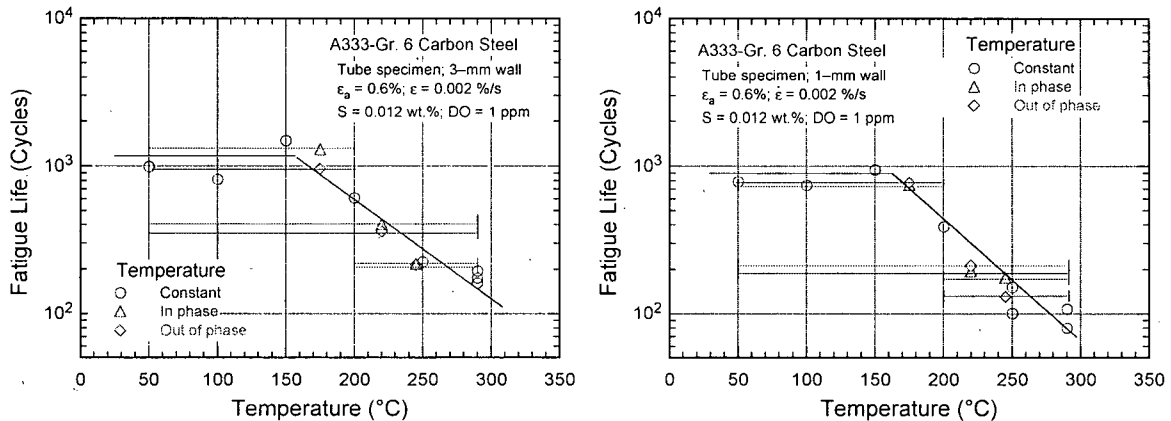


Figure 19. Fatigue life of A333-Gr 6 carbon steel tube specimens under varying temperature, indicated by horizontal bars.

However, the nearly identical fatigue lives of the in-phase and out-of-phase tests are somewhat surprising. If we consider that the tensile-load cycle is primarily responsible for environmentally assisted reduction in fatigue life, and that the applied strain and temperature must be above a minimum threshold value for environmental effects to occur, then fatigue life for the out-of-phase tests should be longer than for the in-phase tests, because applied strains above the threshold strain occur at temperatures above 150°C for in-phase tests, whereas they occur at temperatures below 150°C for the out-of-phase tests. If environmental effects on fatigue life are considered to be minimal below the threshold values of 150°C for temperature and <0.25% for strain range, the average temperatures for the out-of-phase tests at

50–290°C, 50–200°C, and 200–290°C should be 195, 160, and 236°C, respectively, instead of 220, 175, and 245°C, as plotted in Fig. 19. Thus, the fatigue lives of out-of-phase tests should be at least 50% higher than those of the in-phase tests. Most likely, difference in the cyclic hardening behavior of the material is affecting fatigue life of the out-of-phase tests.

- In LWR environments, the effect of temperature on the fatigue life of carbon and low-alloy steels is explicitly considered in F_{en} defined in Eqs. 27 and 28 (Section 4.2.13). Also, an average temperature may be used to calculate F_{en} for a specific stress cycle or load set pair.

4.2.5 Dissolved Oxygen

The dependence of fatigue life of carbon steel on DO content in water^{12,13,16} is shown in Fig. 20. The test temperature, applied strain amplitude, and S content in steel were above, and strain rate was below, the critical threshold value. The results indicate a minimum DO level of 0.04 ppm above which environment decreases the fatigue life of the steel. The effect of DO content on fatigue life saturates at 0.5 ppm, i.e., increases in DO levels above 0.5 ppm do not cause further decreases in life. In Fig. 20, for DO levels between 0.04 and 0.5 ppm, fatigue life appears to decrease logarithmically with DO. Estimates of fatigue life from a trained ANN also show a similar effect of DO on the fatigue life of carbon steels and low-alloy steels.

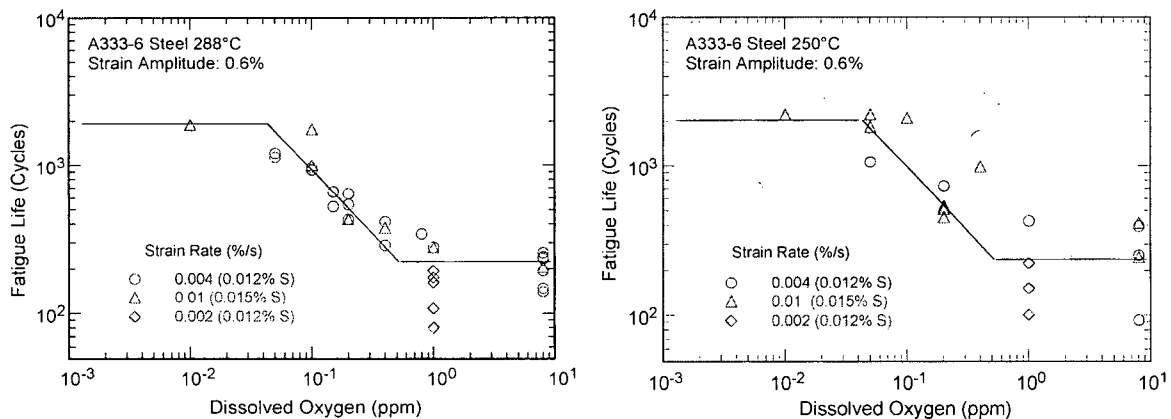


Figure 20. Dependence on DO of fatigue life of carbon steel in high-purity water.

Environmental effects on the fatigue life of carbon and low-alloy steels are minimal at DO levels below 0.04 ppm, i.e., in low-DO PWR or hydrogen-chemistry BWR environments. In contrast, environmental enhancement of CGRs has been observed in low-alloy steels even in low-DO water.¹⁰⁴ This apparent inconsistency of fatigue ϵ -N data with the CGR data may be attributed to differences in the environment at the crack tip. The initiation of environmentally assisted enhancement of CGRs in low-alloy steels requires a critical level of sulfides at the crack tip.¹⁰⁴ The development of this critical sulfide concentration requires a minimum crack extension of 0.33 mm and CGRs in the range of 1.3×10^{-4} to 4.2×10^{-7} mm/s. These conditions are not achieved under typical ϵ -N tests. Thus, environmental effects on fatigue life are expected to be insignificant in low-DO environments.

- In LWR environments, effect of DO level on the fatigue life of carbon and low-alloy steels is explicitly considered in F_{en} defined in Eqs. 27 and 28 (Section 4.2.13).

4.2.6 Water Conductivity

In most studies the DO level in water has generally been considered the key environmental parameter that affects the fatigue life of materials in LWR environments. Studies on the effect of the concentration of anionic impurities in water (expressed as the overall conductivity of water), are somewhat limited. The limited data indicate that the fatigue life of WB36 low-alloy steel at 177°C in water with ≈ 8 ppm DO decreased by a factor of ≈ 6 when the conductivity of water was increased from 0.06 to 0.5 $\mu\text{S}/\text{cm}$.^{48,106} A similar behavior has also been observed in another study of the effect of conductivity on the initiation of short cracks.¹⁰⁷

- Normally, plants are unlikely to accumulate many fatigue cycles under off-normal conditions. Thus, effects of water conductivity on fatigue life have not been considered in the determination of F_{en} .

4.2.7 Sulfur Content in Steel

It is well known that S content and morphology are the most important material-related parameters that determine susceptibility of low-alloy steels to environmentally enhanced fatigue CGRs.¹⁰⁸⁻¹¹¹ A critical concentration of S^{2-} or HS^- ions is required at the crack tip for environmental effects to occur. Both the corrosion fatigue CGRs and threshold stress intensity factor ΔK_{th} are a function of the S content in the range 0.003–0.019 wt.%.¹¹⁰ The probability of environmental enhancement of fatigue CGRs in precracked specimens of low-alloy steels appears to diminish markedly for S contents < 0.005 wt.%.

The fatigue ϵ -N data for low-alloy steels also indicate a dependence of fatigue life on S content. When all the threshold conditions are satisfied, environmental effects on the fatigue life increase with increased S content. The fatigue lives of A508-C1 3 steel with 0.003 wt.% S and A533-Gr B steel with 0.010 wt.% S are plotted as a function of strain rate in Fig. 21. However, the available data sets are too sparse to establish a functional form for dependence of fatigue life on S content and to define either a threshold for S content below which environmental effects are unimportant or an upper limit above which the effect of S on fatigue life may saturate. A linear dependence of fatigue life on S content has been assumed in correlations for estimating fatigue life of carbon steels and low-alloy steels in LWR environments.^{4,79} The limited data suggest that environmental effects on fatigue life saturate at S contents above 0.015 wt.%.⁴

The existing fatigue ϵ -N data also indicate significant reductions in fatigue life of some heats of carbon steel with S levels as low as 0.002 wt.%. The fatigue lives of several heats of A333-Gr 6 carbon

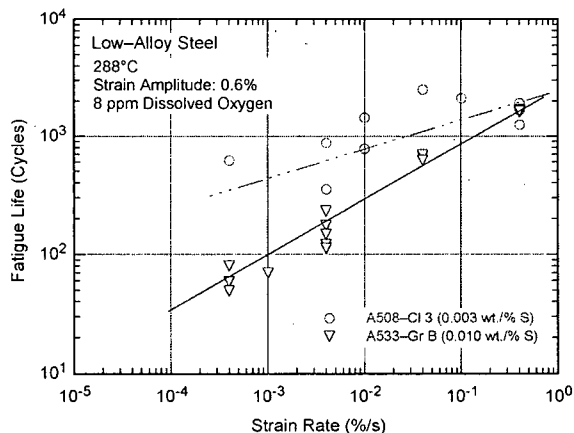


Figure 21.
Effect of strain rate on fatigue life of low-alloy steels with different S contents (JNUFAD database and Ref. 4).

steel with S contents of 0.002–0.015 wt.% in high-DO water at 288°C and 0.6% strain amplitude are plotted as a function of strain rate in Fig. 22.⁴ Environmental effects on the fatigue life of these steels seem to be independent of S content in the range of 0.002–0.015 wt.%. However, these tests were conducted in air-saturated water (≈ 8 ppm DO). The fatigue life of carbon steels seems to be relatively insensitive to S content in very high DO water, e.g., greater than 1 ppm DO; under these conditions, the effect of DO dominates fatigue life. In other words, the saturation DO level of 0.5 ppm most likely is for medium- and high-S steels (i.e., steels with ≥ 0.005 wt.% S); it may be higher for low-S steels.

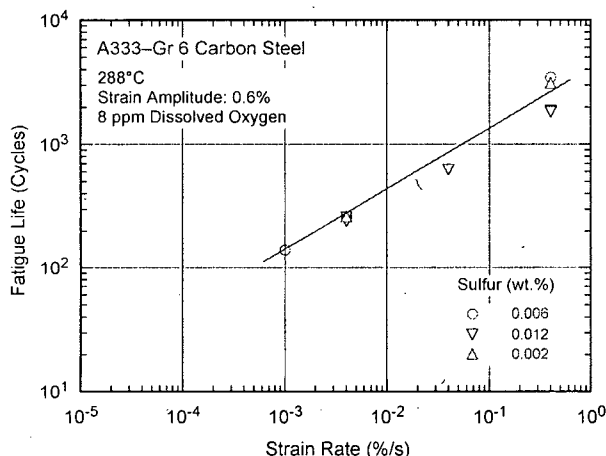


Figure 22. Effect of strain rate on the fatigue life of A333-Gr 6 carbon steels with different S contents.

- In LWR environments, the effect of S content on the fatigue life of carbon and low-alloy steels is explicitly considered in F_{en} , defined in Eqs. 27 and 28 (Section 4.2.13). However, evaluation of experimental data on low-S steels (< 0.005 wt.% S) in water with ≥ 1 ppm DO should be done with caution; the effect of S may be larger than that predicted by Eqs. 27 and 28.

4.2.8 Tensile Hold Period

Fatigue tests conducted using trapezoidal waveforms indicate that a hold period at peak tensile strain decreases the fatigue life of carbon steels in high-DO water at 289°C.^{4,18} However, a detailed examination of the data indicated that these results are either due to limitations of the test procedure or caused by a frequency effect. Loading waveforms, hysteresis loops, and fatigue lives for the tests on A106-Gr B carbon steel in air and water environments are shown in Fig. 23.⁴ A 300-s hold period is sufficient to reduce fatigue life by $\approx 50\%$ (≈ 2000 cycles without and ≈ 1000 cycles with a hold period); a longer hold period of 1800 s results in only slightly lower fatigue life than that with a 300-s hold period. For example, two 300-s hold tests at 288°C and $\approx 0.78\%$ strain range in oxygenated water with 0.7 ppm DO gave fatigue lives of 1,007 and 1,092 cycles; life in a 1800-s hold test was 840 cycles. These tests were conducted in stroke-control mode and are somewhat different from the conventional hold-time test in strain-control mode, where the total strain in the sample is held constant during the hold period. However, a portion of the elastic strain is converted to plastic strain because of stress relaxation. In a stroke-control test, there is an additional plastic strain in the sample due to relaxation of elastic strain from the load train (Fig. 23). Consequently, significant strain changes occur during the hold period; the measured plastic strains during the hold period were $\approx 0.028\%$ from relaxation of the gauge and 0.05–0.06% from relaxation of the load train. These conditions resulted in strain rates of 0.005–0.02%/s during the hold period. The reduction in life may be attributed to the slow strain rates during the hold period. Also, frequency effects may decrease the fatigue life of hold time tests, e.g., in air, the fatigue life of stroke-control test with hold period is $\approx 50\%$ lower than that without the hold period.

Hold-time tests have also been conducted on STS410 carbon steel at 289°C in water with 1 ppm DO. The results are given in Table 5.¹⁸ The most significant observation is that a reduction in fatigue life occurs only for those hold-time tests that were conducted at fast strain rates, e.g., at 0.4%/s. At lower strain rates, fatigue life is essentially the same for the tests with or without hold periods. Based on these results, Higuchi et al.¹⁸ conclude that the procedures for calculating F_{en} need not be revised. Also, as discussed in Section 4.2.11, the differences in fatigue life of these tests are within the data scatter for the fatigue $\epsilon-N$ data in LWR environments.

- The existing data do not demonstrate that hold periods at peak tensile strain affect the fatigue life of carbon and low-alloy steels in LWR environments. Thus, any revision/modification of the method to determine F_{en} is not warranted.

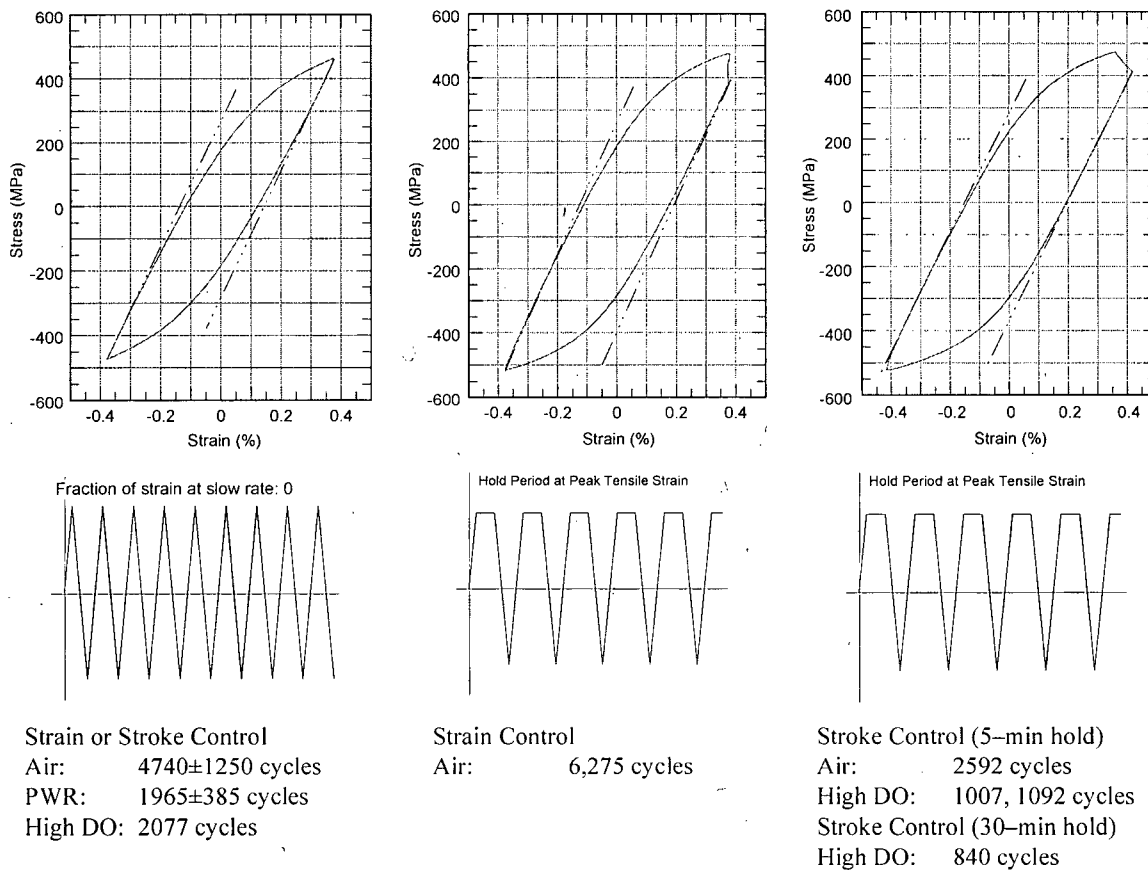


Figure 23. Fatigue life of A106-Gr B steel in air and water environments at 288°C, 0.78% strain range, and hold period at peak tensile strain (Ref. 4). Hysteresis loops are for tests in air.

Table 5. Fatigue data for STS410 steel at 289°C in water with 1 ppm DO and trapezoidal waveform.

Strain Ampl. (%)	Hold Period at Peak Tensile Strain (s)	Tensile / Compressive Strain Rate (%/s)			
		0.4 / 0.4	0.04 / 0.4	0.01 / 0.4	0.004 / 0.4
0.6	0	489	240	-	118
0.6	60	328, 405	238	-	138
0.6	600	173, 217	-	-	-
0.3	0	3270	1290	737	508
0.3	60	1840, 1760	1495	875	587
0.3	600	436, 625	-	-	-

4.2.9 Flow Rate

Nearly all of the fatigue ϵ - N data for LWR environments have been obtained at very low water flow rates. Recent data indicate that, under the environmental conditions typical of operating BWRs, environmental effects on the fatigue life of carbon steels are at least a factor of 2 lower at high flow rates (7 m/s) than at 0.3 m/s or lower.^{19,20,44} The beneficial effects of increased flow rate are greater for high-S steels and at low strain rates.^{19,20} The effect of water flow rate on the fatigue life of high-S (0.016 wt.%) A333-Gr 6 carbon steel in high-purity water at 289°C is shown in Fig. 24. At 0.3% strain amplitude, 0.01%/s strain rate, and all DO levels, fatigue life is increased by a factor of ≈ 2 when the flow rate is increased from $\approx 10^{-5}$ to 7 m/s. At 0.6% strain amplitude and 0.001%/s strain rate, fatigue life is increased by a factor of ≈ 6 in water with 0.2 ppm DO and by a factor of ≈ 3 in water with 1.0 or 0.05 ppm DO. Under similar loading conditions, i.e., 0.6% strain amplitude and 0.001%/s strain rate, a low-S (0.008 wt.%) heat of A333-Gr 6 carbon steel showed only a factor of ≈ 2 increase in fatigue life with increased flow rates. Note that the beneficial effects of flow rate are determined from a single test on each material at very low flow rates; data scatter in LWR environments is typically a factor of ≈ 2 .

A factor of 2 increase in fatigue life was observed (Fig. 25) at KWU during component tests with 180° bends of carbon steel tubing (0.025 wt.% S) when internal flow rates of up to 0.6 m/s were established.⁴⁴ The tests were conducted at 240°C in water that contained 0.2 ppm DO.

- Because of the uncertainties in the flow conditions at or near the locations of crack initiation, the beneficial effect of flow rate on the fatigue life is presently not included in fatigue evaluations.

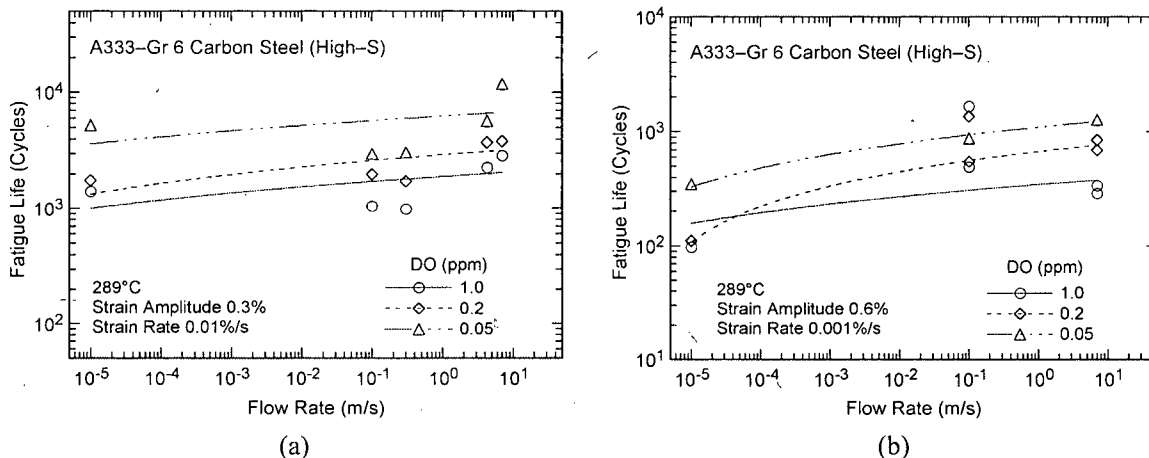


Figure 24. Effect of water flow rate on fatigue life of A333-Gr 6 carbon steel at 289°C and strain amplitude and strain rates of (a) 0.3% and 0.01%/s and (b) 0.6% and 0.001%/s.

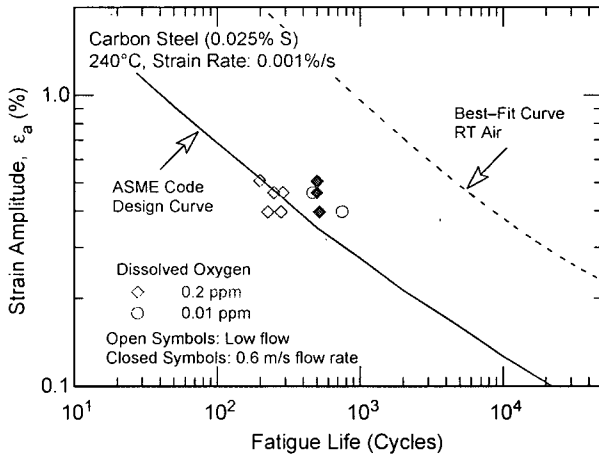


Figure 25. Effect of flow rate on low-cycle fatigue of carbon steel tube bends in high-purity water at 240°C (Ref. 44). RT = room temperature.

4.2.10 Surface Finish

Fatigue testing has been conducted on specimens of carbon and low-alloy steels that were intentionally roughened in a lathe, under controlled conditions, with 50-grit sandpaper to produce circumferential scratches with an average roughness of 1.2 μm and R_q of 1.6 μm (≈ 62 micro in.).³⁹ The results for A106-Gr B carbon steel and A533-Gr B low-alloy steel are shown in Fig. 26. In air, the fatigue life of rough A106-Gr B specimens is a factor of 3 lower than that of smooth specimens, and, in high-DO water, it is the same as that of smooth specimens. In low-DO water, the fatigue life of the roughened A106-Gr B specimen is slightly lower than that of smooth specimens. The effect of surface roughness on the fatigue life of A533-Gr B low-alloy steel is similar to that for A106-Gr B carbon steel; in high-DO water, the fatigue lives of both rough and smooth specimens are the same. The results in water are consistent with a mechanism of growth by a slip oxidation/dissolution process, which seems unlikely to be affected by surface finish. Because environmental effects are moderate in low-DO water, surface roughness would be expected to influence fatigue life.

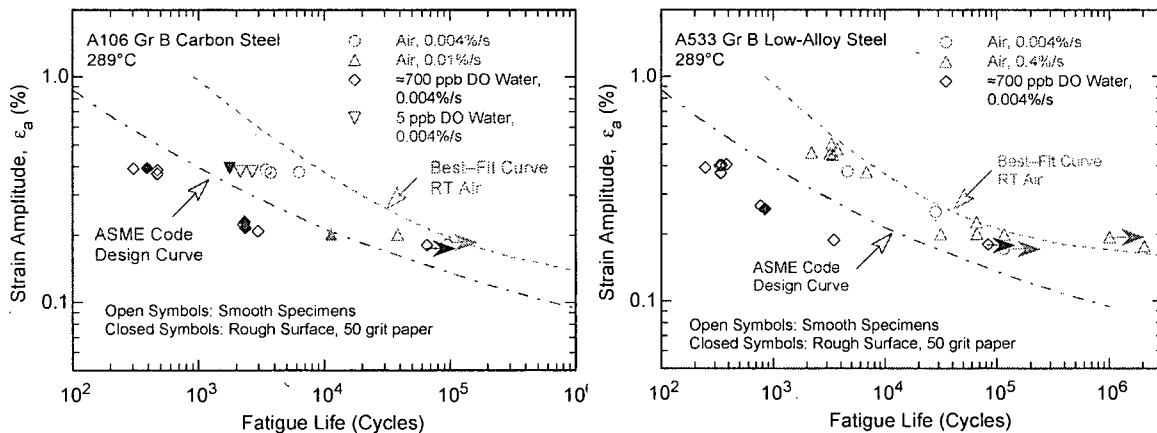


Figure 26. Effect of surface roughness on fatigue life of (a) A106-Gr B carbon steel and (b) A533 low-alloy steel in air and high-purity water at 289°C.

- The effect of surface finish is not considered in the environmental fatigue correction factor; it is included in the subfactor for "surface finish and environment" that is applied to the mean data curve to develop the Code fatigue design curve in air.

4.2.11 Heat-to-Heat Variability

The effect of material variability and data scatter on the fatigue life of carbon and low-alloy steels has also been evaluated for LWR environments. The fatigue behavior of each of the heats or loading conditions is characterized by the value of the constant A in the ANL models (e.g., Eq. 6). The values of A for the various data sets are ordered, and median ranks are used to estimate the cumulative distribution of A for the population. Results for carbon and low-alloy steels in water environments are shown in Fig. 27. The median value of A in water is 5.951 for carbon steels and 5.747 for low-alloy steels. The results indicate that environmental effects are approximately the same for the various heats of these steels. For example, the cumulative distribution of data sets for specific heats is approximately the same in air and water environments. The ANL model seem to overestimate the effect of environment for a few heats, e.g., the ranking for A533-Gr B heat 5 is ≈ 42 percentile in air and ≈ 95 percentile in water, and for A106-Gr B heat A, it is ≈ 17 percentile in air and varies from 2 to 60 percentile in water. Monte Carlo analyses were also performed for the fatigue data in LWR environments.

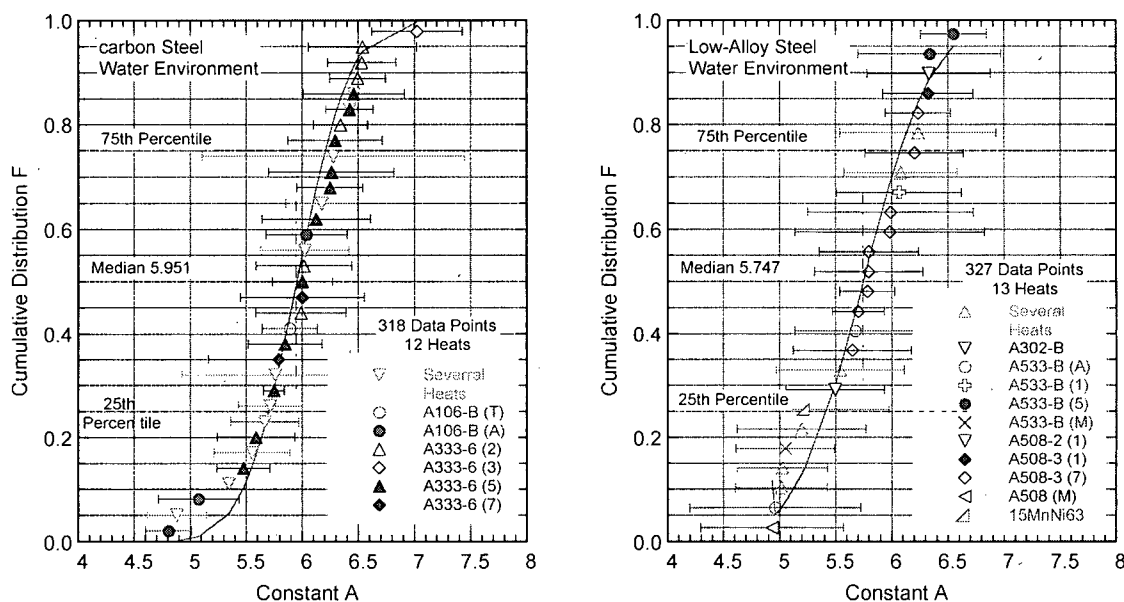


Figure 27. Estimated cumulative distribution of parameter A in the ANL models for fatigue life for heats of carbon and low-alloy steels in LWR environments.

The results for carbon and low-alloy steels in LWR environments are summarized in Tables 6 and 7, respectively, in terms of values for A that provide bounds for the portion of the population and the confidence that is desired in the estimates of the bounds. In LWR environments, the 5th percentile value of parameter A at 95% confidence level is 5.191 for carbon steels and 4.748 for low-alloy steels. From Fig. 27, the median value of A for the sample is 5.951 for carbon steels and 5.747 for low-alloy steels. Thus, the 95/95 value of the margin to account for material variability and data scatter is 2.1 and 2.7 on life for carbon steels and low-alloy steels, respectively. These margins are needed to provide 95% confidence that the resultant life will be greater than that observed for 95% of the materials of interest.

Table 6. Values of parameter A in the ANL fatigue life model for carbon steels in water and the margins on life as a function of confidence level and percentage of population bounded.

Confidence Level	Percentage of Population Bounded (Percentile Distribution of A)				
	95 (5)	90 (10)	75 (25)	67 (33)	50 (50)
	<u>Values of Parameter A</u>				
50	5.333	5.469	5.697	5.786	5.951
75	5.275	5.417	5.652	5.742	5.906
95	5.191	5.342	5.587	5.678	5.840
	<u>Margins on Life</u>				
50	1.9	1.6	1.3	1.2	1.0
75	2.0	1.7	1.3	1.2	1.0
95	2.1	1.8	1.4	1.3	1.1

Table 7. Values of parameter A in the ANL fatigue life model for low-alloy steels in water and the margins on life as a function of confidence level and percentage of population bounded.

Confidence Level	Percentage of Population Bounded (Percentile Distribution of A)				
	95 (5)	90 (10)	75 (25)	67 (33)	50 (50)
	<u>Values of Parameter A</u>				
50	4.950	5.126	5.420	5.534	5.747
75	4.867	5.052	5.355	5.470	5.680
95	4.748	4.944	5.261	5.378	5.585
	<u>Margins on Life</u>				
50	2.2	1.9	1.4	1.2	1.0
75	2.4	2.0	1.5	1.3	1.1
95	2.7	2.2	1.6	1.4	1.2

- *The effect of heat-to-heat variability is not considered in the environmental fatigue correction factor; it is included in the subfactor for "data scatter and material variability" that is applied to the mean data curve to develop the Code fatigue design curve in air.*

4.2.12 Fatigue Life Model

Fatigue-life models for estimating the fatigue lives of carbon and low-alloy steels in LWR environments based on the existing fatigue ϵ -N data have been developed at ANL.^{4,39} The effects of key parameters, such as temperature, strain rate, DO content in water, and S content in the steel, are included in the correlations; the effects of these and other parameters on the fatigue life are discussed below in detail. The functional forms for the effects of strain rate, temperature, DO level in water, and S content in the steel were based on the data trends. For both carbon and low-alloy steels, the model assumes threshold and saturation values of 1.0 and 0.001%/s, respectively, for strain rate; 0.001 and 0.015 wt.%, respectively, for S; and 0.04 and 0.5 ppm, respectively, for DO. It also considers a threshold value of 150°C for temperature.

In the present report these models have been updated based on the analysis presented in Section 4.2.11, e.g., constant A in the models differs from the value reported earlier in NUREG/CR-6583 and -6815. Relative to the earlier model, the fatigue lives predicted by the updated model are $\approx 6\%$ lower for carbon steels and $\approx 2\%$ higher for low-alloy steels. In LWR environments, the fatigue life, N, of carbon steels is represented by

$$\ln(N) = 5.951 - 1.975 \ln(\epsilon_a - 0.113) + 0.101 S^* T^* O^* \dot{\epsilon}^*, \quad (20)$$

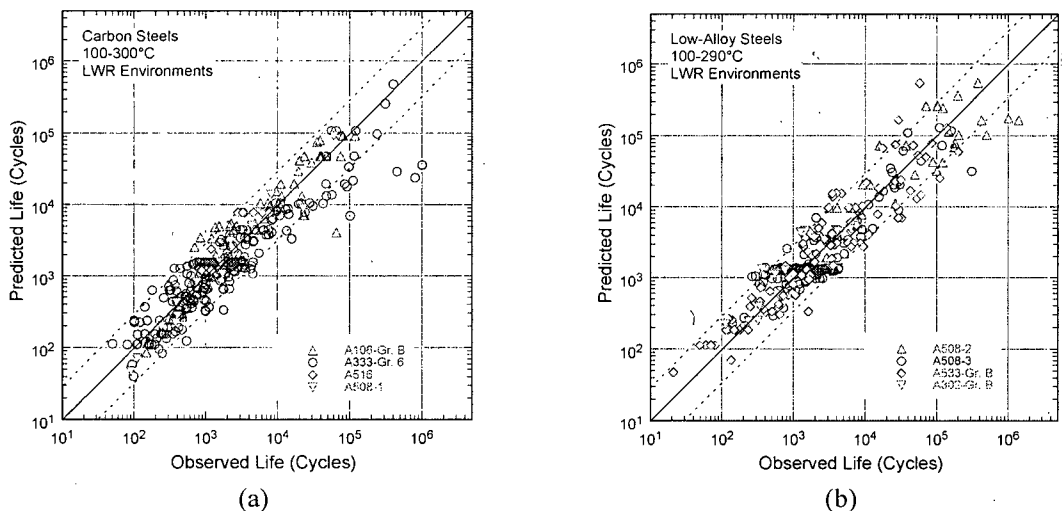


Figure 28. Experimental and predicted fatigue lives of (a) carbon steels and (b) low-alloy steels in LWR environments.

and that of low-alloy steels, by

$$\ln(N) = 5.747 - 1.808 \ln(\epsilon_a - 0.151) + 0.101 S^* T^* O^* \dot{\epsilon}^* \quad (21)$$

where S^* , T^* , O^* , and $\dot{\epsilon}^*$ are transformed S content, temperature, DO level, and strain rate, respectively, defined as:

$$\begin{aligned} S^* &= 0.015 && (\text{DO} > 1.0 \text{ ppm}) \\ S^* &= 0.001 && (\text{DO} \leq 1.0 \text{ ppm and } S \leq 0.001 \text{ wt.}\%) \\ S^* &= S && (\text{DO} \leq 1.0 \text{ ppm and } 0.001 < S \leq 0.015 \text{ wt.}\%) \\ S^* &= 0.015 && (\text{DO} \leq 1.0 \text{ ppm and } S > 0.015 \text{ wt.}\%) \end{aligned} \quad (22)$$

$$\begin{aligned} T^* &= 0 && (T \leq 150^\circ\text{C}) \\ T^* &= T - 150 && (150 < T \leq 350^\circ\text{C}) \end{aligned} \quad (23)$$

$$\begin{aligned} O^* &= 0 && (\text{DO} \leq 0.04 \text{ ppm}) \\ O^* &= \ln(\text{DO}/0.04) && (0.04 \text{ ppm} < \text{DO} \leq 0.5 \text{ ppm}) \\ O^* &= \ln(12.5) && (\text{DO} > 0.5 \text{ ppm}) \end{aligned} \quad (24)$$

$$\begin{aligned} \dot{\epsilon}^* &= 0 && (\dot{\epsilon} > 1\%/s) \\ \dot{\epsilon}^* &= \ln(\dot{\epsilon}) && (0.001 \leq \dot{\epsilon} \leq 1\%/s) \\ \dot{\epsilon}^* &= \ln(0.001) && (\dot{\epsilon} < 0.001\%/s) \end{aligned} \quad (25)$$

These models are recommended for predicted fatigue lives $\leq 10^6$ cycles. Also, as discussed in Section 4.2.7, because the effect of S on the fatigue life of carbon and low-alloy steels appears to depend on the DO level in water, Eqs. 20–25 may yield nonconservative estimates of fatigue life for low-S (< 0.007 wt.%) steels in high-temperature water with > 1 ppm DO. The experimental values of fatigue life and those predicted by Eqs. 20 and 21 are plotted in Fig. 28. The predicted fatigue lives show good agreement with the experimental values; the experimental and predicted values differ by a factor of 3.

- The ANL fatigue life models represent the mean values of fatigue life as a function of applied strain amplitude, temperature, strain rate, DO level in water, and S content of the steel. The effects of parameters (such as mean stress, surface finish, size and geometry, and loading history) that are known to influence fatigue life are not included in the model.

4.2.13 Environmental Fatigue Correction Factor

The effects of reactor coolant environments on fatigue life have also been expressed in terms of environmental fatigue correction factor, F_{en} , which is defined as the ratio of life in air at room temperature, N_{RTair} , to that in water at the service temperature, N_{water} . Values of F_{en} can be obtained from the ANL fatigue life model, where

$$\ln(F_{en}) = \ln(N_{RTair}) - \ln(N_{water}). \quad (26)$$

The environmental fatigue correction factor for carbon steels is given by

$$F_{en} = \exp(0.632 - 0.101 S^* T^* O^* \dot{\epsilon}^*), \quad (27)$$

and for low-alloy steels, by

$$F_{en} = \exp(0.702 - 0.101 S^* T^* O^* \dot{\epsilon}^*), \quad (28)$$

where the constants S^* , T^* , $\dot{\epsilon}^*$, and O^* are defined in Eqs. 22–25. Note that because the ANL fatigue life models have been updated in the present report, the constants 0.632 and 0.702 in Eqs. 27 and 28 are different from the values reported earlier in NUREG/CR-6583 and -6815. Relative to the earlier expressions, correction factors determined from Eq. 27 for carbon steels are $\approx 8\%$ higher, and those determined from Eq. 28 for low-alloy steels are $\approx 18\%$ lower. A threshold strain amplitude (one-half of the applied strain range) is also defined, below which LWR coolant environments have no effect on fatigue life, i.e., $F_{en} = 1$. The threshold strain amplitude is 0.07% (145 MPa stress amplitude) for carbon and low-alloy steels. To incorporate environmental effects into a ASME Section III fatigue evaluation, the fatigue usage for a specific stress cycle of load set pair based on the current Code fatigue design curves is multiplied by the correction factor. Further details for incorporating environmental effects into fatigue evaluations are presented in Appendix A.

- The F_{en} approach may be used to incorporate environmental effects into the Code fatigue evaluations.

4.2.14 Modified Rate Approach

Nearly all of the existing fatigue ϵ - N data were obtained under loading histories with constant strain rate, temperature, and strain amplitude. The actual loading histories encountered during service of nuclear power plants are far more complex. Exploratory fatigue tests have been conducted with waveforms in which the test temperature and strain rate were changed.^{4,15,18} The results of such tests provide guidance for developing procedures and rules for fatigue evaluation of components under complex loading histories.

The modified rate approach has been proposed to predict fatigue life under changing test conditions.^{31,32} It allows calculating F_{en} under conditions where temperature and strain rate are changing. The correction factor, $F_{en}(\dot{\epsilon}, T)$, is assumed to increase linearly from 1 with increments of

strain from a minimum value ϵ_{\min} (%) to a maximum value ϵ_{\max} (%). Increments of F_{en} , dF_{en} , during increments of strain, $d\epsilon$, are calculated from

$$dF_{en} = (F_{en} - 1) d\epsilon / (\epsilon_{\max} - \epsilon_{\min}). \quad (29)$$

Integration of Eq. 29 from ϵ_{\min} to ϵ_{\max} provides the environmental fatigue correction factor under changing temperature and strain rate. The application of the modified rate approach to a strain transient is illustrated in Fig. 29; at each strain increment, $F_{en}(\dot{\epsilon}, T)$ is determined from Eqs. 27 and 28. Thus, F_{en} for the total strain transient is given by

$$F_{en} = \sum_{k=1}^n F_{en,k}(\dot{\epsilon}_k, T_k) \frac{\Delta\epsilon_k}{\epsilon_{\max} - \epsilon_{\min}}, \quad (30)$$

where n is the total number of strain increments, and k is the subscript for the k -th incremental segment.

As discussed in Section 4.2.3, a minimum threshold strain, ϵ_{th} (one-half of the applied strain range), is required for an environmentally assisted decrease in fatigue life. During a strain cycle, environmental effects are significant only after the applied strain level exceeds the threshold value. In application of the modified rate approach when a threshold strain ϵ_{th} is considered, F_{en} for the total strain transient is given by

$$F_{en} = \sum_{k=1}^n F_{en,k}(\dot{\epsilon}_k, T_k) \frac{\Delta\epsilon_k}{\epsilon_{\max} - (\epsilon_{\min} + \epsilon_{th})}. \quad (31)$$

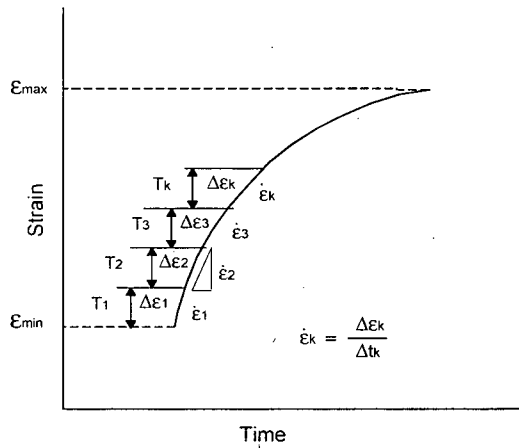


Figure 29. Application of the modified rate approach to determine the environmental fatigue correction factor F_{en} during a transient.

The modified rate approach has been used to evaluate fatigue life under cyclic loading conditions where both temperature and strain rate were varied during the test.^{18,31,32} The studies demonstrate the applicability of the damage rate approach to variable loading conditions such as actual plant transient. Also, the following conclusions may be drawn from these studies.

- (a) The use of a strain threshold, ϵ_{th} , for calculating F_{en} by the modified rate approach (i.e., Eq. 31) is not necessary because it does not improve the accuracy of estimation.³² As discussed earlier in

Section 4.2.3, application of the modified rate approach, without the consideration of a strain threshold, gives the best estimates of fatigue life.

- (b) Under load cycles that involve variable strain rate, estimates of F_{en} based on an average strain rate [i.e., in Fig. 29, total strain ($\epsilon_{max} - \epsilon_{min}$) divided by the total time for the transient] are the most conservative.¹⁸ Thus, calculations of F_{en} based on an average strain rate for the transient will always yield a conservative estimate of fatigue life.
 - (c) An average temperature for the transient may be used to estimate F_{en} during a load cycle.
- *Where information is available regarding the transients associated with a specific stress cycle or load set pair, the modified rate approach may be used to determine F_{en} .*

5 Austenitic Stainless Steels

The relevant fatigue ϵ - N data for austenitic SSs in air include the data compiled by Jaske and O'Donnell⁷² for developing fatigue design criteria for pressure vessel alloys, the JNUFAD database from Japan, studies at EdF in France,⁶⁹ and the results of Conway et al.⁷³ and Keller.⁷⁴ In water, the existing fatigue ϵ - N data include the tests performed by GE in a test loop at the Dresden I reactor;⁸⁻¹¹ the JNUFAD data base; studies at MHI, IHI, and Hitachi in Japan;¹⁸⁻³⁰ the work at ANL;^{6,7,36-40} and the studies sponsored by EdF.⁷⁰⁻⁷¹ Nearly 60% of the tests in air were conducted at room temperature, 20% at 250-325°C, and 20% at 350-450°C. Nearly 90% of the tests in water were conducted at temperatures between 260 and 325°C; the remainder were at lower temperatures. The data on Type 316NG in water have been obtained primarily at DO levels ≥ 0.2 ppm, and those on Type 316 SS, at ≤ 0.005 ppm DO; half of the tests on Type 304 SS are at low-DO and the remaining at high-DO levels.

5.1 Air Environment

5.1.1 Experimental Data

The fatigue ϵ - N data for Types 304, 316, and 316NG SS in air at temperatures between room temperature and 456°C are shown in Fig. 30. The best-fit curve based on the updated ANL fatigue life model (Eq. 32 in Section 5.1.7) and the ASME Section III mean-data curves are included in the figures. The results indicate that the fatigue life of Type 304 SS is comparable to that of Type 316 SS; the fatigue

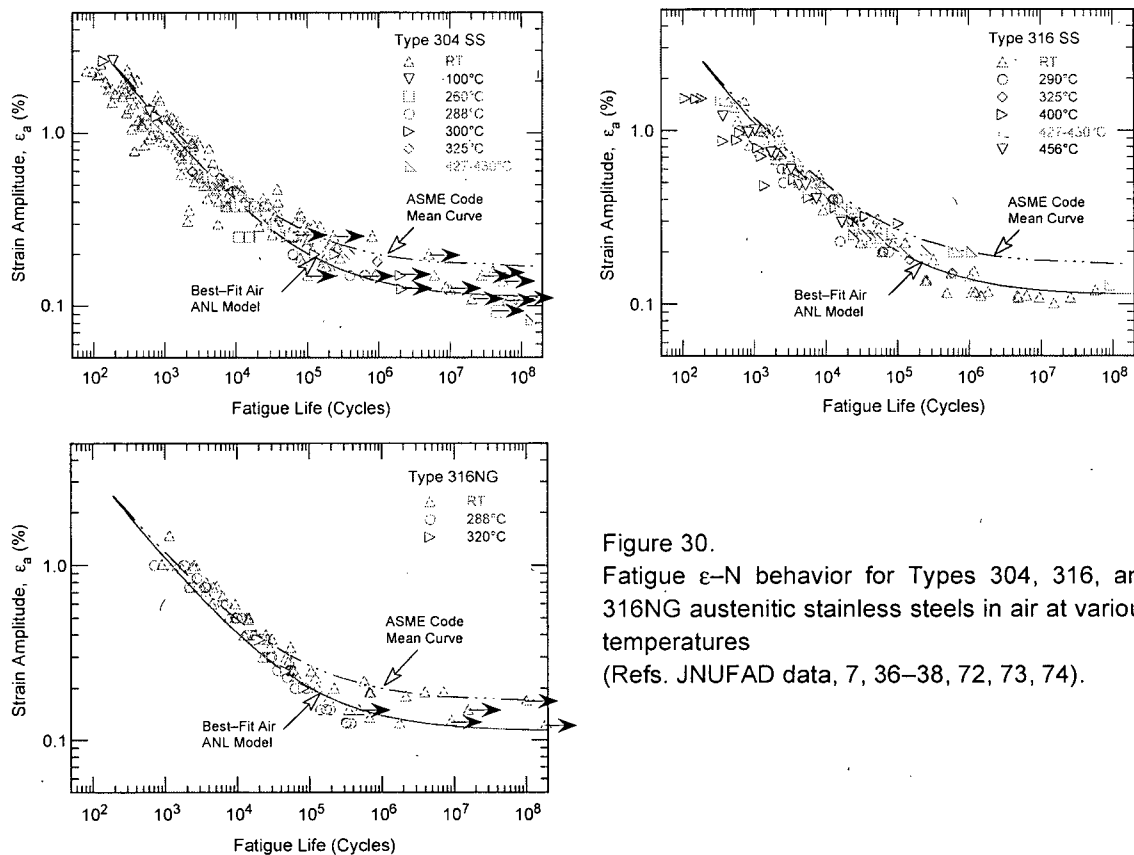


Figure 30.
Fatigue ϵ - N behavior for Types 304, 316, and 316NG austenitic stainless steels in air at various temperatures (Refs. JNUFAD data, 7, 36-38, 72, 73, 74).

life of Type 316NG is slightly higher than that of Types 304 and 316 SS at high strain amplitudes. Some of the tests on Type 316 SS in room-temperature air have been conducted in load-control mode at stress levels in the range of 190–230 MPa. The data are shown as triangles in Fig. 30, with strain amplitudes of 0.1–0.12% and fatigue lives of 7×10^4 – 3×10^7 . For these tests, the strain amplitude was calculated only as elastic strain. Based on cyclic stress-vs.-strain correlations for Type 316 SS,³⁸ actual strain amplitudes for these tests should be 0.23–0.32%. These results were excluded from the analysis of the fatigue ϵ - N data to develop the model for estimating the fatigue life of these steels in air.

The results also indicate that the current Code mean-data curve is not consistent with the existing fatigue ϵ - N data. At strain amplitudes <0.3% (stress amplitudes <585 MPa), the Code mean curve predicts significantly longer fatigue lives than those observed experimentally for several heats of austenitic SSs with composition and tensile strength within the ASME specifications. The difference between the Code mean curve and the best-fit of the available experimental data is due most likely to differences in the tensile strength of the steels. The Code mean curve represents SSs with relatively high strength; the fatigue ϵ - N data obtained during the last 30 years were obtained on SSs with lower tensile strengths.

Furthermore, for the current Code mean curve, the 10^6 cycle fatigue limit (i.e., the stress amplitude at a fatigue life of 10^6 cycles) is 389 MPa, which is greater than the monotonic yield strength of austenitic SSs in more common use (≈ 303 MPa). Consequently, the current Code design curve for austenitic SSs does not include a mean stress correction for fatigue lives below 10^6 cycles. Recent studies by Wire et al.¹¹² and Solomon et al.⁷⁰ on the effect of residual stress on fatigue life clearly demonstrate that mean stress can decrease the 10^6 cycle fatigue limit of the material; the extent of the effect depends on the cyclic hardening behavior of the material and the resultant decrease in strain amplitude developed during load-controlled cycling. Strain hardening is more pronounced at high temperatures (e.g., 288–320°C) or at high mean stress (e.g., >70 MPa); therefore, as observed by Wire et al. and Solomon et al., fatigue life for load-controlled tests with mean stress is actually increased at high temperatures or large values of mean stress. In both studies, under load control, mean stress effects were observed at low temperatures (150°C) or at relatively low mean stress (<70 MPa).

Wire et al.¹¹² performed fatigue tests on two heats of Types 304 SS to establish the effect of mean stress under both strain control and load control. The strain-controlled tests indicated “an apparent reduction of up to 26% in strain amplitude in the low- and intermediate-cycle regime (< 10^6 cycle) for a mean stress of 138 MPa.” However, the results were affected both by mean stress and cold work. Although the composition and vendor-supplied tensile strength for the two heats of Type 304 SS were within the ASME specifications, the measured mechanical properties showed much larger variations than indicated by the vendor properties. Wire et al. state, “at 288°C, yield strength varied from 152–338 MPa. These wide variations are attributed to variations in (cold) working from the surface to the center of the thick cylindrical forgings.” After separating the individual effect of mean stress and cold work, the Wire et al. results indicate a 12% decrease in strain amplitude for a mean stress of 138 MPa. These results are consistent with the predictions based on conventional mean stress models such as the Goodman correlation.

- *The current Code mean data curve, and therefore the Code design curve, is nonconservative with respect to the existing fatigue ϵ - N data for austenitic SSs. A new Code fatigue design curve, which is consistent with the existing fatigue data, has been proposed (see Section 5.1.8 for details).*

5.1.2 Specimen Geometry

The influence of specimen geometry (hourglass vs. gauge length specimens) on the fatigue life of Types 304 and 316 SS is shown in Fig. 31. At temperatures up to 300°C, specimen geometry has little or no effect on the fatigue life of austenitic SSs; the fatigue lives of hourglass specimens are comparable to those of gauge specimens.

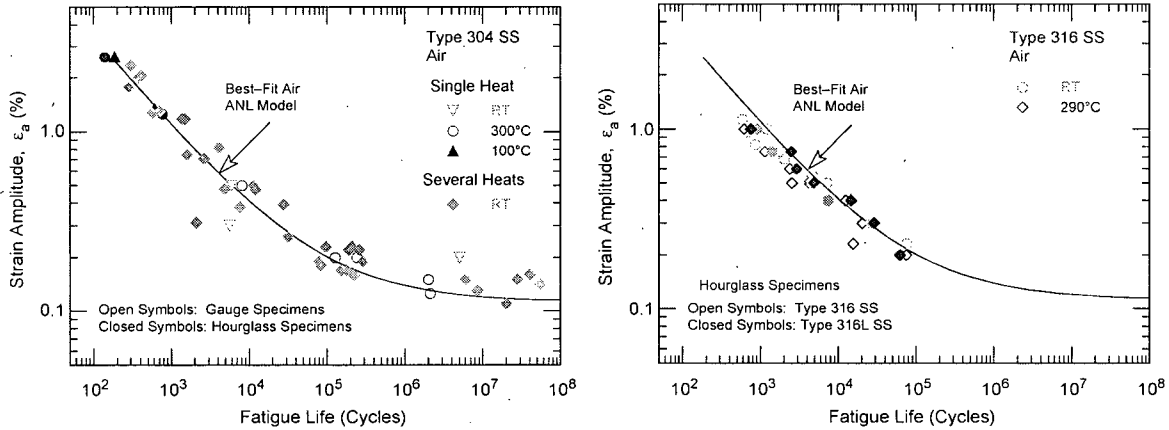


Figure 31. Influence of specimen geometry on fatigue life of Types 304 and 316 stainless steel (JNUFAD data).

- Fatigue $\epsilon-N$ data obtained either on hourglass or straight gauge specimens may be used to develop the Code fatigue design curves.

5.1.3 Temperature

The fatigue life of Types 304 and 316 SS in air at temperatures between 100 and 325°C is plotted in Fig. 32; the best-fit curve based on the ANL model (Eq. 32 in Section 5.1.7) and the ASME Code mean curve are also shown in the figures. In air, the fatigue life of austenitic SSs is independent of temperature from room temperature to 400°C. Although the effect of strain rate on fatigue life seems to be significant

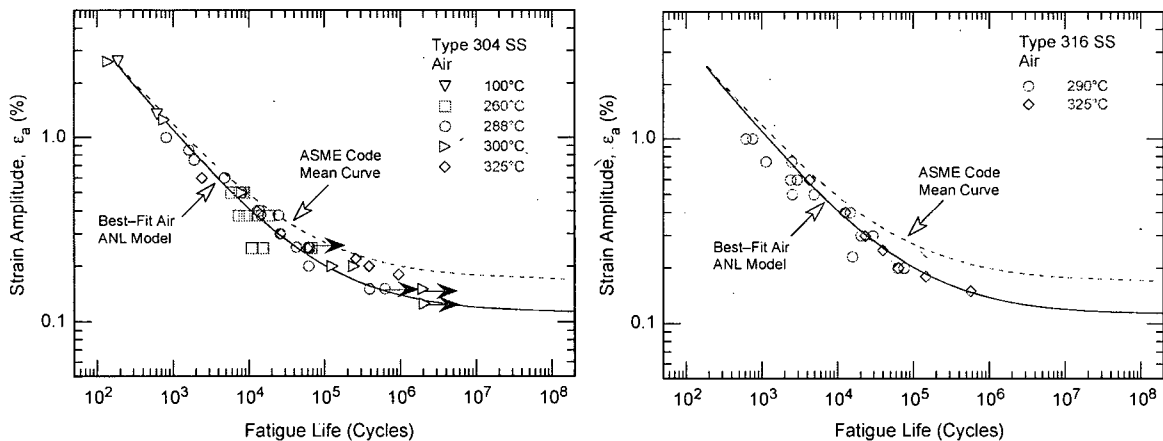


Figure 32. Influence of temperature on fatigue life of Types 304 and 316 stainless steel in air (Ref. 38, JNUFAD database).

at temperatures above 400°C, variations in strain rate in the range of 0.4–0.008%/s have no effect on the fatigue lives of SSs at temperatures up to 400°C.⁶⁹ In air, the fatigue ϵ -N data can be represented by a single curve for temperatures from room temperature up to 400°C.

Recent data indicate that temperature can influence the fatigue limit of austenitic SSs because of differences in the secondary hardening behavior of the material due to dynamic strain aging.⁷¹ For a heat of Type 304L SS, the fatigue limit was higher at 300°C than at 150°C because of significant secondary hardening at 300°C.

- *Temperature has no significant effect on the fatigue life of austenitic SSs at temperatures from room temperature to 400°C. Variations in fatigue life due to the effects of secondary hardening behavior are accounted for in the factor applied on stress to obtain the design curve from the mean data curve.*

5.1.4 Cyclic Strain Hardening Behavior

Under cyclic loading, austenitic SSs exhibit rapid hardening during the first 50–100 cycles; as shown in Fig. 33 the extent of hardening increases with increasing strain amplitude and decreasing temperature and strain rate.³⁸ The initial hardening is followed by a softening and saturation stage at high temperatures, and by continuous softening at room temperature.

- *The cyclic strain hardening behavior is likely to influence the fatigue limit of the material; variations in fatigue life due to such effects are accounted for in the factor of 2 on stress.*

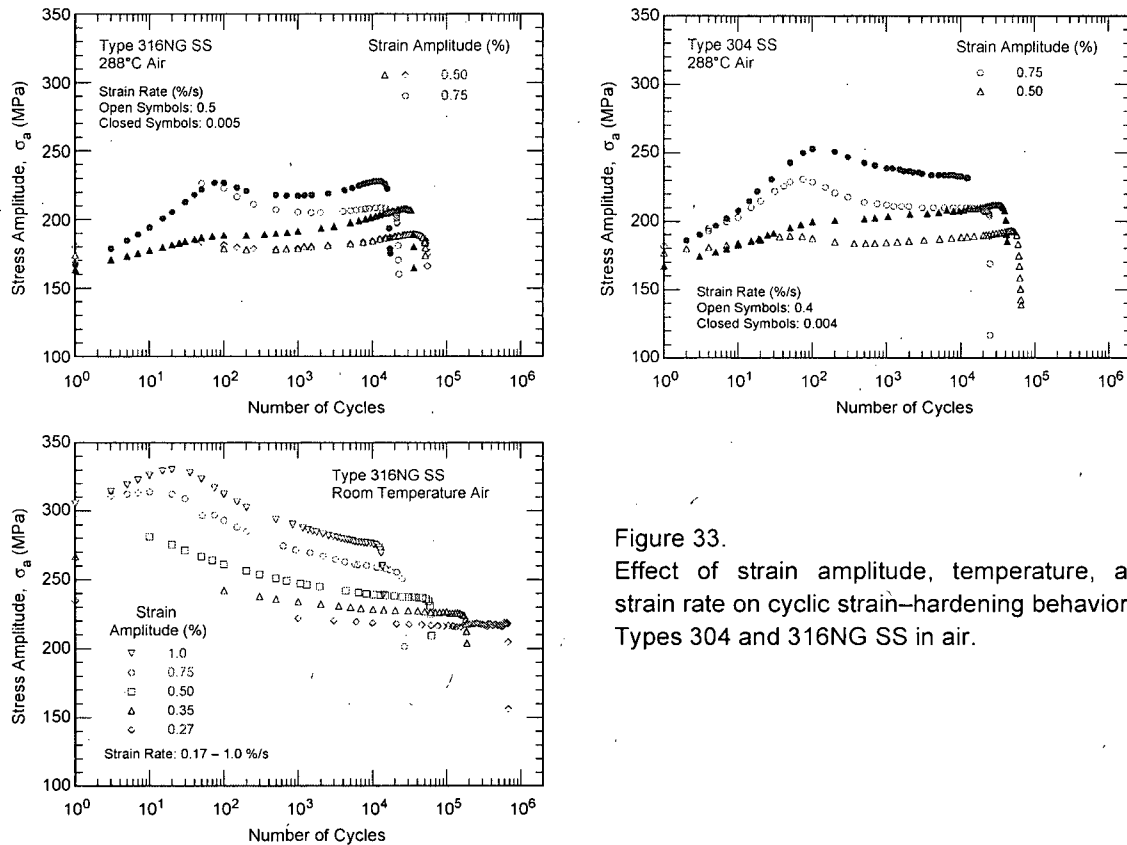


Figure 33. Effect of strain amplitude, temperature, and strain rate on cyclic strain-hardening behavior of Types 304 and 316NG SS in air.

5.1.5 Surface Finish

Fatigue tests have been conducted on Types 304 and 316NG SS specimens that were intentionally roughened in a lathe, under controlled conditions, with 50-grit sandpaper to produce circumferential cracks with an average surface roughness of $1.2\ \mu\text{m}$. The results are shown in Figs. 34a and b, respectively, for Types 316NG and 304 SS. For both steels, the fatigue life of roughened specimens is a factor of ≈ 3 lower than that of the smooth specimens.

- *The effect of surface finish was not investigated in the mean data curve used to develop the Code fatigue design curves; it is included as part of the subfactor that is applied to the mean data curve to account for "surface finish and environment."*

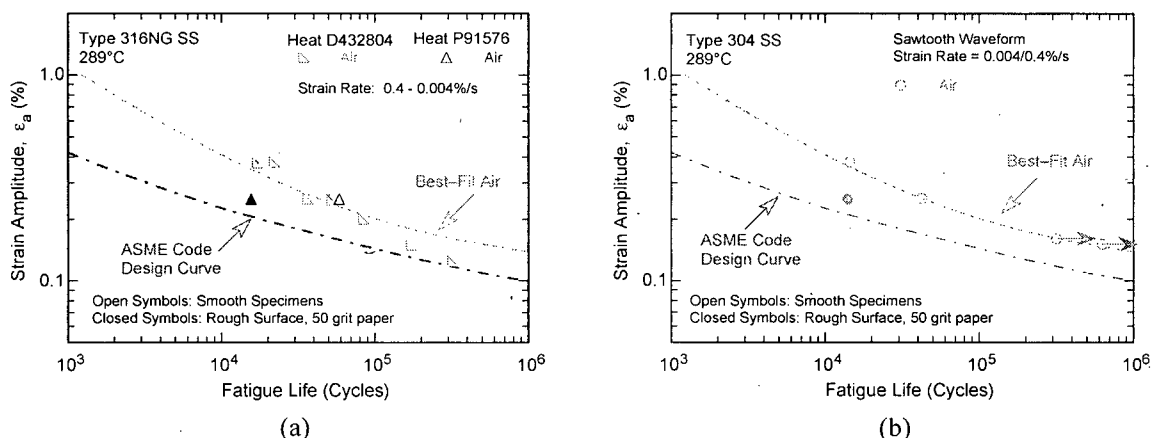


Figure 34. Effect of surface roughness on fatigue life of (a) Type 316NG and (b) Type 304 SSs in air.

5.1.6 Heat-to-Heat Variability

The effects of material variability and data scatter must be included to ensure that the design curves not only describe the available test data well, but also adequately describe the fatigue lives of the much larger number of heats of material that are found in the field. As mentioned earlier for carbon and low-alloy steels, material variability and data scatter in the fatigue ϵ -N data for austenitic SSs are also evaluated by considering the best-fit curves determined from tests on individual heats of materials or loading conditions as samples of the much larger population of heats of materials and service conditions of interest. The fatigue behavior of each of the heats or loading conditions is characterized by the value of the constant A in Eq. 6. The values of A for the various data sets were ordered, and median ranks were used to estimate the cumulative distribution of A for the population. The distributions were fit to lognormal curves. Results for various austenitic SSs in air are shown in Fig. 35. The median value of the constant A is 6.891 for the fatigue life of austenitic SSs in air at temperatures not exceeding 400°C . The values of A that describe the 5th percentile of these distributions give a fatigue ϵ -N curve that is expected to bound the lives of 95% of the heats of austenitic SSs. A Monte Carlo analysis was performed to address the uncertainties in the median value and standard deviation of the sample used for the analysis.

For austenitic SSs, the values for A that provide bounds for the portion of the population and the confidence that is desired in the estimates of the bounds are summarized in Table 8. From Fig. 35, the median value of A for the sample is 6.891. From Table 8, the 95/95 value of the margin to account for material variability and data scatter is 2.3 on life. This margin is needed to provide reasonable confidence that the resultant life will be greater than that observed for 95% of the materials of interest.

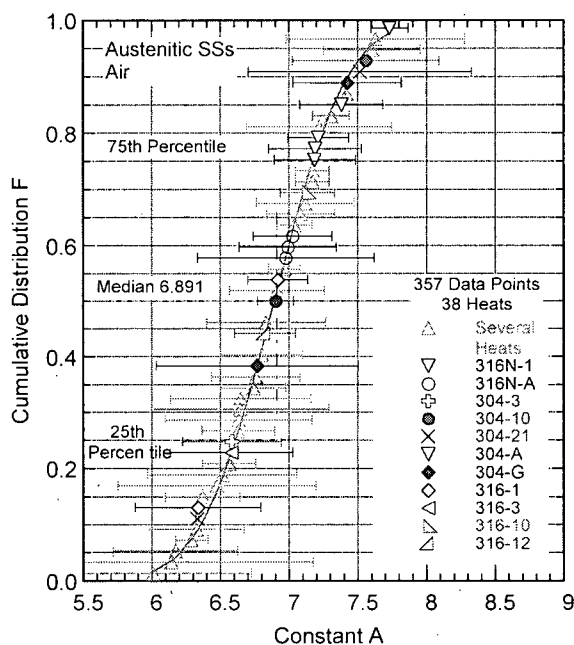


Figure 35. Estimated cumulative distribution of constant A in the ANL model for fatigue life for heats of austenitic SS in air.

Table 8. Values of parameter A in the ANL fatigue life model and the margins on life for austenitic SSs in air as a function of confidence level and percentage of population bounded.

Confidence Level	Percentage of Population Bounded (Percentile Distribution of A)				
	95 (5)	90 (10)	75 (25)	67 (33)	50 (50)
	<u>Values of Parameter A</u>				
50	6.205	6.356	6.609	6.707	6.891
75	6.152	6.309	6.569	6.668	6.851
95	6.075	6.241	6.510	6.611	6.793
	<u>Margins on Life</u>				
50	2.0	1.7	1.3	1.2	1.0
75	2.1	1.8	1.4	1.2	1.0
95	2.3	1.9	1.5	1.3	1.1

- The Code fatigue design curves are based on the mean data curves; heat-to-heat variability is included in the subfactor that is applied to the mean data curve to account for "data scatter and material variability."

5.1.1.7 Fatigue Life Model

The database used to develop the new air mean data curve is much larger and developed for more representative materials than were used as the basis for the existing ASME fatigue design curves. It is an updated version of the PVRC database; the sources are listed in Table 1 of the present report. The data were obtained on smooth specimens tested under strain control with a fully reversed loading (i.e., $R = -1$) in compliance with consensus standard approaches for the development of such data. The database for austenitic SSs consists of some 520 tests on Types 304, 316, 304L, 316L and 316NG SS; ≈ 220 for Type 304 SS; 150 for Type 316 SS; and 150 for Types 316NG, 304L, and 316L SS. The austenitic SSs used in these studies are all in compliance with the compositional and strength requirements of the ASME Code specifications.

Several different best-fit mean ϵ -N curves for austenitic SSs have been proposed in the literature. Examples include Jaske and O'Donnell,⁷² Diercks,¹¹³ Chopra,³⁸ Tsutsumi et al.,²⁸ and Solomon and Amzallag.¹¹⁴ These curves differ by up to 50%, particularly in the 10^4 to 10^7 cycle regime; the differences primarily occur because different database were used in developing the models for the mean ϵ -N curves. The analyses by Jaske and O'Donnell and by Diercks are based on the Jaske and O'Donnell database. The details regarding the database used by Tsutsumi et al. are not available. The database used in NUREG/CR-5704 included the Jaske and O'Donnell data, data obtained in Japan (including the JNUFAD database), and some additional data obtained in the U.S. In the earlier ANL reports, separate models were presented for Type 304 or 316 SS and Type 316NG SS. In the present report, the existing data were reanalyzed to develop a single model for the fatigue ϵ -N behavior of austenitic SSs. The model assumes that the fatigue life in air is independent of temperature and strain rate. Also, to be consistent with the models proposed by Tsutsumi et al.²⁸ and Jaske and O'Donnell,⁷² the value of the constant C in the modified Langer equation (Eq. 6) was lower than that in earlier reports (i.e., 0.112 instead of 0.126). The proposed curve yields an R^2 value of 0.851 when compared with the available data; the R^2 values for the mean curves derived by Tsutsumi et al., Jaske and O'Donnell, and the ASME Code are 0.839, 0.826, and 0.568, respectively.

In air, at temperatures up to 400°C, the fatigue data for Types 304, 304L, 316, 316L, and 316NG SS are best represented by the equation:

$$\ln(N) = 6.891 - 1.920 \ln(\epsilon_a - 0.112) \quad (32)$$

where ϵ_a is applied strain amplitude (%). The experimental values of fatigue life and those predicted by Eq. 32 for austenitic SSs in air are plotted in Fig. 36. The predicted lives show good agreement with the experimental values; for most tests the difference between the experimental and predicted values is within a factor of 3, and for some, the observed fatigue lives are significantly longer than the predicted values.

- *The ANL fatigue life models represent mean values of fatigue life. The effects of parameters such as mean stress, surface finish, size and geometry, and loading history, which are known to influence fatigue life, are not explicitly considered in the model; such effects are accounted for in the factors of 20 on life and 2 on stress that are applied to the mean data curve to obtain the Code fatigue design curve.*

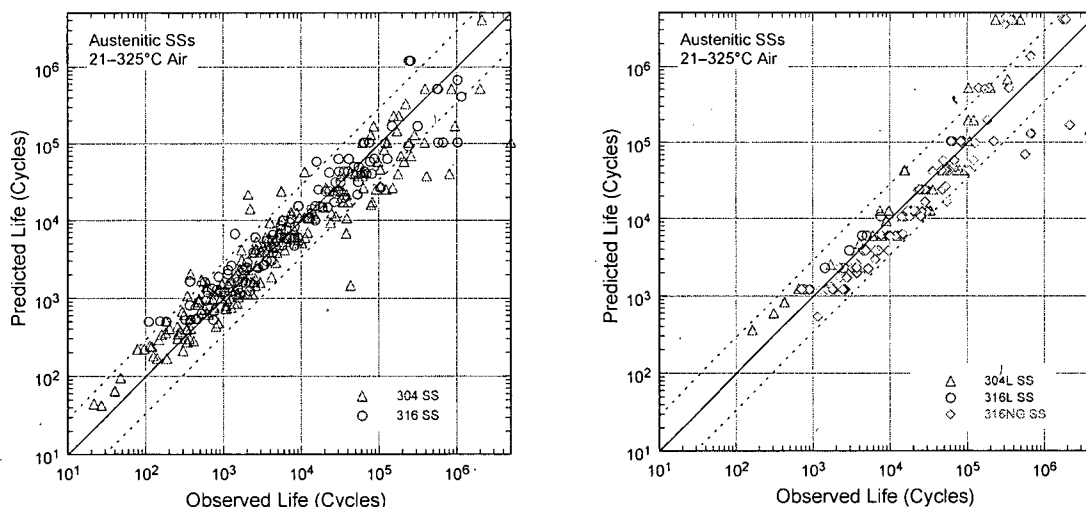


Figure 36. Experimental and predicted fatigue lives of austenitic SSs in air.

5.1.8 New Fatigue Design Curve

As discussed in Section 5.1.1, the current Code mean-data curve that was used to develop the Code fatigue design curve, is not consistent with the existing fatigue ϵ - N data. A fatigue design curve that is consistent with the existing database may be obtained from the ANL model (Eq. 32) by following the same procedure that was used to develop the current ASME Code fatigue design curve. However, the discussions presented later in Section 7.5 indicate that the current Code requirement of a factor of 20 on cycles, to account for the effects of material variability and data scatter, specimen size, surface finish, and loading history, is conservative by at least a factor of 1.7. Thus, to reduce this conservatism, fatigue design curve based on the ANL model for austenitic SSs (Eq. 32) may be developed by first correcting for mean stress effects using the modified Goodman relationship and then lowering the mean-stress-adjusted curve by a factor of 2 on stress or 12 on cycles, whichever is more conservative. This curve and the current Code design curve are shown in Fig. 37; values of stress amplitude vs. cycles for the current and the proposed design curves are given in Table 9. A fatigue design curve that is consistent with the existing fatigue ϵ - N data but is not based on the ANL model (Eq. 32) has also been proposed by the ASME Subgroup on Fatigue Strength.⁸⁹

Table 9. The new and current Code fatigue design curves for austenitic stainless steels in air.

Cycles	Stress Amplitude (MPa/ksi)		Cycles	Stress Amplitude (MPa/ksi)	
	New Design Curve	Current Design Curve		New Design Curve	Current Design Curve
1 E+01	6000 (870)	4881 (708)	2 E+05	168 (24.4)	248 (35.9)
2 E+01	4300 (624)	3530 (512)	5 E+05	142 (20.6)	214 (31.0)
5 E+01	2748 (399)	2379 (345)	1 E+06	126 (18.3)	195 (28.3)
1 E+02	1978 (287)	1800 (261)	2 E+06	113 (16.4)	157 (22.8)
2 E+02	1440 (209)	1386 (201)	5 E+06	102 (14.8)	127 (18.4)
5 E+02	974 (141)	1020 (148)	1 E+07	99 (14.4)	113 (16.4)
1 E+03	745 (108)	820 (119)	2 E+07		105 (15.2)
2 E+03	590 (85.6)	669 (97.0)	5 E+07		98.6 (14.3)
5 E+03	450 (65.3)	524 (76.0)	1 E+08	97.1 (14.1)	97.1 (14.1)
1 E+04	368 (53.4)	441 (64.0)	1 E+09	95.8 (13.9)	95.8 (13.9)
2 E+04	300 (43.5)	383 (55.5)	1 E+10	94.4 (13.7)	94.4 (13.7)
5 E+04	235 (34.1)	319 (46.3)	1 E+11	93.7 (13.6)	93.7 (13.6)
1 E+05	196 (28.4)	281 (40.8)	2 E+10		

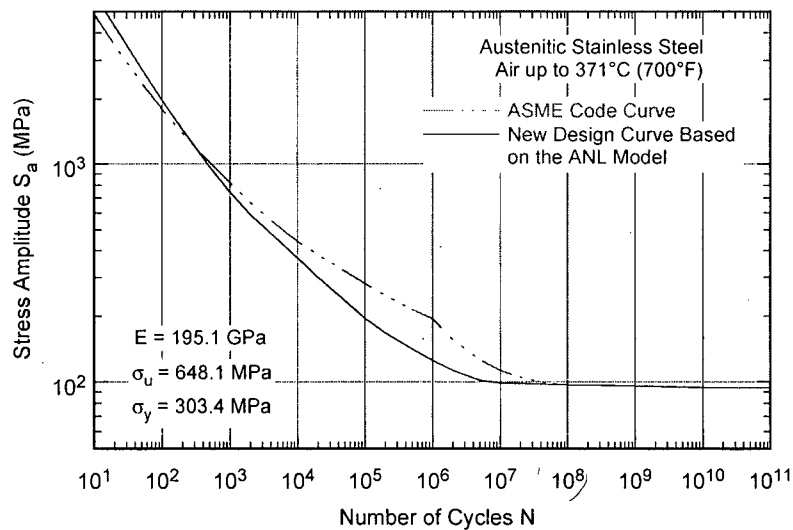


Figure 37. Fatigue design curve for austenitic stainless steels in air.

The proposed curve extends up to 10^{11} cycles; the two curves are the same beyond 10^8 cycles. Although the curve is based primarily on data for Types 304 and 316 SS, it may be used for wrought Types 304, 310, 316, 347, and 348 SS, and cast CF-3, CF-8, and CF-8M SS for temperatures not exceeding 371°C (700°F).

- The current Code fatigue design curve for austenitic stainless steels is nonconservative with respect to the existing fatigue ϵ - N data for fatigue lives in the range of 10^3 to 5×10^6 cycles. A new design curve, that is consistent with the existing data, has been developed. To reduce the conservatism in the current Code requirement of 20 on life, the new curve was obtained by using factors of 12 on life and 2 on stress.

5.2 LWR Environment

5.2.1 Experimental Data

The fatigue lives of austenitic SSs are decreased in LWR environments; the fatigue ϵ - N data for Types 304 and 316NG SS in water at 288°C are shown in Fig. 38. The ϵ - N curves based on the ANL model (Eq. 32 in Section 5.1.7 and Eq. 34 in Section 5.2.13) are also included in the figures. The fatigue life is decreased significantly when three threshold conditions are satisfied simultaneously, viz., applied strain range and service temperature are above a minimum threshold level, and the loading strain rate is below a threshold value. The DO level in the water and, possibly, the composition and heat treatment of the steel are also important parameters for environmental effects on fatigue life. For some steels, fatigue life is longer in high-DO water than in low-DO PWR environments. Although, in air, the fatigue life of Type 316NG SS is slightly longer than that of Types 304 and 316 SS, the effects of LWR environments are comparable for wrought Types 304, 316, and 316NG. Also, limited data indicate that the fatigue life of cast austenitic SSs in both low-DO and high-DO environments is comparable to that of wrought SSs in low-DO environment.

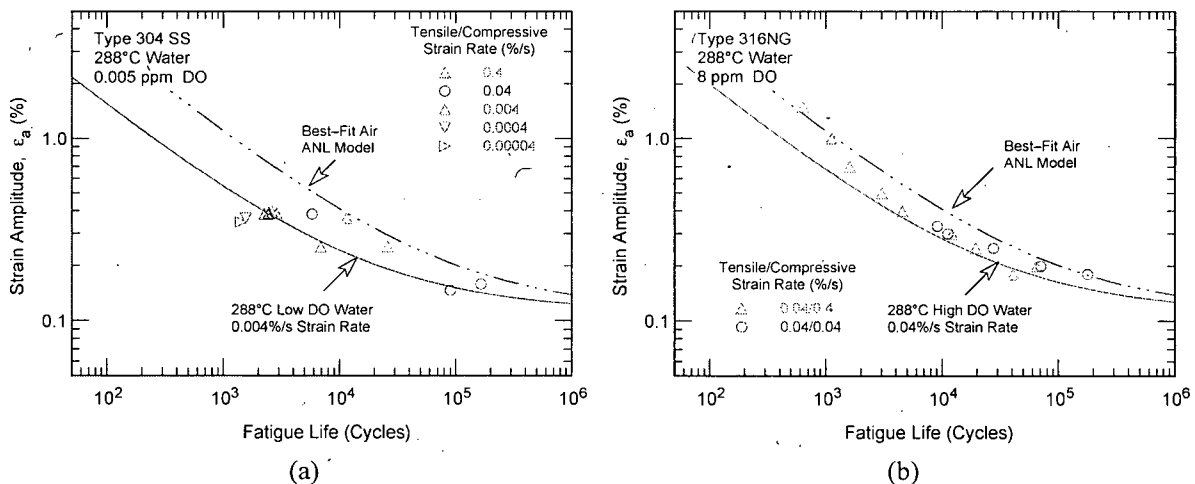


Figure 38. Strain amplitude vs. fatigue life data for (a) Type 304 and (b) Type 316NG SS in water at 288°C (JNUFAD and Refs. 7,38).

The existing fatigue data indicate that a slow strain rate applied during the tensile-loading cycle (i.e., up-ramp with increasing strain) is primarily responsible for the environmentally assisted reduction in fatigue life. Slow rates applied during both tensile- and compressive-loading cycles (i.e., up- and down-ramps) do not further decrease fatigue life compared with that observed for tests with only a slow

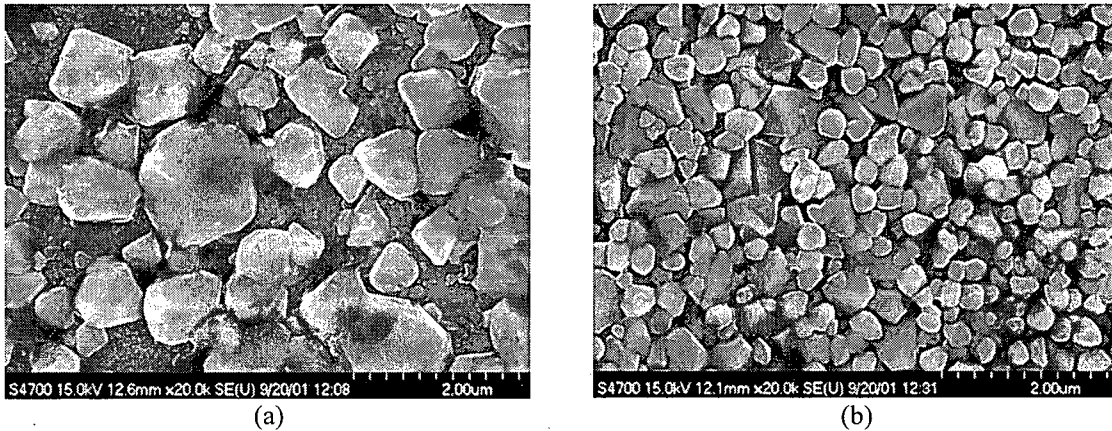


Figure 39. Higher-magnification photomicrographs of oxide films that formed on Type 316NG stainless steel in (a) simulated PWR water and (b) high-DO water.

tensile-loading cycle (Fig. 38b). Consequently, loading and environmental conditions during the tensile-loading cycle (strain rate, temperature, and DO level) are important for environmentally assisted reduction of the fatigue lives of these steels.

For austenitic SSs, lower fatigue lives in low-DO water than in high-DO water are difficult to reconcile in terms of the slip oxidation/dissolution mechanism, which assumes that crack growth rates increase with increasing DO in the water. The characteristics of the surface oxide films that form on austenitic SSs in LWR coolant environments can influence the mechanism and kinetics of corrosion processes and thereby influence the initiation stage, i.e., the growth of MSCs. Also, the reduction of fatigue life in high-temperature water has often been attributed to the presence of surface micropits that may act as stress raisers and provide preferred sites for the formation of fatigue cracks. Photomicrographs of the gauge surfaces of Type 316NG specimens tested in simulated PWR water and high-DO water are shown in Fig. 39. Austenitic SSs exposed to LWR environments develop an oxide film that consists of two layers: a fine-grained, tightly-adherent, chromium-rich inner layer, and a crystalline, nickel-rich outer layer composed of large and intermediate-size particles. The inner layer forms by solid-state growth, whereas the crystalline outer layer forms by precipitation or deposition from the solution. A schematic representation of the surface oxide film is shown in Fig. 40. The structure and composition of the inner and outer layers and their variation with the water chemistry have been identified.^{115,116}

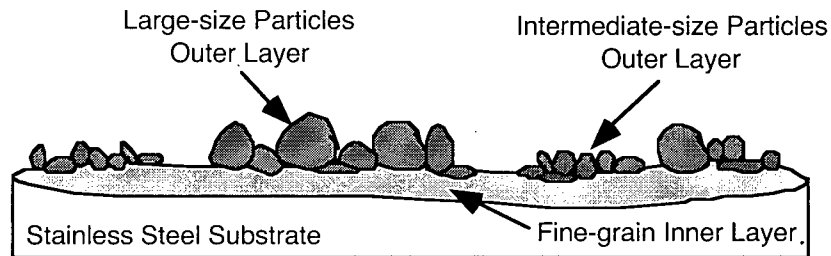


Figure 40. Schematic of the corrosion oxide film formed on austenitic stainless steels in LWR environments.

Experimental data indicate that surface micropits or minor differences in the composition or structure of the surface oxide film have no effect on the formation of fatigue cracks. Fatigue tests were conducted on Type 316NG (Heat P91576) specimens that were preexposed to either low-DO or high-DO water and then tested in air or water environments. The results of these tests, as well as data obtained earlier on this heat and Heat D432804 of Type 316NG SS in air and low-DO water at 288°C, are plotted in Fig. 41. The fatigue life of a specimen preoxidized in high-DO water and then tested in low-DO water is identical to that of specimens tested without preoxidation. Also, fatigue lives of specimens preoxidized at 288°C in low-DO water and then tested in air are identical to those of unoxidized specimens (Fig. 41). If micropits were responsible for the reduction in life, the preexposed specimens should show a decrease in life. Also, the fatigue limit of these steels should be lower in water than in air, but the data indicate this limit is the same in water and air environments. Metallographic examination of the test specimens indicated that environmentally assisted reduction in fatigue lives of austenitic SSs most likely is not caused by slip oxidation/dissolution but some other process, such as hydrogen-induced cracking.^{7,36,37}

- An LWR environment has a significant effect on the fatigue life of austenitic SSs; such effects are not considered in the current Code design curve. Environmental effects may be incorporated into the Code fatigue evaluation using the F_{en} approach described in Section 5.2.14.

5.2.2 Strain Amplitude

As in the case of the carbon and low-alloy steels, a minimum threshold strain range is required for the environmentally induced decrease in fatigue lives of SS to occur. Exploratory fatigue tests have also been conducted on austenitic SSs to determine the threshold strain range beyond which environmental effects are significant during a fatigue cycle.^{24,29} The tests were performed with waveforms in which the slow strain rate is applied during only a fraction of the tensile loading cycle. The results indicate that a minimum threshold strain is required for an environmentally assisted decrease in the fatigue lives of SSs (Fig. 42). The threshold strain range $\Delta\epsilon_{th}$ appears to be independent of material type (weld or base metal) and temperature in the range of 250–325°C, but it tends to decrease as the strain range is decreased.^{24,29} The threshold strain range may be expressed in terms of the applied strain range $\Delta\epsilon$ by the equation

$$\Delta\epsilon_{th}/\Delta\epsilon = -0.22 \Delta\epsilon + 0.65. \quad (33)$$

The results suggest that $\Delta\epsilon_{th}$ is related to the elastic strain range of the test and does not correspond to the strain at which the crack closes.

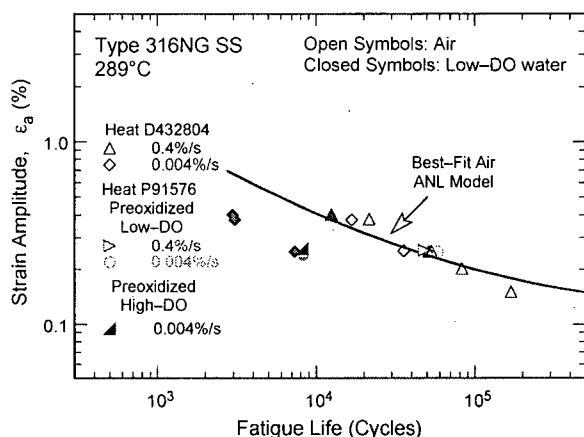


Figure 41. Effects of environment on formation of fatigue cracks in Type 316NG SS in air and low-DO water at 288°C. Preoxidized specimens were exposed for 10 days at 288°C in water that contained either <5 ppb DO and $\approx 23 \text{ cm}^3/\text{kg}$ dissolved H_2 or $\approx 500 \text{ ppb}$ DO and no dissolved H_2 (Ref. 7).

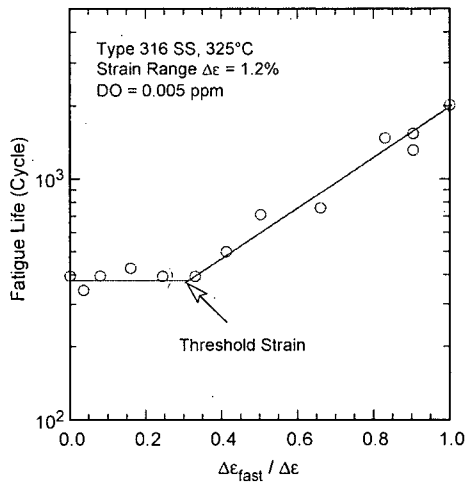


Figure 42. Results of strain rate change tests on Type 316 SS in low-DO water at 325°C. Low strain rate was applied during only a fraction of tensile loading cycle. Fatigue life is plotted as a function of fraction of strain at high strain rate (Refs. 24,29).

- In LWR environments, the procedure for calculating F_{en} , defined in Eq. 38 (Section 5.2.14), includes a threshold strain range below which LWR coolant environments have no effect on fatigue life, i.e., $F_{en} = 1$. However, a threshold strain should not be considered when the damage rate approach is used to determine F_{en} for a stress cycle or load set pair.

5.2.3 Hold-Time Effects

Environmental effects on fatigue life occur primarily during the tensile-loading cycle and at strain levels greater than the threshold value. Information on the effect of hold periods on the fatigue life of austenitic SSs in water is very limited. In high-DO water, the fatigue lives of Type 304 SS tested with a trapezoidal waveform (i.e., hold periods at peak tensile and compressive strain)⁸ are comparable to those tested with a triangular waveform,²⁵ as shown in Fig. 43. As discussed in Section 4.2.8, a similar behavior has been observed for carbon and low-alloy steels: the data show little or no effect of hold periods on fatigue lives of the steels in high-DO water.

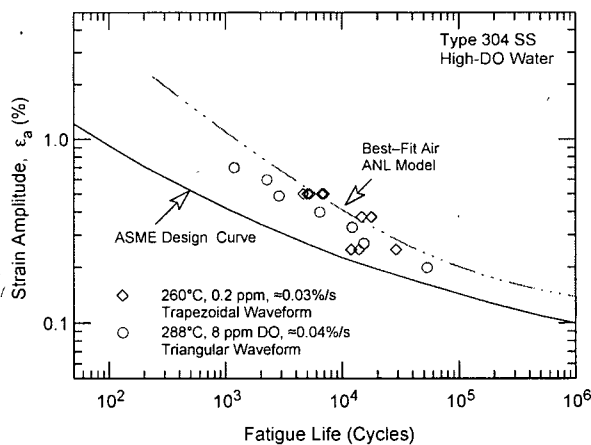


Figure 43. Fatigue life of Type 304 stainless steel tested in high-DO water at 260–288°C with trapezoidal or triangular waveform (Refs. 8,25).

- The existing data do not demonstrate that hold periods at peak tensile strain affect the fatigue life of austenitic SSs in LWR environments. Thus, any revision/modification of the method to determine F_{en} is not warranted.

5.2.4 Strain Rate

The fatigue life of Types 304L and 316 SSs in low-DO water is plotted as a function of tensile strain rate in Fig. 44. In low-DO PWR environment, the fatigue life of austenitic SSs decreases with decreasing strain rate below $\approx 0.4\%/s$; the effect of environment on fatigue life saturates at $\approx 0.0004\%/s$ (Fig. 44).^{7,18,21-25,28,29,38-40} Only a moderate decrease in life is observed at strain rates greater than $0.4\%/s$. A decrease in strain rate from 0.4 to $0.0004\%/s$ decreases the fatigue life by a factor of ≈ 10 .

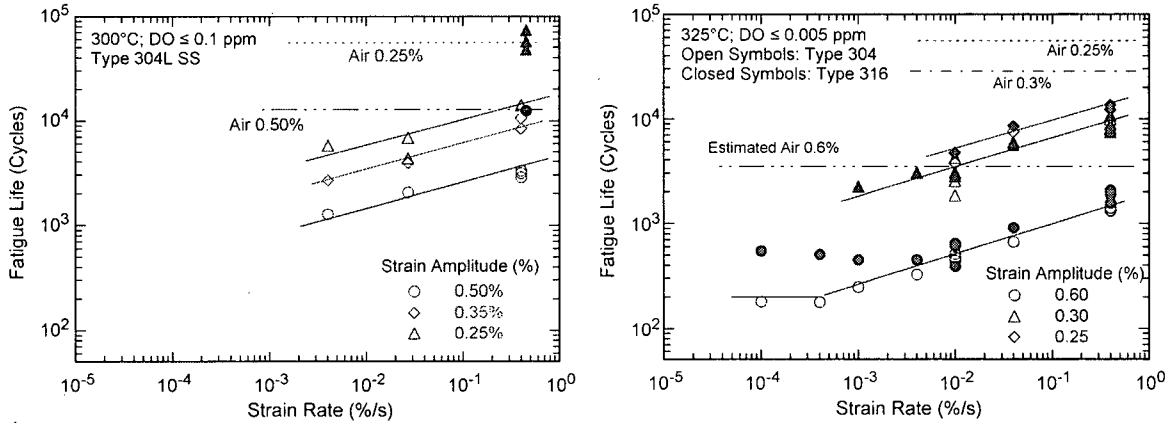


Figure 44. Dependence of fatigue lives of austenitic stainless steels on strain rate in low-DO water (Refs. 7,38,40,71).

In high-DO water, the effect of strain rate may be less pronounced than in low-DO water (Fig. 45). For example, for Heat 30956 of Type 304 SS, strain rate has no effect on fatigue life in high-DO water, whereas life decreases linearly with strain rate in low-DO water (Fig. 45a). For Heat D432804 of Type 316NG, some effect of strain rate is observed in high-DO water, although it is smaller than that in low-DO water (Fig. 45b).

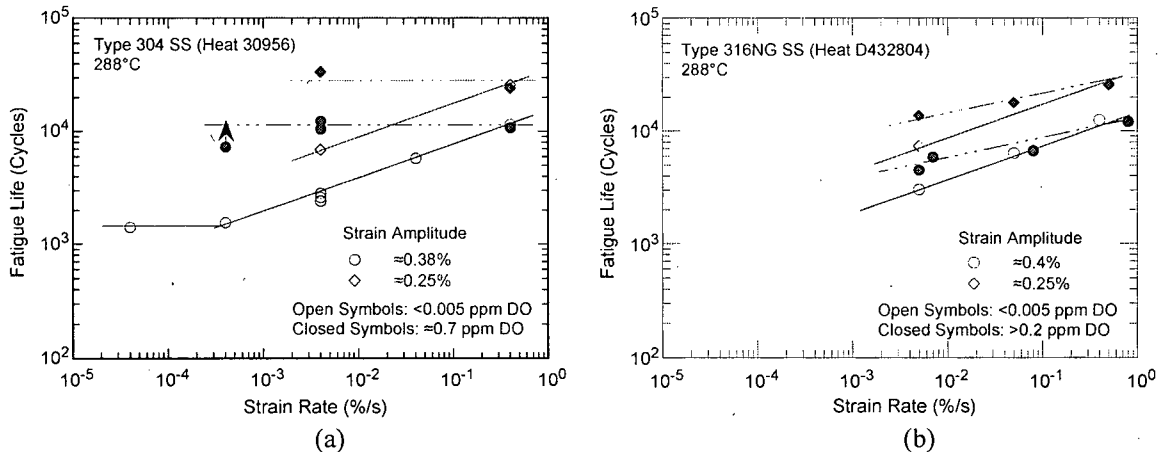


Figure 45. Dependence of fatigue life of Types (a) 304 and (b) 316NG stainless steel on strain rate in high- and low-DO water at 288°C (Ref. 7,38,40).

- In LWR environments, the effect of strain rate on the fatigue life of austenitic SSs is explicitly considered in F_{en} defined in Eq. 38 (Section 5.2.14). Also, guidance is provided to define the strain rate to be used to calculate F_{en} for a specific stress cycle or load set pair.

5.2.5 Dissolved Oxygen

In contrast to the behavior of carbon and low-alloy steels, the fatigue lives of austenitic SSs decrease significantly in low-DO (i.e., <0.05 ppm DO) water. In low-DO water, the fatigue life is not influenced by the composition or heat treatment condition of the steel. The fatigue life, however, continues to decrease with decreasing strain rate and increasing temperature.^{7,18,23-25,28,29,38-40}

In high-DO water, the fatigue lives of austenitic SSs are either comparable to^{23,28} or, in some cases, higher^{7,38,40} than those in low-DO water, i.e., for some SSs, environmental effects may be lower in high-DO than in low-DO water. The results presented in Figs. 45a and 45b indicate that, in high-DO water, environmental effects on the fatigue lives of austenitic SSs are influenced by the composition and heat treatment of the steel. For example, for high-carbon Type 304 SS, environmental effects in high-DO water are insignificant for the mill-annealed (MA) material (Fig. 45a), whereas as discussed in Section 5.2.8, for sensitized material the effect of environment is the same in high- and low-DO water. For the low-C Type 316NG SS, some effect of strain rate is apparent in high-DO water, although it is smaller than that in low-DO water (Fig. 45b). The effect of material heat treatment on the fatigue life of Type 304 SS is discussed in Section 5.2.8; in high-DO water, material heat treatment affects the fatigue life of SSs.

- In LWR environments, the effect of DO on the fatigue life of austenitic SSs is explicitly considered in F_{en} defined in Eq. 38. Also, guidance is provided to define the DO content to be used to calculate F_{en} for a specific stress cycle or load set pair.

5.2.6 Water Conductivity

The studies at ANL indicate that, for fatigue tests in high-DO water, the conductivity of water and the ECP of steel are important parameters that must be held constant.^{7,38,40} During laboratory tests, the time to reach stable environmental conditions depends on the autoclave volume, DO level, flow rate, etc. In the ANL test facility, fatigue tests on austenitic SSs in high-DO water required a soaking period of 5-6 days for the ECP of the steel to stabilize. The steel ECP increased from zero or a negative value to above 150 mV during this period. The results shown in Fig. 45a for MA Heat 30956 of Type 304 SS in high-DO water (closed circles) were obtained for specimens that were soaked for 5-6 days before the test. The same material tested in high-DO water after soaking for only 24 h showed a significant reduction in fatigue life, as indicated by Fig. 46.

The effect of the conductivity of water and the ECP of the steel on the fatigue life of austenitic SSs is shown in Fig. 46. In high-DO water, fatigue life is decreased by a factor of ≈ 2 when the conductivity of water is increased from ≈ 0.07 to $0.4 \mu\text{S}/\text{cm}$. Note that environmental effects appear more significant for the specimens that were soaked for only 24 h. For these tests, the ECP of steel was initially very low and increased during the test.

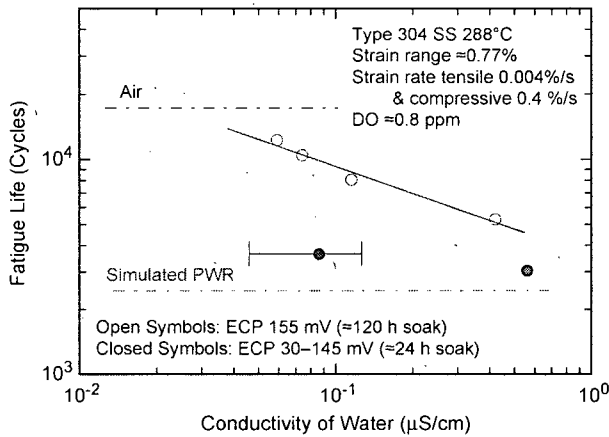


Figure 46. Effects of conductivity of water and soaking period on fatigue life of Type 304 SS in high-DO water (Ref. 7,38).

• Effects of water chemistry on fatigue life have not been considered in the determination of F_{en} . Additional guidance may be needed for excursions of off-normal water chemistry conditions.

5.2.7 Temperature

The change in fatigue lives of austenitic SSs with test temperature at two strain amplitudes and two strain rates is shown in Fig. 47. The results suggest a threshold temperature of 150°C, above which the environment decreases fatigue life in low-DO water if the strain rate is below the threshold of 0.4%/s. In the range of 150–325°C, the logarithm of fatigue life decreases linearly with temperature. Only a moderate decrease in life occurs in water at temperatures below the threshold value of 150°C.

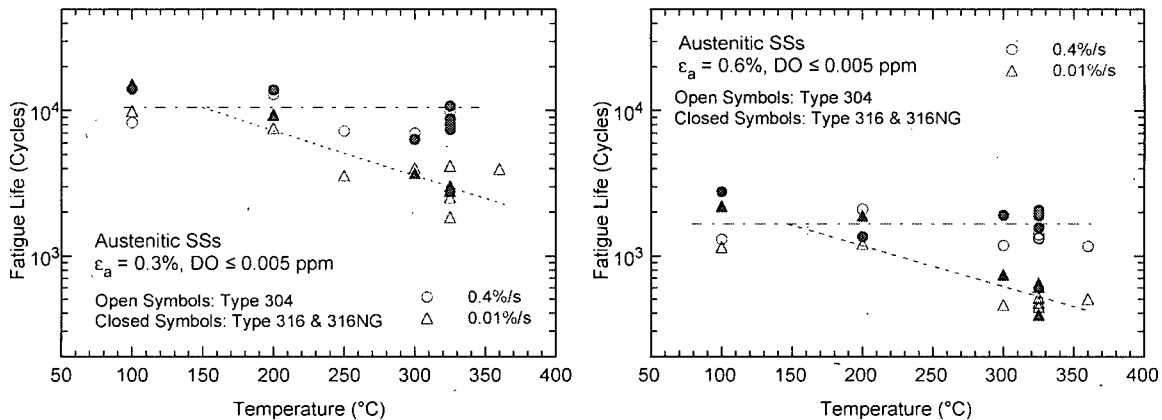


Figure 47. Change in fatigue lives of austenitic stainless steels in low-DO water with temperature (Refs. 7,23–25,28,38–40).

Fatigue tests have been conducted at MHI in Japan on Type 316 SS under combined mechanical and thermal cycling.²³ Triangular waveforms were used for both strain and temperature cycling. Two sequences were selected for temperature cycling: (i) an in-phase sequence, in which temperature cycling was synchronized with mechanical strain cycling, and (ii) a sequence in which temperature and strain were out of phase, i.e., maximum temperature occurred at minimum strain level and vice versa. Two temperature ranges, 100–325°C and 200–325°C, were selected for the tests. The results are shown in Fig. 48, along with data obtained from tests at constant temperature. An average temperature is used in

Fig. 48 for the thermal cycling tests. Because environmental effects are considered to be moderate below threshold values of 150°C for temperature and $\approx 0.25\%$ for strain range, the average temperature for the thermal cycling tests was determined from higher value between 150°C and temperature at threshold strain for in-phase tests, and the lower value between maximum temperature and temperature at threshold strain for out-of-phase tests.

The results in Fig. 48 indicate that for load cycles involving variable temperature, average temperature gives the best estimate of fatigue life. Also, as expected, the fatigue lives of the in-phase tests are shorter than those for the out-of-phase tests. For the thermal cycling tests, fatigue life is longer for out-of-phase tests than for in-phase tests, because applied strains above the threshold strain occur at high temperatures for in-phase tests, whereas they occur at low temperatures for out-of-phase tests. The results from the thermal cycling tests (triangles) agree well with those from the constant-temperature tests (open circles).

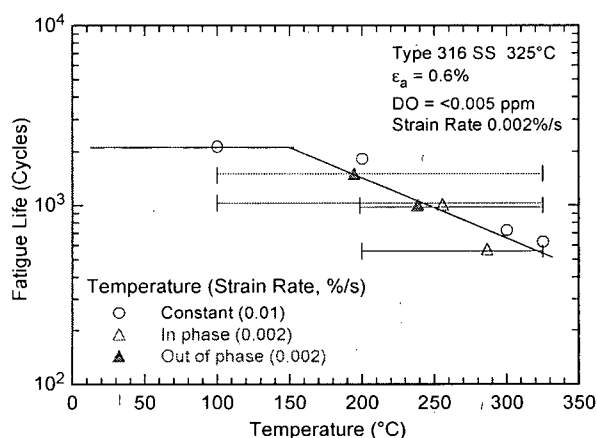


Figure 48. Fatigue life of Type 316 stainless steel under constant and varying test temperature (Ref. 23).

Another study conducted by the Japan Nuclear Safety Organization on Type 316 SS under combined mechanical and thermal cycling in PWR water showed similar results, e.g., the in-phase tests had lower fatigue lives than the out-of-phase tests.^{30,32} These results indicate that load cycles involving variable temperature conditions may be represented by an average temperature.

- In LWR environments, the effect of temperature on the fatigue life of austenitic SSs is explicitly considered in F_{en} , defined in Eq. 38 (Section 5.2.14). Also, guidance is provided to define the temperature to be used to calculate F_{en} for a specific stress cycle or load set pair.

5.2.8 Material Heat Treatment

Limited data indicate that, although heat treatment has little or no effect on the fatigue life of austenitic SSs in low-DO and air environments, in a high-DO environment, fatigue life may be longer for nonsensitized or slightly sensitized SS.⁴⁰ The effect of heat treatment on the fatigue life of Type 304 SS in air, BWR, and PWR environments is shown in Fig. 49. Fatigue life is plotted as a function of the EPR (electrochemical potentiodynamic reactivation) value for the various material conditions. The results indicate that heat treatment has little or no effect on the fatigue life of Type 304 SS in air and PWR environments. In a BWR environment, fatigue life is lower for the sensitized SSs; fatigue life decreases with increasing EPR value.

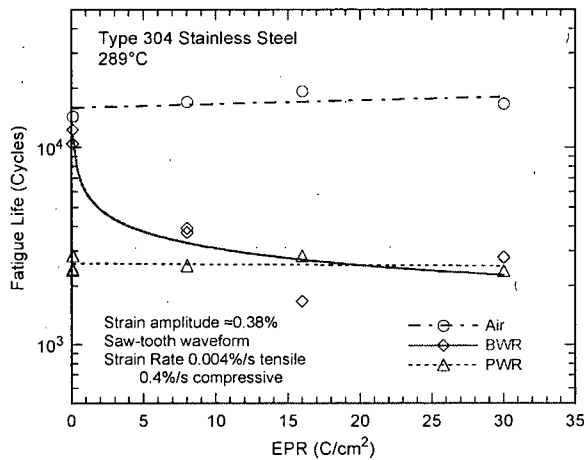


Figure 49.
The effect of material heat treatment on fatigue life of Type 304 stainless steel in air, BWR and PWR environments at 289°C, $\approx 0.38\%$ strain amplitude, sawtooth waveform, and 0.004%/s tensile strain rate (Ref. 40).

These results are consistent with the data obtained at MHI on solution-annealed and sensitized Types 304 and 316 SS.^{21,25} In low-DO (< 0.005 ppm) water at 325°C, a sensitization annealing had no effect on the fatigue lives of these steels. In high-DO (8 ppm) water at 300°C, the fatigue life of sensitized Type 304 SS was a factor of ≈ 2 lower than that of the solution-annealed steel. However, a sensitization anneal had little or no effect on the fatigue life of low-C Type 316NG SS in high-DO water at 288°C, and the lives of solution-annealed and sensitized Type 316NG SS were comparable.

- The effect of heat treatment is not considered in the environmental fatigue correction factor; estimates of F_{en} based on Eq. 38 (Section 5.2.14) may be conservative for some SSs in high-DO water.

5.2.9 Flow Rate

It is generally recognized that flow rate most likely affects the fatigue life of LWR materials because it may cause differences in local environmental conditions in the enclaves of the microcracks formed during early stages in the fatigue ϵ -N test. As discussed in Section 4.2.9, data obtained under typical operating conditions for BWRs indicate that environmental effects on the fatigue life of carbon steels are a factor of ≈ 2 lower at high flow rates (7 m/s) than at low flow rates (0.3 m/s or lower).^{19,20} However, similar tests in both low-DO and high-DO environments indicate that increasing flow rate has no effect or may have a detrimental effect on the fatigue life of austenitic SSs. Figure 50 shows the effect of water flow rate on the fatigue life of Types 316NG and 304 SSs in high-purity water at 289°C. Under

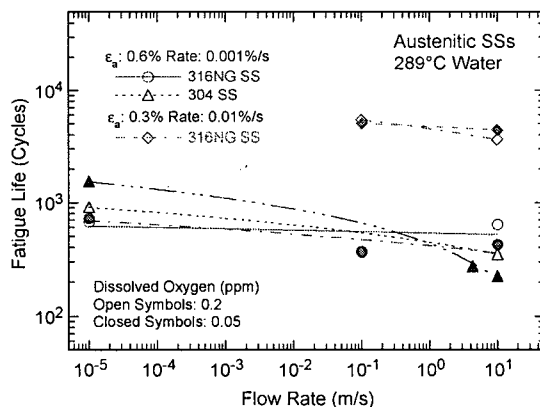


Figure 50.
Effect of water flow rate on the fatigue life of austenitic SSs in high-purity water at 289°C (Ref. 20).

all test conditions, the fatigue lives of these steels are slightly lower at high flow rates than those at lower rates or semi-stagnant conditions.

Fatigue tests conducted on SS pipe bend specimens in simulated PWR primary water at 240°C also indicate that water flow rate has no effect on the fatigue life of austenitic SSs. Increasing the flow rate from 0.005 m/s to 2.2 m/s had no effect on fatigue crack initiation in ≈26.5-mm diameter tube specimens. These results appear to be consistent with the notion that, in LWR environments, the mechanism of fatigue crack initiation in austenitic SSs may differ from that in carbon and low-alloy steels.

- Because of the uncertainties in the flow conditions at or near the locations of crack initiation and the insignificant effect of flow rate, flow rate effects on the fatigue life of austenitic SSs in LWR environments are presently not considered in the fatigue evaluations.

5.2.10 Surface Finish

Fatigue tests have been conducted on Types 304 and 316NG SS specimens that were intentionally roughened in a lathe, under controlled conditions, with 5-grit sandpaper to produce circumferential cracks with an average surface roughness of 1.2 μm. The results are shown in Figs. 51a and b, respectively, for Types 316NG and 304 SS. For both steels, the fatigue life of roughened specimens is lower than that of the smooth specimens in air and low-DO water environments. In high-DO water, the fatigue life of Heat P91576 of Type 316NG is the same for rough and smooth specimens.

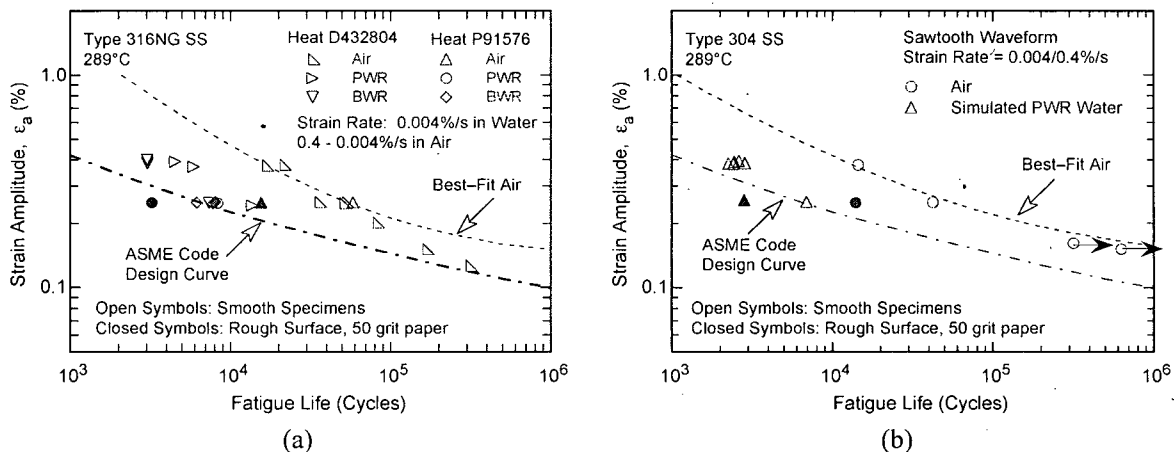


Figure 51. Effect of surface roughness on fatigue life of (a) Type 316NG and (b) Type 304 stainless steels in air and high-purity water at 289°C.

- The effect of surface finish is not considered in the environmental fatigue correction factor; it is included in the subfactor for "surface finish and environment," which is applied to the mean data curve to develop the Code fatigue design curve in air.

5.2.11 Heat-to-Heat Variability

The effect of material variability and data scatter on the fatigue life of austenitic SSs has been evaluated for the data in LWR environments. The fatigue behavior of each of the heats or loading conditions is characterized by the value of the constant A in the ANL model (e.g., Eq. 6). The values of A for the various data sets are ordered, and median ranks are used to estimate the cumulative distribution of A for the population. The results in water environments are shown in Fig. 52. The median value of A

in water is 6.157. The results indicate that environmental effects are approximately the same for the various heats of these steels. For example, the cumulative distribution of data sets for specific heats is approximately the same in air and water environments. The ANL model seems to over-estimate the effect of environment for a few heats, e.g., the ranking for Type 304 SS heat 3 is ≈ 25 percentile in air (Fig. 35) and ≈ 85 percentile in water (Fig. 52).

The values for constant A that provide bounds for the portion of the population and the confidence that is desired in the estimates of the bounds for austenitic SSs in LWR environments are summarized in Table 10. In LWR environments, the 5th percentile value of Parameter A at a 95% confidence level is 5.401. Thus, for the median value of 6.157 for the sample (Table 10), the 95/95 value of the margin to account for material variability and data scatter is 2.3 on life. This margin is needed to provide 95% confidence that the resultant life will be greater than that observed for 95% of the materials of interest.

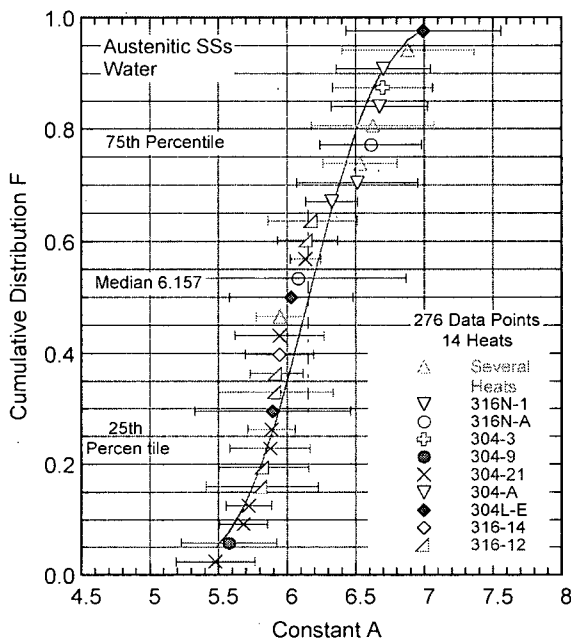


Figure 52. Estimated cumulative distribution of constant A in the ANL model for fatigue life for heats of austenitic SSs in water.

Table 10. Values of parameter A in the ANL fatigue life model and the margins on life for austenitic SSs in water as a function of confidence level and percentage of population bounded.

Confidence Level	Percentage of Population Bounded (Percentile Distribution of A)				
	95 (5)	90 (10)	75 (25)	67 (33)	50 (50)
<u>Values of Parameter A</u>					
50	5.481	5.630	5.880	5.976	6.157
75	5.414	5.570	5.828	5.925	6.104
95	5.317	5.483	5.752	5.851	6.028
<u>Margins on Life</u>					
50	2.0	1.7	1.3	1.2	1.0
75	2.1	1.8	1.4	1.3	1.1
95	2.3	2.0	1.5	1.4	1.1

- The heat-to-heat variability is included in the Code fatigue design curves as part of the subfactor that is applied to the room-temperature mean data curve to account for "data scatter and material variability."

5.2.12 Cast Stainless Steels

Available fatigue ϵ - N data^{23,28,37,38} indicate that, in air, the fatigue lives of cast CF-8 and CF-8M SSs are similar to that of wrought austenitic SSs. The fatigue lives of cast austenitic SSs also decrease in LWR coolant environments. Limited data suggest that the fatigue lives of cast SSs in high-DO water are approximately the same as those in low-DO water. In LWR environments the fatigue lives of cast SSs are comparable to those of wrought SSs in low-DO water. Also, the fatigue lives of these steels are relatively insensitive to changes in ferrite content in the range of 12–28%.^{23,28} Also, existing data are inadequate to establish the dependence of fatigue life on temperature in LWR environments.

The effect of thermal aging at 250–400°C on the fracture toughness properties of cast SSs are well established, fracture toughness is decreased significantly after thermal aging because of the spinodal decomposition of the ferrite phase to form Cr-rich α' phase.^{117,118} The cyclic-hardening behavior of cast austenitic SSs is also influenced by thermal aging.³⁸ At 288°C, cyclic stresses of cast SSs aged for 10,000 h at 400°C are higher than those for unaged material or wrought SSs. Also, strain rate effects on cyclic stress are greater for aged than for unaged steel, i.e., cyclic stresses increase significantly with decreasing strain rate. The existing data are too sparse to establish the effects of thermal aging on strain-rate effects on the fatigue life of cast SSs in air. Limited data in low-DO water at 288°C indicate that thermal aging for 10,000 h at 400°C decreases the fatigue life of CF-8M steels, Fig. 53b.³⁸ Note that thermal aging of another heat of CF-8M steel for 25,200 h at 465°C, Fig. 53a, had little or no effect on fatigue life. The different behavior for the two steels may be attributed to differences in the microstructure produced after thermal aging at 400°C as apposed to 465°C. Thermal aging at 400°C results in spinodal decomposition of the ferrite phase which strengthens the ferrite phase and increases cyclic hardening. Thermal aging at 465°C results in the nucleation and growth of large α' particles and other phases such as sigma phase, which do not change the tensile or cyclic hardening properties of the material.

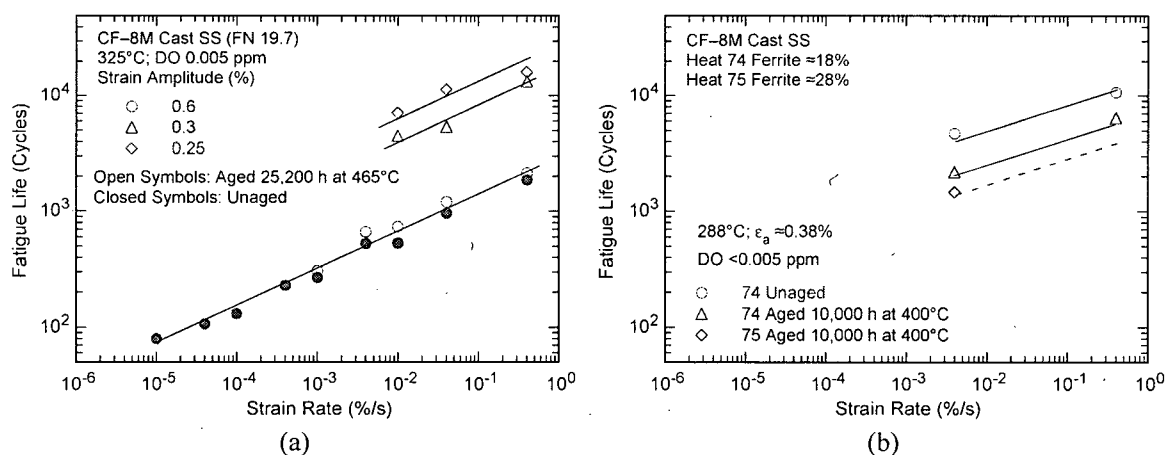


Figure 53. Dependence of fatigue lives of CF-8M cast SSs on strain rate in low-DO water at various strain amplitudes (Refs. 23,28,37,38).

The decrease in fatigue life with decreasing strain rate for three heats of CF-8M cast SS in low-DO water at 325 and 288°C is shown in Fig. 53; the effects of strain rate on the fatigue life of cast SSs are similar to those for wrought SSs. However, for an unaged heat of CF-8M steel with $\approx 20\%$ ferrite, environmental effects on life do not appear to saturate even at strain rates as low as 0.00001%/s.^{23,28} Similar results have also been reported for unaged CF-8M steels in low-DO water at 325°C.¹¹⁹ Based

on these results, the saturation strain rate of 0.0004%/s, recommended for wrought SSs (Eq. 36 in Section 5.2.13), has been decreased to 0.00004%/s for cast SS. However, thermal aging may have influenced the results at very low strain rates. All of the tests at low strain rates were obtained on unaged material; as discussed above, available data indicate that thermal aging decreases the fatigue life of CF-8M steel (Fig. 53b). Limited data indicate that the effects of strain rate are the same in low- and high-DO water. Also, such low strain rates (i.e., less than 0.0004%/s) are not likely to occur in the field. In the present report the effects of strain rate and temperature on the fatigue life of cast austenitic SSs are assumed to be similar to those for wrought SSs.

The estimated cumulative distribution of constant A in the ANL model for fatigue life for austenitic SSs, including several heats of cast SSs, in air and water environments are shown in Fig. 54. The results for cast SSs are evenly distributed and have insignificant effect on the median value of the constant A, e.g., the values with and without the cast SS data are 6.878 and 6.891, respectively, in air, and 6.147 and 6.157, respectively, in water. Thus, the ANL model for austenitic SSs adequately represent both wrought and cast SSs.

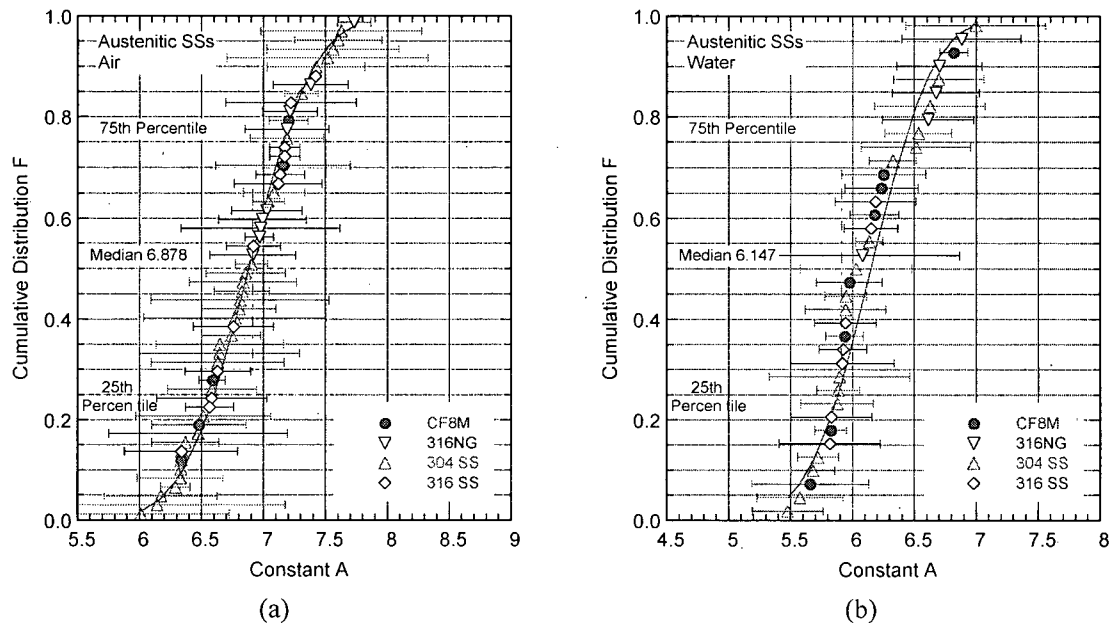


Figure 54. Estimated cumulative distribution of constant A in the ANL model for fatigue life of wrought and cast austenitic stainless steels in (a) air and (b) water environments.

5.2.13 Fatigue Life Model

In LWR environments, the fatigue life of austenitic SSs depends on strain rate, DO level, and temperature; the effects of these and other parameters on the fatigue life of austenitic SSs are discussed in detail below. The functional forms for the effects of strain rate and temperature are based on the data trends. For both wrought and cast austenitic SSs, the model assumes threshold and saturation values of 0.4 and 0.0004%/s, respectively, for strain rate and a threshold value of 150°C for temperature.

The influence of DO level on the fatigue life of austenitic SSs is not well understood. As discussed in Section 5.2.5, the fatigue lives of austenitic SSs are decreased significantly in low-DO water, whereas in high-DO water they are either comparable or, for some steels, higher than those in low-DO water. In

high-DO water, the composition and heat treatment of the steel influence the magnitude of environmental effects on austenitic SSs. Until more data are available to clearly establish the effects of DO level on fatigue life, the effect of DO level on fatigue life is assumed to be the same in low- and high-DO water and for wrought and cast austenitic SSs.

The least-squares fit of the experimental data in water yields a steeper slope for the ϵ -N curve than the slope of the curve obtained in air.^{38,82} These results indicate that environmental effect may be more pronounced at low than at high strain amplitudes. Differing slopes for the ϵ -N curves in air and water environments would add complexity to the determination of the environmental fatigue correction factor F_{en} , discussed in the next section. In the ANL model, the slope of the ϵ -N curve is assumed to be the same in LWR and air environments. In LWR environments, fatigue data for austenitic SSs are best represented by the equation:

$$\ln(N) = 6.157 - 1.920 \ln(\epsilon_a - 0.112) + T' \dot{\epsilon}' O', \quad (34)$$

where T' , $\dot{\epsilon}'$, and O' are transformed temperature, strain rate, and DO, respectively, defined as follows:

$$\begin{aligned} T' &= 0 && (T < 150^\circ\text{C}) \\ T' &= (T - 150)/175 && (150 \leq T < 325^\circ\text{C}) \\ T' &= 1 && (T \geq 325^\circ\text{C}) \end{aligned} \quad (35)$$

$$\begin{aligned} \dot{\epsilon}' &= 0 && (\dot{\epsilon} > 0.4\%/s) \\ \dot{\epsilon}' &= \ln(\dot{\epsilon}/0.4) && (0.0004 \leq \dot{\epsilon} \leq 0.4\%/s) \\ \dot{\epsilon}' &= \ln(0.0004/0.4) && (\dot{\epsilon} < 0.0004\%/s) \end{aligned} \quad (36)$$

$$O' = 0.281 \quad (\text{all DO levels}). \quad (37)$$

These models are recommended for predicted fatigue lives $\leq 10^6$ cycles. Note that Eq. 34 is based on the updated ANL model for austenitic SSs in air (Eq. 32) and the analysis presented in Section 5.2.11. A single expression is used for Types 304, 304L, 316, 316L, and 316NG SSs, and constant A and slope B in the equation are different from the values reported earlier in NUREG/CR-5704, -6815, and -6878. Equations 34-37 can also be used for cast austenitic SSs such as CF-3, CF-8, and CF-8M. Also, because the influence of DO level on the fatigue life of austenitic SSs may be influenced by the material composition and heat treatment, the ANL fatigue life model may be somewhat conservative for some SSs in high-DO water.

The experimental values of fatigue life and those predicted by Eq. 34 for austenitic SSs in LWR environments are plotted in Fig. 55. The predicted fatigue lives show good agreement with the experimental values. The difference between the experimental and predicted values is within a factor of 3 for most tests; the experimental fatigue lives of a few tests on Type 304 SS are up to a factor of ≈ 4 lower than the predicted values, all of these tests were on tube specimens with 1- or 3-mm wall thickness.

- *The ANL model represent the mean values of fatigue life as a function of applied strain amplitude, temperature, strain rate, and DO level in water. The effects of parameters such as mean stress, surface finish, size and geometry, and loading history, which are known to influence fatigue life, are not included in the model.*

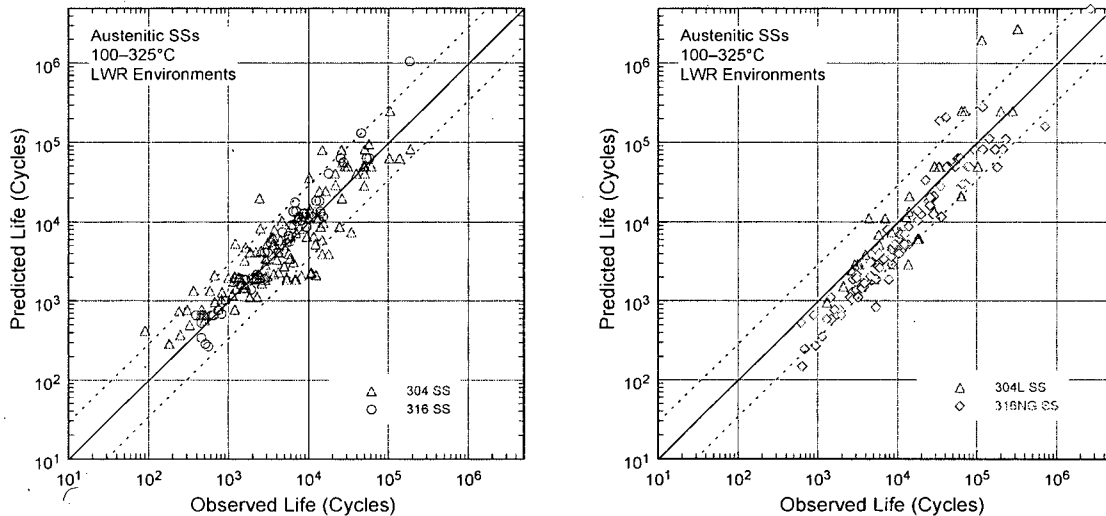


Figure 55. Experimental and predicted values of fatigue lives of austenitic SSs in LWR environments.

5.2.14 Environmental Correction Factor

The effects of reactor coolant environments on fatigue life have also been expressed in terms of a fatigue life correction factor F_{en} , which is defined as the ratio of life in air at room temperature to that in water at the service temperature. The fatigue life correction factor for austenitic SSs, based on the ANL model, is given by

$$F_{en} = \exp(0.734 - T' \epsilon' O'), \quad (38)$$

where the constants T' , ϵ' , and O' are defined in Eqs. 35–37. Note that because the ANL model for austenitic SSs has been updated in the present report, the constant 0.734 in Eq. 38 is different from the values reported earlier in NUREG/CR–5704, 6815, and 6878. Relative to the earlier expressions, correction factors determined from Eq. 38 are 45–60% lower. A threshold strain amplitude (one-half of the applied strain range) is also defined, below which LWR coolant environments have no effect on fatigue life, i.e., $F_{en} = 1$. The threshold strain amplitude is 0.10% (195 MPa stress amplitude) for austenitic SSs. To incorporate environmental effects into a Section III fatigue evaluation, the fatigue usage for a specific stress cycle, based on the proposed new fatigue design curve (Fig. 37 and Table 9 in Section 5.1.8), is multiplied by the correction factor. Further details for incorporating environmental effects into fatigue evaluations are presented in Appendix A.

- The F_{en} approach may be used to incorporate environmental effects into the Code fatigue evaluations.

This page is intentionally left blank.

6 Ni-Cr-Fe Alloys and Welds

The relevant fatigue ϵ - N data for Ni-Cr-Fe alloys and their welds in air and water environments include the data compiled by Jaske and O'Donnell⁷² for developing fatigue design criteria for pressure vessel alloys; the JNUFAD database from Japan; studies at MHI, IHI, and Hitachi in Japan;³³ studies at Knolls Atomic Power Laboratory;^{76,77} work sponsored by EPRI at Westinghouse Electric Corporation;⁷⁵ the tests performed by GE in a test loop at the Dresden I reactor;⁸ and the results of Van Der Sluys et al.⁷⁸ For Alloys 600 and 690, nearly 70% of the tests in air were conducted at room temperature and the remainder at 83–325°C. For Ni-Cr-Fe alloy welds (e.g., Alloys 82, 182, 132, and 152) nearly 85% of the tests in air were conducted at room temperature. In water, nearly 60% of the tests were conducted in simulated BWR environment (≈ 0.2 ppm DO) and 40% in PWR environment (< 0.01 ppm DO); tests in BWR water were performed at 288°C and in PWR water at 315 or 325°C. The existing fatigue data also include some tests in water with all volatile treatment (AVT) and at very high frequencies, e.g., 20 Hz to 40 kHz.⁷⁵ As expected, environmental effects on fatigue life were not observed for these tests; the results in AVT water are not included in the present analysis.

6.1 Air Environment

6.1.1 Experimental Data

The fatigue ϵ - N data for Alloys 600 and 690 in air at temperatures between room temperature and 316°C are shown in Fig. 56, and those for Ni-Cr-Fe alloy welds (e.g., Alloys 82, 182, 132, and 152) in air at temperatures between room temperature and 315°C are shown in Fig. 57. The best-fit curve for austenitic SSs based on the updated ANL model (Eq. 32 in Section 5.1.7) and the ASME Section III mean-data curve are included in the figures. The results indicate that although the data for Alloy 690 are very limited, the fatigue lives of Alloy 690 are comparable to those of Alloy 600 (Fig. 56). Similarly, the fatigue lives of Alloy 152 weld are comparable to those of Alloys 82, 182, and 132 welds (Fig. 57). Also, the fatigue lives of the Ni-Cr-Fe alloy welds are comparable to those of the wrought Alloys 600 and 690 in the low-cycle regime (i.e., $< 10^5$ cycles) and are slightly superior to the lives of wrought materials in the high-cycle regime.

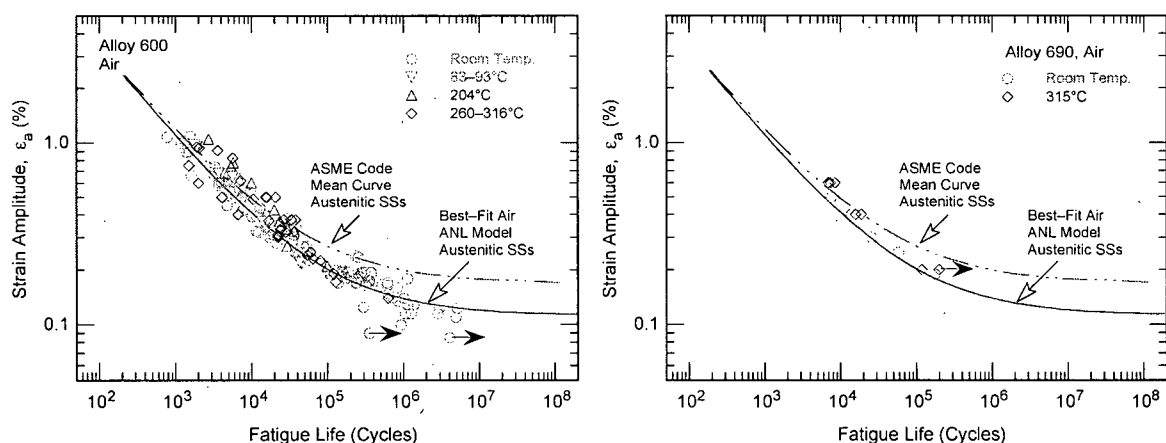


Figure 56. Fatigue ϵ - N behavior for Alloys 600 and 690 in air at temperatures between room temperature and 315°C (Refs. JNUFAD data, 72, 75–78).

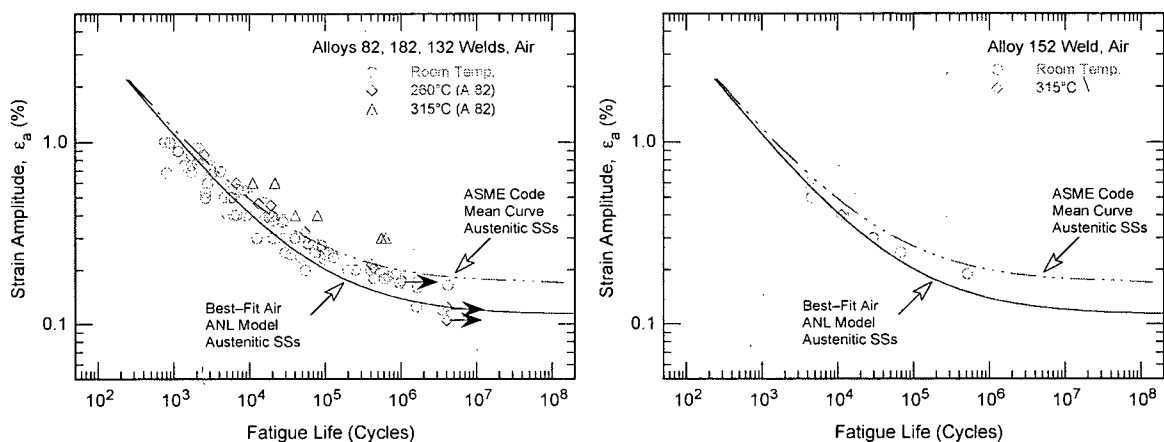


Figure 57. Fatigue ϵ - N behavior for Alloys 82, 182, 132, and 152 welds in air at various temperatures (Refs. JNUFAD data, 72-78).

The fatigue lives of Alloy 600 are generally longer at high temperatures than at room temperature (Fig. 56a).⁷⁵⁻⁷⁷ A similar behavior is observed for its weld metal, e.g., Alloy 82 (Fig. 57a). However, limited data for Alloy 690 (Fig. 56b) and its weld metal, Alloy 152 (Fig. 57b), indicate little or no effect of temperature on their fatigue lives. The existing data are inadequate to determine the effect of strain rate on the fatigue life of Ni-Cr-Fe alloys.

The results also indicate that the fatigue data for Ni-Cr-Fe alloys, including welds, are not consistent with the current ASME Code mean curve for austenitic SSs. The data for Alloys 600 and 690 show very good agreement with the updated ANL fatigue life model for austenitic SSs (Fig. 56a). Also, the fatigue data for Alloys 82, 182, and 132 are consistent with the updated ANL model in the low-cycle regime and somewhat conservative with respect to the model in the high-cycle regime (Fig. 57a).

- For Alloys 600 and 690 and their welds, the updated ANL fatigue life model proposed in the present report for austenitic SSs (Eq. 32) is either consistent or conservative with respect to the fatigue ϵ - N data.

6.1.2 Fatigue Life Model

For Ni-Cr-Fe alloys, fatigue evaluations are based on the fatigue design curve for austenitic SSs. However, the existing fatigue ϵ - N data for Ni-Cr-Fe alloy and their welds are not consistent with the current ASME Code fatigue design curve for austenitic SSs. As discussed above, the data are either comparable or slightly conservative with respect to the updated ANL model for austenitic SSs, e.g., Eq. 32. Thus, the new fatigue design curve proposed in the present report for austenitic SSs and presented in Fig. 37 and Table 9 adequately represents the fatigue ϵ - N behavior of Ni-Cr-Fe alloys and their welds.

- The new design curve for austenitic SSs may also be used for Ni-Cr-Fe alloys and their welds.

6.2 LWR Environment

6.2.1 Experimental Data

The fatigue lives of Ni-Cr-Fe alloys and their welds are also decreased in LWR environments; the fatigue ϵ -N data for various Ni-Cr-Fe alloys in simulated BWR water at $\approx 289^\circ\text{C}$ and PWR water at $315\text{-}325^\circ\text{C}$ are shown in Figs. 58 and 59, respectively. The ϵ -N curves based on the ANL model for austenitic SSs (Eq. 32 in Section 5.1.7) and the ASME Section III mean-data curve for austenitic SSs are also included in the figures. The results indicate that environmental effects on the fatigue life of Ni-Cr-Fe alloys are strongly dependent on key parameters such as strain rate, temperature, and DO level in water. Similar to SSs, the effect of coolant environment on the fatigue life of Ni-Cr-Fe alloys is greater in the low-DO PWR environment than in the high-DO BWR environment. However, under similar loading and environmental conditions, the extent of the effects of environment is considerably less for the Ni-Cr-Fe alloys than for austenitic SSs. In general, environmental effects on fatigue life are the same for wrought and weld alloys.

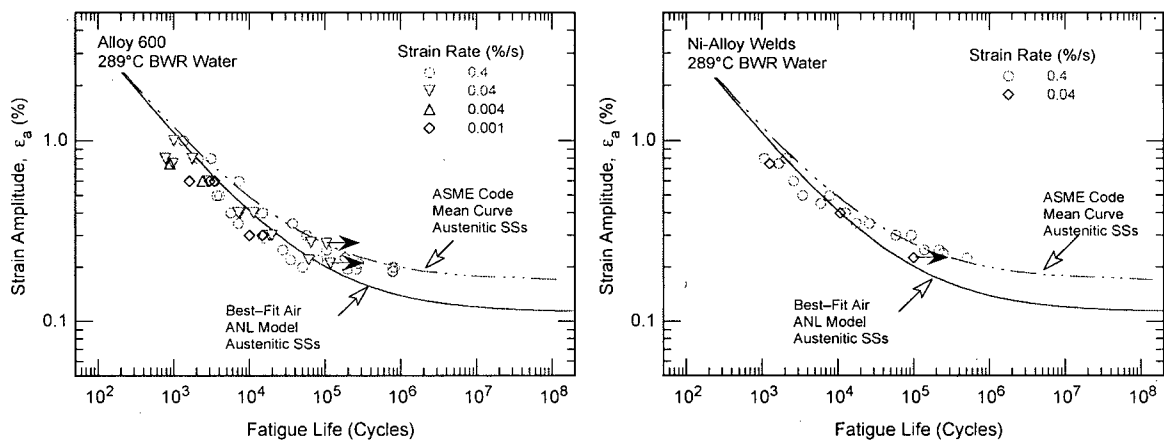


Figure 58. Fatigue ϵ -N behavior for Alloy 600 and its weld alloys in simulated BWR water at $\approx 289^\circ\text{C}$ (Refs. JNUFAD data, 33).

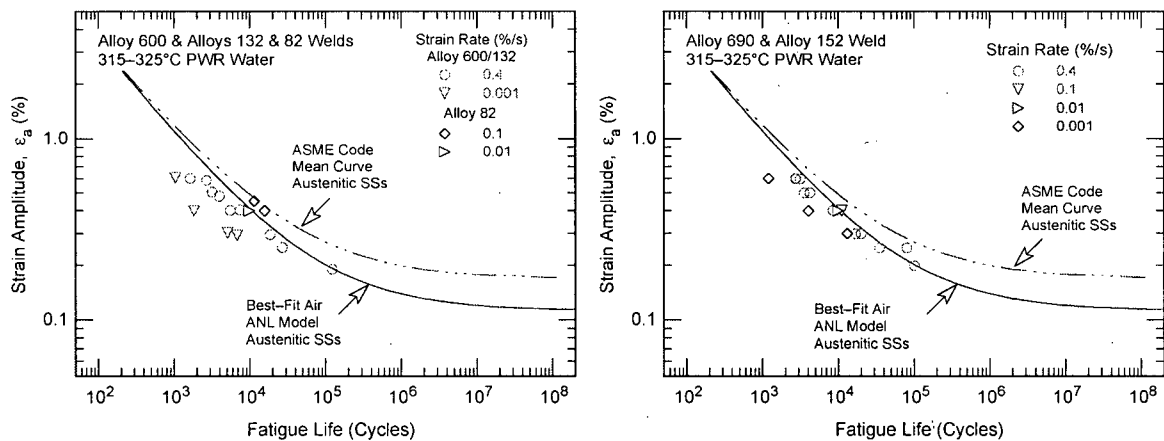


Figure 59. Fatigue ϵ -N behavior for Alloys 600 and 690 and their weld alloys in simulated PWR water at $315\text{ or }325^\circ\text{C}$ (Refs. 33, 78).

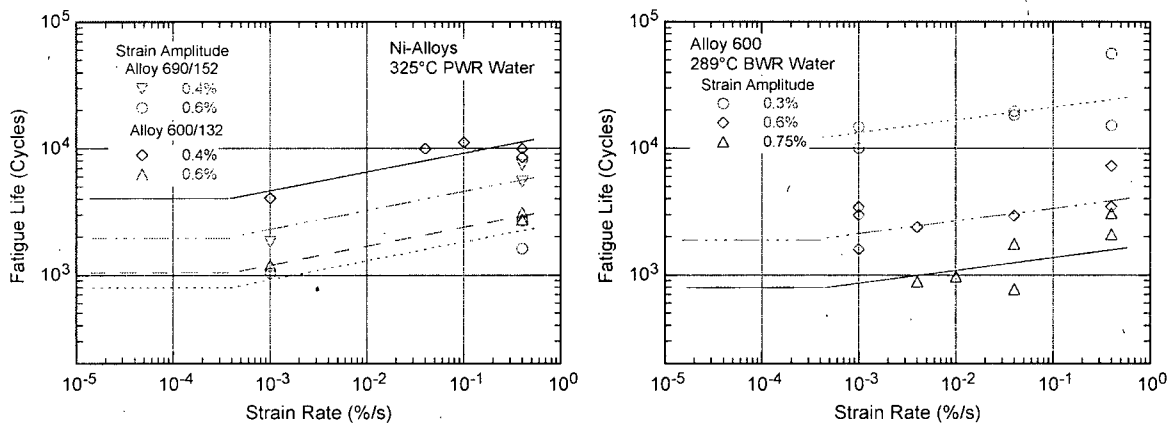


Figure 60. Dependence of fatigue lives of Alloys 690 and 600 and their weld alloys in PWR water at 325°C and Alloy 600 in BWR water at 289°C (Refs. JNUFAD data, 33, 78).

6.2.2 Effects of Key Parameters

The existing fatigue ϵ -N data for Ni-Cr-Fe alloys in LWR environments are very limited; the effects of the key loading and environmental parameters (e.g., strain rate, temperature, and DO level) on fatigue life of these alloys have been evaluated by Higuchi et al.³³ The fatigue lives of Alloys 600 and 690 and their weld metals (e.g., Alloys 132 and 152) in simulated PWR and BWR water at different strain amplitudes are plotted as a function of strain rate in Fig. 60. The fatigue life of these alloys decreases logarithmically with decreasing strain rate. Although fatigue data at strain rates below 0.001%/s are not available, for Ni-Cr-Fe alloys, the effect of strain rate is assumed to be similar to that for austenitic SSs; the effect saturates at 0.0004%/s strain rate. Also, the threshold strain rate below which environmental effects are significant cannot be determined from the present data. Higuchi et al.³³ have defined a threshold strain rate of 1.8%/s in high-DO BWR water and 26.1%/s in low-DO PWR water. As discussed in Section 6.2.3, an average threshold value of 5%/s provides good estimates of fatigue lives of Ni-Cr-Fe alloys in LWR environments.

The results also indicate that the effects of environment are greater in the low-DO PWR water than in high-DO BWR water. For example, a three orders of magnitude decrease in strain rate decreases the fatigue life of these alloys by a factor of ≈ 3 in PWR water and by ≈ 2 in BWR water.

The existing data are inadequate to determine accurately the functional form for the effect of temperature on fatigue life or to define the threshold strain amplitude below which environmental effects on fatigue life do not occur. Such effects are assumed to be similar to those observed in austenitic SSs. It is also assumed that a slow strain rate applied during the tensile-loading cycle (i.e., up-ramp with increasing strain) is primarily responsible for the environmentally assisted reduction in fatigue life. Slow rates applied during both tensile- and compressive-loading cycles (i.e., up- and down-ramps) do not further decrease fatigue life compared with that observed for tests with only a slow tensile-loading cycle. Thus, loading and environmental conditions during the tensile-loading cycle are important for environmentally assisted reduction of the fatigue lives of Ni-Cr-Fe alloys.

6.2.3 Environmental Correction Factor

The effects of reactor coolant environments on fatigue life of Ni-Cr-Fe alloys can also be expressed in terms of a fatigue life correction factor F_{en} , which is defined as the ratio of life in air at room

temperature to that in water at the service temperature. The existing fatigue data are very limited to develop a fatigue life model for estimating the fatigue life of Ni-Cr-Fe alloys in LWR environments. However, as discussed above in Section 6.2.2, environmental effects for these alloys show the same trends as those observed for austenitic SSs. Thus, F_{en} for Ni-Cr-Fe alloys can be expressed as

$$F_{en} = \exp(T' \dot{\epsilon}' O'), \quad (39)$$

where T' , $\dot{\epsilon}'$, and O' are transformed temperature, strain rate, and DO, respectively. The functional forms for these transformed parameters were obtained from the best fit of the experimental data and are defined as follows:

$$\begin{aligned} T' &= T/325 && (T < 325^\circ\text{C}) \\ T' &= 1 && (T \geq 325^\circ\text{C}) \end{aligned} \quad (40)$$

$$\begin{aligned} \dot{\epsilon}' &= 0 && (\dot{\epsilon} > 5.0\%/s) \\ \dot{\epsilon}' &= \ln(\dot{\epsilon}/5.0) && (0.0004 \leq \dot{\epsilon} \leq 5.0\%/s) \\ \dot{\epsilon}' &= \ln(0.0004/5.0) && (\dot{\epsilon} < 0.0004\%/s) \end{aligned} \quad (41)$$

$$\begin{aligned} O' &= 0.09 && (\text{NWC BWR water}) \\ O' &= 0.16 && (\text{PWR or HWC BWR water}). \end{aligned} \quad (42)$$

The fatigue life of Ni-Cr-Fe alloys in LWR environments can be estimated from Eqs. 32 and 39–42. The experimental and estimated fatigue lives of various Ni-Cr-Fe alloys in BWR and PWR water are plotted in Fig. 61; the estimated values are either comparable or longer than those observed experimentally.

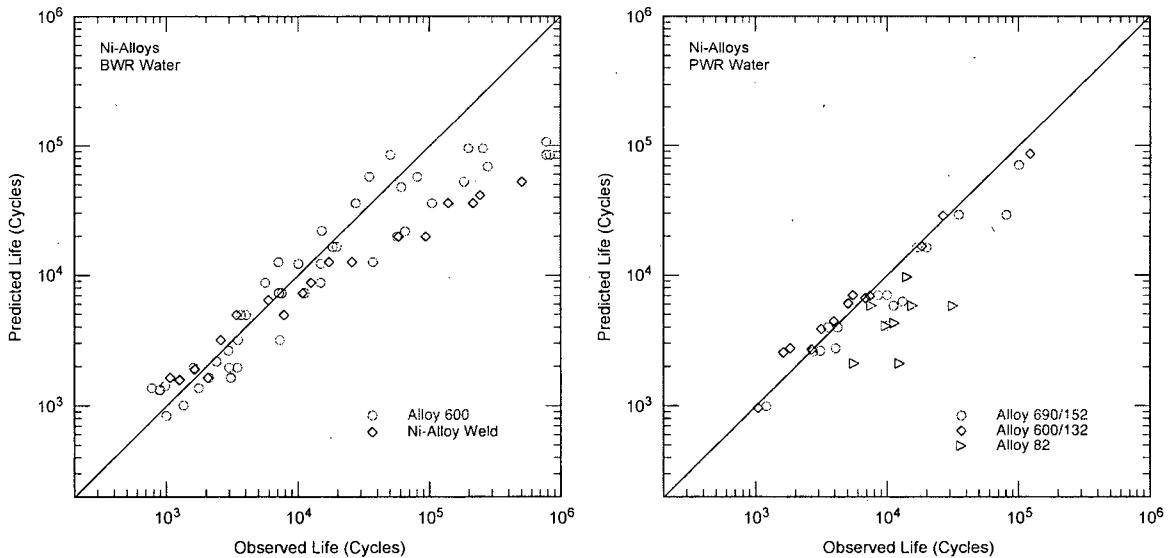


Figure 61. The experimental and estimated fatigue lives of various Ni alloys in BWR and PWR environments (Refs. JNUFAD data, 33, 78).

A threshold strain amplitude (one-half of the applied strain range) is also defined, below which LWR coolant environments have no effect on fatigue life, i.e., $F_{en} = 1$. The value is assumed to be the same as that for austenitic SSs. The threshold strain amplitude is 0.10% (195 MPa stress amplitude) for Ni-Cr-Fe alloys. To incorporate environmental effects into a Section III fatigue evaluation, the fatigue

usage for a specific stress cycle, based on the proposed new fatigue design curve for austenitic SSs (Fig. 37 and Table 9 in Section 5.1.8), is multiplied by the correction factor. Further details for incorporating environmental effects into fatigue evaluations are presented in Appendix A.

- *The F_{en} approach may be used to incorporate environmental effects into the Code fatigue evaluations.*

7 Margins in ASME Code Fatigue Design Curves

Conservatism in the ASME Code fatigue evaluations may arise from (a) the fatigue evaluation procedures and/or (b) the fatigue design curves. The overall conservatism in ASME Code fatigue evaluations has been demonstrated in fatigue tests on components.^{120,121} Mayfield et al.¹²⁰ have shown that, in air, the margins on the number of cycles to failure for elbows and tees were 40–310 and 104–510, respectively, for austenitic SS and 118–2500 and 123–1700, respectively, for carbon steel. The margins for girth butt welds were significantly lower, 6–77 for SS and 14–128 for carbon steel. Data obtained by Heald and Kiss¹²¹ on 26 piping components at room temperature and 288°C showed that the design margin for cracking exceeds 20, and for most of the components, it is >100. In these tests, fatigue life was expressed as the number of cycles for the crack to penetrate through the wall, which ranged in thickness from 6 to 18 mm. Consequently, depending on wall thickness, the actual margins to form a 3-mm crack may be lower by a factor of more than 2.

Deardorff and Smith¹²² discussed the types and extent of conservatism present in the ASME Section III fatigue evaluation procedures and the effects of LWR environments on fatigue margins. The sources of conservatism in the procedures include the use of design transients that are significantly more severe than those experienced in service, conservative grouping of transients, and use of simplified elastic-plastic analyses that lead to higher stresses. The authors estimated that the ratio of the CUFs computed with the mean experimental curve for test specimen data in air and more accurate values of the stress to the CUFs computed with the Code fatigue design curve were ≈ 60 and 90, respectively, for PWR and BWR nozzles. The reductions in these margins due to environmental effects were estimated to be factors of 5.2 and 4.6 for PWR and BWR nozzles, respectively. Thus, Deardorff and Smith¹²² argue that, after accounting for environmental effects, factors of 12 and 20 on life for PWR and BWR nozzles, respectively, account for uncertainties due to material variability, surface finish, size, mean stress, and loading sequence.

However, other studies on piping and components indicate that the Code fatigue design procedures do not always ensure large margins of safety.^{123,124} Southwest Research Institute performed fatigue tests in room-temperature water on 0.91-m-diameter carbon and low-alloy steel vessels.¹²³ In the low-cycle regime, ≈ 5 -mm-deep cracks were initiated slightly above (a factor of < 2) the number of cycles predicted by the ASME Code design curve (Fig. 62a). Battelle-Columbus conducted tests on 203-mm or 914-mm carbon steel pipe welds at room temperature in an inert environment, and Oak Ridge National Laboratory (ORNL) performed four-point bend tests on 406-mm-diameter Type 304 SS pipe removed from the C-reactor at the Savannah River site.¹²⁴ The results showed that the number of cycles to produce a leak was lower, and in some cases significantly lower, than that expected from the ASME Code fatigue design curves (Fig. 62a and b). The most striking results are for the ORNL “tie-in” and flawed “test” weld; these specimens cracked completely through the 12.7-mm-thick wall in a life 6 or 7 times shorter than expected from the Code curve. Note that the Battelle and ORNL results represent a through-wall crack; the number of cycles to initiate a 3-mm crack may be a factor of 2 lower.

Much of the margin in the current evaluations arises from design procedures (e.g., stress analysis rules and cycle counting) that, as discussed by Deardorff and Smith,¹²² are quite conservative. However, the ASME Code permits new and improved approaches to fatigue evaluations (e.g., finite-element analyses, fatigue monitoring, and improved K_e factors) that can significantly decrease the conservatism in the current fatigue evaluation procedures.

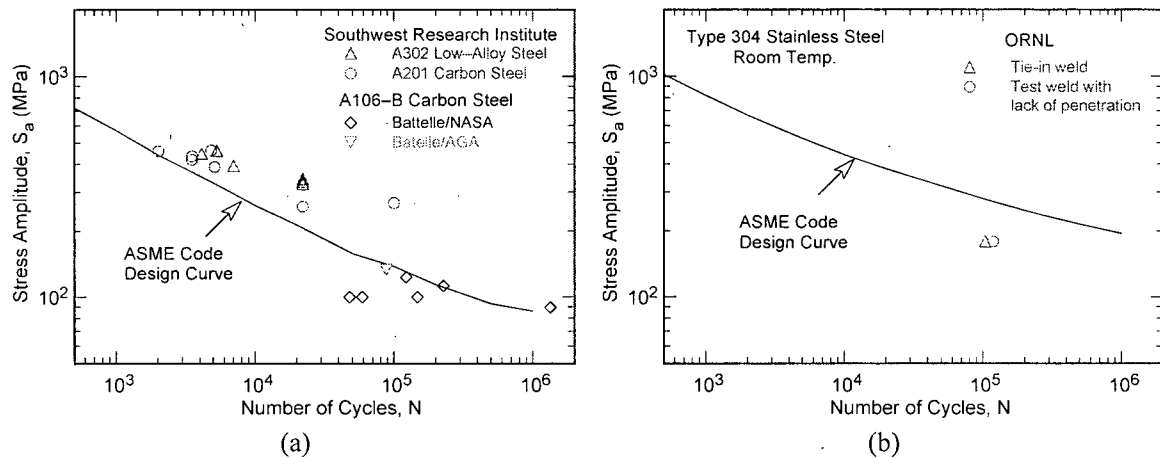


Figure 62. Fatigue data for (a) carbon and low-alloy steel and (b) Type 304 stainless steel components (Refs. 123,124).

The factors of 2 on stress and 20 on cycles used in the Code were intended to cover the effects of variables that can influence fatigue life but were not investigated in the tests that provided the data for the curves. It is not clear whether the particular values of 2 and 20 include possible conservatism. A study sponsored by the PVRC to assess the margins of 2 and 20 in fatigue design curves concluded that these margins should not be changed.¹²⁵

The variables that can affect fatigue life in air and LWR environments can be broadly classified into three groups:

- (a) Material
 - (i) Composition
 - (ii) Metallurgy: grain size, inclusions, orientation within a forging or plate
 - (iii) Processing: cold work, heat treatment
 - (iv) Size and geometry
 - (v) Surface finish: fabrication surface condition
 - (vi) Surface preparation: surface work hardening
- (b) Loading
 - (i) Strain rate: rise time
 - (ii) Sequence: linear damage summation or Miner's rule
 - (iii) Mean stress
 - (iv) Biaxial effects: constraints
- (c) Environment
 - (i) Water chemistry: DO, lithium hydroxide, boric acid concentrations
 - (ii) Temperature
 - (iii) Flow rate

The existing fatigue ϵ - N database covers an adequate range of material parameters (i-iii), a loading parameter (i), and the environment parameters (i-ii); therefore, the variability and uncertainty in fatigue life due to these parameters have been incorporated into the model. The existing data are most likely conservative with respect to the effects of surface preparation because the fatigue ϵ - N data are obtained for specimens that are free of surface cold work. Fabrication procedures for fatigue test specimens

generally follow American Society for Testing and Materials (ASTM) guidelines, which require that the final polishing of the specimens avoid surface work-hardening. Biaxial effects are covered by design procedures and need not be considered in the fatigue design curves.

As discussed earlier, under the conditions typical of operating BWRs, environmental effects on the fatigue life are a factor of ≈ 2 lower at high flow rates (7 m/s) than those at very low flow rates (0.3 m/s or lower) for carbon and low-alloy steels and are independent of flow rate for austenitic SSs.^{19,20} However, because of the uncertainties in the flow conditions at or near the locations of crack initiation, the beneficial effect of flow rate on the fatigue life of carbon and low-alloy steels is presently not included in fatigue evaluations.

Thus, the contributions of four groups of variables, namely, material variability and data scatter, specimen size and geometry, surface finish, and loading sequence (Miner's rule), must be considered in developing fatigue design curves that are applicable to components.

7.1 Material Variability and Data Scatter

The effects of material variability and data scatter must be included to ensure that the design curves not only describe the available test data well, but also adequately describe the fatigue lives of the much larger number of heats of material that are found in the field. The effects of material variability and data scatter have been evaluated for the various materials by considering the best-fit curves determined from tests on individual heats of materials or loading conditions as samples of the much larger population of heats of materials and service conditions of interest. The fatigue behavior of each of the heats or loading conditions is characterized by the value of the constant A in Eq. 6. The values of A for the various data sets are ordered, and median ranks are used to estimate the cumulative distribution of A for the population. The distributions were fit to lognormal curves. The median value of A and standard deviation for each sample, as well as the number of data sets in the sample, are listed in Table 11. The 95/95 value of the margin on the median value to account for material variability and data scatter vary from 2.1 to 2.8 for the various samples. These margins applied to the mean value of life determined from the ANL fatigue life models provide 95% confidence that the fatigue life of 95 percentile of the materials and loading conditions of interest will be greater than the resultant value.

Table 11. The median value of A and standard deviation for the various fatigue ϵ -N data sets used to evaluate material variability and data scatter.

	Air Environment			Water Environment		
	Median Value of A	Standard Deviation	Number of Data Sets	Median Value of A	Standard Deviation	Number of Data Sets
Carbon Steel	6.583	0.477	17	5.951	0.376	33
Low-Alloy Steel	6.449	0.375	32	5.747	0.484	26
Stainless Steel	6.891	0.417	51	6.328	0.462	36

7.2 Size and Geometry

The effect of specimen size on the fatigue life was reviewed in earlier reports.^{6,39} Various studies conclude that "size effect" is not a significant parameter in the design curve margins when the fatigue curve is based on data from axial strain control rather than bending tests. No intrinsic size effect has been observed for smooth specimens tested in axial loading or plain bending. However, a size effect does occur in specimens tested in rotating bending; the fatigue endurance limit decreases by $\approx 25\%$ if the specimen size is increased from 2 to 16 mm but does not decrease further with larger sizes. Also, some effect of size and geometry has been observed on small-scale-vessel tests conducted at the Ecole

Polytechnique in conjunction with the large-size-pressure-vessel tests carried out by the Southwest Research Institute.¹²³ The tests at the Ecole Polytechnique were conducted in room-temperature water on 19-mm-thick shells with ≈ 305 -mm inner diameter nozzles and made of machined bar stock. The results indicate that the fatigue lives determined from tests on the small-scale-vessel are 30–50% lower than those obtained from tests on small, smooth fatigue specimen. However, the difference in fatigue lives in these tests cannot be attributed to specimen size alone, it is due to the effects of both size and surface finish.

During cyclic loading, cracks generally form at surface irregularities either already in existence or produced by slip bands, grain boundaries, second phase particles, etc. In smooth specimens, formation of surface cracks is affected by the specimen size; crack initiation is easier in larger specimens because of the increased surface area and, therefore, increased number of sites for crack initiation. Specimen size is not likely to influence crack initiation in specimens with rough surfaces because cracks initiate at existing irregularities on the rough surface. As discussed in the next section, surface roughness has a large effect on fatigue life. Consequently, for rough surfaces, the effect of specimen size may not be considered in the margin of 20 on life. However, conservatively, a factor of 1.2–1.4 on life may be used to incorporate size effects on fatigue life in the low-cycle regime.

7.3 Surface Finish

The effect of surface finish must be considered to account for the difference in fatigue life expected in actual components with industrial-grade surface finish compared to the smooth polished surface of a test specimen. Fatigue life is sensitive to surface finish; cracks can initiate at surface irregularities that are normal to the stress axis. The height, spacing, shape, and distribution of surface irregularities are important for crack initiation. The effect of surface finish on crack initiation is expressed by Eq. 12 in terms of the RMS value of surface roughness (R_q).

The roughness of machined surfaces or natural finishes can range from ≈ 0.8 to $6.0 \mu\text{m}$. Typical surface finish for various machining processes is in the range of 0.2 – $1.6 \mu\text{m}$ for cylindrical grinding, 0.4 – $3.0 \mu\text{m}$ for surface grinding, 0.8 – $3.0 \mu\text{m}$ for finish turning, and drilling and 1.6 – $4.0 \mu\text{m}$ for milling. For fabrication processes, it is in the range of 0.8 – $3.0 \mu\text{m}$ for extrusion and 1.6 – $4.0 \mu\text{m}$ for cold rolling. Thus, from Eq. 12, the fatigue life of components with such rough surfaces may be a factor of 2–3.5 lower than that of a smooth specimen.

Limited data in LWR environments on specimens that were intentionally roughened indicate that the effects of surface roughness on fatigue life is the same in air and water environments for austenitic SSs, but are insignificant in water for carbon and low-alloy steels. Thus, in LWR environments, a factor of 2.0–3.5 on life may also be used to account for the effects of surface finish on the fatigue life of austenitic SSs, but the factor may be lower for carbon and low-alloy steels, e.g., a factor of 2 may be used for carbon and low-alloy steels.

7.4 Loading Sequence

The effects of variable amplitude loading of smooth specimens were also reviewed in an earlier report.³⁹ In a variable loading sequence, the presence of a few cycles at high strain amplitude causes the fatigue life at smaller strain amplitude to be significantly lower than that at constant-amplitude loading, i.e., the fatigue limit of the material is lower under variable loading histories.

As discussed in Section 2, fatigue life has conventionally been divided into two stages: initiation, expressed as the cycles required to form microstructurally small cracks (MSCs) on the surface, and propagation, expressed as cycles required to propagate these MSCs to engineering size. The transition from initiation to propagation stage strongly depends on applied stress amplitude; at stress levels above the fatigue limit, the transition from initiation to propagation stage occurs at crack depths in the range of 150 to 250 μm . However, under constant loading at stress levels below the fatigue limit of the material (e.g., $\Delta\sigma_1$ in Fig. 1), although microcracks $\approx 10 \mu\text{m}$ can form quite early in life, they do not grow to an engineering size. Under the variable loading conditions encountered during service of power plants, cracks created by growth of MSCs at high stresses ($\Delta\sigma_3$ in Fig. 1) to depths larger than the transition crack depth can then grow to an engineering size even at stress levels below the fatigue limit.

Studies on fatigue damage in Type 304 SS under complex loading histories¹²⁶ indicate that the loading sequence of decreasing strain levels (i.e., high strain level followed by low strain level) is more damaging than that of increasing strain levels. The fatigue life of the steel at low strain levels decreased by a factor of 2–4 under a decreasing-strain sequence. In another study, the fatigue limit of medium carbon steels was lowered even after low-stress high-cycle fatigue; the higher the stress, the greater the decrease in fatigue threshold.¹²⁷ A recent study on Type 316NG and Ti-stabilized Type 316 SS on strain-controlled tests in air and PWR environment with constant or variable strain amplitude reported a factor of 3 or more decrease in fatigue life under variable amplitude compared with constant amplitude.¹²⁸ Although the strain spectrum used in the study was not intended to be representative of real transients, it represents a generic case and demonstrates the effect of loading sequence on fatigue life.

Because variable loading histories primarily influence fatigue life at low strain levels, the mean fatigue ϵ - N curves are lowered to account for damaging cycles that occur below the constant-amplitude fatigue limit of the material. However, conservatively, a factor of 1.2–2.0 on life may be used to incorporate the possible effects of load histories on fatigue life in the low-cycle regime.

7.5 Fatigue Design Curve Margins Summarized

The ASME Code fatigue design curves are currently obtained from the mean data curves by first adjusting for the effects of mean stress, and then reducing the life at each point of the adjusted curve by a factor of 2 on strain and 20 on life, whichever is more conservative. The factors on strain are needed primarily to account for the variation in the fatigue limit of the material caused by material variability, component size, surface finish, and load history. Because these variables affect life through their influence on the growth of short cracks ($<100 \mu\text{m}$), the adjustment on strain to account for such variations is typically not cumulative, i.e., the portion of the life can only be reduced by a finite amount. Thus, it is controlled by the variable that has the largest effect on life. In relating the fatigue lives of laboratory test specimens to those of actual reactor components, the factor of 2 on strain that is currently being used to develop the Code design curves is adequate to account for the uncertainties associated with material variability, component size, surface finish, and load history.

The factors on life are needed to account for variations in fatigue life in the low-cycle regime. Based on the discussions presented above the effects of various material, loading, and environmental parameters on fatigue life may be summarized as follows:

- (a) The results presented in Table 11 may be used to determine the margins that need to be applied to the mean value of life to ensure that the resultant value of life would bound a specific percentile (e.g., 95 percentile) of the materials and loading conditions of interest.

- (b) For rough surfaces, specimen size is not likely to influence fatigue life, and therefore, the effect of specimen size need not be considered in the margin of 20 on life. However, conservatively, a factor of 1.2–1.4 on life may be used to incorporate size effects on fatigue life.
- (c) Limited data indicate that, for carbon and low-alloy steels, the effects of surface roughness on fatigue life are insignificant in LWR environments. A factor of 2 on life may be used for carbon and low-alloy steels in water environments instead of the 2.0–3.5 used for carbon and low-alloy steels in air and for austenitic SSs in both air and water environments.
- (d) Variable loading histories primarily influence fatigue life at low strain levels, i.e., in the high-cycle regime, and the mean fatigue ϵ - N curves are lowered by a factor of 2 on strain to account for damaging cycles that occur below the constant-strain fatigue limit of the material. Conservatively, a factor of 1.2–2.0 on life may be used to incorporate the possible effects of load histories on fatigue life in the low-cycle regime.

The subfactors that are needed to account for the effects of the various material, loading, and environmental parameters on fatigue life are summarized in Table 12. The total adjustment on life may vary from 6 to 27. Because the maximum value represents a relatively poor heat of material and assumes the maximum effects of size, surface finish, and loading history, the maximum value of 27 is likely to be quite conservative. A value of 20 is currently being used to develop the Code design curves from the mean-data curves.

Table 12. Factors on life applied to mean fatigue ϵ - N curve to account for the effects of various material, loading, and environmental parameters.

Parameter	Section III Criterion Document	Present Report
Material Variability and Data Scatter		
(minimum to mean)	2.0	2.1–2.8
Size Effect	2.5	1.2–1.4
Surface Finish, etc.	4.0	2.0–3.5*
Loading History	–	1.2–2.0
Total Adjustment	20	6.0–27.4

*A factor of 2 on life may be used for carbon and low-alloy steels in LWR environments.

To determine the most appropriate value for the design margin on life, Monte Carlo simulations were performed using the material variability and data scatter results given in Table 11, and the margins needed to account for the effects of size, surface finish, and loading history listed in Table 12. A lognormal distribution was also assumed for the effects of size, surface finish, and loading history, and the minimum and maximum values of the adjustment factors, e.g., 1.2–1.4 for size, 2.0–3.5 for surface finish, and 1.2–2.0 for loading history, were assumed to represent the 5th and 95th percentile, respectively. The cumulative distribution of the values of A in the fatigue ϵ - N curve for test specimens and the adjusted curve that represents the behavior of actual components is shown in Fig. 63 for carbon and low-alloy steels and austenitic SSs.

The results indicate that, relative to the specimen curve, the median value of constant A for the component curve decreased by a factor of 5.6 to account for the effects of size, surface finish, and loading history, and the standard deviation of heat-to-heat variation of the component curve increased by 6–10%. The margin that has to be applied to the mean data curve for test specimens to obtain a component curve that would bound 95% of the population, is 11.0–12.7 for the various materials; the values are given in

Table 13. An average value of 12 on life may be used for developing fatigue design curves from the mean data curve. The choice of bounding the 95th percentile of the population for a design curve is somewhat arbitrary. It is done with the understanding that the design curve controls fatigue initiation, not failure. The choice also recognizes that there are conservatisms implied in the choice of log normal distributions, which have an infinite tail, and in the identification of what in many cases are bounding values of the effects as 95th percentile values.

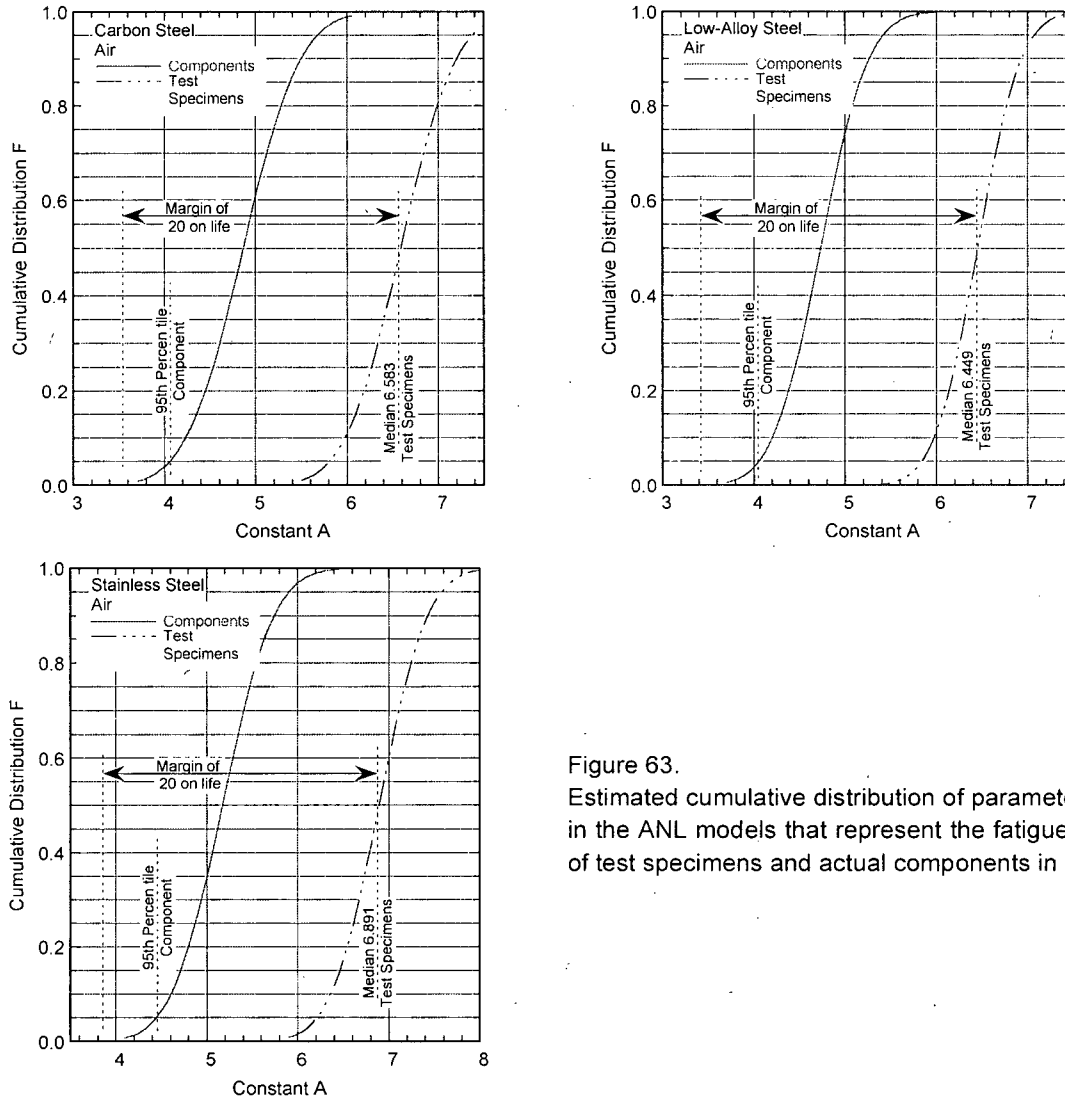


Figure 63. Estimated cumulative distribution of parameter A in the ANL models that represent the fatigue life of test specimens and actual components in air.

Table 13. Margin applied to the mean values of fatigue life to bound 95% of the population.

Material	Air Environment
Carbon Steels	12.6
Low-Alloy Steels	11.0
Austenitic Stainless Steels	11.6

These results suggest that for all materials, the current ASME Code requirements of a factor of 20 on cycles to account for the effects of material variability and data scatter, as well as specimen size, surface finish, and loading history, contain at least a factor of 1.7 conservatism (i.e., $20/12 \approx 1.7$). Thus, to reduce this conservatism, fatigue design curves may be obtained from the mean data curve by first correcting for mean stress effects using the modified Goodman relationship, and then reducing the mean-stress adjusted curve by a factor of 2 on stress or 12 on cycles, whichever is more conservative. Fatigue design curves have been developed from the ANL fatigue life models using this procedure; the curves for carbon and low-alloy steels are presented in Section 4.1.10 and for wrought and cast austenitic SSs in Section 5.1.8.

8 Summary

The existing fatigue ϵ -N data for carbon and low-alloy steels, wrought and cast austenitic SSs, and Ni-Cr-Fe alloys have been evaluated to define the effects of key material, loading, and environmental parameters on the fatigue lives of these steels. The fatigue lives of these materials are decreased in LWR environments; the magnitude of the reduction depends on temperature, strain rate, DO level in water, and, for carbon and low-alloy steels, the S content of the steel. For all steels, environmental effects on fatigue life are significant only when critical parameters (temperature, strain rate, DO level, and strain amplitude) meet certain threshold values. Environmental effects are moderate, e.g., less than a factor of 2 decrease in life, when any one of the threshold conditions is not satisfied. The threshold values of the critical parameters and the effects of other parameters (such as water conductivity, water flow rate, and material heat treatment) on the fatigue life of the steels are summarized.

In air, the fatigue life of carbon and low-alloy steels depends on steel type, temperature, orientation, and strain rate. The fatigue life of carbon steels is a factor of ≈ 1.5 lower than that of low-alloy steels. For both steels, fatigue life decreases with increase in temperature. Some heats of carbon and low-alloy steels exhibit effects of strain rate and orientation. For these heats, fatigue life decreases with decreasing strain rate. Also, based on the distribution and morphology of sulfides, the fatigue properties in the transverse orientation may be inferior to those in the rolling orientation. The data indicate significant heat-to-heat variation; at 288°C, the fatigue life of carbon and low-alloy steels may vary by up to a factor of 3 above or below the mean value. Fatigue life is very sensitive to surface finish; the fatigue life of specimens with rough surfaces may be up to a factor of 3 lower than that of smooth specimens. The results also indicate that in room-temperature air, the ASME mean curve for low-alloy steels is in good agreement with the available experimental data, and the curve for carbon steels is somewhat conservative.

The fatigue lives of both carbon and low-alloy steels are decreased in LWR environments; the reduction depends on temperature, strain rate, DO level in water, and S content of the steel. The fatigue life is decreased significantly when four conditions are satisfied simultaneously, viz., the strain amplitude, temperature, and DO in water are above certain minimum levels, and the strain rate is below a threshold value. The S content in the steel is also important; its effect on life depends on the DO level in water.

Although the microstructures and cyclic-hardening behavior of carbon and low-alloy steels differ significantly, environmental degradation of the fatigue life of these steels is very similar. For both steels, only a moderate decrease in life (by a factor of < 2) is observed when any one of the threshold conditions is not satisfied, e.g., low-DO PWR environment, temperatures $< 150^\circ\text{C}$, or vibratory fatigue. The existing fatigue S-N data have been reviewed to establish the critical parameters that influence fatigue life and define their threshold and limiting values within which environmental effects are significant.

In air, the fatigue lives of Types 304 and 316 SS are comparable; those of Type 316NG are superior to those of Types 304 and 316 SS at high strain amplitudes. The fatigue lives of austenitic SSs in air are independent of temperature in the range from room temperature to 427°C. Also, variation in strain rate in the range of 0.4–0.008%/s has no effect on the fatigue lives of SSs at temperatures up to 400°C. The fatigue ϵ -N behavior of cast SSs is similar to that of wrought austenitic SSs. The results indicate that the ASME mean-data curve for SSs is not consistent with the experimental data at strain amplitudes $< 0.5\%$ or stress amplitudes $< 975\text{ MPa}$ ($< 141\text{ ksi}$); the ASME mean curve predicts significantly longer lives than those observed experimentally.

The fatigue lives of cast and wrought austenitic SSs decrease in LWR environments compared to those in air. The decrease depends on strain rate, DO level in water, and temperature. A minimum threshold strain is required for an environmentally assisted decrease in the fatigue life of SSs, and this strain appears to be independent of material type (weld or base metal) and temperature in the range of 250–325°C. Environmental effects on fatigue life occur primarily during the tensile-loading cycle and at strain levels greater than the threshold value. Strain rate and temperature have a strong effect on fatigue life in LWR environments. Fatigue life decreases with decreasing strain rate below 0.4%/s; the effect saturates at 0.0004%/s. Similarly, the fatigue ϵ -N data suggest a threshold temperature of 150°C; in the range of 150–325°C, the logarithm of life decreases linearly with temperature.

The effect of DO level may be different for different steels. In low-DO water (i.e., <0.01 ppm DO) the fatigue lives of all wrought and cast austenitic SSs are decreased significantly; composition or heat treatment of the steel has little or no effect on fatigue life. However, in high-DO water, the environmental effects on fatigue life appear to be influenced by the composition and heat treatment of the steel; the effect of high-DO water on the fatigue lives of different compositions and heat treatment of SSs is not well established. Limited data indicate that for a high-C Type 304 SS, environmental effects are significant only for sensitized steel. For a low-C Type 316NG SS, some effect of environment was observed even for mill-annealed steel (nonsensitized steel) in high-DO water, although the effect was smaller than that observed in low-DO water. Limited fatigue ϵ -N data indicate that the fatigue lives of cast SSs are approximately the same in low- and high-DO water and are comparable to those observed for wrought SSs in low-DO water. In the present report, environmental effects on the fatigue lives of wrought and cast austenitic SSs are considered to be the same in high-DO and low-DO environments.

The fatigue ϵ -N data for Ni-Cr-Fe alloys indicate that although the data for Alloy 690 are very limited, the fatigue lives of Alloy 690 are comparable to those of Alloy 600. Also, the fatigue lives of the Ni-Cr-Fe alloy welds are comparable to those of the wrought Alloys 600 and 690 in the low-cycle regime, i.e., $<10^5$ cycles, and are slightly superior to the lives of wrought materials in the high-cycle regime. The fatigue data for Ni-Cr-Fe alloys in LWR environments are very limited; the effects of key loading and environmental parameters on fatigue life are similar to those for austenitic SSs. For example, the fatigue life of these steels decreases logarithmically with decreasing strain rate. Also, the effects of environment are greater in the low-DO PWR water than the high-DO BWR water. The existing data are inadequate to determine accurately the functional form for the effect of temperature on fatigue life.

Fatigue life models developed earlier to predict fatigue lives of small smooth specimens of carbon and low-alloy steels and wrought and cast austenitic SSs as a function of material, loading, and environmental parameters have been updated/revised using a larger fatigue ϵ -N database. The functional form and bounding values of these parameters were based on experimental observations and data trends. The models are applicable for predicted fatigue lives $\leq 10^6$ cycles. The ANL fatigue life model proposed in the present report for austenitic SSs in air is also recommended for predicting the fatigue lives of small smooth specimens of Ni-Cr-Fe alloys.

An approach, based on the environmental fatigue correction factor, is discussed to incorporate the effects of LWR coolant environments into the ASME Code fatigue evaluations. To incorporate environmental effects into a Section III fatigue evaluation, the fatigue usage for a specific stress cycle of load set pair based on the current Code fatigue design curves is multiplied by the correction factor.

The report also presents a critical review of the ASME Code fatigue design margins of 2 on stress and 20 on life and assesses the possible conservatism in the current choice of design margins. These factors cover the effects of variables that can influence fatigue life but were not investigated in the tests

that provided the data for the design curves. Although these factors were intended to be somewhat conservative, they should not be considered safety margins because they were intended to account for variables that are known to affect fatigue life. Data available in the literature have been reviewed to evaluate the margins on cycles and stress that are needed to account for the differences and uncertainties. Monte Carlo simulations were performed to determine the margin on cycles needed to obtain a fatigue design curve that would provide a somewhat conservative estimate of the number of cycles to initiate a fatigue crack in reactor components. The results suggest that for both carbon and low-alloy steels and austenitic SSs, the current ASME Code requirements of a factor of 20 on cycles to account for the effects of material variability and data scatter, as well as size, surface finish, and loading history, contain at least a factor of 1.7 conservatism. Thus, to reduce this conservatism, fatigue design curves have been developed from the ANL model by first correcting for mean stress effects, and then reducing the mean-stress adjusted curve by a factor of 2 on stress and 12 on cycles, whichever is more conservative. A detailed procedure for incorporating environmental effects into fatigue evaluations is also presented in Appendix A.

This page is intentionally left blank.

References

1. Langer, B. F., "Design of Pressure Vessels for Low-Cycle Fatigue," ASME J. Basic Eng. 84, 389-402, 1962.
2. "Criteria of the ASME Boiler and Pressure Vessel Code for Design by Analysis in Sections III and VIII, Division 2," The American Society of Mechanical Engineers, New York, 1969.
3. Cooper, W. E., "The Initial Scope and Intent of the Section III Fatigue Design Procedure," Welding Research Council, Inc., Technical Information from Workshop on Cyclic Life and Environmental Effects in Nuclear Applications, Clearwater, Florida, Jan. 22-21, 1992.
4. Chopra, O. K., and W. J. Shack, "Effects of LWR Coolant Environments on Fatigue Design Curves of Carbon and Low-Alloy Steels," NUREG/CR-6583, ANL-97/18, March 1998.
5. Gavenda, D. J., P. R. Luebbbers, and O. K. Chopra, "Crack Initiation and Crack Growth Behavior of Carbon and Low-Alloy Steels," Fatigue and Fracture I, Vol. 350, S. Rahman, K. K. Yoon, S. Bhandari, R. Warke, and J. M. Bloom, eds., American Society of Mechanical Engineers, New York, pp. 243-255, 1997.
6. Chopra, O. K., and W. J. Shack, "Environmental Effects on Fatigue Crack Initiation in Piping and Pressure Vessel Steels," NUREG/CR-6717, ANL-00/27, May 2001.
7. Chopra, O. K., "Mechanisms and Estimation of Fatigue Crack Initiation in Austenitic Stainless Steels in LWR Environments," NUREG/CR-6787, ANL-01/25, Aug. 2002.
8. Hale, D. A., S. A. Wilson, E. Kiss, and A. J. Gianuzzi, "Low-Cycle Fatigue Evaluation of Primary Piping Materials in a BWR Environment," GEAP-20244, U.S. Nuclear Regulatory Commission, Sept. 1977.
9. Hale, D. A., S. A. Wilson, J. N. Kass, and E. Kiss, "Low Cycle Fatigue Behavior of Commercial Piping Materials in a BWR Environment," J. Eng. Mater. Technol. 103, 15-25, 1981.
10. Ranganath, S., J. N. Kass, and J. D. Heald, "Fatigue Behavior of Carbon Steel Components in High-Temperature Water Environments," BWR Environmental Cracking Margins for Carbon Steel Piping, EPRI NP-2406, Appendix 3, Electric Power Research Institute, Palo Alto, CA, May 1982.
11. Ranganath, S., J. N. Kass, and J. D. Heald, "Fatigue Behavior of Carbon Steel Components in High-Temperature Water Environments," Low-Cycle Fatigue and Life Prediction, ASTM STP 770, C. Amzallag, B. N. Leis, and P. Rabbe, eds., American Society for Testing and Materials, Philadelphia, pp. 436-459, 1982.
12. Nagata, N., S. Sato, and Y. Katada, "Low-Cycle Fatigue Behavior of Pressure Vessel Steels in High-Temperature Pressurized Water," ISIJ Intl. 31 (1), 106-114, 1991.
13. Higuchi, M., and K. Iida, "Fatigue Strength Correction Factors for Carbon and Low-Alloy Steels in Oxygen-Containing High-Temperature Water," Nucl. Eng. Des. 129, 293-306, 1991.

14. Katada, Y., N. Nagata, and S. Sato, "Effect of Dissolved Oxygen Concentration on Fatigue Crack Growth Behavior of A533 B Steel in High Temperature Water," *ISIJ Intl.* 33 (8), 877–883, 1993.
15. Kanasaki, H., M. Hayashi, K. Iida, and Y. Asada, "Effects of Temperature Change on Fatigue Life of Carbon Steel in High Temperature Water," *Fatigue and Crack Growth: Environmental Effects, Modeling Studies, and Design Considerations*, PVP Vol. 306, S. Yukawa, ed., American Society of Mechanical Engineers, New York, pp. 117–122, 1995.
16. Nakao, G., H. Kanasaki, M. Higuchi, K. Iida, and Y. Asada, "Effects of Temperature and Dissolved Oxygen Content on Fatigue Life of Carbon and Low-Alloy Steels in LWR Water Environment," *Fatigue and Crack Growth: Environmental Effects, Modeling Studies, and Design Considerations*, PVP Vol. 306, S. Yukawa, ed., American Society of Mechanical Engineers, New York, pp. 123–128, 1995.
17. Higuchi, M., K. Iida, and Y. Asada, "Effects of Strain Rate Change on Fatigue Life of Carbon Steel in High-Temperature Water," *Fatigue and Crack Growth: Environmental Effects, Modeling Studies, and Design Considerations*, PVP Vol. 306, S. Yukawa, ed., American Society of Mechanical Engineers, New York, pp. 111–116, 1995; also *Proc. of Symp. on Effects of the Environment on the Initiation of Crack Growth*, ASTM STP 1298, American Society for Testing and Materials, Philadelphia, 1997.
18. Higuchi, M., K. Iida, and K. Sakaguchi, "Effects of Strain Rate Fluctuation and Strain Holding on Fatigue Life Reduction for LWR Structural Steels in Simulated PWR Water," *Pressure Vessel and Piping Codes and Standards*, PVP Vol. 419, M. D. Rana, ed., American Society of Mechanical Engineers, New York, pp. 143–152, 2001.
19. Hirano, A., M. Yamamoto, K. Sakaguchi, T. Shoji, and K. Iida, "Effects of Water Flow Rate on Fatigue Life of Ferritic and Austenitic Steels in Simulated LWR Environment," *Pressure Vessel and Piping Codes and Standards – 2002*, PVP Vol. 439, M. D. Rana, ed., American Society of Mechanical Engineers, New York, pp. 143–150, 2002.
20. Hirano, A., M. Yamamoto, K. Sakaguchi, and T. Shoji, "Effects of Water Flow Rate on Fatigue Life of Carbon and Stainless Steels in Simulated LWR Environment," *Pressure Vessel and Piping Codes and Standards – 2004*, PVP Vol. 480, American Society of Mechanical Engineers, New York, pp. 109–119, 2004.
21. Fujiwara, M., T. Endo, and H. Kanasaki, "Strain Rate Effects on the Low-Cycle Fatigue Strength of 304 Stainless Steel in High-Temperature Water Environment. Fatigue Life: Analysis and Prediction," *Proc. Intl. Conf. and Exposition on Fatigue, Corrosion Cracking, Fracture Mechanics, and Failure Analysis*, ASM, Metals Park, OH, pp. 309–313, 1986.
22. Mimaki, H., H. Kanasaki, I. Suzuki, M. Koyama, M. Akiyama, T. Okubo, and Y. Mishima, "Material Aging Research Program for PWR Plants," *Aging Management Through Maintenance Management*, PVP Vol. 332, I. T. Kisisel, ed., American Society of Mechanical Engineers, New York, pp. 97–105, 1996.
23. Kanasaki, H., R. Umehara, H. Mizuta, and T. Suyama, "Fatigue Lives of Stainless Steels in PWR Primary Water," *Trans. 14th Intl. Conf. on Structural Mechanics in Reactor Technology (SMiRT 14)*, Lyon, France, pp. 473–483, 1997.

24. Kanasaki, H., R. Umehara, H. Mizuta, and T. Suyama, "Effects of Strain Rate and Temperature Change on the Fatigue Life of Stainless Steel in PWR Primary Water," Trans. 14th Intl. Conf. on Structural Mechanics in Reactor Technology (SMiRT 14), Lyon, France, pp. 485-493, 1997.
25. Higuchi, M., and K. Iida, "Reduction in Low-Cycle Fatigue Life of Austenitic Stainless Steels in High-Temperature Water," Pressure Vessel and Piping Codes and Standards, PVP Vol. 353, D. P. Jones, B. R. Newton, W. J. O'Donnell, R. Vecchio, G. A. Antaki, D. Bhavani, N. G. Cofie, and G. L. Hollinger, eds., American Society of Mechanical Engineers, New York, pp. 79-86, 1997.
26. Hayashi, M., "Thermal Fatigue Strength of Type 304 Stainless Steel in Simulated BWR Environment," Nucl. Eng. Des. 184, 135-144, 1998.
27. Hayashi, M., K. Enomoto, T. Saito, and T. Miyagawa, "Development of Thermal Fatigue Testing with BWR Water Environment and Thermal Fatigue Strength of Austenitic Stainless Steels," Nucl. Eng. Des. 184, 113-122, 1998.
28. Tsutsumi, K., H. Kanasaki, T. Umakoshi, T. Nakamura, S. Urata, H. Mizuta, and S. Nomoto, "Fatigue Life Reduction in PWR Water Environment for Stainless Steels," Assessment Methodologies for Preventing Failure: Service Experience and Environmental Considerations, PVP Vol. 410-2, R. Mohan, ed., American Society of Mechanical Engineers, New York, pp. 23-34, 2000.
29. Tsutsumi, K., T. Dodo, H. Kanasaki, S. Nomoto, Y. Minami, and T. Nakamura, "Fatigue Behavior of Stainless Steel under Conditions of Changing Strain Rate in PWR Primary Water," Pressure Vessel and Piping Codes and Standards, PVP Vol. 419, M. D. Rana, ed., American Society of Mechanical Engineers, New York, pp. 135-141, 2001.
30. Tsutsumi, K., M. Higuchi, K. Iida, and Y. Yamamoto, "The Modified Rate Approach to Evaluate Fatigue Life under Synchronously Changing Temperature and Strain Rate in Elevated Temperature Water," Pressure Vessel and Piping Codes and Standards - 2002, PVP Vol. 439, M. D. Rana, ed., American Society of Mechanical Engineers, New York, pp. 99-107, 2002.
31. Higuchi, M., T. Hirano, and K. Sakaguchi, "Evaluation of Fatigue Damage on Operating Plant Components in LWR Water," Pressure Vessel and Piping Codes and Standards - 2004, PVP Vol. 480, American Society of Mechanical Engineers, New York, pp. 129-138, 2004.
32. Nomura, Y., M. Higuchi, Y. Asada, and K. Sakaguchi, "The Modified Rate Approach Method to Evaluate Fatigue Life under Synchronously Changing Temperature and Strain Rate in Elevated Temperature Water in Austenitic Stainless Steels," Pressure Vessel and Piping Codes and Standards - 2004, PVP Vol. 480, American Society of Mechanical Engineers, New York, pp. 99-108, 2004.
33. Higuchi, M., K. Sakaguchi, A. Hirano, and Y. Nomura, "Revised and New Proposal of Environmental Fatigue Life Correction Factor (F_{en}) for Carbon and Low-Alloy Steels and Nickel Alloys in LWR Water Environments," Proc. of the 200 ASME Pressure Vessels and Piping Conf., July 23-27, 2006, Vancouver, BC, Canada, paper # PVP2006-ICPVT-93194.

34. Chopra, O. K., and W. J. Shack, "Evaluation of Effects of LWR Coolant Environments on Fatigue Life of Carbon and Low-Alloy Steels," Effects of the Environment on the Initiation of Crack Growth, ASTM STP 1298, W. A. Van Der Sluys, R. S. Piascik, and R. Zawierucha, eds., American Society for Testing and Materials, Philadelphia, pp. 247-266, 1997.
35. Chopra, O. K., and W. J. Shack, "Low-Cycle Fatigue of Piping and Pressure Vessel Steels in LWR Environments," Nucl. Eng. Des. 184, 49-76, 1998.
36. Chopra, O. K., and D. J. Gavenda, "Effects of LWR Coolant Environments on Fatigue Lives of Austenitic Stainless Steels," J. Pressure Vessel Technol. 120, 116-121, 1998.
37. Chopra, O. K., and J. L. Smith, "Estimation of Fatigue Strain-Life Curves for Austenitic Stainless Steels in Light Water Reactor Environments," Fatigue, Environmental Factors, and New Materials, PVP Vol. 374, H. S. Mehta, R. W. Swindeman, J. A. Todd, S. Yukawa, M. Zako, W. H. Bamford, M. Higuchi, E. Jones, H. Nickel, and S. Rahman, eds., American Society of Mechanical Engineers, New York, pp. 249-259, 1998.
38. Chopra, O. K., "Effects of LWR Coolant Environments on Fatigue Design Curves of Austenitic Stainless Steels," NUREG/CR-5704, ANL-98/31, 1999.
39. Chopra, O. K., and W. J. Shack, "Review of the Margins for ASME Code Design Curves - Effects of Surface Roughness and Material Variability," NUREG/CR-6815, ANL-02/39, Sept. 2003.
40. Chopra, O. K., B. Alexandreanu, and W. J. Shack, "Effect of Material Heat Treatment on Fatigue Crack Initiation in Austenitic Stainless Steels in LWR Environments," NUREG/CR-6878, ANL-03/35, July 2005.
41. Terrell, J. B., "Fatigue Life Characterization of Smooth and Notched Piping Steel Specimens in 288°C Air Environments," NUREG/CR-5013, EM-2232 Materials Engineering Associates, Inc., Lanham, MD, May 1988.
42. Terrell, J. B., "Fatigue Strength of Smooth and Notched Specimens of ASME SA 106-B Steel in PWR Environments," NUREG/CR-5136, MEA-2289, Materials Engineering Associates, Inc., Lanham, MD, Sept. 1988.
43. Terrell, J. B., "Effect of Cyclic Frequency on the Fatigue Life of ASME SA-106-B Piping Steel in PWR Environments," J. Mater. Eng. 10, 193-203, 1988.
44. Lenz, E., N. Wieling, and H. Muenster, "Influence of Variation of Flow Rates and Temperature on the Cyclic Crack Growth Rate under BWR Conditions," Environmental Degradation of Materials in Nuclear Power Systems - Water Reactors, The Metallurgical Society, Warrendale, PA, 1988.
45. Garud, Y. S., S. R. Paterson, R. B. Dooley, R. S. Pathania, J. Hickling, and A. Bursik, "Corrosion Fatigue of Water Touched Pressure Retaining Components in Power Plants," EPRI TR-106696, Final Report, Electric Power Research Institute, Palo Alto, Nov. 1997.
46. Faigy, C., T. Le Courtois, E. de Fraguier, J-A Leduff, A. Lefrancois, and J. Dechelotte, "Thermal Fatigue in French RHR System," Int. Conf. on Fatigue of Reactor Components, Napa, CA, July 31-August 2, 2000.

47. Kussmaul, K., R. Rintamaa, J. Jansky, M. Kemppainen, and K. Törrönen, "On the Mechanism of Environmental Cracking Introduced by Cyclic Thermal Loading," in IAEA Specialists Meeting, Corrosion and Stress Corrosion of Steel Pressure Boundary Components and Steam Turbines, VTT Symp. 43, Espoo, Finland, pp. 195-243, 1983.
48. Hickling, J., "Strain Induced Corrosion Cracking of Low-Alloy Reactor Pressure Vessel Steels under BWR Conditions," Proc. 10th Intl. Symp. on Environmental Degradation of Materials in Nuclear Power Systems - Water Reactors, F. P. Ford, S. M. Bruemmer, and G. S. Was, eds., The Minerals, Metals, and Materials Society, Warrendale, PA, CD-ROM, paper 0156, 2001.
49. Hickling, J., "Research and Service Experience with Environmentally Assisted Cracking of Low-Alloy Steel," Power Plant Chem., 7 (1), 4-15, 2005.
50. Iida, K., "A Review of Fatigue Failures in LWR Plants in Japan," Nucl. Eng. Des. 138, 297-312, 1992.
51. NRC IE Bulletin No. 79-13, "Cracking in Feedwater System Piping," U.S. Nuclear Regulatory Commission, Washington, DC, June 25, 1979.
52. NRC Information Notice 93-20, "Thermal Fatigue Cracking of Feedwater Piping to Steam Generators," U.S. Nuclear Regulatory Commission, Washington, DC, March 24, 1993.
53. Kussmaul, K., D. Blind, and J. Jansky, "Formation and Growth of Cracking in Feed Water Pipes and RPV Nozzles," Nucl. Eng. Des. 81, 105-119, 1984.
54. Gordon, B. M., D. E. Delwiche, and G. M. Gordon, "Service Experience of BWR Pressure Vessels," Performance and Evaluation of Light Water Reactor Pressure Vessels, PVP Vol.-119, American Society of Mechanical Engineers, New York, pp. 9-17, 1987.
55. Lenz, E., B. Stellwag, and N. Wieling, "The Influence of Strain-Induced Corrosion Cracking on the Crack Initiation in Low-Alloy Steels in HT-Water - A Relation Between Monotonic and Cyclic Crack Initiation Behavior," in IAEA Specialists Meeting Corrosion and Stress Corrosion of Steel Pressure Boundary Components and Steam Turbines, VTT Symp. 43, Espoo, Finland, pp. 243-267, 1983.
56. Hickling, J., and D. Blind, "Strain-Induced Corrosion Cracking of Low-Alloy Steels in LWR Systems - Case Histories and Identification of Conditions Leading to Susceptibility," Nucl. Eng. Des. 91, 305-330, 1986.
57. Hirschberg, P., A. F. Deardorff, and J. Carey, "Operating Experience Regarding Thermal Fatigue of Unisolable Piping Connected to PWR Reactor Coolant Systems," Int. Conf. on Fatigue of Reactor Components, Napa, CA, July 31-August 2, 2000.
58. NRC Information Notice 88-01, "Safety Injection Pipe Failure," U.S. Nuclear Regulatory Commission, Washington, DC (Jan. 27, 1988).
59. NRC Bulletin No. 88-08, "Thermal Stresses in Piping Connected to Reactor Coolant Systems," U.S. Nuclear Regulatory Commission, Washington, DC, June 22; Suppl. 1, June 24; Suppl. 2, Aug. 4, 1988; Suppl. 3, April 1989.

60. Sakai, T., "Leakage from CVCS Pipe of Regenerative Heat Exchanger Induced by High-Cycle Thermal Fatigue at Tsuruga Nuclear Power Station Unit 2," Int. Conf. on Fatigue of Reactor Components, Napa, CA, July 31–August 2, 2000.
61. Hoshino, T., T. Ueno, T. Aoki, and Y. Kutomi, "Leakage from CVCS Pipe of Regenerative Heat Exchanger Induced by High-Cycle Thermal Fatigue at Tsuruga Nuclear Power Station Unit 2," Proc. 8th Intl. Conf. on Nuclear Engineering, 1.01 Operational Experience/Root Cause Failure Analysis, Paper 8615, American Society of Mechanical Engineers, New York, 2000.
62. Stephan, J.-M., and J. C. Masson, "Auxiliary+ Feedwater Line Stratification and Coufast Simulation," Int. Conf. on Fatigue of Reactor Components, Napa, CA, July 31–August 2, 2000.
63. Kilian, R., J. Hickling, and R. Nickell, "Environmental Fatigue Testing of Stainless Steel Pipe Bends in Flowing, Simulated PWR Primary Water at 240°C," Third Intl. Conf. Fatigue of Reactor Components, MRP-151, Electric Power Research Institute, Palo Alto, CA, Aug. 2005.
64. NRC Bulletin No. 88–11, "Pressurizer Surge Line Thermal Stratification," U.S. Nuclear Regulatory Commission, Washington, DC, Dec. 20, 1988.
65. Majumdar, S., O. K. Chopra, and W. J. Shack, "Interim Fatigue Design Curves for Carbon, Low-Alloy, and Austenitic Stainless Steels in LWR Environments," NUREG/CR–5999, ANL–93/3, 1993.
66. Keisler, J., O. K. Chopra, and W. J. Shack, "Fatigue Strain–Life Behavior of Carbon and Low-Alloy Steels, Austenitic Stainless Steels, and Alloy 600 in LWR Environments," NUREG/CR–6335, ANL–95/15, 1995.
67. Park, H. B., and O. K. Chopra, "A Fracture Mechanics Approach for Estimating Fatigue Crack Initiation in Carbon and Low-Alloy Steels in LWR Coolant Environment," Assessment Methodologies for Preventing Failure: Service Experience and Environmental Considerations, PVP Vol. 410-2, R. Mohan, ed., American Society of Mechanical Engineers, New York, pp. 3–11, 2000.
68. O'Donnell, T. P., and W. J. O'Donnell, "Stress Intensity Values in Conventional S-N Fatigue Specimens," Pressure Vessels and Piping Codes and Standard: Volume 1 – Current Applications, PVP Vol. 313–1, K. R. Rao and Y. Asada, eds., American Society of Mechanical Engineers, New York, pp. 191–192, 1995.
69. Amzallag, C., P. Rabbe, G. Gallet, and H.-P. Lieurade, "Influence des Conditions de Sollicitation Sur le Comportement en Fatigue Oligocyclique D'aciers Inoxydables Austénitiques," *Memoires Scientifiques Revue Metallurgie Mars*, pp. 161–173, 1978.
70. Solomon, H. D., C. Amzallag, A. J. Vallee, and R. E. De Lair, "Influence of Mean Stress on the Fatigue Behavior of 304L SS in Air and PWR Water," Proc. of the 2005 ASME Pressure Vessels and Piping Conf., July 17–21, 2005, Denver, CO, paper # PVP2005–71064.
71. Solomon, H. D., C. Amzallag, R. E. De Lair, and A. J. Vallee, "Strain Controlled Fatigue of Type 304L SS in Air and PWR Water," Proc. Third Intl. Conf. on Fatigue of Reactor Components, Seville, Spain, Oct. 3–6, 2004.

72. Jaske, C. E., and W. J. O'Donnell, "Fatigue Design Criteria for Pressure Vessel Alloys," *Trans. ASME J. Pressure Vessel Technol.* 99, 584-592, 1977.
73. Conway, J. B., R. H. Stentz, and J. T. Berling, "Fatigue, Tensile, and Relaxation Behavior of Stainless Steels," TID-26135, U.S. Atomic Energy Commission, Washington, DC, 1975.
74. Keller, D. L., "Progress on LMFBR Cladding, Structural, and Component Materials Studies During July, 1971 through June, 1972, Final Report," Task 32, Battelle-Columbus Laboratories, BMI-1928, 1977.
75. Jacko, R. J., "Fatigue Performance of Ni-Cr-Fe Alloy 600 under Typical PWR Steam Generator Conditions," EPRI NP-2957, Electric Power Research Institute, Palo Alto, CA, March 1983.
76. Dinerman, A. E., "Cyclic Strain Fatigue of Inconel at 75 to 600°F," KAPL-2084, Knolls Atomic Power Laboratory, Schenectady, NY, August 1960.
77. Mowbray, D. F., G. J. Sokol, and R. E. Savidge, "Fatigue Characteristics of Ni-Cr-Fe Alloys with Emphasis on Pressure-Vessel Cladding," KAPL-3108, Knolls Atomic Power Laboratory, Schenectady, NY, July 1965.
78. Van Der Sluys, W. A., B. A. Young, and D. Doyle, "Corrosion Fatigue Properties on Alloy 690 and Some Nickel-Based Weld Metals," *Assessment Methodologies for Preventing Failure: Service Experience and Environmental Considerations*, PVP Vol. 410-2, R. Mohan, ed., American Society of Mechanical Engineers, New York, pp. 85-91, 2000.
79. Iida, K., T. Bannai, M. Higuchi, K. Tsutsumi, and K. Sakaguchi, "Comparison of Japanese MITI Guideline and Other Methods for Evaluation of Environmental Fatigue Life Reduction," *Pressure Vessel and Piping Codes and Standards*, PVP Vol. 419, M. D. Rana, ed., American Society of Mechanical Engineers, New York, pp. 73-81, 2001.
80. Chopra, O. K., and W. J. Shack, "Overview of Fatigue Crack Initiation in Carbon and Low-Alloy Steels in Light Water Reactor Environments," *J. Pressure Vessel Technol.* 121, 49-60, 1999.
81. Higuchi, M., "Revised Proposal of Fatigue Life Correction Factor F_{en} for Carbon and Low Alloy Steels in LWR Water Environments," *Assessment Methodologies for Preventing Failure: Service Experience and Environmental Considerations*, PVP Vol. 410-2, R. Mohan, ed., American Society of Mechanical Engineers, New York, pp. 35-44, 2000.
82. Leax, T. R., "Statistical Models of Mean Stress and Water Environment Effects on the Fatigue Behavior of 304 Stainless Steel," *Probabilistic and Environmental Aspects of Fracture and Fatigues*, PVP Vol. 386, S. Rahman, ed., American Society of Mechanical Engineers, New York, pp. 229-239, 1999.
83. Ford, F. P., S. Ranganath, and D. Weinstein, "Environmentally Assisted Fatigue Crack Initiation in Low-Alloy Steels - A Review of the Literature and the ASME Code Design Requirements," EPRI Report TR-102765, Electric Power Research Institute, Palo Alto, CA, Aug. 1993.

84. Ford, F. P., "Prediction of Corrosion Fatigue Initiation in Low-Alloy and Carbon Steel/Water Systems at 288°C," Proc. 6th Intl. Symp. on Environmental Degradation of Materials in Nuclear Power Systems – Water Reactors, R. E. Gold and E. P. Simonen, eds., The Metallurgical Society, Warrendale, PA, pp. 9–17, 1993.
85. Mehta, H. S., and S. R. Gosselin, "Environmental Factor Approach to Account for Water Effects in Pressure Vessel and Piping Fatigue Evaluations," Nucl. Eng. Des. 181, 175–197, 1998.
86. Mehta, H. S., "An Update on the Consideration of Reactor Water Effects in Code Fatigue Initiation Evaluations for Pressure Vessels and Piping," Assessment Methodologies for Preventing Failure: Service Experience and Environmental Considerations, PVP Vol. 410-2, R. Mohan, ed., American Society of Mechanical Engineers, New York, pp. 45–51, 2000.
87. Van Der Sluys, W. A., and S. Yukawa, "Status of PVRC Evaluation of LWR Coolant Environmental Effects on the S–N Fatigue Properties of Pressure Boundary Materials," Fatigue and Crack Growth: Environmental Effects, Modeling Studies, and Design Considerations, PVP Vol. 306, S. Yukawa, ed., American Society of Mechanical Engineers, New York, pp. 47–58, 1995.
88. Van Der Sluys, W. A., "PVRC's Position on Environmental Effects on Fatigue Life in LWR Applications," Welding Research Council Bulletin 487, Welding Research Council, Inc., New York, Dec. 2003.
89. O'Donnell, W. J., W. J. O'Donnell, and T. P. O'Donnell, "Proposed New Fatigue Design Curves for Austenitic Stainless Steels, Alloy 600, and Alloy 800," Proc. of the 2005 ASME Pressure Vessels and Piping Conf., July 17–21, 2005, Denver, CO, paper # PVP2005–71409.
90. O'Donnell, W. J., W. J. O'Donnell, and T. P. O'Donnell, "Proposed New Fatigue Design Curves for Carbon and Low-Alloy Steels in High Temperature Water," Proc. of the 2005 ASME Pressure Vessels and Piping Conf., July 17–21, 2005, Denver, CO, paper # PVP2005–71410.
91. Abdel-Raouf, H., A. Plumtree, and T. H. Topper, "Effects of Temperature and Deformation Rate on Cyclic Strength and Fracture of Low-Carbon Steel," Cyclic Stress–Strain Behavior – Analysis, Experimentation, and Failure Prediction, ASTM STP 519, American Society for Testing and Materials, Philadelphia, pp. 28–57, 1973.
92. Lee, B. H., and I. S. Kim, "Dynamic Strain Aging in the High-Temperature Low-Cycle Fatigue of SA 508 Cl. 3 Forging Steel," J. Nucl. Mater. 226, 216–225, 1995.
93. Maiya, P. S., and D. E. Busch, "Effect of Surface Roughness on Low-Cycle Fatigue Behavior of Type 304 Stainless Steel," Met. Trans. 6A, 1761–1766, 1975.
94. Maiya, P. S., "Effect of Surface Roughness and Strain Range on Low-Cycle Fatigue Behavior of Type 304 Stainless Steel," Scripta Metall. 9, 1277–1282, 1975.
95. Stout, K. J., "Surface Roughness – Measurement, Interpretation, and Significance of Data," Mater. Eng. 2, 287–295, 1981.
96. Iida, K., "A Study of Surface Finish Effect Factor in ASME B & PV Code Section III," Pressure Vessel Technology, Vol. 2, L. Cengdian and R. W. Nichols, eds., Pergamon Press, New York, pp. 727–734, 1989.

97. Manjoine, M. J., and R. L. Johnson, "Fatigue Design Curves for Carbon and Low Alloy Steels up to 700°F (371°C)," *Material Durability/Life Prediction Modeling: Materials for the 21st Century*, PVP-Vol. 290, American Society of Mechanical Engineers, New York, 1994.
98. Johnson, L. G., "The Median Ranks of Sample Values in Their Population with an Application to Certain Fatigue Studies," *Ind. Math.* 2, 1-9, 1951.
99. Lipson, C., and N. J. Sheth, *Statistical Design and Analysis of Engineering Experiments*, McGraw Hill, New York, 1973.
100. Beck, J., and K. Arnold, *Parameter Estimation in Engineering and Science*, J. Wiley, New York, 1977.
101. Stambaugh, K. A., D. H. Leeson, F. V. Lawrence, C. Y. Hou, and G. Banas, "Reduction of S-N Curves for Ship Structural Details," *Welding Research Council* 398, January 1995.
102. Ford, F. P., and P. L. Andresen, "Stress Corrosion Cracking of Low-Alloy Pressure Vessel Steel in 288°C Water," *Proc. 3rd Int. Atomic Energy Agency Specialists' Meeting on Subcritical Crack Growth*, NUREG/CP-0112, Vol. 1, pp. 37-56, Aug. 1990.
103. Ford, F. P., "Overview of Collaborative Research into the Mechanisms of Environmentally Controlled Cracking in the Low Alloy Pressure Vessel Steel/Water System," *Proc. 2nd Int. Atomic Energy Agency Specialists' Meeting on Subcritical Crack Growth*, NUREG/CP-0067, MEA-2090, Vol. 2, pp. 3-71, April 1986.
104. Wire, G. L., and Y. Y. Li, "Initiation of Environmentally-Assisted Cracking in Low-Alloy Steels," *Fatigue and Fracture Vol. 1*, PVP Vol. 323, H. S. Mehta, ed., American Society of Mechanical Engineers, New York, pp. 269-289, 1996.
105. Pleune, T. T., and O. K. Chopra, "Artificial Neural Networks and Effects of Loading Conditions on Fatigue Life of Carbon and Low-Alloy Steels," *Fatigue and Fracture Vol. 1*, PVP Vol. 350, S. Rahman, K. K. Yoon, S. Bhandari, R. Warke, and J. M. Bloom, eds., American Society of Mechanical Engineers, New York, pp. 413-423, 1997.
106. Solomon, H. D., R. E. DeLair, and A. D. Unruh, "Crack Initiation in Low-Alloy Steel in High-Purity Water," *Effects of the Environment on the Initiation of Crack Growth*, ASTM STP 1298, W. A. Van Der Sluys, R. S. Piascik, and R. Zawierucha, eds., American Society for Testing and Materials, Philadelphia, pp. 135-149, 1997.
107. Solomon, H. D., R. E. DeLair, and E. Tolksdorf, "LCF Crack Initiation in WB36 in High-Temperature Water," *Proc. 9th Intl. Symp. on Environmental Degradation of Materials in Nuclear Power Systems - Water Reactors*, F. P. Ford, S. M. Bruemmer, and G. S. Was, eds., The Minerals, Metals, and Materials Society, Warrendale, PA, pp. 865-872, 1999.
108. Cullen, W. H., M. Kemppainen, H. Hänninen, and K. Törrönen, "The Effects of Sulfur Chemistry and Flow Rate on Fatigue Crack Growth Rates in LWR Environments," *NUREG/CR-4121*, 1985.

109. Van Der Sluys, W. A., and R. H. Emanuelson, "Environmental Acceleration of Fatigue Crack Growth in Reactor Pressure Vessel Materials and Environments," *Environmentally Assisted Cracking: Science and Engineering*, ASTM STP 1049, W. B. Lisagor, T. W. Crooker, and B. N. Leis, eds., American Society for Testing and Materials, Philadelphia, PA, pp. 117-135, 1990.
110. Atkinson, J. D., J. Yu, and Z.-Y. Chen, "An Analysis of the Effects of Sulfur Content and Potential on Corrosion Fatigue Crack Growth in Reactor Pressure Vessel Steels," *Corros. Sci.* 38 (5), 755-765, 1996.
111. Auten, T. A., S. Z. Hayden, and R. H. Emanuelson, "Fatigue Crack Growth Rate Studies of Medium Sulfur Low Alloy Steels Tested in High Temperature Water," *Proc. 6th Int. Symp. on Environmental Degradation of Materials in Nuclear Power Systems - Water Reactors*, R. E. Gold and E. P. Simonen, eds., The Metallurgical Society, Warrendale, PA, pp. 35-40, 1993.
112. Wire, G. L., T. R. Leax, and J. T. Kandra, "Mean Stress and Environmental Effects on Fatigue in Type 304 Stainless Steel," in *Probabilistic and Environmental Aspects of Fracture and Fatigues*, PVP Vol. 386, S. Rahman, ed., American Society of Mechanical Engineers, New York, pp. 213-228, 1999.
113. Diercks, D. R., "Development of Fatigue Design Curves for Pressure Vessel Alloys Using a Modified Langer Equation," *Trans. ASME J. Pressure Vessel Technol.* 101, 292-297, 1979.
114. Solomon, H. D., and C. Amzallag, "Comparison of Models Predicting the Fatigue Behavior of Austenitic Stainless Steels," *Proc. of the 2005 ASME Pressure Vessels and Piping Conf.*, July 17-21, 2005, Denver, CO, paper # PVP2005-71063.
115. Kim, Y. J., "Characterization of the Oxide Film Formed on Type 316 Stainless Steel in 288°C Water in Cyclic Normal and Hydrogen Water Chemistries," *Corrosion* 51 (11), 849-860, 1995.
116. Kim, Y. J., "Analysis of Oxide Film Formed on Type 304 Stainless Steel in 288°C Water Containing Oxygen, Hydrogen, and Hydrogen Peroxide," *Corrosion* 55 (1), 81-88, 1999.
117. Chopra, O. K., "Estimation of Fracture Toughness of Cast Stainless Steels During Thermal Aging in LWR Systems," NUREG/CR-4513, ANL-93/22, Aug. 1994.
118. Chopra, O. K., "Effect of Thermal Aging on Mechanical Properties of Cast Stainless Steels," in *Proc. of the 2nd Int. Conf. on Heat-Resistant Materials*, K. Natesan, P. Ganesan, and G. Lai, eds., ASM International, Materials Park, OH, pp. 479-485, 1995.
119. Higuchi, M., "Review and Consideration of Unsettled Problems on Evaluation of Fatigue Damage in LWR Water," *Proc. of the 2005 ASME Pressure Vessels and Piping Conf.*, July 17-21, 2005, Denver, CO, paper # PVP2005-71306.
120. Mayfield, M. E., E. C. Rodabaugh, and R. J. Eiber, "A Comparison of Fatigue Test Data on Piping with the ASME Code Fatigue Evaluation Procedure," ASME Paper 79-PVP-92, American Society of Mechanical Engineers, New York, 1979.
121. Heald, J. D., and E. Kiss, "Low Cycle Fatigue of Nuclear Pipe Components," *J. Pressure Vessel Technol.* 74, PVP-5, 1-6, 1974.

122. Deardorff, A. F., and J. K. Smith, "Evaluation of Conservatism and Environmental Effects in ASME Code, Section III, Class 1 Fatigue Analysis," SAND94-0187, prepared by Structural Integrity Associates, San Jose, CA, under contract to Sandia National Laboratories, Albuquerque, NM, 1994.
123. Kooistra, L. F., E. A. Lange, and A. G. Pickett, "Full-Size Pressure Vessel Testing and Its Application to Design," *J. Eng. Power* 86, 419-428, 1964.
124. Scott, P. M., and G. M. Wilkowski, "A Comparison of Recent Full-Scale Component Fatigue Data with the ASME Section III Fatigue Design Curves," in *Fatigue and Crack Growth: Environmental Effects, Modeling Studies, and Design Considerations*, PVP Vol. 306, S. Yukawa, ed., American Society of Mechanical Engineers, New York, pp. 129-138, 1995.
125. Hechmer, J., "Evaluation Methods for Fatigue - A PVRC Project," in *Fatigue, Environmental Factors, and New Materials*, PVP Vol. 374, H. S. Mehta, R. W. Swindeman, J. A. Todd, S. Yukawa, M. Zako, W. H. Bamford, M. Higuchi, E. Jones, H. Nickel, and S. Rahman, eds., American Society of Mechanical Engineers, New York, pp. 191-199, 1998.
126. Manjoine, M. J., "Fatigue Damage Models for Annealed Type 304 Stainless Steel under Complex Strain Histories," *Trans. 6th Intl. Conf. on Structural Mechanics in Reactor Technology (SMiRT)*, Vol. L, 8/1, North-Holland Publishing Co., pp. 1-13, 1981.
127. Nian, L., and Du Bai-Ping, "The Effect of Low-Stress High-Cycle Fatigue on the Microstructure and Fatigue Threshold of a 40Cr Steel," *Int. J. Fatigue* 17 (1), 43-48, 1995.
128. Solin, J. P., "Fatigue of Stabilized SS and 316NG Alloy in PWR Environment," *Proc. of the 2006 ASME Pressure Vessels and Piping Conf.*, July 23-27, 2006, Vancouver, BC, Canada, paper # PVP2006-ICPVT-93833.

This page is intentionally left blank.

APPENDIX A

Incorporating Environmental Effects into Fatigue Evaluations

A1 Scope

This Appendix provides the environmental fatigue correction factor (F_{en}) methodology that is considered acceptable for incorporating the effects of reactor coolant environments on fatigue usage factor evaluations of metal components for new reactor construction. The methodology for performing fatigue evaluations for the four major categories of structural materials, e.g., carbon steel, low-alloy steels, wrought and cast austenitic stainless steels, and Ni-Cr-Fe alloys, is described.

A2 Environmental Correction Factor (F_{en})

The effects of reactor coolant environments on the fatigue life of structural materials are expressed in terms of a nominal environmental fatigue correction factor, $F_{en,nom}$, which is defined as the ratio of fatigue life in air at room temperature ($N_{air,RT}$) to that in water at the service temperature (N_{water}):

$$F_{en,nom} = N_{air,RT}/N_{water} \quad (A.1)$$

The nominal environmental fatigue correction factor, $F_{en,nom}$, for carbon steels is expressed as

$$F_{en,nom} = \exp(0.632 - 0.101 S^* T^* O^* \dot{\epsilon}^*), \quad (A.2)$$

and for low-alloy steels, it is expressed as

$$F_{en,nom} = \exp(0.702 - 0.101 S^* T^* O^* \dot{\epsilon}^*), \quad (A.3)$$

where S^* , T^* , O^* , and $\dot{\epsilon}^*$ are transformed S content, temperature, DO level, and strain rate, respectively, defined as:

$$\begin{aligned} S^* &= 0.001 && (S \leq 0.001 \text{ wt.}\%) \\ S^* &= S && (S \leq 0.015 \text{ wt.}\%) \\ S^* &= 0.015 && (S > 0.015 \text{ wt.}\%) \end{aligned} \quad (A.4)$$

$$\begin{aligned} T^* &= 0 && (T < 150^\circ\text{C}) \\ T^* &= T - 150 && (T = 150\text{--}350^\circ\text{C}) \end{aligned} \quad (A.5)$$

$$\begin{aligned} O^* &= 0 && (\text{DO} \leq 0.04 \text{ ppm}) \\ O^* &= \ln(\text{DO}/0.04) && (0.04 \text{ ppm} < \text{DO} \leq 0.5 \text{ ppm}) \\ O^* &= \ln(12.5) && (\text{DO} > 0.5 \text{ ppm}) \end{aligned} \quad (A.6)$$

$$\begin{aligned} \dot{\epsilon}^* &= 0 && (\dot{\epsilon} > 1\%/s) \\ \dot{\epsilon}^* &= \ln(\dot{\epsilon}) && (0.001 \leq \dot{\epsilon} \leq 1\%/s) \\ \dot{\epsilon}^* &= \ln(0.001) && (\dot{\epsilon} < 0.001\%/s) \end{aligned} \quad (A.7)$$

For both carbon and low-alloy steels, a threshold value of 0.07% for strain amplitude (one-half the strain range for the cycle) is defined, below which environmental effects on the fatigue life of these steels do not occur. Thus,

$$F_{en,nom} = 1 \quad (\epsilon_a \leq 0.07\%). \quad (A.8)$$

For wrought and cast austenitic stainless steels,

$$F_{en,nom} = \exp(0.734 - T' O' \dot{\epsilon}'). \quad (A.9)$$

where T' , $\dot{\epsilon}'$, and O' are transformed temperature, strain rate, and DO level, respectively, defined as:

$$\begin{aligned} T' &= 0 & (T < 150^\circ\text{C}) \\ T' &= (T - 150)/175 & (150 \leq T < 325^\circ\text{C}) \\ T' &= 1 & (T \geq 325^\circ\text{C}) \end{aligned} \quad (A.10)$$

$$\begin{aligned} \dot{\epsilon}' &= 0 & (\dot{\epsilon} > 0.4\%/s) \\ \dot{\epsilon}' &= \ln(\dot{\epsilon}/0.4) & (0.0004 \leq \dot{\epsilon} \leq 0.4\%/s) \\ \dot{\epsilon}' &= \ln(0.0004/0.4) & (\dot{\epsilon} < 0.0004\%/s) \end{aligned} \quad (A.11)$$

$$O' = 0.281 \quad (\text{all DO levels}). \quad (A.12)$$

For wrought and cast austenitic stainless steels, a threshold value of 0.10% for strain amplitude (one-half the strain range for the cycle) is defined, below which environmental effects on the fatigue life of these steels do not occur. Thus,

$$F_{en,nom} = 1 \quad (\epsilon_a \leq 0.10\%). \quad (A.13)$$

For Ni-Cr-Fe alloys,

$$F_{en,nom} = \exp(-T' \dot{\epsilon}' O'), \quad (A.14)$$

where T' , $\dot{\epsilon}'$, and O' are transformed temperature, strain rate, and DO, respectively, defined as:

$$\begin{aligned} T' &= T/325 & (T < 325^\circ\text{C}) \\ T' &= 1 & (T \geq 325^\circ\text{C}) \end{aligned} \quad (A.15)$$

$$\begin{aligned} \dot{\epsilon}' &= 0 & (\dot{\epsilon} > 5.0\%/s) \\ \dot{\epsilon}' &= \ln(\dot{\epsilon}/5.0) & (0.0004 \leq \dot{\epsilon} \leq 5.0\%/s) \\ \dot{\epsilon}' &= \ln(0.0004/5.0) & (\dot{\epsilon} < 0.0004\%/s) \end{aligned} \quad (A.16)$$

$$\begin{aligned} O' &= 0.09 & (\text{NWC BWR water}) \\ O' &= 0.16 & (\text{PWR or HWC BWR water}). \end{aligned} \quad (A.17)$$

For Ni-Cr-Fe alloys, a threshold value of 0.10% for strain amplitude (one-half the strain range for the cycle) is defined, below which environmental effects on the fatigue life of these alloys do not occur. Thus,

$$F_{en,nom} = 1 \quad (\epsilon_a \leq 0.10\%) \quad (A.18)$$

A3 Fatigue Evaluation Procedure

The evaluation method uses as its input the partial fatigue usage factors $U_1, U_2, U_3, \dots, U_n$, determined in Class 1 fatigue evaluations. To incorporate environmental effects into the Section III fatigue evaluation, the partial fatigue usage factors for a specific stress cycle or load set pair, based on the current Code fatigue design curves, is multiplied by the environmental fatigue correction factor:

$$U_{en,1} = U_1 \cdot F_{en,1} \quad (A.19)$$

In the Class 1 design-by-analysis procedure, the partial fatigue usage factors are calculated for each type of stress cycle in paragraph NB-3222.4(e)(5). For Class 1 piping products designed using the NB-3600 procedure, Paragraph NB-3653 provides the procedure for the calculation of partial fatigue usage factors for each of the load set pairs. The partial usage factors are obtained from the Code fatigue design curves provided they are consistent, or conservative, with respect to the existing fatigue ϵ - N data. For example, the Code fatigue design curve for austenitic SSs developed in the 1960s is not consistent with the existing fatigue database and, therefore, will yield nonconservative estimates of usage factors for most heats of austenitic SSs that are used in the construction of nuclear reactor components. Examples of calculating partial usage factors are as follows:

- (1) For carbon and low-alloy steels with ultimate tensile strength ≤ 552 MPa (≤ 80 ksi), the partial fatigue usage factors are obtained from the ASME Code fatigue design curve, i.e., Fig. I-9.1 of the mandatory Appendix I to Section III of the ASME Code. As an alternative, to reduce conservatism in the current Code requirement of a factor of 20 on life, partial usage factors may be determined from the fatigue design curves that were developed from the ANL fatigue life model, i.e., Figs. A.1 and A.2 and Table A.1.

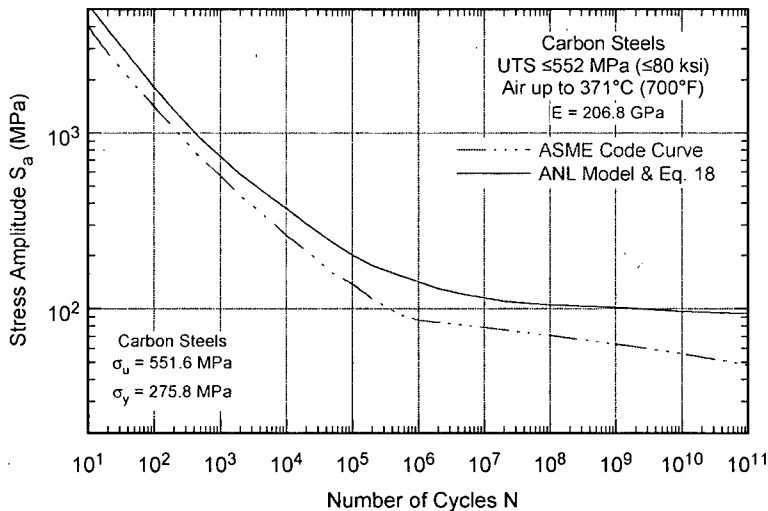


Figure A.1.
Fatigue design curve for carbon steels in air. The curve developed from the ANL model is based on factors of 12 on life and 2 on stress.

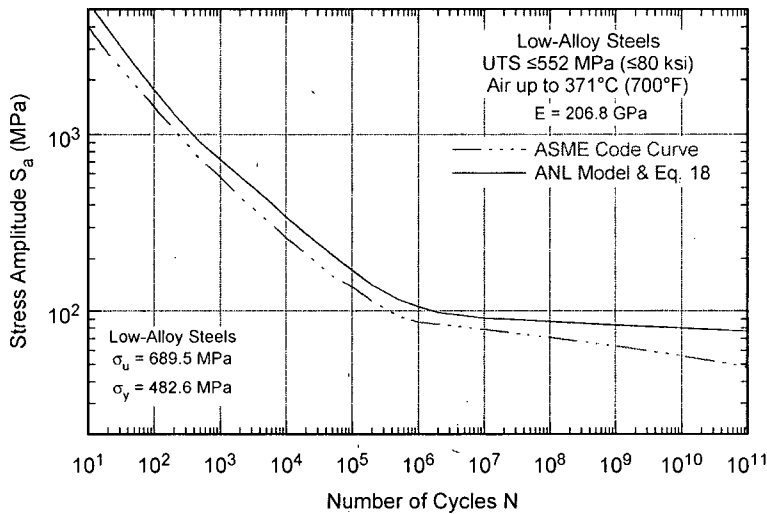


Figure A.2. Fatigue design curve for low-alloy steels in air. The curve developed from the ANL model is based on factors of 12 on life and 2 on stress.

Table A.1. Fatigue design curves for carbon and low-alloy steels and proposed extension to 10¹¹ cycles.

Cycles	Stress Amplitude (MPa/ksi)			Cycles	Stress Amplitude (MPa/ksi)		
	ASME Code Curve	Eqs. 15 & 18 Carbon Steel	Eqs. 16 & 18 Low-Alloy Steel		ASME Code Curve	Eqs. 15 & 18 Carbon Steel	Eqs. 16 & 18 Low-Alloy Steel
1 E+01	3999 (580)	5355 (777)	5467 (793)	2 E+05	114 (16.5)	176 (25.5)	141 (20.5)
2 E+01	2827 (410)	3830 (556)	3880 (563)	5 E+05	93 (13.5)	154 (22.3)	116 (16.8)
5 E+01	1896 (275)	2510 (364)	2438 (354)	1 E+06	86 (12.5)	142 (20.6)	106 (15.4)
1 E+02	1413 (205)	1820 (264)	1760 (255)	2 E+06		130 (18.9)	98 (14.2)
2 E+02	1069 (155)	1355 (197)	1300 (189)	5 E+06		120 (17.4)	94 (13.6)
5 E+02	724 (105)	935 (136)	900 (131)	1 E+07	76.5 (11.1)	115 (16.7)	91 (13.2)
1 E+03	572 (83)	733 (106)	720 (104)	2 E+07		110 (16.0)	90 (13.1)
2 E+03	441 (64)	584 (84.7)	576 (83.5)	5 E+07		107 (15.5)	88 (12.8)
5 E+03	331 (48)	451 (65.4)	432 (62.7)	1 E+08	68.3 (9.9)	105 (15.2)	87 (12.6)
1 E+04	262 (38)	373 (54.1)	342 (49.6)	1 E+09	60.7 (8.8)	102 (14.8)	83 (12.0)
2 E+04	214 (31)	305 (44.2)	276 (40.0)	1 E+010	54.5 (7.9)	97 (14.1)	80 (11.6)
5 E+04	159 (23)	238 (34.5)	210 (30.5)	1 E+011	48.3 (7.0)	94 (13.6)	77 (11.2)
1 E+05	138 (20.0)	201 (29.2)	172 (24.9)				

- (2) For wrought or cast austenitic SSs and Ni-Cr-Fe alloys, the partial fatigue usage factors are obtained from the new fatigue design curve proposed in the present report for austenitic SSs, i.e., Fig. A.3 and Table A.2.

The cumulative fatigue usage factor, U_{en} , considering the effects of reactor coolant environments is then calculated as the following:

$$U_{en} = U_1 \cdot F_{en,1} + U_2 \cdot F_{en,2} + U_3 \cdot F_{en,3} + U_i \cdot F_{en,i} \dots + U_n \cdot F_{en,n}, \quad (A.20)$$

where $F_{en,i}$ is the nominal environmental fatigue correction factor for the "i"th stress cycle (NB-3200) or load set pair (NB-3600). Because environmental effects on fatigue life occur primarily during the tensile-loading cycle (i.e., up-ramp with increasing strain or stress), this calculation is performed only for the tensile stress producing portion of the stress cycle constituting a load pair. Also, the values for key parameters such as strain rate, temperature, dissolved oxygen in water, and for carbon and low-alloy steels S content, are needed to calculate F_{en} for each stress cycle or load set pair. As discussed in Sections 4 and 5 of this report, the following guidance may be used to determine these parameters:

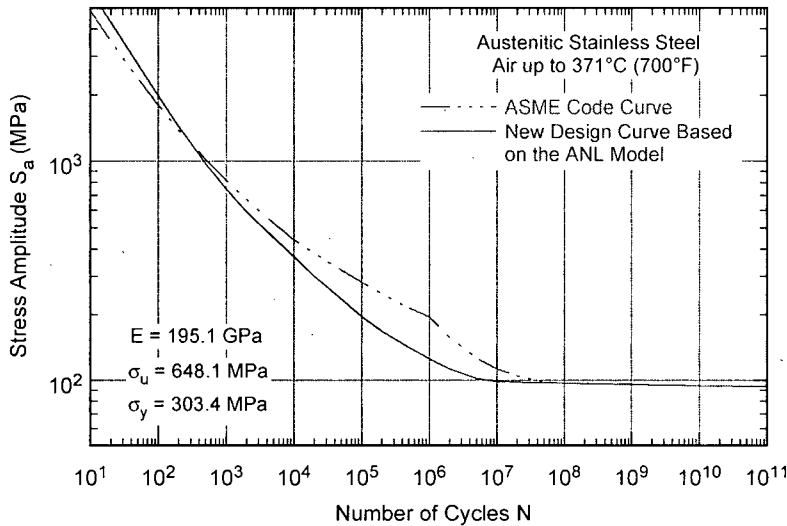


Figure A.3.
Fatigue design curve for austenitic stainless steels in air.

Table A.2. The new and current Code fatigue design curves for austenitic stainless steels in air.

Cycles	Stress Amplitude (MPa/ksi)		Cycles	Stress Amplitude (MPa/ksi)	
	New Design Curve	Current Design Curve		New Design Curve	Current Design Curve
1 E+01	6000 (870)	4881 (708)	2 E+05	168 (24.4)	248 (35.9)
2 E+01	4300 (624)	3530 (512)	5 E+05	142 (20.6)	214 (31.0)
5 E+01	2748 (399)	2379 (345)	1 E+06	126 (18.3)	195 (28.3)
1 E+02	1978 (287)	1800 (261)	2 E+06	113 (16.4)	157 (22.8)
2 E+02	1440 (209)	1386 (201)	5 E+06	102 (14.8)	127 (18.4)
5 E+02	974 (141)	1020 (148)	1 E+07	99 (14.4)	113 (16.4)
1 E+03	745 (108)	820 (119)	2 E+07		105 (15.2)
2 E+03	590 (85.6)	669 (97.0)	5 E+07		98.6 (14.3)
5 E+03	450 (65.3)	524 (76.0)	1 E+08	97.1 (14.1)	97.1 (14.1)
1 E+04	368 (53.4)	441 (64.0)	1 E+09	95.8 (13.9)	95.8 (13.9)
2 E+04	300 (43.5)	383 (55.5)	1 E+10	94.4 (13.7)	94.4 (13.7)
5 E+04	235 (34.1)	319 (46.3)	1 E+11	93.7 (13.6)	93.7 (13.6)
1 E+05	196 (28.4)	281 (40.8)	2 E+10		

- (1) An average strain rate for the transient always yields a conservative estimate of F_{en} . The lower bound or saturation strain rate of 0.001%/s for carbon and low-alloy steels or 0.0004%/s for austenitic SSs can be used to perform the most conservative evaluation.
- (2) For the case of a constant strain rate and a linear temperature response, an average temperature (i.e., average of the maximum and minimum temperatures for the transients) may be used to calculate F_{en} . In general, the "average" temperature that should be used in the calculations should produce results that are consistent with the results that would be obtained using the modified rate approach described in Section 4.2.14 of this report. The maximum temperature can be used to perform the most conservative evaluation.
- (3) The DO value is obtained from each transient constituting the stress cycle. For carbon and low-alloy steels, the dissolved oxygen content, DO, associated with a stress cycle is the highest oxygen level in the transient, and for austenitic stainless steels, it is the lowest oxygen level in the transient. A value of 0.4 ppm for carbon and low-alloy steels and 0.05 ppm for austenitic stainless steels can be used for the DO content to perform a conservative evaluation.

- (4) The sulfur content, S, in terms of weight percent might be obtained from the certified material test report or an equivalent source. If the sulfur content is unknown, then its value shall be assumed as the maximum value specified in the procurement specification or the applicable construction Code.

The detailed procedures for incorporating environmental effects into the Code fatigue evaluations have been presented in several articles. The following two may be used for guidance:

- (1) Mehta, H. S., "An Update on the Consideration of Reactor Water Effects in Code Fatigue Initiation Evaluations for Pressure Vessels and Piping," Assessment Methodologies for Preventing Failure: Service Experience and Environmental Considerations, PVP Vol. 410-2, R. Mohan, ed., American Society of Mechanical Engineers, New York, pp. 45-51, 2000.
- (2) Nakamura, T., M. Higuchi, T. Kusunoki, and Y. Sugie, "JSME Codes on Environmental Fatigue Evaluation," Proc. of the 2006 ASME Pressure Vessels and Piping Conf., July 23-27, 2006, Vancouver, BC, Canada, paper # PVP2006-ICPVT11-93305.

NRC FORM 335 (2-89) NRCM 1102, 3201, 3202	U. S. NUCLEAR REGULATORY COMMISSION	1. REPORT NUMBER (Assigned by NRC. Add Vol., Supp., Rev., and Addendum Numbers, if any.) NUREG/CR-6909 ANL-06/08				
BIBLIOGRAPHIC DATA SHEET (See instructions on the reverse)		2. TITLE AND SUBTITLE Effect of LWR Coolant Environments on the Fatigue Life of Reactor Materials Final Report				
5. AUTHOR(S) O. K. Chopra and W. J. Shack		3. DATE REPORT PUBLISHED <table border="1" style="width: 100%; text-align: center;"> <tr> <td>MONTH</td> <td>YEAR</td> </tr> <tr> <td>February</td> <td>2007</td> </tr> </table> 4. FIN OR GRANT NUMBER N6187	MONTH	YEAR	February	2007
MONTH	YEAR					
February	2007					
8. PERFORMING ORGANIZATION - NAME AND ADDRESS (If NRC, provide Division, Office or Region, U.S. Nuclear Regulatory Commission, and mailing address; if contractor, provide name and mailing address.) Argonne National Laboratory 9700 South Cass Avenue Argonne, IL 60439		6. TYPE OF REPORT Technical 7. PERIOD COVERED (Inclusive Dates)				
9. SPONSORING ORGANIZATION - NAME AND ADDRESS (If NRC, type "Same as above"; if contractor, provide NRC Division, Office or Region, U.S. Nuclear Regulatory Commission, and mailing address.) Division of Fuel, Engineering, and Radiological Research Office of Nuclear Regulatory Research U.S. Nuclear Regulatory Commission Washington, DC 20555-0001						
10. SUPPLEMENTARY NOTES H. J. Gonzalez, NRC Project Manager						
11. ABSTRACT (200 words or less) The existing fatigue strain-vs.-life ($\epsilon-N$) data illustrate potentially significant effects of LWR coolant environments on the fatigue resistance of pressure vessel and piping steels. Under certain environmental and loading conditions, fatigue lives in water relative to those in air can be a factor of ≈ 12 lower for austenitic stainless steels, ≈ 3 lower for Ni-Cr-Fe alloys, and ≈ 17 lower for carbon and low-alloy steels. This report summarizes the work performed at Argonne National Laboratory on the fatigue of piping and pressure vessel steels in LWR environments. The existing fatigue $\epsilon-N$ data have been evaluated to identify the various material, environmental, and loading parameters that influence fatigue crack initiation, and to establish the effects of key parameters on the fatigue life of these steels. Statistical models are presented for estimating fatigue life as a function of material, loading, and environmental conditions. The environmental fatigue correction factor for incorporating the effects of LWR environments into ASME Section III fatigue evaluations is described. The report also presents a critical review of the ASME Code fatigue design margins of 2 on stress (or strain) and 20 on life and assesses the possible conservatism in the current choice of design margins.						
12. KEY WORDS/DESCRIPTORS (List words or phrases that will assist researchers in locating this report.) Fatigue crack initiation Fatigue life Environmental effects Carbon and low-alloy steels Austenitic stainless steels Ni-Cr-Fe alloys BWR environment PWR environment	13. AVAILABILITY STATEMENT Unlimited 14. SECURITY CLASSIFICATION (This Page) Unclassified (This Report) Unclassified 15. NUMBER OF PAGES 16. ICE PR					

NUCLEAR REGULATORY COMMISSION

Title: Advisory Committee on Reactor Safeguards
Subcommittee on Materials, Metallurgy and
Reactor Fuels

Docket Number: (not applicable)

Location: Rockville, Maryland

Date: Wednesday, December 6, 2006

Work Order No.: NRC-1347

Pages 1-162

NEAL R. GROSS AND CO., INC.
Court Reporters and Transcribers
1323 Rhode Island Avenue, N.W.
Washington, D.C. 20005
(202) 234-4433

1
2
3
4
5
6
7
8
9
10
11
12
13
14
15
16
17
18
19
20
21
22
23
24
25

UNITED STATES OF AMERICA
NUCLEAR REGULATORY COMMISSION

+ + + + +

ADVISORY COMMITTEE ON REACTOR SAFEGUARDS
SUBCOMMITTEE ON MATERIALS, METALLURGY, AND
REACTOR FUELS

+ + + + +

WEDNESDAY,
December 6, 2006

+ + + + +

The meeting was convened in Room T-2B3 of
Two White Flint North, / 11545 Rockville Pike,
Rockville, Maryland, at 1:30 p.m., Dr. J. Sam Armijo,
Chairman of the subcommittee, presiding.

MEMBERS PRESENT:

- J. SAM ARMIJO, CHAIRMAN
- MARIO V. BONACA, ACRS MEMBER
- SAID ABDET KHALIK, ACRS MEMBER
- SANJOY BANERJEE, ACRS MEMBER
- THOMAS S. KRESS, ACRS MEMBER
- JOHN D. SIEBER, ACRS MEMBER
- GRAHAM WALLIS, ACRS MEMBER
- CHARLES G. HAMMER, DESIGNATED FEDERAL OFFICIAL
- CAXETANO SANTOS, ACRS STAFF

1	<u>I N D E X</u>	2
2	Opening Remarks, S. Armijo, ACRS	3
3	Overview of Regulatory Guide 1.207 (DG-1144)	
4	H. Gonzalez, RES	4
5	Discussion of Technical Basis for Regulatory	
6	Guide 1.207 and NUREG/CF-6909, O. Chopra,	
7	Argonne National Laboratory	11
8	Discussion of Public Comments and Staff	
9	Responses for Regulatory Guide 1.207	
10	and NUREG/CR-6909, H. Gonzalez, RES and	
11	O. Chopra, ANL	77
12	ASME Presentation, E. Ennis, ASME	85
13	AREVA Presentation, D. Cofflin, AREVA	142
14	Adjourn	161
15		
16		
17		
18		
19		
20		
21		
22		
23		
24		
25		

P-R-O-C-E-E-D-I-N-G-S

1:31 P.M.

1
2
3 CHAIRMAN ARMIJO: The meeting will now
4 come to order. This is a meeting of the Materials,
5 Metallurgy and Reactor Fuels Subcommittee. My name is
6 Sam Armijo, Chairman of the Committee. ACRS Members
7 in attendance are Dr. Mario Bonaca, Mr. Jack Sieber,
8 Dr. Bill Shack is sitting as a member of the audience
9 or staff at this point, Dr. Thomas Kress and Dr.
10 Graham Wallis are also present.

11 Gary Hammer of the ACRS staff is the
12 Designated Federal Official for this meeting.

13 The purpose of this meeting is to discuss
14 Regulatory Guide 1.207, guidelines for evaluating
15 fatigue analyses incorporating the life reduction of
16 metal components due to the effects of light-water
17 reactor environments for new reactors. We will hear
18 presentations from the NRC's Office of Nuclear
19 Regulatory Research and their contractor, Argonne
20 National Laboratory.

21 We will also hear presentations from
22 representatives of the American Society of Mechanical
23 Engineers and AREVA.

24 The Subcommittee will gather information,
25 analyze relevant issues and facts, and formulate

NEAL R. GROSS
COURT REPORTERS AND TRANSCRIBERS
1323 RHODE ISLAND AVE., N.W.
WASHINGTON, D.C. 20005-3701

1 proposed positions and actions, as appropriate for
2 deliberation by the Full Committee.

3 The rules for participation in today's
4 meeting have been announced as part of the notice of
5 this meeting previously published in the Federal
6 Register. We have received no written comments from
7 members of the public regarding today's meeting.

8 A transcript of the meeting is being kept
9 and will be made available as stated in the Federal
10 Register notice. Therefore, we request that
11 participants in this meeting use the microphones
12 located throughout the meeting when addressing the
13 Subcommittee.

14 Participants should first identify
15 themselves and speak with sufficient clarity and
16 volume so that they may be readily heard.

17 We will now proceed with the meeting and
18 I call on Mr. Hipolito Gonzales of the Office of
19 Nuclear Regulatory Research to begin.

20 MR. GONZALEZ: Thank you. I am Hipolito
21 Gonzalez. I'm the Project Manager for Regulatory
22 Guide 1.207. I'm from the Corrosion and Metallurgy
23 Branch and with me, Omesh Chopra. He's from Argonne
24 National Lab. He's going to be presenting part of the
25 regulatory basis, technical regulatory basis.

1 I would like to acknowledge William Cullen
2 from the Office of Research and John Ferrer, NRR, for
3 their helpful reviews and comments on this project.

4 Next slide.

5 The agenda today, we're going to be
6 discussing Regulatory Guide 1.207. I'm going to give
7 a quick historical perspective and then we're going to
8 go over an overview the reg. guide. And then Omesh
9 will present the technical basis which is the NUREG
10 report CR, NUREG CR 6909, Revision 1.

11 I'm going to give a summary of the
12 regulatory positions. And the last presentation is
13 going to be the resolution of public comments.

14 The ASME Section 3, fatigue design curves
15 were developed in the late 1960s and the early 1970s.
16 The tests conducted were in laboratory environments at
17 ambient temperatures. And the design curves included
18 adjusted factors of 2 constraint and 20 on cyclic life
19 to account for variations in materials, surface
20 finish, data scatter and size.

21 Results from the studies in Japan and
22 others in ANL, Argonne National Lab, as illustrated.
23 Potential significant effects of the light-water
24 reactor coolant environment on the fatigue life of the
25 steel, steel components.

1 Next slide.

2 Since the late 1980s, the NRC staff has
3 been involved in the discussion with ASME co-
4 committees, the PVRC and Technical Community to
5 address the issues related to the environmental
6 effects on fatigue.

7 In 1991, the ASME Board of Nuclear Code
8 and Standards requested the PVRC to examine worldwide
9 fatigue strain versus like data and develop
10 recommendations.

11 In 1995, it was resolution for GSI 166
12 which established that the risk to core damage from
13 fatigue failure of the reactor coolant system was
14 small. So no action was required for current plant
15 design life of 40 years. Also, the NRC staff
16 concluded that fatigue issues should be evaluated for
17 extended period of operation for license renewal and
18 this is under GSI-190.

19 In 1999, we had GSI-190 and the fatigue
20 evaluation of metal components for 60-year life plant,
21 plant life. Staff concluded that consistent with
22 requirements of 10 CFR 54.21, that aging management
23 programs for license renewal should address components
24 of fatigue including the effects of the environment.

25 On December 1, 1999, by letter to the

1 Chairman of the ASME Board of Nuclear Code and
2 Standards, the NRC requested ASME to revise the code
3 to include the environmental effects on the fatigue
4 design components.

5 Next slide.

6 ASME initiated the PVRC Steering Committee
7 on cyclic life and environmental effects and the PVRC
8 Committee recommended revising the code for design
9 fatigue curves. This was to WRC Bulletin 487.

10 After more than 25 years of deliberation,
11 there hasn't been any consensus regarding
12 environmental effects on fatigue life on the light-
13 water reactor environments.

14 The NRR requested research under user need
15 requests to 504 to develop guidance for determining
16 the acceptable fatigue life of ASME pressure boundary
17 components with consideration of the light water
18 reactor environment and this guidance will be used for
19 supporting reviews of application that the Agency
20 expects to receive for new reactors. The industry was
21 immediately notified that the NRC staff initiated this
22 work, the development of the reg. guide. In addition,
23 this is one of the high priority reg. guides to be
24 completed by March 2007.

25 In February and August this year, NRC

1 staff and ANL, we had presented at the ASME Code
2 Meetings the technical basis draft, NUREG CR6909. On
3 July 24, 2006, both the draft reg. guide and the NUREG
4 technical basis report were published for public
5 comments and the public comment period ended September
6 25.

7 In addition, on July 25, ANL presented a
8 paper on the technical basis again.

9 CHAIRMAN ARMIJO: Just to clarify
10 something, new reactors, does that include -- do these
11 rules apply to already certified design, such as the
12 ABWR and the AP1000? Are they grandfathered by virtue
13 of their certification?

14 MR. FERRER: This is John Ferrer from NRR
15 staff. They're grandfathered by virtue of their
16 certification that's already been addressed in the
17 reviews there, so we're not backfitting this reg.
18 guide to those certified designs.

19 DR. SIEBER: For 40 years though.

20 CHAIRMAN ARMIJO: Well, actually, if you
21 read the safety evaluation, the way it was written
22 said that they were evaluated for 60 years.

23 DR. SIEBER: Okay.

24 CHAIRMAN ARMIJO: That's kind of an
25 inconsistency in a way because they haven't been built

1 in the United States and if they were being certified
2 after this reg. guide is issued, that would be the
3 rule -- that would control the design, wouldn't it?

4 MR. FERRER: I wish I -- I agree with you.
5 Unfortunately, the way certified design works is once
6 we certify it, we'd have to go through a backfit
7 evaluation if we were going to apply this. And what
8 happened in the backfit evaluation, if you go back a
9 couple of slides on the GSI-166 and the GSI-190, we
10 did a backfit evaluation and showed the risk was not
11 high enough to justify a backfit, but the reason we
12 implemented it on license renewal was the fact that
13 the probability of leakage increased significantly
14 within 40 and 60 years.

15 But again, the risk which is the
16 probability of getting a pipe rupture that would lead
17 to core damage was still low.

18 CHAIRMAN ARMIJO: Thank you.

19 MR. GONZALEZ: Now I am going to go to an
20 overview of the reg. guide.

21 Next slide.

22 How the reg. guide 1.207 relates to the
23 regulatory requirements. GDC criterion, general
24 design criterion 1, quality standards and waivers.
25 And the part says that safety-related systems,

1 structures and components must be designed,
2 fabricated, erected and tested to the quality standard
3 commensurate with the importance of the safety
4 function performed.

5 GDC-30 states, in part, that components
6 included in a reactor pressure boundary must be
7 designed, fabricated, erected and tested to the
8 highest practical quality standards.

9 In 10 CFR 50.55A endorses the ASME boiler
10 pressure vessel code for design of safety-related
11 systems and components. These are Class 1 components.

12 ASME Code Section 3 includes the design
13 fatigue, includes the fatigue design curves. But
14 these fatigue design curves do not address the impact
15 of the reactor coolant system environment.

16 The objective of this regulatory guide is
17 to provide guidance for determining the acceptable
18 fatigue life of ASME pressure boundary components with
19 the consideration of the light water reactor
20 environment for major structural materials that will
21 be carbon steel, low-alloy steels, austenitic
22 stainless steel and nickel-based alloys. For example,
23 alloy-600, 690.

24 So in this guide, describes an approach
25 that the NRC staff considers acceptable to support

NEAL R. GROSS

COURT REPORTERS AND TRANSCRIBERS
1323 RHODE ISLAND AVE., N.W.
WASHINGTON, D.C. 20005-3701

1 reviews about the applications that the Agency expects
2 to receive for new reactors.

3 Implementation, this will only apply to
4 new plants. And no backfitting is intended. And this
5 is due to the conservatism in the current fleet of
6 reactors because of the design practices for fatigue
7 work conservatisms all plants were designed.

8 Next slide, please.

9 Now I'm going to -- how the technical
10 basis was developed. Omesh is going to give the
11 presentation on the technical basis report.

12 MR. CHOPRA: Thanks, Hipo.

13 DR. BONACA: I have a question regarding
14 your last statement. No backfitting is intended,
15 conservatism on coolant reactors. If the approach was
16 conservative on coolant reactors, I mean could it be
17 used also for new reactors?

18 MR. FERRER: Let me try to answer that.
19 In reviewing GSI-166 which was backfit to current
20 operating plants, we evaluated the as-existing fatigue
21 analyses and there were a number of conservatisms in
22 the specification of transients and the methodology
23 and the analysis.

24 We don't know whether or not that same
25 conservatism will be applied in the new reactors. In

NEAL R. GROSS

COURT REPORTERS AND TRANSCRIBERS
1323 RHODE ISLAND AVE., N.W.
WASHINGTON, D.C. 20005-3701

1 addition, there have been some changes in the ASME
2 code criteria since those original analyses were done
3 that removed some of the conservatisms in the
4 analysis. So if somebody were to do code analysis to
5 the current code criteria may not have the same level
6 of conservatisms.

7 DR. BONACA: I understand. Thank you.

8 MR. CHOPRA: The issue we are discussing
9 here today is effect of light water reactor coolant
10 environments on the fatigue life of structural steels.
11 Over the last 20 to 30 years, there's been sufficient
12 data accumulated, both in the U.S. and worldwide,
13 especially in Japan, which shows that coolant
14 environments can have a significant effect on the
15 fatigue life of these steels.

16 And this data is very consistent. It
17 doesn't matter where it has been rated, all show
18 similar trends without any exception. And also, the
19 fatigue data is consistent with a much larger database
20 on fatigue crack growth rates affect on environment of
21 fatigue crack growth rates. There's no inconsistency.
22 The mechanisms are very similar and both show similar
23 trends, effects of radius parameters, material loading
24 and environmental parameters have similar inference on
25 fatigue crack initiation and fatigue crack growth.

NEAL R. GROSS

COURT REPORTERS AND TRANSCRIBERS
1323 RHODE ISLAND AVE., N.W.
WASHINGTON, D.C. 20005-3701

1 And this fatigue data has been evaluated
2 to clearly define which are the important parameters.
3 They're well defined and also the range of these
4 parameters for which environmental effects are
5 significant, it's clearly defined.

6 So we know the conditions under which
7 environment would have an effect on fatigue life. The
8 question is do these conditions exist in the fleet?
9 If they exist, we will have an effect on the
10 environment and it should be considered. We know from
11 subsection 31.32.21 that the current fatigue design
12 curves do not include the effect of aggressive
13 environment which can accelerate fatigue failures and
14 has to be considered.

15 So the burden is on the designer to better
16 define these transients, to know what conditions
17 occurred during these transients and whether
18 environment would be involved.

19 Next, before getting into the
20 environmental effects, I just want to cover a few
21 background information. We are talking about the
22 effect of environment on fatigue life. Let's
23 understand what do we mean by fatigue life? The
24 current code design curves were based on data which
25 was where the specimens were tested to failure. Quite

NEAL R. GROSS

COURT REPORTERS AND TRANSCRIBERS
1323 RHODE ISLAND AVE., N.W.
WASHINGTON, D.C. 20005-3701

1 often, these design curves are termed as failure
2 codes, but I think the intent was to define fatigue
3 life as to prevent fatigue crack initiation, because
4 the data which has been obtained in the last 20 to 30
5 years in these results fatigue life is defined as the
6 number of sitings for the peak load to decrease by 25
7 percent.

8 And for the type of specimen, size of
9 specimens used in these tests, mostly quarter inch or
10 three-eighth round cylindrical specimens, this would
11 correspond to creating a three millimeter crack. So
12 we can say the fatigue life is the number of cycles
13 for a given strain condition to initiate a three
14 millimeter crack and from several studies we know that
15 surface crack, about 10 micron deep form quite early
16 during fatigue cycling.

17 So we can say that fatigue life is nothing
18 but it's associated with growth of these cracks from
19 a 10 micron size to 3 millimeter size and typically
20 this is the behavior of the growth of these cracks is
21 in this shape where crack length is a fraction of
22 fatigue life varies like this and it's divided into
23 two stages, initiation stage and a propagation stage.
24 Initiation stage is characterized by decrease in crack
25 growth rates. It's very sensitive to micro structure.

1 It involves sheer crack growth which is 45 degrees to
2 the stress axis, whereas propagation stage is not very
3 sensitive to microstructure. It was tensile crack
4 growth which is perpendicular to the stress axis and
5 this is the stage where you see on the fracture
6 surface well defined striations.

7 Various studies have shown that this
8 transition from an initiation stage to a propagation
9 stage occurs around -- depending on the material, 150
10 micron or 300 micron, that range.

11 So initiation stage is growth of crack up
12 to 300 microns. Propagation stage is beyond that to
13 3000 or 3 millimeter size.

14 Next slide.

15 CHAIRMAN ARMIJO: Before you leave that
16 curve, just for the benefit of people who don't
17 understand these curves, what is the time difference
18 between or the fatigue life difference from the three
19 millimeter crack initiated crack to through-wall
20 failure in the case of let's say a one-inch pipe, one-
21 inch wall thickness?

22 MR. CHOPRA: We would use the crack growth
23 rate data.

24 CHAIRMAN ARMIJO: Would that typically
25 increase the number of cycles by a factor of 2 or a

NEAL R. GROSS

COURT REPORTERS AND TRANSCRIBERS
1323 RHODE ISLAND AVE., N.W.
WASHINGTON, D.C. 20005-3701

1 factor of 10?

2 MR. CHOPRA: It depends on the conditions,
3 loading conditions and environment and so on. So we
4 know what the crack growth rates are for various
5 conditions. So we have to use that. But maybe I can
6 answer another way. In a test specimen, the
7 difference between 25 percent load drop and complete
8 failure of a specimen is very small. It's less than
9 one or two percent.

10 So whether we call it failure of a
11 specimen or defining it 25 percent drop, would be very
12 small difference. The idea of using 25 percent load
13 drop was to be consistent so that we define life as
14 some consistent -- all the labs do the same thing. So
15 that was the idea.

16 Otherwise, for a real component, if we
17 deal with three millimeter steel in a tube, it would
18 depend on crack growth rates.

19 CHAIRMAN ARMIJO: Okay.

20 MR. CHOPRA: Now the same curve I've
21 plotted a slightly different way where I plotted still
22 our cracked growth rates was the crack depths,
23 decreasing growth rates in the initiation stage and
24 increasing growth rates.

25 Now of course, crack growth would depend

1 on applied stress ranges. The higher the stress
2 range, the higher the crack growth. The delta sigma
3 one at very low stresses, the cracks which form during
4 cyclic loading may not growth to large enough size
5 that they can -- the propagation stage takes over.

6 DR. WALLIS: Crack velocity is really
7 growth rate and microns per cycle, not per unit of
8 time.

9 MR. CHOPRA: Right, but depending on the
10 time period one could convert it to --

11 DR. WALLIS: I know, but velocity is a
12 strange word.

13 MR. CHOPRA: Yes, maybe this should be
14 crack growth rate.

15 DR. WALLIS: If there's no cycling,
16 there's no crack growth.

17 MR. CHOPRA: Yes, yes. Beta sigma one,
18 when the stresses are very low, cracks may grow to
19 large enough size for the propagation to take over and
20 this is known as the fatigue limit of the material.
21 This is true for constant loading.

22 MR. BANERJEE: What's the mechanism that
23 changes the velocity so much?

24 MR. CHOPRA: Initial sheer crack growth.
25 It will extent maximum couple of degrees. So it's a

NEAL R. GROSS

COURT REPORTERS AND TRANSCRIBERS
1323 RHODE ISLAND AVE., N.W.
WASHINGTON, D.C. 20005-3701

1 shear crack growth, 45 degrees, whereas, once you go
2 deep enough, large enough size, you get into a
3 different process where actually fracture mechanics
4 methodology can be used to express that. It's a
5 tensile crack growth.

6 MR. BANERJEE: It's a multi-grain sort of
7 size and then it starts -- a different mechanism.

8 MR. CHOPRA: Typically, a couple of
9 grains. Fatigue limit is applicable only under
10 constant stress conditions. If we have random
11 loading, as in the case of a real component, then we
12 can have situations where we have higher stresses, few
13 cycles of higher stresses, where cracks can grow
14 beyond this depth that you can grow even at stresses
15 which are much lower than fatigue limit.

16 So the history of cycling is also
17 important for evaluating fatigue damage.

18 DR. WALLIS: Delta sigma is the magnitude
19 of this?

20 MR. CHOPRA: Of the stress range, applied
21 extracted stress range. And environment also.

22 DR. WALLIS: Does it matter if it's 10
23 silo or compressible?

24 MR. CHOPRA: On the tests which are used
25 for obtaining fatigue data, the strain range ratio is

1 -1, completely reversed. So we go from tensile to
2 compressive.

3 Even in environment, corrosion processes
4 can cause the cracks to grow beyond this and then
5 propagation can take over. So environment also could
6 accelerate. So the question is which part -- which of
7 these stages is affected by environment? Initiation
8 or propagation, or both?

9 DR. WALLIS: Your scales are linear, are
10 they?

11 MR. CHOPRA: This is a schematic.

12 DR. WALLIS: Schematic.

13 MR. CHOPRA: This portion is plotted here
14 where I have actual numbers. And I just wanted to
15 show you that we know from crack growth studies that
16 crack growth rates are affected by environment and
17 it's very well documented.

18 DR. WALLIS: These data look unreasonably
19 well behaved for materials data.

20 (Laughter.)

21 MR. CHOPRA: If we plotted a few tests, we
22 will see this happen.

23 CHAIRMAN ARMIJO: Agreement is log, log.

24 DR. WALLIS: Even so, I mean.

25 MR. CHOPRA: Anyway, effect of environment

NEAL R. GROSS

COURT REPORTERS AND TRANSCRIBERS
1323 RHODE ISLAND AVE., N.W.
WASHINGTON, D.C. 20005-3701

1 is also, has been studied in fatigue crack initiation.

2 DR. WALLIS: These are real data?

3 MR. CHOPRA: These are real data. But we
4 have calculated the crack growth rates in the fatigue
5 samples by benchmarking the fatigue crack front at
6 different stages during fatigue life. And so we can
7 see the three environments here: high oxygen -- high
8 dissolved oxygen water; low dissolved oxygen; PWR
9 water and air. And we see if you take 100 micron
10 crack length and air -- it took about 3,000 cycles to
11 reach that. In water, it took only 40 cycles, which
12 gives me an average growth rate of 2.5 micron per
13 cycle and this is this region here, average of this.

14 In this case, it's .0033 microns per
15 cycle. So we see two orders of magnitude effect of
16 environment which suggests that even the initiation
17 stage may be affected even more than what crack growth
18 rate is affected.

19 I just wanted to show you that both stages
20 are affected by the environment, even the growth of
21 very small cracks.

22 Now next, the design curves, what do the
23 design curves --

24 DR. WALLIS: Presumably, this is not just
25 one batch of data like this.

1 MR. CHOPRA: There's lots of data. I'm
2 just giving --

3 DR. WALLIS: There's a whole lot of data.

4 MR. CHOPRA: I'm just giving you one set,
5 yes. There's a lot of data.

6 DR. WALLIS: Because if there were
7 uncertainty in these, these curves might switch
8 positions.

9 MR. CHOPRA: sure, but I'm just presenting
10 that data to show that environment has a large effect.
11 It's the relative difference between air and water
12 which I was trying to show, not absolute crack growth
13 rates, just to show that it took only 40 cycles in
14 high oxygen water compared to 3,000 which suggests
15 that environment has a large effect on fatigue crack
16 initiation.

17 Now the design curves, we have -- the data
18 which we have obtained is on small specimens. They
19 are absolutely smooth and they were tested in room
20 temperature air. This is what was used to generate
21 the design curves in the current code. And all of
22 them were tested under strain control, fully reversed,
23 strain ratio of -1.

24 Now this gives me the best behavior of a
25 specimen when a crack would be initiated in a

1 specimen. To apply those results to actual reactor
2 component we need to adjust these results to account
3 for parameters or variables which we know affect
4 fatigue life, but are not included in this data. And
5 these variables are mean stress, surface finish, size,
6 loading history.

7 DR. WALLIS: Does the humidity of the air
8 make a difference?

9 MR. CHOPRA: Actually, if you look at the
10 basis document of the current code, they use a
11 subfactor which included surface roughness and
12 environment and by that environment they meant a lab,
13 well-controlled lab environment.

14 DR. WALLIS: Does the humidity of the air
15 make a difference?

16 MR. CHOPRA: In some cases it would, but
17 again, that is not studied as a -- it's not addressed
18 as an explicit parameter in defining fatigue life.
19 All data which was used was room temperature air to
20 generate the design curves.

21 DR. WALLIS: Room temperature means 20
22 degrees Centigrade or something?

23 MR. CHOPRA: Yes, 25, yes. To account for
24 these other variables like mean stress, surface
25 roughness and so on, what the current code --

1 DR. WALLIS: I'm sorry, when you -- maybe
2 you just said it. When you say PWR water, you mean at
3 room temperature or --

4 MR. CHOPRA: No, no. The design curves do
5 not address environment at all.

6 DR. WALLIS: But your data that you showed
7 us, the well-behaved data.

8 MR. CHOPRA: Those are higher
9 temperatures.

10 DR. WALLIS: Those are higher
11 temperatures.

12 MR. CHOPRA: They would be at reactive
13 temperatures.

14 DR. WALLIS: Okay. Could be a temperature
15 effect as well as an environment effect?

16 MR. CHOPRA: There is and I'll come to
17 that actually. In water, temperature is a very
18 important parameter. And to convert this data on
19 specimens to a real component, what the current code
20 does now is take the best --

21 DR. WALLIS: Is the PWR water that is
22 borated at initial strength or something?

23 MR. CHOPRA: PWR is. It both has boron
24 and lithium.

25 DR. WALLIS: There's some sort of average

NEAL R. GROSS

COURT REPORTERS AND TRANSCRIBERS
1323 RHODE ISLAND AVE., N.W.
WASHINGTON, D.C. 20005-3701

1 condition throughout the cycle?

2 MR. CHOPRA: Right, right. Typically,
3 people test around 1,000 ppm boron and 2ppm lithium.

4 To adjust these curves to an actual
5 reactor component, what the code does is we take the
6 best of the specimen data and adjust it for mean
7 stress correction and then apply these adjustment
8 factors of two on stress. We decrease the specimen
9 curve by a factor of two on stress and 20 on life,
10 whichever is the lower gets the design curve. But as
11 I mentioned, it does not include the effect of an
12 aggressive environment. In this case, what we are
13 talking about is light-water reactor environments.

14 Now to summarize some of the effects of
15 environment on carbon and low-alloy steels, there are
16 several parameters which are important. Steel type,
17 all of the data shows irrespective of steel type, it
18 doesn't matter which grade of carbon steel or low-
19 alloy steel, effect of environment is about the same.
20 There is a strain threshold below which environments
21 do not -- environmental effects do not occur. And
22 this threshold is very close to slightly above the
23 fatigue life of the steel. Strain rate is an
24 important parameter. There is a threshold, 1 percent
25 per second above that. Environmental effects are more

NEAL R. GROSS

COURT REPORTERS AND TRANSCRIBERS
1323 RHODE ISLAND AVE., N.W.
WASHINGTON, D.C. 20005-3701

1 great and lower the strain rate, higher the effect.
2 And it diffuses the saturation at around .001 percent
3 per second.

4 Similarly, temperature is very important.
5 Once again, there is a threshold; 150 degree C.
6 Higher temperatures, there's greater effect. Below
7 150 --

8 DR. WALLIS: Strain rate's lowest point is
9 .001 percent a second makes a difference?

10 MR. CHOPRA: Yes. I'll show you some of
11 the results.

12 DR. WALLIS: Really? That's awfully slow,
13 isn't it?

14 MR. CHOPRA: Some of the transients are.

15 DR. WALLIS: Abnormally slow.

16 MR. CHOPRA: Temperature also, there is
17 only a moderate effect below 150. Typically, when I
18 mean moderate effect, up to a factor of 2. Any water
19 touched surface may have up to a factor of --

20 DR. WALLIS: Linear decrease doesn't tell
21 me how fast it is. Linear decrease in life after 150
22 doesn't tell me how rapidly it decreases.

23 MR. CHOPRA: There are some slides, I'll
24 show you how much of a different it is.

25 MR. SANTOS: Do you have an equation?

NEAL R. GROSS

COURT REPORTERS AND TRANSCRIBERS
1323 RHODE ISLAND AVE., N.W.
WASHINGTON, D.C. 20005-3701

1 MR. CHOPRA: Yes.

2 DR. WALLIS: Which goes right through the
3 data?

4 MR. CHOPRA: Absolutely.

5 DR. WALLIS: Is this an Argonne equation
6 or a universal equation?

7 CHAIRMAN ARMIJO: You'll see.

8 DR. WALLIS: We'll see, okay.

9 MR. CHOPRA: Dissolved oxygen is also
10 similar. There's a threshold. In this case, low
11 oxygen environmental effects on carbon low-allow
12 steels are less. There's a threshold .04 ppm. Higher
13 dissolved oxygen has an environmental effect,
14 saturates around .05 ppm.

15 DR. WALLIS: How much sulfur is there in
16 the reactor?

17 CHAIRMAN ARMIJO: That's in the steel.

18 DR. WALLIS: In the steel, I'm sorry. I
19 thought you were talking about the environment. Now
20 you're talking about the steel?

21 MR. CHOPRA: These are --

22 DR. WALLIS: Dissolved oxygen in the
23 steel.

24 MR. CHOPRA: These are loading parameters.
25 Some are environmental parameters. Some are material

1 parameters.

2 DR. WALLIS: Okay.

3 MR. CHOPRA: Sulfur also has a large
4 effect on fatigue crack initiation.

5 DR. WALLIS: There's no other effects,
6 copper and stuff like that? There's no other effects?

7 MR. CHOPRA: In the steel? No. At least
8 the ones which we have looked at. Sulfur is the one
9 because it deals with the mechanism. Actually, the
10 reason why these are higher for carbon and low-alloy
11 steels which these are very well documented. It's the
12 sulfite iron density of the cracking. If we reach a
13 critical sulfite iron density crack enhancement
14 occurs. So these are very well documented in the
15 data. This is a mechanism. That's why sulfur is
16 important.

17 Roughness effects, we know if we have a
18 rough specimen surface it provides sites for
19 initiation. Life goes down. And in carbon low-alloy
20 steel, in air, there is an effect of surface
21 roughness, but some limited data suggests that in
22 water, rough and smooth specimens have about the same
23 life. So roughness effects may not be there for
24 carbon low-alloy steel.

25 Flow rate also, most of the data has been

1 obtained on very low flow rates or semi-stagnant
2 conditions. If we do these tests in higher flow
3 rates, effect of the environment does go down. Means
4 fatigue life would increase in high flow rates by a
5 factor of about 2.

6 Similarly, the effects on austenitic
7 stainless steels, same parameters, steel type, again
8 different grades of austenitic stainless steel,
9 similar effects and even cast austenitic stainless
10 steel have similar effects on the environment.

11 Once again we see a strain threshold below
12 which there is no effect and it's very close to the
13 fatigue limit. The dependence of strain rate and
14 temperature are very similar to what we see in carbon
15 and low-alloy steels.

16 The next three, dissolved oxygen, surface
17 roughness and flow rate, the effects are very
18 different from carbon and low-alloy steels. In this
19 case, for austenitic stainless steel, it's the low
20 oxygen which gives you a larger effect. And
21 irrespective of what steel type we use or what heat
22 treatment, heat treatment that means sensitization.
23 Sensitized stainless steel or solution in the
24 stainless steel both show similar life in low oxygen.

25 DR. WALLIS: That extends down to zero

1 oxygen?

2 MR. CHOPRA: Pardon me?

3 DR. WALLIS: That extends down --

4 MR. CHOPRA: If we can achieve that, you
5 know, but typically in a PWR, we have around -- it's
6 a low -- less than 50 ppm.

7 Yes, low oxygen, irrespective of the steel
8 type or heat treatment, there's a large effect on
9 environment, but in high oxygen, non-water chemistry,
10 PWR conditions, some steels show less effect and these
11 are solution annealed high-carbon steels which are not
12 sensitized. All low carbon grades such as 316 nuclear
13 grade or 304 L may have less effect in high oxygen.

14 Surface roughness and this is both in air
15 and water environments, there's a reduction in life.
16 Even in water. In carbonate steel we did not see a
17 reduction in life for rough samples. In this case,
18 both in air and water there is an effect of roughness.
19 And flow rate, there is no effect of flow rate on
20 fatigue life for austenitic stainless steels in water.

21 The differences between these three
22 suggests that the mechanism may be different for
23 austenitic stainless steels compared to carbon and
24 low-alloy steel. I mention the mechanism for carbon
25 and low-alloy steels, the sulfite iron density of the

1 crack depth. In this case, it's not well known --
2 there's no agreement on what is the mechanism. One
3 possible mechanism would be that as we expose stress
4 surface, hydrogen is created which changes the
5 definition of behavior and of the crack depth. But
6 this is one possible mechanism.

7 The next slides are details of what I
8 summarized. Unless there are specific questions, I'm
9 going to skip these next eight slides which basically
10 give the data which I summarized in the previous.

11 CHAIRMAN ARMIJO: I think it would be
12 better if you just highlight these things, just to
13 make the key points from these charts because I think
14 they're important.

15 MR. CHOPRA: This is the strain rate
16 effect. You were asking about the strain rate. I
17 plotted fatigue life for low-alloy steel, carbon steel
18 under certain conditions, strain amplitudes. In air,
19 PWR water and BWR.

20 DR. WALLIS: Are you claiming there's a
21 significant difference between air and PWR?

22 MR. CHOPRA: It's up to about a factor of
23 2 and this could be a factor of 15 or 20 lower

24 DR. WALLIS: We're not going to put in
25 that much oxygen, are we?

1 MR. CHOPRA: BWR has 200 to 300 ppb oxygen
2 and in this case, there are correlations which will
3 tell you how much -- depending on the oxygen, what
4 would be the effect.

5 This is the maximum effect because this is
6 I think .7. Saturation is at .5. So this is the
7 maximum effect under these conditions.

8 This is strain threshold which I
9 mentioned, the threshold about which effect of
10 environment is there. This gives you dissolved oxygen
11 at .04, this is carbon steel, higher oxygen levels,
12 things go down. And again, in PWR there's only a
13 modern effect.

14 I mentioned that for stainless steel, the
15 effect of dissolved oxygen is different. Here, this
16 is now three or four stainless at two different
17 strainless amplitude. There are two different tests
18 at different conditions, .25 and .33 and high oxygen,
19 no effect upstream rate and low oxygen, it goes down.
20 Whereas, a 316 NG or low carbon grade shows some
21 reduction in life in high oxygen, but not at the same
22 extent as you see in low oxygen.

23 So these are just a few examples I'm
24 showing. There's a lot of data in Japan and Europe
25 which shows similar trends. This shows the effect of

NEAL R. GROSS

COURT REPORTERS AND TRANSCRIBERS
1323 RHODE ISLAND AVE., N.W.
WASHINGTON, D.C. 20005-3701

1 sensitization. Sensitization is defined as a number,
2 EPI number. Degree of sensitization is increasing and
3 same conditions. In air, low oxygen, high oxygen and
4 we see in high oxygen it decreases with degree of
5 sensitization.

6 Effect of -- this is temperature again at
7 150 and lower, depending on what are the strain rates
8 and what are the dissolved oxygen conditions. If it's
9 very low, no effect. These are low oxygen conditions,
10 no effect. High oxygen, depending on the strain rate
11 and dissolved oxygen levels to the extent of the
12 effect in pieces.

13 DR. WALLIS: You're just talking about a
14 hundred cycles there, failure.

15 MR. CHOPRA: No, a thousand. In some
16 cases in the environment, it is.

17 DR. WALLIS: Right.

18 MR. CHOPRA: There is up to a factor of 20
19 reduction in life.

20 Surface roughness again, stainless steel,
21 open circles, smooth specimens; closed circles are
22 symbols are rough samples. A factor of 3 in air,
23 factor about the same in water.

24 CHAIRMAN ARMIJO: I don't want to belabor
25 this, but I looked at these data and the one that

1 shows -- the curve on the left for the air data, the
2 right triangles. They don't go through the best fit
3 curve at all.

4 MR. CHOPRA: Actually, this is 316 NG.
5 316 NG has a steeper slope, but for convenience we are
6 using a curve for all steels.

7 CHAIRMAN ARMIJO: So that's the best fit
8 curve there is for all --

9 MR. CHOPRA: All stainless steels, all
10 grades, including high or low-carbon grades.

11 DR. WALLIS: The purpose of the ASME curve
12 is to be below all the data, is that the idea?

13 MR. CHOPRA: Once we take into account,
14 you know I mentioned those adjustment factors of 20 on
15 fatigue and 2 on stress. Once we take that into
16 account, once we do that adjustment, then we want to
17 make sure that we are above that.

18 But these are best fit curves. So they
19 give you the average behavior for all --

20 DR. WALLIS: The ASME code has a factor of
21 2 in it or something? I don't see that.

22 MR. CHOPRA: I'll come to that. Give me
23 a

24 --

25 DR. WALLIS: Okay. But the factor of 2 is

1 in this curve here?

2 MR. CHOPRA: No, these are --

3 CHAIRMAN ARMIJO: ASME codes.

4 MR. CHOPRA: The code curve has the factor
5 of 2.

6 DR. WALLIS: No safety factor.

7 MR. CHOPRA: This is the best fit. These
8 are showing that even --

9 DR. WALLIS: Oh, I see. So you've give up
10 your margin of 2?

11 MR. CHOPRA: Right.

12 DR. WALLIS: Okay.

13 MR. CHOPRA: What we are saying is only
14 the margin or adjustment factors are gone for the --

15 CHAIRMAN ARMIJO: That's it.

16 MR. CHOPRA: Environment has taken care of
17 all that and still be within bound for a lot of other
18 factors like surface roughness and so on.

19 DR. WALLIS: You're going to tell us what
20 you're going to do about that?

21 MR. CHOPRA: Sure.

22 DR. WALLIS: Okay.

23 (Laughter.)

24 CHAIRMAN ARMIJO: Absolutely.

25 MR. CHOPRA: This gives you the effect of

1 flow rate. I mentioned that for carbon and low-alloy
2 steels, effect of environment is less.

3 Now a few slides for nickel alloy.
4 There's much less data on nickel alloys. Here, I've
5 plotted the data which is available --

6 DR. WALLIS: Much less data. So you're
7 showing us more than you showed us for steel?

8 MR. CHOPRA: What we do is rather than
9 coming with a new curve for nickel alloys, unless we
10 have enough data, what I'm trying to show is that we
11 can use the austenitic stainless steel to represent
12 the nickel alloys and even the few data we have for
13 alloy 690 suggests that we can use the austenitic
14 stainless steel code to determine usage factors,
15 fatigue usage factors for nickel alloys in air.

16 MR. BANERJEE: So temperature has almost
17 no effect here.

18 MR. CHOPRA: For carbon and low-alloy
19 steels there is some effect. Going from room
20 temperature to 300 may reduce life by about 50
21 percent, but stainless up to 400. There's not much
22 effect.

23 MR. BANERJEE: Including nickel alloys?

24 MR. CHOPRA: Nickel alloys, no. At 400,
25 in fact, they show longer life. But again, the data

NEAL R. GROSS

COURT REPORTERS AND TRANSCRIBERS
1323 RHODE ISLAND AVE., N.W.
WASHINGTON, D.C. 20005-3701

1 is very limited. There's few data sets at 400 which
2 actually show longer life for alloy 600. But again,
3 at present, since all curves are based on room
4 temperature data, we are not taking any temperature
5 dependence for air. But for water effects,
6 temperature is important and explicitly defined in the
7 expressions to calculate fatigue life in water.

8 DR. WALLIS: That means it is through the
9 median of the data in some way?

10 MR. CHOPRA: I'll show you how we got the
11 best fit curves.

12 DR. WALLIS: It's supposed to be an
13 average right through the middle of the data.

14 MR. CHOPRA: Right.

15 DR. WALLIS: It's not best fit to a 95
16 percentile or something like that? You'll get to that
17 too, but what you're showing here is --

18 MR. CHOPRA: Average, right. These
19 results show nickel alloy data for alloy 600 and some
20 of the welds. In BWR, normal water chemistry, BWR
21 environment and PWR environment and again, what we see
22 is the effects are similar to what we get for
23 austenitic stainless steels. There's larger effect in
24 low oxygen than in high oxygen. PWR environment has
25 larger effect than BWR, but the focal effect is much

NEAL R. GROSS

COURT REPORTERS AND TRANSCRIBERS
1323 RHODE ISLAND AVE., N.W.
WASHINGTON, D.C. 20005-3701

1 less than what you would see for austenitic stainless
2 steel.

3 Typically, under certain conditions in,
4 austenitic stainless steel we see a reduction of a
5 factor of 14 or 15. In this, the maximum is a factor
6 of 3. So the effect is much less, but we can use this
7 limited data to define the important parameters and
8 how to estimate environmental effects.

9 Now we have all this data. How do we
10 generate the expressions? All -- in air, all data,
11 fatigue data I expressed by this modified Langer
12 equation where fatigue life is expressed in terms of
13 strain amplitude and these constants A, B, C --

14 DR. WALLIS: Is this an equation because
15 you plotted the data on log paper, is that why it is?

16 MR. CHOPRA: This is the expression used
17 and it presents the data best.

18 DR. WALLIS: It's because you plotted it
19 on log paper. It looks good on log paper and it's
20 linear.

21 MR. CHOPRA: Well, the trend is also -- it
22 does represent the trend.

23 DR. WALLIS: Okay.

24 MR. CHOPRA: And C is the fatigue limit or
25 related with the fatigue limit of the material. B is

1 the slope of that curve. A is a constant which would
2 vary with heat to heat. Depending on a more resistant
3 material would give a higher A or lower means it's
4 less resistant to fatigue damage.

5 We can do a best fit of the data and also
6 use this A to represent heat to heat variability and
7 come up with a median value, how median material would
8 behave. Best fit gives me the average behavior,
9 whereas a distribution would give me how various
10 materials behave and I get a median curve and then
11 come up with a number which would bound 95 percent of
12 the materials. And that's what I'm going to show.

13 One more thing, another term, D can be
14 added to impute in 1, which would include parameters
15 like temperature, strain rate and so on.

16 DR. WALLIS: Does the ASME curve have a
17 similar equation?

18 MR. CHOPRA: Yes. The Langer equation is
19 very -- yes.

20 This shows for low-alloy steels in air and
21 water various heats. Now each did define even if I
22 have 10 data points, it's 1 point. Another may have
23 500 data points. But if it's the same material, it's
24 just one point on this plot. This way, I can give
25 you, we can determine the median value for the

1 materials and if I select a fifth percentile number,
2 in this case, 5.56, if I select the A or 5.56, that
3 curve would bound 95 percent of the --/

4 DR. WALLIS: It's the coefficient.

5 MR. CHOPRA: So this is how we obtain the
6 design curve by defining what subfactors I need to
7 adjust the best fit curve for average curve to come up
8 with a design curve which would bound 95 percent of
9 the materials.

10 I'll give the loca probability of track
11 initiation.

12 MR. BANERJEE: There's B and C as well,
13 right?

14 MR. CHOPRA: B and C, what I do is use it
15 for normalizing to get A for each heat which is the
16 average heat and I get a standard deviation. That's
17 what I've plotted here. For the particular heat, I've
18 given the average value and the standard deviation for
19 the data set.

20 MR. BANERJEE: You lost me.

21 CHAIRMAN ARMIJO: B and C are relatively
22 constant.

23 MR. CHOPRA: A is the one that changes.

24 MR. BANERJEE: So you fix B and C to some
25 value?

1 MR. CHOPRA: Right, right. And we know
2 even environment does not change. The strain
3 threshold was close to fatigue limit so I don't have
4 to change the fatigue limit. And there is no data
5 which suggests that C changes, means that the fatigue
6 limit changes for material.

7 DR. WALLIS: The range of that is not very
8 big, but if N is E to the A, so it's a factor of about
9 10 on the whole range.

10 MR. CHOPRA: Right.

11 MR. BANERJEE: Do B and C govern the shape
12 of the curve?

13 MR. CHOPRA: Yes. Right. The slope is B.
14 C is where at 10^6 or 10^7 .

15 DR. WALLIS: I see where it's flat.

16 CHAIRMAN ARMIJO: So all the environmental
17 effects are just put into the A constant?

18 MR. CHOPRA: Right.

19 CHAIRMAN ARMIJO: Okay.

20 MR. CHOPRA: Now we come up with these
21 expressions which can be used for predicting fatigue
22 life under various conditions. Again, Langer equation
23 A, constant A; slope B and C. And this is the
24 environmental term B which would have these -- which
25 would depend on these three parameters for carbon low-

NEAL R. GROSS

COURT REPORTERS AND TRANSCRIBERS
1323 RHODE ISLAND AVE., N.W.
WASHINGTON, D.C. 20005-3701

1 alloy steel, same for content, given by these
2 expressions, temperature, dissolved oxygen and strain
3 rate.

4 CHAIRMAN ARMIJO: Now the A is the five
5 percent number?

6 MR. CHOPRA: No. These are still the
7 average numbers.

8 CHAIRMAN ARMIJO: These are average
9 numbers.

10 MR. CHOPRA: Next, I'll get to where we
11 apply those adjustment factors to get the design
12 growth.

13 DR. WALLIS: What does N mean here?

14 MR. CHOPRA: Cycles --

15 DR. WALLIS: Environment. N for
16 environment, is that PWR?

17 MR. CHOPRA: No, this is in error what the
18 expression is. This is in the light water reactor.

19 DR. WALLIS: Okay.

20 MR. CHOPRA: It doesn't matter whether
21 it's BWR or PWR because these are the parameters which
22 will change in various environments, reactor
23 environments.

24 MR. BANERJEE: Is there no effective
25 hydrogen on it at all?

1 MR. CHOPRA: In BWR environment, there's
2 about 2 ppm dissolved hydrogen, but I think it's the
3 hydrogen which is created by the austenitic reaction
4 which is more important than what is -- it does
5 control ECP, the electrical potential of the
6 environment. So hydrogen would change the ECP, but
7 below -250 electrical potential, effects are not that
8 much different. But you know, in crack growth rates
9 there is some effect, depending on -- well, in this
10 case all -- we use only 2 PPM hydrogen.

11 MR. BANERJEE: These are all done in
12 autoclaves or whatever?

13 MR. CHOPRA: And we do simulate these
14 conditions. BWR, it's high oxygen, high purity, very
15 high purity. And pressurized water reactor, again
16 high purity. Then we had boron or boric acid to get
17 boron, 1,000 PPM and 2 PPM lithium, by adding lithium
18 hydroxide. And measure the pH. We measure the
19 conductivity and maintain all these water chemistry
20 parameters constant during the test.

21 CHAIRMAN ARMIJO: These are flowing a loop
22 type --

23 MR. CHOPRA: Very small flow rates. I
24 think if you look at the -- my plot, they would amount
25 to 10^{-5} meter per second. Very low.

1 CHAIRMAN ARMIJO: They're not static
2 autoclaves?

3 MR. CHOPRA: They're not static and they
4 are continuously reconditioned. So if they are, it's
5 once through. They're not repeated.

6 DR. WALLIS: How long are the tests done
7 typically?

8 MR. CHOPRA: Depends on the conditions.
9 At low strain amplitudes and low strain rates, it may
10 take up to 5 to 8 months and those results are very
11 limited. In the range which people have -- we have
12 tested .25 to .4 strain amplifies, it can take
13 anywhere from a few days to a month or two, depending
14 on the environmental effects. In air, they're much
15 longer. So one has to consider all of these. We
16 can't just dedicate and that's why you see very low,
17 less data under conditions which have very long
18 durations.

19 Now I just want to mention that these
20 expressions are average behavior after median
21 material. Same thing for rod and gas stainless steel.
22 Now as you mentioned that the slope of the 360 NG was
23 different, what we have done is we have used a single
24 expression to represent all grades of steel and this
25 number, the fatigue limit we chose what studies in

1 Japan have established. And Jaske and O'Donnell in
2 1978 pointed this out that the current design curve
3 for stainless steel was not consistent with the
4 experimental data.

5 DR. WALLIS: I want to check this about
6 oxygen. You say it's worse to have less oxygen?

7 MR. CHOPRA: Pardon me?

8 DR. WALLIS: N goes down when you have
9 less oxygen?

10 MR. CHOPRA: In stainless steel, life goes
11 down dissolved oxygen is low.

12 DR. WALLIS: But these it goes the other
13 way?

14 MR. CHOPRA: No. The oxygen, there's a
15 constant factor --

16 DR. WALLIS: In the one before, the carbon
17 and low-alloy steels?

18 MR. CHOPRA: Yes. Now in carbon and low-
19 alloy steel it's the high oxygen which is more
20 damaging.

21 DR. WALLIS: Then it doesn't make -- okay,
22 okay. That's right. Okay. Because I thought it was
23 the other way around. That's a negative --

24 MR. CHOPRA: The strain rate term is a
25 negative.

1 DR. WALLIS: That's right. I was crawling
2 through that and then I was trying to go back to
3 before.

4 MR. CHOPRA: Actually, this whole term is
5 --

6 DR. WALLIS: I understand that. Just
7 before, but the other with the stainless steel, the
8 low oxygen is bad.

9 MR. CHOPRA: Right.

10 DR. WALLIS: Okay, that's what I'm trying
11 to --

12 MR. CHOPRA: I just mentioned that we
13 established a single curve and this we selected from
14 what was proposed by these studies.

15 Now we have the specimen data. We know
16 how to predict what will happen with specimens.

17 DR. WALLIS: What effect does this have on
18 welds of dissimilar metals?

19 MR. CHOPRA: Welds have different --

20 DR. WALLIS: All together different?

21 MR. CHOPRA: Yes.

22 DR. WALLIS: Is there some basis for that?

23 MR. CHOPRA: It depends on the data.

24 DR. WALLIS: You're not addressing that?

25 MR. CHOPRA: No. This is the current code

1 design curves for these grades or types of structural
2 steel.

3 CHAIRMAN ARMIJO: For example, a welded
4 stainless steel is like a cast stainless steel, a weld
5 --

6 MR. CHOPRA: I think the behavior is very
7 similar. But --

8 CHAIRMAN ARMIJO: If it's similar, there's
9 a difference.

10 MR. CHOPRA: Because in some cases there
11 may be difference. We are just looking at here the
12 rod products.

13 CHAIRMAN ARMIJO: Stainless.

14 DR. WALLIS: Is there any effect of
15 fluence on this?

16 MR. CHOPRA: Irradiation? I'm sorry, I
17 didn't get that?

18 DR. WALLIS: Is there any effect of
19 fluence?

20 MR. CHOPRA: We're not studying that.
21 There is an effect, but that's not -- in the design
22 curve --

23 DR. WALLIS: It's all synergistic.

24 MR. CHOPRA: No environment is considered
25 and the designer has to account for other environments

NEAL R. GROSS

COURT REPORTERS AND TRANSCRIBERS
1323 RHODE ISLAND AVE., N.W.
WASHINGTON, D.C. 20005-3701

1 which are not considered in their design.

2 We have the data for specimens. Now to
3 use it to come up with a design curve for components,
4 I mention that they apply this adjustment factor of 20
5 on life and this factor is made up of effects of
6 material availability, data scatter, size, surface
7 finish, loading history.

8 In the current code, these are the
9 subfactors which are defined in the basis document.
10 Loading history was not considered, a total of 20
11 adjustment factors. In our study, based on the
12 distribution I showed for individual materials, this
13 subfactor can vary anywhere from a minimum of 2.1 to
14 2.8. These numbers are taken from studies in the
15 literature. Size can have an effect, minimum 1.2, 1.4
16 and so on. So we see a minimum of 6, maximum of 27.
17 When we take a large number, for example, 20, what we
18 are basically saying is I have a very bad material
19 which is very poor in fatigue resistance. I have
20 rough surfaces and I have the worse loading history.

21 So we used a Monte Carlo simulation and
22 using these as a log normal distribution to simulate
23 what would be the best adjustment needed to define the
24 behavior of components.

25 CHAIRMAN ARMIJO: So the present study,

1 you've agglomerated the data for carbon steels and
2 austenitic stainless steels and all these factors are
3 all pushed together.

4 MR. CHOPRA: Right.

5 CHAIRMAN ARMIJO: But you've separated
6 them. Are they different?

7 MR. CHOPRA: No, these are not the effects
8 of materialability is here and that depends on the
9 material. But effects of surface finish of the
10 component, size of the component or loading history
11 means random loading, high stress cycle followed by
12 low stress cycles. These -- in the current data,
13 these effects are not included. So somehow I need to
14 include these effects to come up with a design curve
15 which would be applicable to a real actual reactor
16 component.

17 Now the question is 20 was selected with
18 some basis. Is this reasonable because quite often,
19 this is what is being questioned. There may be
20 conservatism in this which we need to eliminate. So
21 we are trying to see what possible conservatism might
22 be there in this margin or the adjustment factor of
23 20.

24 DR. BONACA: Twenty was arbitrarily taken
25 as a bounding number, right?

1 Where did you get the 27?

2 MR. CHOPRA: I just took from the
3 literature what people have observed, effect of
4 surface -- surface finish is very well documented.
5 Depending on the average surface finish, an autonomous
6 value of surface finish, they have a harmless
7 reduction in light. So I can use typical finish for
8 grinding or milling operation and so on. It's well
9 documented. We can come up with what would be a
10 typical fabrication process, minimum and maximum. So
11 that's how we came up with this number.

12 DR. WALLIS: What is the basis of the
13 numbers? Is it trying to bound the data or bound the
14 95th percentile?

15 MR. CHOPRA: To come up with a design
16 curve which will be applicable to components.

17 DR. WALLIS: What's the basis of this? Is
18 there a rationale?

19 MR. CHOPRA: Right, 95 percent.

20 DR. WALLIS: Ninety-five, 99, 95?

21 MR. CHOPRA: Ninety-five?

22 DR. WALLIS: Why is 95 good enough?

23 MR. CHOPRA: Well --

24 DR. WALLIS: Why not 99?

25 MR. CHOPRA: We can do a statistical

1 analysis to see what are the probabilities.

2 CHAIRMAN ARMIJO: I think 95/5 basis is
3 sort of a typical basis we've used in a lot of other
4 studies on failure data. But the reason that 95/5 is
5 okay is we've already done risk studies with fatigue
6 cracks initiating and growing to failure and growing
7 to leakage and the fact of a 95/5 probability of
8 fatigue crack initiation still keeps you in acceptably
9 low probability of getting a failure.

10 DR. WALLIS: Okay, so it's related to the
11 overall --

12 CHAIRMAN ARMIJO: Overall margin, yes. If
13 it were just a 95/5 to failure it would be an
14 unacceptable criteria.

15 DR. WALLIS: If the consequence were much
16 worse, you'd need to have a --

17 CHAIRMAN ARMIJO: Yes.

18 MR. BANERJEE: Can you expand a bit more
19 by what you mean by this log normal distribution?

20 MR. CHOPRA: We assumed that the effects
21 of all of these parameters have a log normal.

22 MR. BANERJEE: Of some mean?

23 MR. CHOPRA: Right. And I took these two
24 ranges as the 5th and 95th percentile of that
25 distribution.

1 MR. BANERJEE: So what happens if you
2 chose a different distribution? Does it make any
3 difference to the results?

4 MR. CHOPRA: We have tried three
5 different, I think Bill tried and this gets the best
6 --

7 MR. BANERJEE: Best in what sense?

8 MR. CHOPRA: Very consistent result.
9 There's not much difference between normal and log
10 normal was not much difference. And log normal -- you
11 want to --

12 DR. SHACK: It's basically sort of an
13 arbitrary engineering judgment question. Experience
14 has indicated that when we have enough data, these
15 things do seem to be distributed log normally.

16 We generally don't have enough data,
17 actually, to determine the distribution. So we have
18 sort of just made the engineering judgment that the
19 log normal is close enough.

20 As John was explaining --

21 MR. BANERJEE: It doesn't affect the
22 results.

23 DR. SHACK: It doesn't affect the results
24 very much. What we're trying to do is to bound the
25 data in some reasonable fashion because the

1 consequence is not core damage when we're done. The
2 fact that we're not highly precise on this is not
3 something that concerns us, but we think we've built
4 in sufficient conservatism to account for these
5 variables in a sensible way without going overboard.

6 And the fact that these affects can be
7 considered as independent is also something we don't
8 have data on. We have to sort of work on an
9 engineering judgment basis. So the Monte Carlo
10 simulation that we do assumes the log normal
11 distribution, assumes the independence.

12 MR. CHOPRA: I want to add one more, quite
13 often, actually in the welding research that WRC
14 Bulletin by industry, they are suggesting that in this
15 margin of 20, we can use a factor of 3 to offset
16 environment. This kind of analysis can suggest or
17 show that 3 number is very high. We do not have that,
18 at least what is the possible --

19 DR. KRESS: Is it a theoretical basis for
20 assuming the log normal? There may be, you know. You
21 can look at the physical phenomena and --

22 DR. SHACK: Well, the loading, probably --

23 DR. KRESS: Loading you would think would
24 be log normal. I'm not sure about the effects of the
25 other things.

1 DR. SHACK: The log normal turns out to be
2 slightly more conservative than the normal and so
3 those were my -- if I don't have enough data to define
4 a distribution --

5 DR. KRESS: You might as well use --

6 DR. SHACK: I pick one or the other, sort
7 of on some sort of engineering judgment. The
8 differences are not very large between the two and we
9 just pick the log normal.

10 DR. WALLIS: If you know the distribution,
11 why do you need -- if you know the equation for the
12 distribution, why do you have to do a Monte Carlo
13 analysis?

14 DR. SHACK: Because I'm taking a bunch of
15 random variables.

16 DR. KRESS: That's the way you find the
17 mean, right?

18 MR. CHOPRA: There are four or five of
19 these things.

20 DR. SHACK: There are four or five
21 distributed variables.

22 DR. WALLIS: Easier to do it than to try
23 to go through the mathematics of predicting.

24 DR. SHACK: Yes, it's easier. Yes, I
25 could do it the other way, right.

NEAL R. GROSS

COURT REPORTERS AND TRANSCRIBERS
1323 RHODE ISLAND AVE., N.W.
WASHINGTON, D.C. 20005-3701

1 DR. KRESS: Is the 95 value four times the
2 mean?

3 DR. SHACK: No.

4 DR. KRESS: It has to be if it's log
5 normal.

6 DR. WALLIS: Four times the mean on a
7 constant A would be horrendous.

8 DR. KRESS: You've got to find the mean
9 value.

10 DR. WALLIS: Mean value is about five.

11 CHAIRMAN ARMIJO: Let's move on.

12 MR. CHOPRA: Doing this simulation, we get
13 these curves where this dash curve is now for the
14 specimen, the distribution of A for the specimen and
15 solid would be the distribution for the real
16 component. And we see that the median value has
17 shifted by about 5.3.

18 And 95 of 5th percentile is a factor of
19 12. So we can say that in this factor of 20, there is
20 some conservatism and we can use adjustment factor of
21 12 on life instead of 20.

22 DR. WALLIS: Where did 20 come from?

23 MR. CHOPRA: It's in the design basis
24 document of the current code.

25 DR. WALLIS: It's the judgment of a few

NEAL R. GROSS

COURT REPORTERS AND TRANSCRIBERS
1323 RHODE ISLAND AVE., N.W.
WASHINGTON, D.C. 20005-3701

1 wise men?

2 CHAIRMAN ARMIJO: Many years ago.

3 MR. CHOPRA: Basically, that's what it
4 was.

5 MR. BANERJEE: Not so bad.

6 MR. CHOPRA: The design has several --
7 yes.

8 I've covered -- there is some conservatism in the
9 fatigue evaluations and often this conservatism is
10 used to offset environmental effects and there are two
11 sources of conservatism, in the procedures themselves,
12 the way we define design stresses and design cycles or
13 this adjustment factors of 2 and 20.

14 I showed there's not much margin, only 1.7
15 in this factor of 20, but the current code procedures
16 --

17 DR. WALLIS: Is there enough to account
18 for environmental effects?

19 MR. CHOPRA: No, environmental effects can
20 be as high as a factor of 15.

21 DR. WALLIS: Yes.

22 MR. CHOPRA: Or carbon C would be even
23 higher.

24 DR. WALLIS: These are all reactor data
25 you've got, right?

1 MR. CHOPRA: Those are -- unless you
2 define the operating transient conditions. In certain
3 conditions those may be possible, but again, it's up
4 to the designer to define what are the conditions
5 during a transient, mean strain rates, temperatures
6 and so forth.

7 MR. BANERJEE: But I'm wondering whether
8 in your database you have anything which you've
9 evaluated from N reactor data or reactor data. Do you
10 have any information at all?

11 MR. CHOPRA: There are some components and
12 so on and I list a few examples where there have been
13 some studies. And I'll show you near the end of this.

14 DR. SHACK: The trouble with doing this
15 with field data is it's hard to control variables like
16 knowing that the strain range and because that has
17 such a strong effect on it. Unless you know that
18 accurate, it's hard to back out the result.

19 MR. CULLEN: Bill Cullen, Office of
20 Research. I'd like to explore Dr. Banerjee's question
21 a little more to find out what's behind it.

22 Are you concerned about irradiation
23 effects which really do not come into play for
24 pressure boundary? Or are you concerned about the
25 actual aqueous environment and its characteristics?

1 I'm not sure -- what is the basis?

2 MR. BANERJEE: Well, the basis is more --
3 it would be nice to see some validation under field
4 conditions. There are always sort of surprises
5 between the lab and what happens in the field and even
6 if this sort of validation is not all that thorough,
7 a couple of data points would set your mind at rest
8 that it's not some unexpected factor that comes in.

9 It's more like -- I have a concern always
10 of going from the lab to a real field situation. It's
11 not for any specific issue, not like radiation or
12 combination of factors or boron plus temperature in
13 fatigue cycles which are slow. All these things may
14 or may not be there but just a general question, more
15 a general question.

16 MR. CULLEN: I understand the general
17 question. I'm a little concerned about your word
18 about there always are surprises when you go from the
19 laboratory to the actuality.

20 MR. CHOPRA: Maybe that's too strong.

21 MR. CULLEN: A little bit.

22 (Laughter.)

23 DR. WALLIS: Oftentimes, surprises may be
24 small.

25 MR. CULLEN: Thank you.

NEAL R. GROSS

COURT REPORTERS AND TRANSCRIBERS
1323 RHODE ISLAND AVE., N.W.
WASHINGTON, D.C. 20005-3701

1 MR. BANERJEE: I don't mean to say that
2 this stuff should not be used or anything. Right.

3 MR. CHOPRA: I mentioned that in fatigue
4 evaluations the procedures are quite conservative, but
5 the code allows us to use improved approaches, for
6 example, finite element analysis, fatigue monitoring
7 to define the design stresses and cycles more
8 accurately. So most of this conservatism can be
9 removed with better methods for defining these design
10 conditions.

11 So in that case, there is a need to
12 address the effect of environment explicitly in these
13 procedures.

14 Now the two approaches which we can use
15 either come up with new set of design curves or use
16 some kind of correction factor, F_{en} . Now since
17 environmental effects depend on a whole lot of
18 parameters, temperature, strain rate and so on, either
19 we come up with several sets of design curves to cover
20 the possible conditions which occur in the reactor or
21 field conditions or if you use a bounding curve, it
22 would be very conservative for most of the conditions.

23 Whereas this correction factor, F_{en}
24 approach is relatively simple. You can -- it's very
25 flexible. You can calculate the environmental effects

1 for a specific condition. And this is what is being
2 proposed in this reg. guide.

3 The correction factor is nothing, and this
4 was proposed in 1991 by the Japanese. A correction
5 factor is nothing but a ratio of fatigue life and air
6 versus life and water. So we have these expressions
7 I showed you in the previous slides and we can then
8 calculate F_{en} for different steels, carbon steel, low-
9 alloy steel, and below a strain threshold there's no
10 environmental effects, so the correction factor would
11 be one.

12 Other than that, we use these expressions,
13 actual conditions, temperature, strain rates and so on
14 to calculate the correction factor. To incorporate
15 environmental effects, we take the usage, partial
16 usage factors obtain for specific transients in air,
17 U_1 , U_2 and so on, multiplied by the corresponding
18 correction factor and we get usage factor in the
19 environment.

20 Now to calculate usage factors in air, we
21 should use design curves which are consistent with or
22 conservative with respect to the existing data. And
23 as has been pointed out quite a few years back, the
24 current code curve for stainless steel is not
25 consistent with the current existing data and should

NEAL R. GROSS

COURT REPORTERS AND TRANSCRIBERS
1323 RHODE ISLAND AVE., N.W.
WASHINGTON, D.C. 20005-3701

1 not be used for obtaining usage. And I just want to
2 show before I get to that, these are the expressions
3 for nickel allows. Correction factor, again, as a
4 function of these three variables. And usage and air
5 would be obtained from the curve for austenitic
6 stainless steels.

7 Now I mentioned that the current design
8 curve for austenitic stainless steel is not consistent
9 with the data. I plotted the fatigue data for 316,
10 304 stainless in air, different temperatures and this
11 dashed curve is the curve, current code mean curve.
12 This is the mean curve which was used to obtain the
13 design curve.

14 DR. WALLIS: Where is your design curve?

15 MR. CHOPRA: Design curve would be what
16 you adjust this curve for mean curve correction.

17 DR. WALLIS: Your recommended curve would
18 actually bound the data, wouldn't it?

19 MR. CHOPRA: This is the best -- actually,
20 this data, the curve is based on austenitic stainless
21 steel.

22 DR. WALLIS: I thought you were
23 recommending a bounding curve with this factor.

24 MR. CHOPRA: I'm just trying to show that
25 the current --

1 DR. WALLIS: What's your design curve?
2 You should show that, shouldn't you?

3 MR. CHOPRA: These are mean curves.

4 DR. SHACK: This is air data, mean curve.
5 If we put a design curve on here, we could have a
6 design curve in air and a design curve in --

7 DR. WALLIS: There's all this air data.
8 Are you going to get to your -- it's so far down the
9 road, I can't -- okay.

10 CHAIRMAN ARMIJO: I think he's just trying
11 to show the difference between the two sets of means.

12 MR. CHOPRA: That the current means --

13 DR. WALLIS: You do show the effect of the
14 F factors yet.

15 MR. CHOPRA: No. I'm just trying to show
16 --

17 DR. WALLIS: We've just been talking about
18 --

19 DR. SHACK: What he's trying to
20 demonstrate here is that the F factor requires him to
21 take the ratio in air. He's got to have the right air
22 curve.

23 MR. CHOPRA: And the current mean curve
24 for air, for austenitic stainless steel, is not
25 consistent with the data.

1 Now I'd like to mention one thing, it's
2 been suggested that this curve, the data may be
3 different from the mean curve because of the way
4 fatigue life has been defined or the way we conduct
5 experiments. I can assure you that this difference in
6 the mean curve and the data is not due to any artifact
7 of test procedures or the way the fatigue life is
8 defined in terms of failure or 25 percent load drop.

9 DR. WALLIS: What occurs to me is the ASME
10 code mean curve was a mean curve to something.

11 MR. CHOPRA: Right.

12 DR. WALLIS: And it was presumably through
13 other data.

14 MR. CHOPRA: This curve, the current code
15 curve was based on very limited data. Now we have
16 much more. So I'm just showing that the data which
17 has been obtained since then is not consistent with
18 what we have.

19 DR. WALLIS: You have a much broader data
20 base.

21 MR. CHOPRA: Right.

22 DR. WALLIS: Okay, that's why yours is
23 better?

24 (Laughter.)

25 MR. CHOPRA: We are saying we should

1 change the current code curve. The current code curve
2 is not consistent with --

3 DR. WALLIS: It must have been based on
4 something.

5 MR. CHOPRA: And that data is somewhere in
6 here, up here. But since then we have much more data.

7 DR. WALLIS: Either that, or steels have
8 been getting weaker.

9 MR. CHOPRA: Actually, that is the reason.
10 Mostly like because of the strength of the steel,
11 probably these curves were obtained on steel which was
12 stronger.

13 DR. WALLIS: Wait a minute --

14 MR. CHOPRA: Possible difference.

15 MR. CULLEN: Bill Cullen, Office of
16 Research again. Omesh, if you could go back to that,
17 I'd like to also point out that the curves on which
18 the original ASME code were based I think the data
19 only went out to a factor of about, fatigue life of
20 10^6 or something.

21 MR. CHOPRA: Not even 6.

22 MR. CULLEN: So you've got two orders of
23 magnitude extrapolation there that we're doing now to
24 illustrate. But the other thing again is those tests
25 were all done at room temperature and you're showing

1 data from a wide variety of temperatures up to and
2 including operational.

3 MR. CHOPRA: Stainless does not --

4 MR. CULLEN: Doesn't show much difference,
5 right. To me, that's kind of the point. It all hangs
6 together on the lower curve.

7 MR. CHOPRA: This difference is genuine.
8 We need to use a different curve. And we have now
9 proposed a design curve for air for austenitic
10 stainless steels, the solid line. The current dashed
11 line is the current code of 10^6 and the high cycle
12 extension in the code. And the solid line curve is
13 based on the Argonne model plus adjustment factors of
14 12 on life and 2 on stress. It's not 20 and 2. It's
15 12 and 2.

16 DR. WALLIS: Now the kink that you have
17 here at 10^6 doesn't appear in the previous curve you
18 showed.

19 MR. CHOPRA: The design curve extends only
20 up to 10^6 .

21 DR. WALLIS: So you've just extrapolated
22 it here in your figure?

23 MR. CHOPRA: Yes, because now there is a
24 need to go all the way to 10^{11} .

25 DR. WALLIS: But you're saying mean curve,

1 so where do you stop at 10°?

2 CHAIRMAN ARMIJO: Two different things
3 here, hold on.

4 MR. FERRER: This is John Ferrer. I think
5 originally the stainless steel curve went out to 10°.
6 Later, they got more data at high cycles and the data
7 was clearly showing that there was a drop off and so
8 they -- this is an artifact of fairing the two curves
9 together and the new correction we're doing really is
10 straightening out what they should have straightened
11 out to begin with.

12 DR. WALLIS: Well, it's a curve, it can't
13 be straightened out.

14 (Laughter.)

15 MR. FERRER: For the earlier slide was the
16 man curve through the data. Now we are talking about
17 the code curve which would include these factors.

18 DR. WALLIS: Okay.

19 MR. GURDAL: There is still a curve A, B
20 and C.

21 My name is Robert Gurdal. I'm AREVA,
22 Lynchburg, Virginia. Those curves is because before
23 just now there are three curves, there is A, B and C
24 and they are not indicated there. I just wanted to be
25 sure everybody knows.

1 The reason you have the lower one which is
2 called a curve C --

3 MR. CHOPRA: But the region which we are
4 talking about is this 10^6 to 10 --

5 MR. GURDAL: You go above 10^6 , you have a
6 curve A, curve B and curve C.

7 MR. CHOPRA: I have plotted that.

8 MR. GURDAL: The correct curve is curve A
9 which is the top one.

10 DR. WALLIS: So it's C on this figure and
11 it's A on the previous figure.

12 MR. GURDAL: Maybe, it could be.

13 DR. WALLIS: Maybe. It probably doesn't
14 matter that much.

15 MR. GURDAL: And the C is for the heat
16 affected zone compared to the A.

17 DR. WALLIS: This is the A in this one.

18 MR. GURDAL: That one could be the A,
19 because it does not have the kink.

20 MR. CHOPRA: This is the mean curve.

21 MR. GURDAL: Oh, that's the mean curve.
22 Sorry about that. But the design curve, if you go to
23 the design, there is a curve continuing without any
24 disconnection.

25 DR. WALLIS: Without any kink, yes. Okay.

1 MR. GURDAL: And that's the A. This one
2 is a C.

3 MR. CHOPRA: But the region we are talking
4 about is this.

5 MR. GURDAL: Okay, but the question was
6 about 10^6 .

7 MR. CHOPRA: Which needs to be corrected.

8 DR. WALLIS: Okay, we've resolved that, I
9 think. Thank you. That's very good.

10 CHAIRMAN ARMIJO: Which gets to the point,
11 your design curve treats the weld heat affected zones
12 or the base material, everything as the same as
13 opposed to the code.

14 MR. CHOPRA: Yes, I think so.

15 MR. FERRER: I think so. In the code, I
16 think the previous gentleman was talking about their
17 -- in the high cycle regime, there are three separate
18 curves proposed by ASME that extend past the 10^6
19 cycles.

20 In our proposal we've just bounded that
21 with one curve.

22 MR. CHOPRA: We also have generated design
23 curves for carbon and low-alloy steels based on the
24 same approach using the Argonne models and adjustment
25 factors of 12 and 2. This is for carbon steel and

1 next is for low alloy.

2 Now current code curve for these is only
3 10^6 and now this is the current code curve and an
4 extension has been proposed by a subgroup, fatigue
5 strength. This was proposed a few years back, and it's
6 still not approved by the ASME code committees. We
7 are -- we have another approach to define extension of
8 this curve beyond 10^6 cycle. I just wanted to give a
9 couple of slides to show that.

10 What the subgroup fatigue strength
11 proposed was extension of the curve which is based on
12 load control data and the data extends only up to 10^6
13 and they use maximum effect of mean stress and they
14 propose extension which is expressed by applied stress
15 amplitude given in terms of life with an exponent of
16 $-.05$ which means 5 percent decrease in life, in stress
17 every decade. And since the data only extends up to
18 5 times 10^6 , extrapolation to 10^{11} may give
19 conservative estimates.

20 Another way of extending this curve would
21 be to use the approach with Manjoine had proposed a
22 few years back where the high-cycle fatigue is
23 represented by elastic strain with life blots and if
24 we use existing data which we have extending up to 10^8
25 cycles for these various speeds, we get a slope of -

NEAL R. GROSS

COURT REPORTERS AND TRANSCRIBERS
1323 RHODE ISLAND AVE., N.W.
WASHINGTON, D.C. 20005-3701

1 007. Manjoine proposed -.01 and we can use this
2 expression where the exponent is smaller and which is
3 consistent with the data and this would be for the
4 mean curve.

5 Now we take this adjusted for mean stress
6 correction using Goodman relation which is a
7 conservative approach and actually if we do that this
8 exponent would be .017. So it's slightly lower than
9 what is being proposed by the subgroup fatigue
10 strength, but we can use this expression and that's
11 what we have used to define that extension to the
12 curve.

13 DR. WALLIS: When you make these
14 proposals, did you negotiate something with ASME or
15 did you just say this is what we use --

16 MR. CHOPRA: This has been presented to
17 them.

18 DR. WALLIS: There wasn't any give and
19 take. It was just -- you deduced this from your data?

20 MR. CHOPRA: I attended the subgroup
21 fatigue strength and all our work has been presented
22 there.

23 DR. WALLIS: But the proposal is
24 essentially yours. It isn't some compromise proposal.
25 It's your proposal.

1 MR. CHOPRA: This was proposed by Manjoine
2 a few years back, so this is nothing new.

3 DR. WALLIS: All these green curves are
4 Argonne curves, proposed by Argonne?

5 MR. CHOPRA: No, the best fit curves are
6 what we have defined.

7 DR. WALLIS: Right, so they're not
8 something which has been negotiated and agreed on or
9 anything like that?

10 CHAIRMAN ARMIJO: It's certainly been
11 discussed.

12 DR. WALLIS: It's been discussed. IT's
13 been presented. ASME hasn't come around and said yes,
14 you guys are right.

15 DR. SHACK: One thing to think about for
16 the carbon and low-alloy steels, there's really in air
17 there's no disagreement over the mean curve. The
18 shape may shift just a smidgen, but the only real
19 difference between this design curve and the current
20 is they use a factor of 12 instead of 20. Then you do
21 have the discussion over how to extend it.

22 The environmental effect is a --

23 DR. WALLIS: It's the big one.

24 DR. SHACK: That's the big one.

25 CHAIRMAN ARMIJO: In the reg. guide, does

1 this curve really extend out to 10^{11} or does it -- is
2 it truncated at 10^7 , since there seem to be a big
3 difference.

4 MR. CHOPRA: The proposal is up to 10^{11} .

5 CHAIRMAN ARMIJO: Up to 10^1 , but compared
6 to the ASME code for this particular steel, your curve
7 is nonconservative.

8 MR. CHOPRA: Well, this is --

9 CHAIRMAN ARMIJO: You predict a much
10 longer life.

11 MR. CHOPRA: This is based on the data we
12 have.

13 CHAIRMAN ARMIJO: Right, but nobody has
14 data out to 10^{11} .

15 MR. CHOPRA: No.

16 CHAIRMAN ARMIJO: It's a less conservative
17 --

18 DR. WALLIS: You have a C. You have a
19 constant C or --

20 CHAIRMAN ARMIJO: Right.

21 DR. WALLIS: I'm surprised it isn't
22 completely flat to a green curve.

23 MR. CHOPRA: Made up of two. I mentioned
24 that extension is a different slope.

25 DR. WALLIS: Do they ever have 10^1 cycles

1 in a nuclear environment?

2 MR. FERRER: Vibration --

3 DR. WALLIS: Shaking things that shake.

4 MR. CHOPRA: So the method to apply the
5 correction would be to use for carbon low-alloy steel
6 you can use either the current code design curves or
7 the curves I've mentioned to reduce some conservatism.

8 As you see, it's -- they're based on
9 adjustment factors of 12, rather than 20.

10 For austenitic stainless steels and nickel
11 alloys, we use a new design curve for austenitic
12 stainless steels. And in the appendix to NUREG, there
13 are certain examples given to determine some of the
14 parameters.

15 For example, lab data shows quite often
16 people don't know how to calculate, how to define the
17 strain rates. Lab data shows average strain rate
18 always is a conservative approach.

19 And similarly, if we have a well-defined
20 linear transient temperature change, that can be
21 represented by average temperature and it could be
22 okay.

23 Now this one shows two more slides and
24 I'll be done. There was a question that lab data does
25 not represent the feed. There are certain reports

1 where some operating reports where some operating
2 experience and component test results have been
3 published.

4 This is EPRI report, 1997, and gives a
5 complete chapter, a couple of them, giving examples of
6 corrosion fatigue effects on nuclear power plant
7 components.

8 Similarly, studies in Germany, MPA and
9 other places have shown the conditions which lead to
10 what they call strain-induced corrosion cracking.
11 This was demonstrated for BWR environments. And there
12 are examples, even these examples are component test
13 results. We support the lab data.

14 I want to just show the results of one
15 particular test, component test, recent tests, again,
16 sponsored by EPRI where they used tube u-bend tests
17 tested in PWR water at 240. And I'm just plotting the
18 results for a given strain amplitude what was the
19 fatigue life they measured.

20 In earth environment, these are the
21 triangles. So that serves as a baseline you would
22 expect in air. Then they tested in PWR water in two
23 conditions: a strain rate of .01 percent per second
24 and diamonds are .005 percent per second. And this
25 would give me for this strain amplitude a life in air

1 of 12,500. This is about 36,000. This is 1700. And
2 you can determine for a component test what is the
3 environmental factor.

4 In this test, inert environment cracks
5 were on the OD. And they were biaxial conditions.
6 And the water, they were on the ID. And nearly
7 uniaxial. So since there was a conversion, there's a
8 question whether this number is accurate.

9 There's another way we can determine the
10 baseline life. They have a very well-defined strain
11 rate effect between these two. I applauded the
12 component test results with the lab data, exactly the
13 same slope and we know somewhere there's a threshold.
14 That would be the life in air. So I've got a number
15 8,000; 12,000. I use an average of 10. Gives me a
16 reduction of 5.8 for one strain rate; 2.8.

17 And the F_{en} we have presented, give you
18 5.5 and 3.6. I think these are very reasonable
19 comparisons from a real component test.

20 MR. BANERJEE: So the test was done
21 outside the reactor, right?

22 MR. CHOPRA: This is a component test,
23 where they took an actual u-bend tube and strained it.
24 So it's not a small specimen. They are testing a real
25 component -- it demonstrates that lab data is

1 applicable to actual component test conditions.

2 CHAIRMAN ARMIJO: Did you compare any of
3 the other component tests that you referenced in the
4 previous slide with your data to see how your data
5 predicts?

6 MR. CHOPRA: Some of the earlier, no, we
7 have not.

8 MR. BANERJEE: Do you have any idea of the
9 -- is there anything which happened in a reactor where
10 you have the strain history or something for a period
11 of time?

12 MR. FERRER: I think the answer to that is
13 it's very difficult to have the exact data on the
14 strain history in an actual operating event. We've
15 tried to estimate it and the best you can do is
16 estimate it. I think Omesh presented some references.
17 I think the EPRI one which attributed some of the
18 cracking to environment, but you couldn't prove it
19 absolutely because you just don't have the exact
20 temperature measurements and the strain measurements
21 at the location of your cracks.

22 MR. BANERJEE: But you can estimate them,
23 right? Based on those estimates, what does it look
24 like?

25 MR. FERRER: If you go back to the

1 reference EPRI report, you know, I think based on
2 their estimates they attribute some of it to
3 environmental, but I say those estimates are very
4 crude. They're not nearly as controlled as the lab
5 data and if you look at fatigue, the -- at the low
6 cycle end, the small change in stress gives you a
7 fairly large change in the number of cycles if you
8 look at the shape of the curve.

9 And so it's not that easy. There are some
10 estimates, but they're more judgmental than accurate
11 calculations.

12 MR. BANERJEE: But the evidence or
13 supports -- what you're saying --

14 MR. FERRER: Well, there's some evidence.
15 What you'll hear from -- probably from ASME is the
16 overall operating experience doesn't show that there's
17 a big problem there.

18 MR. BANERJEE: Okay.

19 CHAIRMAN ARMIJO: Okay. That's it?

20 MR. CHOPRA: Yes.

21 CHAIRMAN ARMIJO: Any other questions from
22 the Committee?

23 MR. GONZALEZ: I would like to go back to
24 the reg. guide to present a summary of the three
25 regulatory positions.

1 Regulation position 1, we are endorsing
2 that we will calculate fatigue using air with ASME
3 code analysis procedures plus use the ASME code air
4 curves for new ANL modern air curves. This is for
5 carbon and alloy steels only.

6 Then we will calculate the F_{en} using the
7 appendix A of the NUREG for carbon and alloy steels
8 and this will be applied to calculate the
9 environmental uses factor.

10 But we're given the option of using the
11 ASME curve or the new air curve from the ANL model.
12 Or austenitic stainless steel, we will calculate the
13 fatigue use factoring there with the ASME code
14 analysis procedure, plus the new ANL model air
15 stainless steel curve.

16 We'll use the -- also the F_{en} equation for
17 stainless steel and then calculate the environmental
18 usage factor.

19 For nickel chrome alloys, will be Alloy
20 600, 690. You will use again the ASME code analysis
21 procedure plus the new ANL model air stainless steel
22 curve. As the reason was it was explained before was
23 because of the new data.

24 And if the F_{en} specifically for nickel
25 alloys and calculate the usage factor -- the

1 environmental fatigue usage factor.

2 In summary, Reg. Guide 1.207 will endorse
3 the use of a new air curve for austenitic stainless
4 steels and also will endorse the F_{en} methodology. It
5 will give guidance on incorporating the environmental
6 correction factor, the fatigue design analysis and
7 this is described in Appendix A of the NUREG report
8 and also the NUREG report will describe in detail the
9 technical basis.

10 That's it. Any more questions?

11 CHAIRMAN ARMIJO: Okay, any questions?
12 We're scheduled for a break about now, but we're a
13 little bit ahead of schedule. I don't know if we can
14 reconvene in 15 minutes or do we have to wait until
15 3:35?

16 We'll just take a 15-minute break. Be
17 back at 3:25. Is that right? 3:25, thank you.

18 (Off the record.)

19 CHAIRMAN ARMIJO: Okay, we've got --
20 incredibly we're about five minutes ahead of schedule,
21 so that's good.

22 So Mr. Gonzalez, would you like to
23 continue?

24 MR. GONZALEZ: This is our second part,
25 second presentation. It's in the resolution to public

NEAL R. GROSS AND CO., INC.

Title: Advisory Committee on Reactor Safeguards
549th Meeting

Docket Number: (n/a)

Location: Rockville, Maryland

Date: Thursday, February 7th, 2008

Work Order No.: NRC-2007

Pages 1-346

NEAL R. GROSS AND CO., INC.
Court Reporters and Transcribers
1323 Rhode Island Avenue, N.W.
Washington, D.C. 20005
(202) 234-4433

much done. The question I have: is there any question for the staff here? Any questions for Mr. Hopenfeld from members?

MEMBER ARMIJO: I'd like to ask with respect to the last presenter's comments about new data. Is the staff familiar with -- no, I'm asking the staff if they're aware of the new data that you referred to

MR. FAIR: Hi. I'm John Fair with Division of Engineering who did a lot of the reviews on environmental fatigue.

Yes, we are. The new data is the latest Argonne data that was being applied in new design certifications. Basically the criteria they're using ins license renewal was criteria that was developed quite a while back, and we made a decision at that time that we would, as criteria, we would maintain that criteria because there were a lot of applications in process. So we didn't want to keep changing the rules as these people were putting in new applications. And a lot of the criteria had changed and was massaged over the years.

Actually if you go back and look at the latest criteria we're applying to new reactors, it's not as conservative as the old criteria because we

NEAL R. GROSS

COURT REPORTERS AND TRANSCRIBERS

1323 RHODE ISLAND AVE., N.W.

WASHINGTON, D.C. 20005-3701

(202) 234-4433

www.nealrgross.com

changed the basis for deriving the curves. So if you go and look at the Fen factors themselves using the new criteria, they'll generally be lower.

MEMBER ARMIJO: Okay. Thank you.

VICE CHAIRMAN BONACA: Any other questions?

If not, Mr. Chairman, I'll turn the meeting back to you.

CHAIRMAN SHACK: Okay. Well, it's five minutes late. I'd like to take a break now. I thank the presenters, staff and the industry, for a good presentation, I think, very informative and Mr. Hopenfeld for his comments.

We're slated for 15 minutes. So we'll be back at ten of.

(Whereupon, the foregoing matter went off the record at 10:35 a.m. and went back on the record at 10:55 a.m.)

CHAIRMAN SHACK: The next topic is a draft final Revision 1 to Regulatory Guide 1.45, "Guidance on Monitoring and Responding to Reactor Coolant System Leakage, and, Sam, I think you're going to take us through that.

MEMBER ARMIJO: Right. Thank you, Mr. Chairman.

NEAL R. GROSS

COURT REPORTERS AND TRANSCRIBERS
1323 RHODE ISLAND AVE., N.W.
WASHINGTON, D.C. 20005-3701

NEC-JH 29

Heat and Mass Transfer

by E. R. G. ECKERT

*Professor of Mechanical Engineering
and Director of the Heat Transfer Laboratory
University of Minnesota*

WITH PART A, HEAT CONDUCTION
AND APPENDIX OF PROPERTY VALUES

by ROBERT M. DRAKE, Jr.

*Professor and Chairman
Mechanical Engineering Department Princeton University*

Second Edition of

INTRODUCTION TO THE TRANSFER OF HEAT AND MASS

McGRAW-HILL BOOK COMPANY, INC.

New York Toronto London

1959

ENGINEERING

g. Editors

Expri-

Richard G.
f. Susselaer

H. Hausen¹ gave the expression for the average Nusselt number:

$$\bar{Nu}_d = 0.116[(Re_d)^{2/3} - 125](Pr)^{1/4} \left[1 + \left(\frac{d}{x}\right)^{1/4} \right] \left(\frac{\mu_B}{\mu_w}\right)^{0.14}$$

where μ_B is the viscosity at bulk liquid temperature and μ_w the viscosity at tube-wall temperature. Apart from the latter, the property values are to be inserted at t_B . This formula takes into account the conditions in the intake region. It also satisfactorily reproduces the values in the transition zone $Re_d = 2,300$ to $6,000$. This relation is expected to be especially applicable to fluids for which the variation of viscosity is the

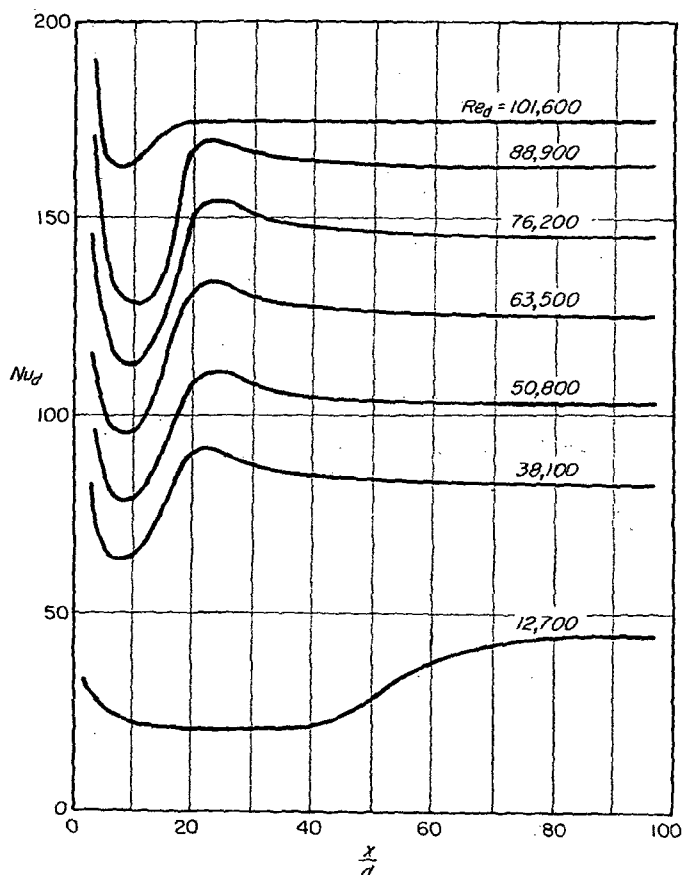


FIG. 8-9. Local Nusselt numbers for flow through a tube near the entrance with simultaneous development of the flow and temperature field. [From W. Linke and H. Kunze, *Allgem. Wärmetech.*, 4:73-79 (1953).]

¹ H. Hausen, *Z. Ver. deut. Ingr., Beih. Verfahrenstech.*, no. 4, 1943, pp. 91-98.

Boundary Layer Theory

NEC-JH 30

BY

Dr HERMANN SCHLICHTING

Professor at the Engineering University of Braunschweig

Director of the Aerodynamische Versuchsanstalt Göttingen

Head of the Institute for Aerodynamics of

the Deutsche Forschungsanstalt für Luft- und Raumfahrt, Braunschweig, Germany

Translated by

Dr J. KESTIN

Professor at Brown University in Providence, Rhode Island

Fourth Edition

McGRAW-HILL BOOK COMPANY, INC.
NEW YORK · TORONTO · LONDON
VERLAG G. BRAUN · KARLSRUHE

a common maximum at $h/d \approx -0.5$. Further small local maxima occur at $-h/d \approx 0.1$ and 1.0 . The minima between them occur at $-h/d \approx 0.2, 0.8,$ and 1.35 . Depending on the depth of the cavity it may sometimes happen that regular vortex patterns are formed in it, leading to the different values of drag. As seen from the symmetry of the curves about $h/d = 0$ shallow cavities of up to $-d/h = 0.1$ give the same increase in drag as corresponding small protuberances.

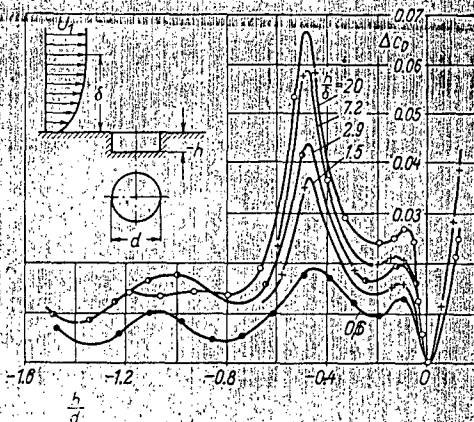


Fig. 21.14. Resistance coefficient of circular cavities of varying depth in a flat wall, as measured by Wieghardt [54]

The flow pattern which exists behind an obstacle placed in the boundary layer near a wall differs markedly from that behind an obstacle placed in the free stream. This circumstance emerges clearly from an experiment performed by H. Schlichting [38] and illustrated in Fig. 21.15. The experiment consisted in the measurement of the velocity field behind a row of spheres placed on a smooth flat surface. The pattern of curves of constant velocity clearly shows a kind of *negative wake effect*. The smallest velocities have been measured in the free gaps in which no spheres are present over the whole length of the plate; on the other hand, the largest velocities have been measured behind the rows of spheres where precisely the smaller velocities

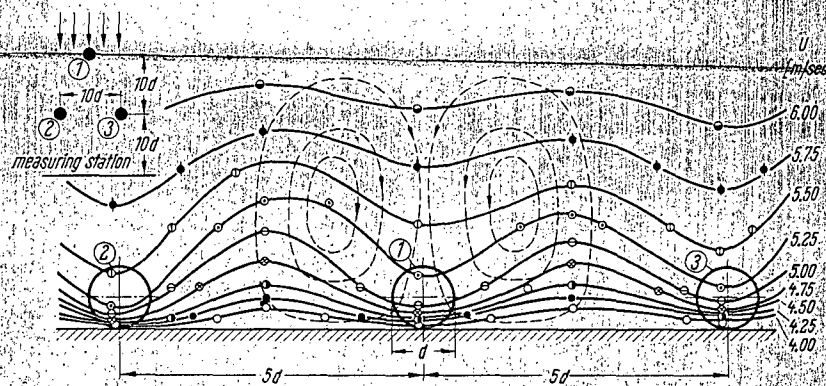


Fig. 21.15. Curves of constant velocity in the flow field behind a row of spheres (full lines) as measured by H. Schlichting [38], and accompanying it the secondary flow (broken lines) in the boundary layer behind sphere (1), as calculated by F. Schultz-Grunow [46]. In the neighbourhood of the wall, the velocity behind the spheres is larger than that in the gaps. The spheres produce a "negative wake effect" which is explained by the existence of secondary flow. Diameter of spheres $d = 4$ mm

Heat Transfer

Fifth Edition

J. P. Holman

Professor of Mechanical Engineering
Southern Methodist University

McGraw-Hill Book Company

New York St. Louis San Francisco Auckland
Bogotá Hamburg Johannesburg London Madrid
Mexico Montreal New Delhi Panama
Paris São Paulo Singapore
Sydney Tokyo
Toronto

Gift

7-14-87

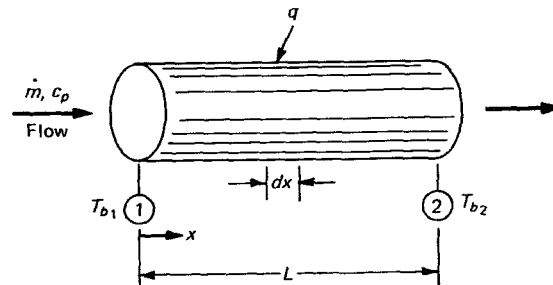
NEC-JH_31 \$44.00

0042539

QC
320
1H64
1981

CENTRAL LIBRARY
U.S. NAVAL AIR STATION
PATUXENT RIVER, MD. 20670

Fig. 6-1 Total heat transfer in terms of bulk-temperature difference.



plicated problems may sometimes be solved analytically, but the solutions, when possible, are very tedious. For design and engineering purposes, empirical correlations are usually of greatest practical utility. In this section we present some of the more important and useful empirical relations and point out their limitations.

First let us give some further consideration to the bulk-temperature concept which is important in all heat-transfer problems involving flow inside closed channels. In Chap. 5 we noted that the bulk temperature represents energy average or "mixing cup" conditions. Thus, for the tube flow depicted in Fig. 6-1 the total energy added can be expressed in terms of a bulk-temperature difference by

$$q = \dot{m}c_p(T_{b2} - T_{b1}) \quad \dot{m} = \rho V A \quad (6-1)$$

provided c_p is reasonably constant over the length. In some differential length dx the heat added dq can be expressed either in terms of a bulk-temperature difference or in terms of the heat-transfer coefficient

$$dq = \dot{m}c_p dT_b = h(2\pi r) dx (T_w - T_b) \quad (6-2)$$

where T_w and T_b are the wall and bulk temperatures at the particular location. The total heat transfer can also be expressed as

$$q = hA(T_w - T_b)_{av} \quad (6-3)$$

where A is the total surface area for heat transfer. Because both T_w and T_b can vary along the length of the tube, a suitable averaging procedure must be adopted for use with Eq. (6-3). In this chapter most of the attention will be focused on methods for determining h , the convective heat-transfer coefficient. Chapter 10 will discuss different methods for taking proper account of temperature variations in heat exchangers.

For fully developed turbulent flow in smooth tubes the following correlation is recommended by Dittus and Boelter [1]:

$$Nu_d = 0.023 Re_d^{0.8} Pr^n$$

The properties in this equation are evaluated at the fluid bulk temperature and the exponent n has the following values:

This may be restructured as

$$\bar{h}^{3/4} = C \left[\frac{\rho(\rho - \rho_v)gk^3}{\mu^2} \frac{\mu P}{4\dot{m}} \frac{4 \sin \phi A/P}{L} \right]^{1/4}$$

and we may solve for \bar{h} as

$$\bar{h} = C^{4/3} \left[\frac{\rho(\rho - \rho_v)gk^3}{\mu^2} \frac{\mu P}{4\dot{m}} \frac{4 \sin \phi A/P}{L} \right]^{1/3} \quad (9-23)$$

We now define a new dimensionless group, the *condensation number* Co , as

$$Co = \bar{h} \left[\frac{\mu^2}{k^3 \rho(\rho - \rho_v)g} \right]^{1/3} \quad (9-24)$$

so that Eq. (9-23) can be expressed in the form

$$Co = C^{4/3} \left(\frac{4 \sin \phi A/P}{L} \right)^{1/3} Re_f^{-1/3} \quad (9-25)$$

For a vertical plate $A/PL = 1.0$, and we obtain, using the constant from Eq. (9-10),

$$Co = 1.47 Re_f^{-1/3} \quad \text{for } Re_f < 1800 \quad (9-26)$$

For a horizontal cylinder $A/PL = \pi$ and

$$Co = 1.514 Re_f^{-1/3} \quad \text{for } Re_f < 1800 \quad (9-27)$$

When turbulence is encountered in the film, an empirical correlation by Kirkbride [2] may be used:

$$Co = 0.0077 Re_f^{0.4} \quad \text{for } Re_f > 1800 \quad (9-28)$$

9-4 Film condensation inside horizontal tubes

Our discussion of film condensation so far has been limited to *exterior surfaces*, where the vapor and liquid condensate flows are not restricted by some overall flow-channel dimensions. Condensation inside tubes is of considerable practical interest because of applications to condensers in refrigeration and air-conditioning systems, but unfortunately these phenomena are quite complicated and not amenable to a simple analytical treatment. The overall flow rate of vapor strongly influences the heat-transfer rate in the forced convection-condensation system, and this in turn is influenced by the rate of liquid accumulation on the walls. Because of the complicated flow phenomena involved we shall present only two empirical relations for heat transfer and refer to reader to Rohsenow [37] for more complete information.

Chato [38] obtained the following expression for condensation of refrigerants at low vapor velocities inside horizontal tubes:

$$\bar{h} = 0.555 \left[\frac{\rho(\rho - \rho_v)gk^3 h_{fg}}{\mu d(T_g - T_w)} \right]^{1/4} \quad (9-29)$$

**VERMONT YANKEE
NUCLEAR POWER CORPORATION**

NEC-JH_32

185 OLD FERRY ROAD, PO BOX 7002, BRATTLEBORO, VT 05302-7002
(802) 257-5271

August 20, 2001
BVY 01-66

U.S. Nuclear Regulatory Commission
ATTN: Document Control Desk
Washington, D.C. 20555

**Subject: Vermont Yankee Nuclear Power Station
License No. DPR-28 (Docket No. 50-271)
Vermont Yankee 2001 Summary Reports for
In-service Inspection and Repairs or Replacements**

In accordance with Article IWA-6000 of Section XI of the ASME Boiler and Pressure Vessel Code, Vermont Yankee (VY) hereby submits the Owner's Report for In-service Inspections (Form NIS-1) and the Owner's Report for Repairs and Replacements (Form NIS-2). These reports describe the in-service examinations, repairs and replacements performed during the period from December 4, 1999 to May 20, 2001 (including Refueling Outage 22). VY's third ten-year interval began September 1, 1993.

We trust that the information provided is adequate; however, should you have questions or require additional information, please contact Mr. Jim DeVincentis at (802) 258-4236.

Sincerely,

VERMONT YANKEE NUCLEAR POWER CORPORATION


Gautam Sen
Licensing Manager

Attachments

cc: USNRC Region 1 Administrator
USNRC Resident Inspector - VYNPS
USNRC Project Manager - VYNPS
Vermont Department of Public Service
Inspection Agency - Arkwright

AD47

SUMMARY OF VERMONT YANKEE COMMITMENTS

BVY NO.: 01-66

The following table identifies commitments made in this document by Vermont Yankee. Any other actions discussed in the submittal represent intended or planned actions by Vermont Yankee. They are described to the NRC for the NRC's information and are not regulatory commitments. Please notify the Licensing Manager of any questions regarding this document or any associated commitments.

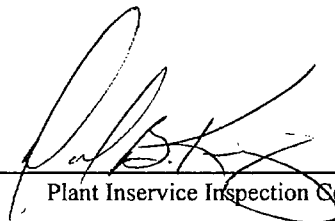
COMMITMENT	COMMITTED DATE OR "OUTAGE"
None	N/A

Vermont Yankee Nuclear Power Corporation

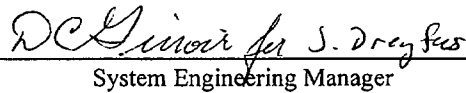
**2001 Form NIS-1 Owner's Summary Report
for
Inservice Inspections**

December 4, 1999 through May 20, 2001

Reviewed by: _____

 8/2/01
Plant Inservice Inspection Coordinator

Approved by: _____

 8/2/01
System Engineering Manager

FORM NIS-1 OWNER'S REPORT FOR INSERVICE INSPECTIONS
As Required by the Provisions of the ASME Code Rules

1. Owner Vermont Yankee Nuclear Power Corporation, 185 Old Ferry Road, PO Box 7002, Brattleboro VT 05302-7002
(Name and Address of Owner)
2. Plant Vermont Yankee Nuclear Power Station, P.O. Box 157, Governor Hunt Road, Vernon, VT 05354-0157
(Name and Address of Plant)
3. Plant Unit 1 4. Owner Certificate of Authorization (if required) DPR-28
5. Commercial Service Date 11/30/1972 6. National Board Number for Unit NONE
7. Components Inspected - SEE ATTACHED PAGES 2 THROUGH 13.
8. Examination Dates 12/04/1999 to 05/20/2001 9. Inspection Interval from 09/1/1993 to 08/31/2003
10. Applicable Editions of Section XI 1986, no Addenda; 1992 w/1992 Addenda (IWE) and 1995 w/1996 Addenda (ASME Appendix VIII)
11. Abstract of Examinations Including a list of examinations and a statement concerning status of work required for current interval - SEE ATTACHED PAGES 2 THROUGH 21.
12. Abstract of Conditions Noted - SEE ATTACHED PAGES 22 THROUGH 25.
13. Abstract of Corrective Measures Recommended and Taken - SEE ATTACHED PAGES 22 THROUGH 25.

We certify that the statements made in this report are correct and the examinations and corrective measures taken conform to the rules of the ASME Code, Section XI.

Certificate of Authorization No. (If applicable) DPR-28 Expiration Date 3/21/2012
Date August 16 20 01 Signed [Signature] By Vermont Yankee Nuclear Power
Owner

CERTIFICATE OF INSERVICE INSPECTION

I, the undersigned, holding a valid commission issued by the National Board of Boiler and Pressure Vessel Inspectors and/or the State or Province of Vermont and employed by Factory Mutual Insurance Co. of Johnston RI have inspected the components described in this Owner's Report during the period December 4, 1999 to May 20, 2001 and state to the best of my knowledge and belief, the Owner has performed examinations and taken corrective measures described in this Owner's Report in accordance with the requirements of the ASME Code, Section XI.

By signing this certificate neither the inspector nor his employer makes any warranty, expressed or implied, concerning the examinations and corrective measures described in this Owner's Report. Furthermore, neither the Inspector nor his employer shall be liable in any manner for any personal injury or property damage or a loss of any kind arising from or connected with this inspection.

[Signature] Commissions VT-345
Inspector's Signature National Board, State, Province, and Endorsements
Date 8-16, 2001

FORM NIS-1 OWNER'S DATA REPORT FOR INSERVICE INSPECTIONS
As Required by the Provisions of the ASME Code rules

Vermont Yankee Nuclear Power Corporation
 Vermont Yankee Nuclear Power Station
 Owner Certification: DPR-28
 Commercial Service Date: 11/30/72

Components Inspected/Abstract of examinations
Sections 7 and 11

<i>ASME Category</i>	<i>Component ID</i>	<i>Exam Type</i>	<i>System ID</i>	<i>Drawing No.</i>	<i>Examination Results</i>
B-D	N2F	UT	Nuclear Boiler	ISI-RPV-103	Acceptable
B-D	N2F-IR	UT Inner Radius	Nuclear Boiler	ISI-RPV-103	Acceptable
B-D	N2G	UT	Nuclear Boiler	ISI-RPV-103	Acceptable
B-D	N2G-IR	UT Inner Radius	Nuclear Boiler	ISI-RPV-103	Acceptable
B-D	N2H	UT	Nuclear Boiler	ISI-RPV-103	Acceptable
B-D	N2H-IR	UT Inner Radius	Nuclear Boiler	ISI-RPV-103	Acceptable
B-D	N2J	UT	Nuclear Boiler	ISI-RPV-103	Acceptable
B-D	N2J-IR	UT Inner Radius	Nuclear Boiler	ISI-RPV-103	Acceptable
B-D	N2K	UT	Nuclear Boiler	ISI-RPV-103	Acceptable
B-D	N2K-IR	UT Inner Radius	Nuclear Boiler	ISI-RPV-103	Acceptable
B-D	N4A-IR	UT Inner Radius	Feedwater	ISI-RPV-103	Acceptable - Automated Inner Radius examination in accordance with General Electric Nuclear Energy document GE-NE-523-A71-0594-A, Revision 1 and VY Calculation VYC-1005
B-D	N4B-IR	UT Inner Radius	Feedwater	ISI-RPV-103	Acceptable - Automated Inner Radius examination in accordance with General Electric Nuclear Energy document GE-NE-523-A71-0594-A, Revision 1 and VY Calculation VYC-1005

FORM NIS-1 OWNER'S DATA REPORT FOR INSERVICE INSPECTIONS
As Required by the Provisions of the ASME Code rules

Vermont Yankee Nuclear Power Corporation
 Vermont Yankee Nuclear Power Station
 Owner Certification: DPR-28
 Commercial Service Date: 11/30/72

Components Inspected/Abstract of examinations
Sections 7 and 11

<i>ASME Category</i>	<i>Component ID</i>	<i>Exam Type</i>	<i>System ID</i>	<i>Drawing No.</i>	<i>Examination Results</i>
B-D	N4C-IR	UT Inner Radius	Feedwater	ISI-RPV-103	Acceptable - Automated Inner Radius examination in accordance with General Electric Nuclear Energy document GE-NE-523-A71-0594-A, Revision 1 and VY Calculation VYC-1005
B-D	N4D-IR	UT Inner Radius	Feedwater	ISI-RPV-103	Acceptable - Automated Inner Radius examination in accordance with General Electric Nuclear Energy document GE-NE-523-A71-0594-A, Revision 1 and VY Calculation VYC-1005
B-F	N11A WELD	PT	Nuclear Boiler	ISI-RPV-103	Acceptable
B-F	N11B WELD	PT	Nuclear Boiler	ISI-RPV-103	Acceptable
B-F	N12A-SE	PT	Nuclear Boiler	ISI-RPV-103	Acceptable
B-F	N1B-SE	PT	Nuclear Boiler	ISI-RPV-103	Acceptable - Examination performed as follow up to indication removal during RFO-21
B-F	N2F-SE	UT, PT	Nuclear Boiler	ISI-RPV-103	Acceptable
B-F	N2G-SE	UT, PT	Nuclear Boiler	ISI-RPV-103	Acceptable
B-F	N2H-SE	UT, PT	Nuclear Boiler	ISI-RPV-103	Acceptable
B-F	N2J-SE	UT, PT	Nuclear Boiler	ISI-RPV-103	Acceptable
B-F	N2K-SE	UT, PT	Nuclear Boiler	ISI-RPV-103	Acceptable

FORM NIS-1 OWNER'S DATA REPORT FOR INSERVICE INSPECTIONS
As Required by the Provisions of the ASME Code rules

Vermont Yankee Nuclear Power Corporation
 Vermont Yankee Nuclear Power Station
 Owner Certification: DPR-28
 Commercial Service Date: 11/30/72

Components Inspected/Abstract of examinations
Sections 7 and 11

<i>ASME Category</i>	<i>Component ID</i>	<i>Exam Type</i>	<i>System ID</i>	<i>Drawing No.</i>	<i>Examination Results</i>
B-F	N6B-SE	UT, PT	Nuclear Boiler	ISI-RPV-103	Acceptable
B-F	N8A-SE	UT, PT	Nuclear Boiler	ISI-RPV-103	Acceptable
B-F	N8B-SE	UT, PT	Nuclear Boiler	ISI-RPV-103	Acceptable
B-G-1	01A-N/W Recirculation Pump P-18-1A Bolting	VT-1	Nuclear Boiler	ISI-RPV-104	Acceptable - IDR # 01-09 generated for corrosion/plating concern - See Sections 12 and 13
B-G-1	02A-N/W Recirculation Pump P-18-1A Bolting	VT-1	Nuclear Boiler	ISI-RPV-104	Acceptable - IDR # 01-09 generated for corrosion/plating concern - See Sections 12 and 13
B-G-1	03A-N/W Recirculation Pump P-18-1A Bolting	VT-1	Nuclear Boiler	ISI-RPV-104	Acceptable - IDR # 01-09 generated for corrosion/plating concern - See Sections 12 and 13
B-G-1	04A-N/W Recirculation Pump P-18-1A Bolting	VT-1	Nuclear Boiler	ISI-RPV-104	Acceptable - IDR # 01-09 generated for corrosion/plating concern - See Sections 12 and 13
B-G-1	05A-N/W Recirculation Pump P-18-1A Bolting	VT-1	Nuclear Boiler	ISI-RPV-104	Acceptable - IDR # 01-09 generated for corrosion/plating concern - See Sections 12 and 13
B-G-1	06A-N/W Recirculation Pump P-18-1A Bolting	VT-1	Nuclear Boiler	ISI-RPV-104	Acceptable - IDR # 01-09 generated for corrosion/plating concern - See Sections 12 and 13
B-G-1	07A-N/W Recirculation Pump P-18-1A Bolting	VT-1	Nuclear Boiler	ISI-RPV-104	Acceptable - IDR # 01-09 generated for corrosion/plating concern - See Sections 12 and 13

FORM NIS-1 OWNER'S DATA REPORT FOR INSERVICE INSPECTIONS
As Required by the Provisions of the ASME Code rules

Vermont Yankee Nuclear Power Corporation
Vermont Yankee Nuclear Power Station
Owner Certification: DPR-28
Commercial Service Date: 11/30/72

Components Inspected/Abstract of examinations
Sections 7 and 11

<i>ASME Category</i>	<i>Component ID</i>	<i>Exam Type</i>	<i>System ID</i>	<i>Drawing No.</i>	<i>Examination Results</i>
B-G-1	08A-N/W Recirculation Pump P-18-1A Bolting	VT-1	Nuclear Boiler	ISI-RPV-104	Acceptable - IDR # 01-09 generated for corrosion/plating concern - See Sections 12 and 13
B-G-1	09A-N/W Recirculation Pump P-18-1A Bolting	VT-1	Nuclear Boiler	ISI-RPV-104	Acceptable - IDR # 01-09 generated for corrosion/plating concern - See Sections 12 and 13
B-G-1	10A-N/W Recirculation Pump P-18-1A Bolting	VT-1	Nuclear Boiler	ISI-RPV-104	Acceptable - IDR # 01-09 generated for corrosion/plating concern - See Sections 12 and 13
B-G-1	11A-N/W Recirculation Pump P-18-1A Bolting	VT-1	Nuclear Boiler	ISI-RPV-104	Acceptable - IDR # 01-09 generated for corrosion/plating concern - See Sections 12 and 13
B-G-1	12A-N/W Recirculation Pump P-18-1A Bolting	VT-1	Nuclear Boiler	ISI-RPV-104	Acceptable - IDR # 01-09 generated for corrosion/plating concern - See Sections 12 and 13
B-G-1	13A-N/W Recirculation Pump P-18-1A Bolting	VT-1	Nuclear Boiler	ISI-RPV-104	Acceptable - IDR # 01-09 generated for corrosion/plating concern - See Sections 12 and 13
B-G-1	14A-N/W Recirculation Pump P-18-1A Bolting	VT-1	Nuclear Boiler	ISI-RPV-104	Acceptable - IDR # 01-09 generated for corrosion/plating concern - See Sections 12 and 13
B-G-1	15A-N/W Recirculation Pump P-18-1A Bolting	VT-1	Nuclear Boiler	ISI-RPV-104	Acceptable - IDR # 01-09 generated for corrosion/plating concern - See Sections 12 and 13

FORM NIS-1 OWNER'S DATA REPORT FOR INSERVICE INSPECTIONS
As Required by the Provisions of the ASME Code rules

Vermont Yankee Nuclear Power Corporation
Vermont Yankee Nuclear Power Station
Owner Certification: DPR-28
Commercial Service Date: 11/30/72

Components Inspected/Abstract of examinations
Sections 7 and 11

<i>ASME Category</i>	<i>Component ID</i>	<i>Exam Type</i>	<i>System ID</i>	<i>Drawing No.</i>	<i>Examination Results</i>
B-G-1	16A-N/W Recirculation Pump P-18-1A Bolting	VT-1	Nuclear Boiler	ISI-RPV-104	Acceptable - IDR # 01-09 generated for corrosion/plating concern - See Sections 12 and 13
B-J	CS4B-F3ADW	UT, PT	Core Spray	ISI-5920-9206	Acceptable
B-J	CS4B-MF5	UT, PT	Core Spray	ISI-5920-9206	Acceptable
B-J	CS4B-MF5B	UT, PT	Core Spray	ISI-5920-9206	Acceptable
B-J	CS4B-MF6A	UT, PT	Core Spray	ISI-5920-9206	Acceptable
B-J	FW20-F1	UT/FAC	Feedwater	ISI-FDW-PART 5A	Acceptable - Code Case N-560 examination
B-J	FW20-F1B	UT/FAC	Feedwater	ISI-FDW-PART 5A	Acceptable - Code Case N-560 examination
B-J	FW20-F3B	UT/FAC	Feedwater	ISI-FDW-PART 5A	Acceptable - Code Case N-560 examination
B-J	SL11-F28	PT	Standby Liquid Control	ISI-SLC-PART 4	Acceptable
B-J	SL11-F29	PT	Standby Liquid Control	ISI-SLC-PART 4	Acceptable
B-K	270 DEG RPV BRKT	PT	Nuclear Boiler	ISI-RPV-103	Acceptable
B-K	RPV SUPPORT SKIRT	MT	Nuclear Boiler	ISI-RPV-103	Acceptable
B-K	RR-34	PT	Nuclear Boiler	ISI-5920-6802 Sh.2	Acceptable
B-K	RR-35	PT	Nuclear Boiler	ISI-5920-6802 Sh.2	Acceptable
B-O	26-03SH	PT	Control Rod Drive	ISI-RPV-104	Acceptable
B-O	34-39SH	PT	Control Rod Drive	ISI-RPV-104	Acceptable

FORM NIS-1 OWNER'S DATA REPORT FOR INSERVICE INSPECTIONS
As Required by the Provisions of the ASME Code rules

Vermont Yankee Nuclear Power Corporation
 Vermont Yankee Nuclear Power Station
 Owner Certification: DPR-28
 Commercial Service Date: 11/30/72

Components Inspected/Abstract of examinations
Sections 7 and 11

<i>ASME Category</i>	<i>Component ID</i>	<i>Exam Type</i>	<i>System ID</i>	<i>Drawing No.</i>	<i>Examination Results</i>
C-C	ACSP-H22	MT	Standby Gas Treatment	ISI-5920-9200	Acceptable
C-C	ACSP-H23	MT	Standby Gas Treatment	ISI-5920-9200	Acceptable
C-C	RHR-H192	MT	Residual Heat Removal	ISI-RHR-PART 11 Sh.4	Acceptable
C-C	RHR-H98	MT	Residual Heat Removal	ISI-5920-9208	Acceptable
C-C	RHR-HD25	PT	Residual Heat Removal	ISI-RHR-PART 16 Sh.1	Acceptable - Successive examination
C-F-2	CR4A-S5	UT, MT	Control Rod Drive	ISI-5920-9528	Acceptable
C-F-2	CR6A-S57	UT, MT	Control Rod Drive	ISI-5920-9527	Acceptable
C-F-2	CR6-S10	UT, MT	Control Rod Drive	ISI-5920-9527	Acceptable
C-F-2	CR6-S22	UT, MT	Control Rod Drive	ISI-5920-9527	Acceptable
C-F-2	CR6-S26	UT, MT	Control Rod Drive	ISI-5920-9527	Acceptable
C-F-2	CS1B-S30	UT, MT	Core Spray	ISI-5920-9210	Acceptable
C-F-2	CT27-S30	UT, MT	Core Spray	ISI-5920-9210	Acceptable
C-F-2	FW17-S5	UT, MT	Feedwater	ISI-FDW-PART 5A	Acceptable
C-F-2	HP15A-S101	UT, MT	High Pressure Coolant Injection	ISI-HPCI-PART 5	Acceptable
C-F-2	RH14-T373	UT, MT	Core Spray	ISI-5920-9208	Acceptable
C-F-2	RH1B-S47	UT, MT	Residual Heat Removal	ISI-5920-9285	Acceptable
C-F-2	RH2B-S113	UT, MT	Residual Heat Removal	ISI-5920-9285	Acceptable

FORM NIS-1 OWNER'S DATA REPORT FOR INSERVICE INSPECTIONS
As Required by the Provisions of the ASME Code rules

Vermont Yankee Nuclear Power Corporation
Vermont Yankee Nuclear Power Station
Owner Certification: DPR-28
Commercial Service Date: 11/30/72

Components Inspected/Abstract of examinations
Sections 7 and 11

<i>ASME Category</i>	<i>Component ID</i>	<i>Exam Type</i>	<i>System ID</i>	<i>Drawing No.</i>	<i>Examination Results</i>
C-F-2	RH2B-S115	UT, MT	Residual Heat Removal	ISI-5920-9285	Acceptable
C-F-2	RH3B-S170	UT, MT	Residual Heat Removal	ISI-5920-9288	Acceptable
C-F-2	RH3D-S200	UT, MT	Residual Heat Removal	ISI-5920-9288	Acceptable
C-F-2	RH3D-S206	UT, MT	Residual Heat Removal	ISI-5920-9288	Acceptable
C-F-2	RH3D-T182	UT, MT	Residual Heat Removal	ISI-5920-9288	Acceptable
C-F-2	RH7-S284	UT, MT	Residual Heat Removal	ISI-5920-9287	Acceptable
C-F-2	RH9-S314	UT, MT	Residual Heat Removal	ISI-RHR-PART 11 Sh.4	Acceptable
C-F-2	RH9-S320	UT, MT	Residual Heat Removal	ISI-RHR-PART 11 Sh.4	Acceptable
C-FAUG	CS2A-S62	UT, MT	Core Spray	ISI-5920-9211	Acceptable
C-FAUG	CS2A-S64	UT, MT	Core Spray	ISI-5920-9211	Acceptable
C-FAUG	CS2A-S65	UT, MT	Core Spray	ISI-5920-9211	Acceptable
C-FAUG	CS2A-S67	UT, MT	Core Spray	ISI-5920-9211	Acceptable
C-FAUG	CT1-S54	UT, PT	Core Spray	ISI-CST-PART 4	Acceptable
C-FAUG	CT1-S56	UT, PT	Core Spray	ISI-CST-PART 4	Acceptable
C-FAUG	RC3-S13	UT, MT	Reactor Core Isolation Cooling	ISI-5920-9255	Acceptable
C-FAUG	RC3-S14	UT, MT	Reactor Core Isolation Cooling	ISI-5920-9255	Acceptable

FORM NIS-1 OWNER'S DATA REPORT FOR INSERVICE INSPECTIONS
As Required by the Provisions of the ASME Code rules

Vermont Yankee Nuclear Power Corporation
Vermont Yankee Nuclear Power Station
Owner Certification: DPR-28
Commercial Service Date: 11/30/72

Components Inspected/Abstract of examinations
Sections-7 and 11

<i>ASME Category</i>	<i>Component ID</i>	<i>Exam Type</i>	<i>System ID</i>	<i>Drawing No.</i>	<i>Examination Results</i>
C-NAUG	MS1D-F9	UT, MT	Main Steam	5920-FS-I1	Acceptable
C-NAUG	MS2D-F1	UT, MT	Main Steam	5920-FS-I1	Acceptable
D-A	RSW-H171	VT-1	Residual Heat Removal	ISI-SW-PART 9	Acceptable
D-A	RSW-H261	VT-1	Residual Heat Removal	ISI-SW-PART 9	Acceptable - IDR # 01-01 generated for arc strikes - See Sections 12 and 13
D-A	RSW-HD261B	VT-1	Residual Heat Removal	ISI-SW-PART 9	Acceptable - IDR # 01-01 generated for arc strikes - See Sections 12 and 13
E-A	Class MC Containment	General Visual	Class MC Containment	5920-13, 5920-41, 5920-42, 6202-200	Acceptable - General Visual Examination as required by ASME Subsection IWE has been 100% completed for the first period of the first IWE Interval. IDR # 01-07 generated for pitting and general corrosion in the Vent Header. IDR # 01-07 generated for pitting and general corrosion in the Vent Header. Also, IDR # 01-08 was generated for general corrosion and material loss in Penetrations X-207A through X-207H. See Sections 12 and 13
E-A	Vent Line Areas (X-5B)	VT-1	Class MC Containment	5920-13	Acceptable
E-A	Vent Line Areas (X-5C)	VT-1	Class MC Containment	5920-13	Acceptable
E-A	Vent Line Areas (X-5D)	VT-1	Class MC Containment	5920-13	Acceptable
E-A	Vent Line Areas (X-5E)	VT-1	Class MC Containment	5920-13	Acceptable

FORM NIS-1 OWNER'S DATA REPORT FOR INSERVICE INSPECTIONS
As Required by the Provisions of the ASME Code rules

Vermont Yankee Nuclear Power Corporation
Vermont Yankee Nuclear Power Station
Owner Certification: DPR-28
Commercial Service Date: 11/30/72

Components Inspected/Abstract of examinations
Sections 7 and 11

<i>ASME Category</i>	<i>Component ID</i>	<i>Exam Type</i>	<i>System ID</i>	<i>Drawing No.</i>	<i>Examination Results</i>
E-C	Drywell Seal Area	VT-1	Class MC Containment	6202-2	Acceptable
E-C	Drywell Seal Area	VT-3	Class MC Containment	6202-2	Acceptable
E-G	Pen. X-200A	VT-1	Class MC Containment	6202-208	Acceptable
E-G	Pen. X-200B	VT-1	Class MC Containment	6202-208	Acceptable
E-G	V16-19-5A	VT-1	Class MC Containment	5920-675	Acceptable
E-G	V16-19-5B	VT-1	Class MC Containment	5920-675	Acceptable
E-G	V16-19-5C	VT-1	Class MC Containment	5920-675	Acceptable
E-G	V16-19-5D	VT-1	Class MC Containment	5920-675	Acceptable
E-G	V16-19-5E	VT-1	Class MC Containment	5920-675	Acceptable
E-G	V16-19-5F	VT-1	Class MC Containment	5920-675	Acceptable
E-G	V16-19-5H	VT-1	Class MC Containment	5920-675	Acceptable
F-A	ACSP-H22	VT-3	Standby Gas Treatment	ISI-5920-9200	Acceptable
F-A	ACSP-H23	VT-3	Standby Gas Treatment	ISI-5920-9200	Acceptable
F-A	CS-HD60A	VT-3	Core Spray	ISI-5920-9210	Acceptable
F-A	FDW-HD39	VT-3	Feedwater	ISI-FDW-PART 5A	Acceptable - IDR # 01-12 generated for debris/corrosion - See Sections 12 and 13
F-A	H-P-44-1B	VT-3	High Pressure Coolant Injection	ISI-HPCI-PART 13A	Acceptable

FORM NIS-1 OWNER'S DATA REPORT FOR INSERVICE INSPECTIONS
As Required by the Provisions of the ASME Code rules

Vermont Yankee Nuclear Power Corporation
Vermont Yankee Nuclear Power Station
Owner Certification: DPR-28
Commercial Service Date: 11/30/72

Components Inspected/Abstract of examinations
Sections 7 and 11

<i>ASME Category</i>	<i>Component ID</i>	<i>Exam Type</i>	<i>System ID</i>	<i>Drawing No.</i>	<i>Examination Results</i>
F-A	HPCI-1	VT-3	High Pressure Coolant Injection	ISI-HPCI-PART 2	Acceptable
F-A	HPCI-2	VT-3	High Pressure Coolant Injection	ISI-HPCI-PART 2	Acceptable
F-A	RHR-H129	VT-3	Residual Heat Removal	ISI-5920-9288	Acceptable
F-A	RHR-H191	VT-3	Residual Heat Removal	ISI-RHR-PART 11 Sh.4	Acceptable
F-A	RHR-H192	VT-3	Residual Heat Removal	ISI-RHR-PART 11 Sh.4	Acceptable - IDR # 01-02 generated for gouge - See Sections 12 and 13
F-A	RHR-H83	VT-3	Residual Heat Removal	ISI-RHR-PART 11 Sh.4	Acceptable
F-A	RHR-H98	VT-3	Residual Heat Removal	ISI-5920-9208	Acceptable
F-A	RHR-HD127C	VT-3	Residual Heat Removal	ISI-5920-9285	Acceptable
F-A	RHR-HD127E	VT-3	Residual Heat Removal	ISI-5920-9285	Acceptable - Successive Examination
F-A	RHR-HD127G	VT-3	Residual Heat Removal	ISI-5920-9285	Acceptable
F-A	RHR-HD188A	VT-3	Residual Heat Removal	ISI-5920-9288	Acceptable
F-A	RPV SUPPORT SKIRT	VT-3	Nuclear Boiler	ISI-RPV-103	Acceptable
F-A	RR-15	VT-3	Nuclear Boiler	ISI-5920-6802 Sh.2	Acceptable
F-A	RR-16	VT-3	Nuclear Boiler	ISI-5920-6802 Sh.2	Acceptable
F-A	RR-17	VT-3	Nuclear Boiler	ISI-5920-6802 Sh.2	Acceptable
F-A	RR-2	VT-3	Nuclear Boiler	ISI-5920-6802 Sh.2	Acceptable

FORM NIS-1 OWNER'S DATA REPORT FOR INSERVICE INSPECTIONS
As Required by the Provisions of the ASME Code rules

Vermont Yankee Nuclear Power Corporation
 Vermont Yankee Nuclear Power Station
 Owner Certification: DPR-28
 Commercial Service Date: 11/30/72

Components Inspected/Abstract of examinations
Sections 7 and 11

<i>ASME Category</i>	<i>Component ID</i>	<i>Exam Type</i>	<i>System ID</i>	<i>Drawing No.</i>	<i>Examination Results</i>
F-A	RR-35	VT-3	Nuclear Boiler	ISI-5920-6802 Sh.2	Acceptable
F-A	RR-44	VT-3	Nuclear Boiler	ISI-5920-6802 Sh.2	Acceptable - IDR # 01-04 generated for setting - See Sections 12 and 13
F-A	RR-52	VT-3	Nuclear Boiler	ISI-5920-6802 Sh.2	Acceptable - IDR # 01-05 generated for setting - See Sections 12 and 13
F-A	RR-7,8	VT-3	Nuclear Boiler	ISI-5920-6802 Sh.2	Acceptable - IDR # 01-06 generated for setting - See Sections 12 and 13
F-A	RSW-H167	VT-3	Residual Heat Removal	ISI-SW-PART 1 Sh.2	Acceptable
F-A	RSW-H171	VT-3	Residual Heat Removal	ISI-SW-PART 9	Acceptable
F-A	RSW-H172	VT-3	Residual Heat Removal	ISI-SW-PART 6 Sh.1	Acceptable
F-A	RSW-H241	VT-3	Residual Heat Removal	ISI-SW-PART 1 Sh.2	Acceptable
F-A	RSW-H261	VT-3	Residual Heat Removal	ISI-SW-PART 9	Acceptable
F-A	RSW-HD261B	VT-3	Residual Heat Removal	ISI-SW-PART 9	Acceptable
F-A	SDV-N-R02	VT-3	Control Rod Drive	ISI-5920-9527	Acceptable
F-A	SDV-N-R05	VT-3	Control Rod Drive	ISI-5920-9527	Acceptable
F-AUG	ACSP-H203	VT-3	Standby Gas Treatment	ISI-5920-9201	Acceptable
F-AUG	ACSP-HD203E	VT-3	Standby Gas Treatment	ISI-5920-9201	Acceptable
F-AUG	ACSP-HD203F	VT-3	Standby Gas Treatment	ISI-5920-9201	Acceptable

FORM NIS-1 OWNER'S DATA REPORT FOR INSERVICE INSPECTIONS
As Required by the Provisions of the ASME Code rules

Vermont Yankee Nuclear Power Corporation
Vermont Yankee Nuclear Power Station
Owner Certification: DPR-28
Commercial Service Date: 11/30/72

Components Inspected/Abstract of examinations
Sections 7 and 11

<i>ASME Category</i>	<i>Component ID</i>	<i>Exam Type</i>	<i>System ID</i>	<i>Drawing No.</i>	<i>Examination Results</i>
F-AUG	RHR-HD25	VT-3, PT	Residual Heat Removal	ISI-RHR-PART 16 Sh.1	Acceptable
N/A	ACSP-H201B	VT-3	Standby Gas Treatment	ISI-AC PART 5	Acceptable
NNS	HPCI-HD28	VT-3	High Pressure Coolant Injection	ISI-HPCI-PART 4 Sh.1	Acceptable
NNS	RHR-HD235	VT-3	Residual Heat Removal	VYI-RHR-PART 7B	Acceptable

FORM NIS-1 OWNER'S DATA REPORT FOR INSERVICE INSPECTIONS
As Required by the Provisions of the ASME Code rules

Vermont Yankee Nuclear Power Corporation
 Vermont Yankee Nuclear Power Station
 Owner Certification: DPR-28
 Commercial Service Date: 11/30/72

Components Inspected/Abstract of examinations
 Sections 7 and 11

<i>Code Category</i>	<i>Quantity Inspected 2001 Outage</i>	<i>Quantity Previously Inspected, Third Interval</i>	<i>Quantity Scheduled, Third Interval</i>	<i>Percent of Third Interval Complete</i>
B-A	0	15	16	94%
B-D	10	38	58	83%
B-F	12	19	35	89%
B-G-1	16	152	288	58%
B-G-2	0	77	109	71%
B-J (Code Case N-560 selection)	9	0 (Code Case N-560 was first used for selection during RFO-22)	15	60% (Previously 64% of the standard ASME Category B-J 25% selection had been completed)
B-J (These are ASME Category B-J, Item B9.40 socket welds which are not included in the Code Case N- 560 selection. They are selected in accordance with Category B-J 25% criteria.)	2	14	23	70%
B-K	4	3	10	70%
B-L-2	0	0	Per approved Relief Request No. B-1	N/A
B-M-2	0	26	Per approved Relief Request No. B-2	N/A

FORM NIS-1 OWNER'S DATA REPORT FOR INSERVICE INSPECTIONS
As Required by the Provisions of the ASME Code rules

Vermont Yankee Nuclear Power Corporation
 Vermont Yankee Nuclear Power Station
 Owner Certification: DPR-28
 Commercial Service Date: 11/30/72

Components Inspected/Abstract of examinations
 Sections 7 and 11

<i>Code Category</i>	<i>Quantity Inspected 2001 Outage</i>	<i>Quantity Previously Inspected, Third Interval</i>	<i>Quantity Scheduled, Third Interval</i>	<i>Percent of Third Interval Complete</i>
B-N-1	0	2	Each Period	N/A
B-N-2	0	Partial	1	N/A
B-O	2	4	7	86%
C-A	0	3	4	75%
C-B	0	6	8	75%
C-C	4	12	20	80%
C-F-2	20	43	72	88%
D-A	3	6	11	82%
E-A	20%	80%	100%	100%
E-C	100%	100%	100%	100%
E-D				
E-G				
F-A	33	59	119	77%

FORM NIS-1 OWNER'S DATA REPORT FOR INSERVICE INSPECTIONS
As Required by the Provisions of the ASME Code rules

Vermont Yankee Nuclear Power Corporation
Vermont Yankee Nuclear Power Station
Owner Certification: DPR-28
Commercial Service Date: 11/30/72

ABSTRACT OF CONDITIONS NOTED/CORRECTIVE MEASURES TAKEN
 Sections 12 and 13

<i>Code Category</i>	<i>Item Identification</i>	<i>Conditions Noted and Corrective Measures Taken</i>
B-G-1	01A-N/W through 16A-N/W	VT-1 examination of Recirculation pump P-18-1A bolting identified possible missing protective thread coating (the bolting was examined in place, under tension). The examination also revealed corrosion on the exposed bolting. Inservice Discrepancy Report # 01-09 was generated to request Engineering evaluation of these indications. Technical Evaluation (TE) 2001-034 was generated and contains: The pump casing cover/body bolting will perform its design function with the as-noted surface conditions. Margin exists in the 2 1/2" diameter cap screws for future corrosion. No additional and/or augmented inspections other than planned inservice inspection is required.
C-C	RHR-H192	VT-3 examination of rigid strut support RHR-H192 revealed a gouge on the pipe clamp. Inservice Discrepancy Report # 01-02 was generated to request Mechanical Design Engineering evaluation of this condition. Technical Evaluation 2001-015 was issued containing: a) The gouge does not extend behind the lugs therefore the lugs have full bearing surface on the clamp. b) The reduction of a maximum of 1/32" of depth on an 8" deep clamp is insignificant (<1%). These indications were determined to be caused during initial installation/fabrication.
D-A	RSW-H172	VT-3 examination of rigid frame support RSW-H172 revealed a crack in the concrete wall adjacent to the base plate. Inservice Discrepancy Report # 01-03 was generated to request Mechanical Design Engineering evaluation of this condition. Technical Evaluation 2001-017 was issued containing: a) The support and the associated anchor bolts will perform their intended design functions in the as-found condition. b) The cracking has been determined to be a surface hairline crack that is the result of normal aging and/or as-expected normal shrinkage cracking of the concrete. This area is monitored in accordance with Vermont Yankee procedure PP 7030 "Structures Monitoring Program" which implements 10 CFR 50.65.

FORM NIS-1 OWNER'S DATA REPORT FOR INSERVICE INSPECTIONS
As Required by the Provisions of the ASME Code rules

Vermont Yankee Nuclear Power Corporation
 Vermont Yankee Nuclear Power Station
 Owner Certification: DPR-28
 Commercial Service Date: 11/30/72

ABSTRACT OF CONDITIONS NOTED/CORRECTIVE MEASURES TAKEN
 Sections 12 and 13

<i>Code Category</i>	<i>Item Identification</i>	<i>Conditions Noted and Corrective Measures Taken</i>
D-A	RSW-H261	VT-3 examination of spring hanger RSW-H261 revealed several arc strikes and a poor weld profile on integrally attached pipe lugs (these lugs are used in common with spring hanger RSW-HD261B - see below) . Inservice Discrepancy Report # 01-01 was generated to request Mechanical Design Engineering evaluation of these conditions. Technical Evaluation 2001-014 was issued containing: a) None of the arc strikes contained cracking b) The maximum recordable depth of any arc strike was .03" c) No overstress conditions exist. d) The weld in question is an "extra weld" not called for in the engineering qualification of the pipe lug (the lug is only required to be welded on 2 sides, this weld is on the third (not required) side. These indications were determined to be caused during initial installation or modification.
D-A	RSW-HD261B	VT-3 examination of spring hanger RSW-HD261B revealed several arc strikes and a poor weld profile on integrally attached pipe lugs (these lugs are used in common with spring hanger RSW-H261 - see above). Inservice Discrepancy Report # 01-01 was generated to request Mechanical Design Engineering evaluation of these conditions. Technical Evaluation 2001-014 was issued containing: a) None of the arc strikes contained cracking b) The maximum recordable depth of any arc strike was .03" c) No overstress conditions exist. d) The weld in question is an "extra weld" not called for in the engineering qualification of the pipe lug (the lug is only required to be welded on 2 sides, this weld is on the third (not required) side. These indications were determined to be caused during initial installation or modification.
E-A	Penetrations X-207A through X-207H	During General Visual examination general corrosion and material loss was found. Inservice Discrepancy Report # 01-08 was generated to request Mechanical Design Engineering evaluation of this condition. Technical Evaluation (TE) 2001-025 was generated and contains: The condition is acceptable as found as there is significant margin remaining to code minimum wall thickness accompanied by a low expected rate of galvanic corrosion in the inerted containment.

FORM NIS-1 OWNER'S DATA REPORT FOR INSERVICE INSPECTIONS
As Required by the Provisions of the ASME Code rules

Vermont Yankee Nuclear Power Corporation
Vermont Yankee Nuclear Power Station
Owner Certification: DPR-28
Commercial Service Date: 11/30/72

ABSTRACT OF CONDITIONS NOTED/CORRECTIVE MEASURES TAKEN
 Sections 12 and 13

<i>Code Category</i>	<i>Item Identification</i>	<i>Conditions Noted and Corrective Measures Taken</i>
E-A	Vent Header	During General Visual examination pitting and general corrosion in excess of the allowable values provided by Mechanical Design Engineering were found. The corrosion and pitting are accompanied by loss of coating. There was also significant standing water in Vent Header bowl H. Inservice Discrepancy Report # 01-07 was generated to request Mechanical Design Engineering evaluation of this condition. Technical Evaluation (TE) 2001-025 was generated and contains: a) The observed pitting in the Vent Header is acceptable. b) The standing water was removed and the source was identified and corrected prior to drywell closeout.
F-A	FDW-HD39	VT-3 examination of anchor FDW-HD39 revealed debris in the form of paint chips, insulation and minor corrosion in a required 1/16" gap between a trunion and the base plate. Inservice Discrepancy Report # 01-12 was generated to request Mechanical Design Engineering evaluation of this condition. Technical Evaluation (TE) 2001-038 was generated and contains: The as found condition of the support/anchor is acceptable with the exception of the identified debris. The trunions are not "bound up" restricting thermal growth/movement of the pipe, and the debris does not adversely impact the overall function of the support/anchor. The debris was subsequently cleaned from the anchor.
F-A	RR-44	VT-3 examination of spring hanger RR-44 revealed a spring can setting that was out of tolerance by greater than $\pm 5\%$ provided by Mechanical Design Engineering. Inservice Discrepancy Report # 01-04 was generated to request Mechanical Design Engineering evaluation of this condition. Technical Evaluation (TE) 2001-021 was generated and contains: The setting was determined to have not affected the supports structural or functional capability. It was noted that the support was "adjusted" as far as possible, i.e., there was no more thread remaining on the rod at the adjustment nut. This condition will be revisited during the next extended refueling outage (RFO-23) to determine if any further action would be warranted.

FORM NIS-1 OWNER'S DATA REPORT FOR INSERVICE INSPECTIONS
As Required by the Provisions of the ASME Code rules

Vermont Yankee Nuclear Power Corporation
Vermont Yankee Nuclear Power Station
Owner Certification: DPR-28
Commercial Service Date: 11/30/72

ABSTRACT OF CONDITIONS NOTED/CORRECTIVE MEASURES TAKEN
Sections 12 and 13

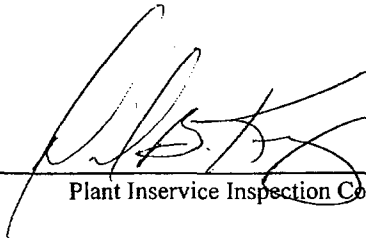
<i>Code Category</i>	<i>Item Identification</i>	<i>Conditions Noted and Corrective Measures Taken</i>
F-A	RR-52	VT-3 examination of spring hanger RR-52 revealed a spring can setting that was out of tolerance by greater than $\pm 5\%$ provided by Mechanical Design Engineering. Inservice Discrepancy Report # 01-05 was generated to request Mechanical Design Engineering evaluation of this condition. Technical Evaluation (TE) 2001-022 was generated and contains: The setting was determined to have not affected the supports structural or functional capability. It was noted that the support was "adjusted" as far as possible, i.e., there was no more thread remaining on the rod at the adjustment nut. This condition will be revisited during the next extended refueling outage (RFO-23) to determine if any further action would be warranted.
F-A	RR-7, 8	VT-3 examination of spring hanger RR-7, 8 revealed a spring can setting that was out of tolerance by greater than $\pm 5\%$ provided by Mechanical Design Engineering. Inservice Discrepancy Report # 01-06 was generated to request Mechanical Design Engineering evaluation of this condition. Technical Evaluation (TE) 2001-023 was generated and contains: a) The setting was determined to have not affected the supports structural or functional capability. b) The spring cans are capable of performing their intended design function in the as-found, as-left condition. This condition will be revisited during the next extended refueling outage (RFO-23) to determine if any further action would be warranted.

Vermont Yankee Nuclear Power Corporation

**2001 Form NIS-2 Owner's Summary Report
for
Repairs or Replacements**

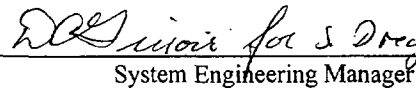
December 4, 1999 through May 20, 2001

Reviewed by:

 8/2/01

Plant Inservice Inspection Coordinator

Approved by:

 8/2/01

System Engineering Manager

FORM NIS-2 OWNER'S REPORT FOR REPAIRS OR REPLACEMENTS
As required by the Provisions of the ASME Code Section XI

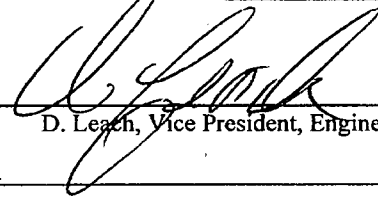
1. Owner Vermont Yankee Nuclear Power Corporation Date _____
Name
185 Old Ferry Road, PO Box 7002, Brattleboro VT 05302-7002 Sheet 2 of 14
Address
2. Plant Vermont Yankee Nuclear Power Station Unit 1
Name
P.O. Box 157, Governor Hunt Road, Vernon, VT 05354-0157 N/A
Address Repair Organization P.O. No., Job No., etc.
3. Work Performed by Vermont Yankee Nuclear Power Corporation Type Code Symbol Stamp N/A
Name
185 Old Ferry Road, PO Box 7002, Brattleboro VT 05302-7002 Authorization No. N/A
Address Expiration Date N/A
4. Identification of System See attached table, pages 4 through 14
5. (a) Applicable Construction Code B.31.1 1967 Edition, No Addenda, No Code Case
(b) Applicable Edition of Section XI Utilized for Repairs or Replacements 1986 Edition No Addenda
6. Identification of Components Repaired or Replaced and Replacement Components See attached table, pages 4
through 14
7. Description of Work See attached table, pages 4 through 14
8. Tests Conducted See attached table, pages 4 through 14
9. Remarks See attached table, pages 4 through 14

CERTIFICATE OF COMPLIANCE

We certify that the statements made in the report are correct and these repairs/replacements conform to the rules of ASME Code, Section XI.

Type Code Symbol Stamp _____ N/A _____

Certificate of Authorization Number _____ N/A _____ Expiration Date _____ N/A _____

Signed  Date August 16, 20 01
D. Leach, Vice President, Engineering

CERTIFICATE OF INSERVICE INSPECTION

I, the undersigned, holding a valid commission issued by the National Board of Boiler and Pressure Vessel Inspectors and the State or Province of Vermont and employed by Factory Mutual Insurance Co. of Johnston RI have inspected the components described in this Owner's Report during the period December 4, 1999 to May 20, 2001 and state to the best of my knowledge and belief, the Owner has performed examinations and taken corrective measures described in this Owner's Report in accordance with the requirements of the ASME Code, Section XI.

By signing this certificate neither the inspector nor his employer makes any warranty, expressed or implied, concerning the examinations and corrective measures described in this Owner's Report. Furthermore, neither the inspector nor his employer shall be liable in any manner for any personal injury or property damage or a loss of any kind arising from or connected with this inspection.

 Commissions VT-345
Inspector's Signature National Board, State, Province, and Endorsements

Date Aug 16 20 01

FORM NIS-2 OWNER'S REPORT FOR REPAIRS OR REPLACEMENTS
As required by the provisions of the ASME Code, Section XI, 1986 Edition, No Addenda

Vermont Yankee Nuclear Power Plant Unit 1
P.O. Box 157, Vernon, VT, 05354

Construction Code B31.1, 1967 Edition, No Addenda, No Code Case

<i>Component Equipment Number</i>	<i>System Identification</i>	<i>Name of Manufacturer</i>	<i>Manufacturer Serial Number</i>	<i>National Board Number</i>	<i>Other Identification (Work Order No., Minor Modification, Design Change, etc.)</i>	<i>Year Built</i>	<i>Repaired, Replaced, or Replacement</i>	<i>ASME Code Stamped</i>	<i>Description of Work</i>	<i>Test Conducted</i>
P-7-1B	SW	Byron Jackson	691-N-0362	N/A	WO 99-009059-000	1972	Repaired	N/A	Repaired Pump internals	System Leakage
RRU-8	HVAC	H. K. Porter	M-24442	N/A	WO 00-001039-000	1972	Repaired	N/A	Repaired Leak	System inservice
RCW-H88	RBCCW	Plant Fabricated	N/A	N/A	MM 99-05 WO 97-008451-020	1972	Repaired	N/A	Structural Hanger Modifications	N/A - repair made to structural components only
RCW-H89	RBCCW	Plant Fabricated	N/A	N/A	MM 99-05 WO 97-008451-020	1972	Repaired	N/A	Structural Hanger Modifications	N/A - repair made to structural components only
DG-1-1A	DG	Fairbanks Morse	38D870011TDS M12	N/A	MM 2000-001 WO 99-004206-000	1972	Replaced	N/A	Replaced Cooling Water Bellows	System inservice
SFP (Spent Fuel Pool)	SFPC	Plant Fabricated	N/A	N/A	MM 99-064 WO 00-000377-000	1972	Repaired	N/A	Obstacle Removal in Support of Spent Fuel Rack installation	N/A - repair made to structural components only
V13-16	RCIC	Walworth	SMB-00	N/A	WO 00-002526-000 WO 00-001746-002	1972	Repaired	N/A	Replaced Stem and Bonnet, Moved Packing To Repair Leak	System Leakage
SR-10-80B	RHRWS	Consolidated - Dresser	C31419	N/A	WO 00-001935-000	1972	Replaced	N/A	Replaced Relief Valve	System Leakage
SR-10-80A	RHRWS	Consolidated - Dresser	TK43762	N/A	WO 00-001943-000	1972	Replaced	N/A	Replaced Relief Valve	System inservice

FORM NIS-2 OWNER'S REPORT FOR REPAIRS OR REPLACEMENTS
 As required by the provisions of the ASME Code, Section XI, 1986 Edition, No Addenda

Vermont Yankee Nuclear Power Plant Unit 1
 P.O. Box 157, Vernon, VT, 05354

Construction Code B31.1, 1967 Edition, No Addenda, No Code Case

<i>Component Equipment Number</i>	<i>System Identification</i>	<i>Name of Manufacturer</i>	<i>Manufacturer Serial Number</i>	<i>National Board Number</i>	<i>Other Identification (Work Order No., Minor Modification, Design Change, etc.)</i>	<i>Year Built</i>	<i>Repaired, Replaced, or Replacement</i>	<i>ASME Code Stamped</i>	<i>Description of Work</i>	<i>Test Conducted</i>
DG-1-1A	DG	Fairbanks Morse	38D870011TDS M12	N/A	WO 99-004206-002	1972	Repaired	N/A	Performed Weld Repair To Eroded Area	System inservice
VG-9B	CAD	Target Rock	Model # 75E002	N/A	WO 00-002632-000	1972	Repaired	N/A	Rebuilt Valve	System Leakage
3"SW-5E	SW	Plant Fabricated	N/A	N/A	WO 00-003663-000	1972	Replacement	N/A	Replaced Section of 3"SW-5E Piping	System Leakage
V70-1A	SW	Walworth	Model # 5341WE	N/A	WO 96-012700-000	1972	Repaired	N/A	Perform Weld Build Up Valve Body in Hinge Pin Area	System Leakage
TK-3-125-10-19	HCU	Liquidonics	200L-8.2-5	N/A	WO 00-005412-001	1972	Replaced	N/A	Replaced Accumulator Tank	System Functional
TK-3-125-06-35	HCU	General Electric	P/N 921D59G2	N/A	WO 00-005412-000	1972	Replaced	N/A	Replaced Accumulator Tank	System Functional
DG-1-1B	DG	Fairbanks Morse	38D70006TDS M12	N/A	WO 00-005379-000	1972	Repaired	N/A	Machined Eroded Area On Flange Faces.	System Functional
V70-7A	SW	Crane	Cat. 487 1/2	N/A	WO 00-003806-000	1972	Replaced	N/A	Replaced Valve	System Leakage
P-7-1A	SW	Byron Jackson	691-N-0361	N/A	WO 00-004971-001	1972	Repaired	N/A	Rebuilt Pump	System Leakage
V70-101	SW	Walworth	Mod. # 5202WE	N/A	WO 95-005089-000	1972	Replaced	N/A	Replaced Valve	System Leakage
TK-3-125-14-35	HCU	Liquidonics	200L-8.2-5	N/A	WO 00-005489-000	1972	Replaced	N/A	Replaced Accumulator	System Leakage
V70-111A/B	SW	Walworth	Mod. # 5275WE	N/A	MM 2000-01 WO 98-012624-000	1972	Replaced	N/A	Replaced Valves	System Leakage
V11-12A	SLC	Powell	N/A	N/A	WO 00-004934-000	1972	Replaced	N/A	Replaced Valve Bonnet Studs	System Leakage

FORM NIS-2 OWNER'S REPORT FOR REPAIRS OR REPLACEMENTS
As required by the provisions of the ASME Code, Section XI, 1986 Edition, No Addenda

Vermont Yankee Nuclear Power Plant Unit 1
P.O. Box 157, Vernon, VT, 05354

Construction Code B31.1, 1967 Edition, No Addenda, No Code Case

<i>Component Equipment Number</i>	<i>System Identification</i>	<i>Name of Manufacturer</i>	<i>Manufacturer Serial Number</i>	<i>National Board Number</i>	<i>Other Identification (Work Order No., Minor Modification, Design Change, etc.)</i>	<i>Year Built</i>	<i>Repaired, Replaced, or Replacement</i>	<i>ASME Code Stamped</i>	<i>Description of Work</i>	<i>Test Conducted</i>
V13-15	RCIC	Walworth	SMB-00	N/A	WO 96-011053-000	1972	Replaced	N/A	Replaced Valve	System Leakage
LCV-3-33D	CRD	BW/IP	N/A	N/A	WO 99-008912-000	1972	Repair	N/A	Replaced Valve Seats	System Leakage
LCV-3-33C	CRD	BW/IP	N/A	N/A	WO 99-008911-000	1972	Repair	N/A	Replaced Valve Seats	System Leakage
SB-16-19-7B	PCAC	Allis Chalmers	00616-11	N/A	WO 99-011315-000	1972	Replaced	N/A	Replaced Flange Bolts	Tested in accordance with Operations Procedure OP 4202
P-7-1B	SW	Byron Jackson	691-N-0362	N/A	WO 00-004971-001	1972	Repaired	N/A	Rebuilt Pump	System Leakage
V70-1A	SW	Walworth	Mod. # 5341WE	N/A	WO 96-012700-000	1972	Repaired	N/A	Weld Buildup of Valve Body in Hinge Pin Area	System Leakage
DG-1-1A	DG	Fairbanks Morse	38D870011TDS M12	N/A	WO 99-008333-000	1972	Replaced	N/A	Replaced Bolting	System inservice
DG-1-1A	DG	Fairbanks Morse	38D870011TDS M12	N/A	WO 99-009496-000	1972	Replaced	N/A	Replaced Bolting	System inservice
DG-1-1B	DG	Fairbanks Morse	38D70006TDS M12	N/A	WO 99-011236-000	1972	Replaced	N/A	Replaced Support Clamp	N/A - repair made to structural components only

FORM NIS-2 OWNER'S REPORT FOR REPAIRS OR REPLACEMENTS
 As required by the provisions of the ASME Code, Section XI, 1986 Edition, No Addenda

Vermont Yankee Nuclear Power Plant Unit 1
 P.O. Box 157, Vernon, VT, 05354

Construction Code B31.1, 1967 Edition, No Addenda, No Code Case

<i>Component Equipment Number</i>	<i>System Identification</i>	<i>Name of Manufacturer</i>	<i>Manufacturer Serial Number</i>	<i>National Board Number</i>	<i>Other Identification (Work Order No., Minor Modification, Design Change, etc.)</i>	<i>Year Built</i>	<i>Repaired, Replaced, or Replacement</i>	<i>ASME Code Stamped</i>	<i>Description of Work</i>	<i>Test Conducted</i>
DG-1-1B	DG	Fairbanks Morse	38D70006TDS M12	N/A	WO 99-010257-000	1972	Replaced	N/A	Replaced Support Clamp	N/A - repair made to structural components only
DG-1-1B	DG	Fairbanks Morse	38D70006TDS M12	N/A	WO 99-009229-000	1972	Replaced	N/A	Replaced Bolting	System inservice
DG-1-1B	DG	Fairbanks Morse	38D70006TDS M12	N/A	WO 99-009500-000	1972	Replaced	N/A	Replaced Bolting	System inservice
TK-3-125-22-35	HCU	Liquidonics	200L-8.2-5	N/A	WO 00-006190-000	1972	Replaced	N/A	Replaced Accumulator	System Leakage
TK-3-125-14-31	HCU	Liquidonics	200L-8.2-5	N/A	WO 00-006191-000	1972	Replaced	N/A	Replaced Accumulator	System Leakage
P-7-1A	SW	Byron Jackson	691-N-0361	N/A	WO 00-006381-000	1972	Replaced/Repaired	N/A	Rebuilt Pump Assembly - Replaced With Spare	System Leakage
S-3-1B	SW	R. P. Adams	106047	N/A	WO 00-006231-000	1972	Repaired	N/A	Opened and Cleaned Strainer	System Leakage
Small Bore Piping at P-18-1A/B Recirc. Pumps	NB	Byron Jackson	671-S-1108	N/A	MM 2000-042 WO 00-001839-000	1972	Repaired	N/A	RBCCW thermal Stress Modifications To Small Bore Piping At P-18-1A/B	System Leakage
SR-16-19-77	N2	Kunkle Valve Co.	L-3072	N/A	WO 00-000596-000	1972	Repaired/Replaced	N/A	Repaired Relief Valve - Replaced With Spare	System Leakage
V11-41	SLC	Powell	Mod. # 3003 WE	N/A	WO 00-006999-000	1972	Replaced	N/A	Replaced Bonnet Studs and Nuts	System Leakage

FORM NIS-2 OWNER'S REPORT FOR REPAIRS OR REPLACEMENTS
As required by the provisions of the ASME Code, Section XI, 1986 Edition, No Addenda

Vermont Yankee Nuclear Power Plant Unit 1
P.O. Box 157, Vernon, VT, 05354

Construction Code B31.1, 1967 Edition, No Addenda, No Code Case

<i>Component Equipment Number</i>	<i>System Identification</i>	<i>Name of Manufacturer</i>	<i>Manufacturer Serial Number</i>	<i>National Board Number</i>	<i>Other Identification (Work Order No., Minor Modification, Design Change, etc.)</i>	<i>Year Built</i>	<i>Repaired, Replaced, or Replacement</i>	<i>ASME Code Stamped</i>	<i>Description of Work</i>	<i>Test Conducted</i>
RV-10-210A/B	RHR	Consolidated Dresser	Mod. # 1685	N/A	MM 2000-043 WO 00-006249-000	1972	Repaired	N/A	Removed Valves Rv-10-210a/B	System Leakage
SR-10-80 A&B	RHRSW	Consolidated Dresser	TK43762	N/A	WO 00-001935-004 WO 00-001943-005 WO 00-007021-000	1972	Repaired	N/A	Rebuilt Safety Relief Valve	System Leakage
CRD-06-31	CRD	General Electric	Mod. # 7RDB144BG1	N/A	WO 00-004225-002	1972	Replaced	N/A	Replaced Control Rod Drive	System Leakage
CRD-06-11	CRD	General Electric	Mod. # 7RDB144BG1	N/A	WO 00-004225-003	1972	Replaced	N/A	Replaced Control Rod Drive	System Leakage
CRD-14-31	CRD	General Electric	Mod. # 7RDB144BG1	N/A	WO 00-004225-004	1972	Replaced	N/A	Replaced Control Rod Drive	System Leakage
CRD-42-27	CRD	General Electric	Mod. # 7RDB144BG1	N/A	WO 00-004225-005	1972	Replaced	N/A	Replaced Control Rod Drive	System Leakage
CRD-18-39	CRD	General Electric	Mod. # 7RDB144BG1	N/A	WO 00-004225-006	1972	Replaced	N/A	Replaced Control Rod Drive	System Leakage
CRD-26-15	CRD	General Electric	Mod. # 7RDB144BG1	N/A	WO 00-004225-007	1972	Replaced	N/A	Replaced Control Rod Drive	System Leakage
CRD-34-31	CRD	General Electric	Mod. # 7RDB144BG1	N/A	WO 00-004225-008	1972	Replaced	N/A	Replaced Control Rod Drive	System Leakage
CRD-34-39	CRD	General Electric	Mod. # 7RDB144BG1	N/A	WO 00-004225-009	1972	Replaced	N/A	Replaced Control Rod Drive	System Leakage
P-45-1A	SLC	Union Pump Co.	P-C274713	N/A	WO 99-009881-000	1972	Replaced	N/A	Replaced Stuffing Box Studs and Nuts	System Functional
P-45-1A	SLC	Union Pump Co.	P-C274713	N/A	WO 00-006269-000	1972	Replaced	N/A	Replaced Cylinder Flange Tie Studs and Nuts	System Functional
P-45-1B	SLC	Union Pump Co.	P-C274714	N/A	WO 98-011881-000	1972	Replaced	N/A	Replaced Stuffing Box Studs and Nuts	System Functional

FORM NIS-2 OWNER'S REPORT FOR REPAIRS OR REPLACEMENTS
 As required by the provisions of the ASME Code, Section XI, 1986 Edition, No Addenda

Vermont Yankee Nuclear Power Plant Unit 1
 P.O. Box 157, Vernon, VT, 05354

Construction Code B31.1, 1967 Edition, No Addenda, No Code Case

<i>Component Equipment Number</i>	<i>System Identification</i>	<i>Name of Manufacturer</i>	<i>Manufacturer Serial Number</i>	<i>National Board Number</i>	<i>Other Identification (Work Order No., Minor Modification, Design Change, etc.)</i>	<i>Year Built</i>	<i>Repaired, Replaced, or Replacement</i>	<i>ASME Code Stamped</i>	<i>Description of Work</i>	<i>Test Conducted</i>
P-45-1B	SLC	Union Pump Co.	P-C274714	N/A	WO 00-006266-000	1972	Replaced	N/A	Replaced Cylinder Flange Tie Studs and Nuts	System Functional
TK-3-125-18-43	HCU	General Electric	P/N 921D595G2	N/A	WO 00-005707-000	1972	Replaced	N/A	Replaced HCU Piston Accumulator	System Leakage
TK-3-125-02-27	HCU	Liquidonics	Mod. # 200L-8.2-5	N/A	WO 00-005708-000	1972	Replaced	N/A	Replaced HCU Piston Accumulator	System Leakage
SR-10-86A	RHR	Dresser	Mod. # 9352774	N/A	WO 97-002364-000	1972	Replaced	N/A	Replaced Valve	System Leakage
HPCI-HD103FN (Snubber S/N ADH-301-1597 removed for functional testing and returned to stock S/N ADH-301-1598 installed)	HPCI	Anchor Darling	ADH-301-1598	N/A	WO 00-001027-000	1972	Repaired/ Replaced	N/A	Replaced and Rebuilt Snubber	N/A - replacement of snubber only
RHR-H185 (Snubber S/N 32198 removed for functional testing and returned to stock S/N 26351 installed)	RHR	Grinnell	Fig. 200 S/N 32198	N/A	WO 00-000995-000	1972	Repaired/ Replaced	N/A	Replaced and Rebuilt Snubber	N/A - replacement of snubber only
RR-3 (Snubber S/N 32197 removed for functional testing and returned to stock S/N 26347 installed)	NB	Grinnell	Miller Model	N/A	WO 00-000993-000	1972	Repaired/ Replaced	N/A	Replaced and Rebuilt Snubber	N/A - replacement of snubber only
CS-HD54A (Snubber S/N 32195 removed for functional testing and returned to stock S/N 26348 installed)	CS	Miller	Fig. 201	N/A	WO 00-000991-000	1972	Repaired/ Replaced	N/A	Replaced and Rebuilt Snubber	N/A - replacement of snubber only

FORM NIS-2 OWNER'S REPORT FOR REPAIRS OR REPLACEMENTS
As required by the provisions of the ASME Code, Section XI, 1986 Edition, No Addenda

Vermont Yankee Nuclear Power Plant Unit 1
P.O. Box 157, Vernon, VT, 05354

Construction Code B31.1, 1967 Edition, No Addenda, No Code Case

<i>Component Equipment Number</i>	<i>System Identification</i>	<i>Name of Manufacturer</i>	<i>Manufacturer Serial Number</i>	<i>National Board Number</i>	<i>Other Identification (Work Order No., Minor Modification, Design Change, etc.)</i>	<i>Year Built</i>	<i>Repaired, Replaced, or Replacement</i>	<i>ASME Code Stamped</i>	<i>Description of Work</i>	<i>Test Conducted</i>
RHR-H197A (Snubber S/N 32196 removed for functional testing and returned to stock S/N 26349 installed)	RHR	Lynair	Fig. 200	N/A	WO 00-000989-000	1972	Repaired/ Replaced	N/A	Replaced and Rebuilt Snubber	N/A - replacement of snubber only
RR-35 (Snubber S/N 322003 removed for functional testing and returned to stock S/N 30034 installed)	NB	Miller	Fig. 200	N/A	WO 00-000906-000	1972	Repaired/ Replaced	N/A	Replaced and Rebuilt Snubber	N/A - replacement of snubber only
MSSRV S/N 249	NB	Target Rock	249	N/A	PO VY009397	1972	Repaired/ Replaced	N/A	Replaced/Rebuilt Main Steam Safety Relief Valve	System Leakage
MSSRV S/N 250	NB	Target Rock	250	N/A	PO VY009397	1972	Repaired/ Replaced	N/A	Replaced/Rebuilt Main Steam Safety Relief Valve	System Leakage
MSSRV S/N 67-HH-14	NB	Target Rock	67-HH-14	N/A	PO VY009397	1972	Repaired/ Replaced	N/A	Replaced/Rebuilt Main Steam Safety Relief Valve	System Leakage
MSSRV S/N BL 1134	NB	Target Rock	BL 1134	N/A	PO VY009397	1972	Repaired/ Replaced	N/A	Replaced/Rebuilt Main Steam Safety Relief Valve	System Leakage
MSSRV S/N BL-1137	NB	Target Rock	BL-1137	N/A	PO VY009397	1972	Repaired/ Replaced	N/A	Replaced/Rebuilt Main Steam Safety Relief Valve	System Leakage
Alternate Cooling System to Standby Fuel Pool Cooling System	SFPC	Plant Fabricated	N/A	N/A	VYDC 2000-024 WO 00-005772-000	1972	Repaired	N/A	Installed Alternate Cooling System To Standby Fuel Pool Cooling System Design Change	Hydrostatic and System leakage

FORM NIS-2 OWNER'S REPORT FOR REPAIRS OR REPLACEMENTS
 As required by the provisions of the ASME Code, Section XI, 1986 Edition, No Addenda

Vermont Yankee Nuclear Power Plant Unit 1
 P.O. Box 157, Vernon, VT, 05354

Construction Code B31.1, 1967 Edition, No Addenda, No Code Case

<i>Component Equipment Number</i>	<i>System Identification</i>	<i>Name of Manufacturer</i>	<i>Manufacturer Serial Number</i>	<i>National Board Number</i>	<i>Other Identification (Work Order No., Minor Modification, Design Change, etc.)</i>	<i>Year Built</i>	<i>Repaired, Replaced, or Replacement</i>	<i>ASME Code Stamped</i>	<i>Description of Work</i>	<i>Test Conducted</i>
NG-13A	CAD	Target Rock	Mod. # 75E001 S/N	N/A	WO 00-004690-000	1972	Repaired	N/A	Valve internals inspection and Bonnet Tack Weld	
NG-13B	CAD	Target Rock	Mod. # 75E001 S/N 3	N/A	WO 00-004691-000	1972	Repaired	N/A	Valve internals inspection and Bonnet Tack Weld	System Leakage
NG-11B	CAD	Target Rock	Mod. # 75E001 S/N 3	N/A	WO 00-004687-000	1972	Repaired	N/A	Valve internals inspection and Bonnet Tack Weld	System Leakage
NG-12B	CAD	Target Rock	Mod. # 75E001 S/N 4	N/A	WO 00-004689-000	1972	Repaired	N/A	Valve internals inspection and Bonnet Tack Weld	System Leakage
NG-12A	CAD	Target Rock	Mod. # 75E001 S/N 2	N/A	WO 00-004688-000	1972	Repaired	N/A	Valve internals inspection and Bonnet Tack Weld	System Leakage
NG-11A	CAD	Target Rock	Mod. # 75E001	N/A	WO 00-004393-000	1972	Repaired	N/A	Valve internals inspection and Bonnet Tack Weld	System Leakage
P-8-1D	RHRSW	Byron Jackson	Mod. # VTP S/N 691-N-0366	N/A	WO 01-001098-000	1972	Replaced	N/A	Replaced Pump Rotating Assembly	System Leakage
DG-1-1A	DG	Fairbanks Morse	38D870011TDS M12	N/A	WO 01-000804-000	1972	Replaced	N/A	Replaced the Collar Stud Assembly	System inservice
DG-1-1B	DG	Fairbanks Morse	38D70006TDS M12	N/A	WO 01-001101-000	1972	Replaced	N/A	Replaced Broken OCS Scavenging Air Piping Stud	System inservice
SR-72-3A	SA	Kunkle Valve Co.	N/A	N/A	WO 00-000597-000	1972	Replaced	N/A	Replaced Relief Valve	System Leakage
RV-2-71A	NB	Target Rock	Mod. # 67F-000-15 6X10	N/A	WO 00-004226-000	1972	Replaced	N/A	Replaced Relief Valve	System Leakage

FORM NIS-2 OWNER'S REPORT FOR REPAIRS OR REPLACEMENTS
 As required by the provisions of the ASME Code, Section XI, 1986 Edition, No Addenda

Vermont Yankee Nuclear Power Plant Unit 1
 P.O. Box 157, Vernon, VT, 05354

Construction Code B31.1, 1967 Edition, No Addenda, No Code Case

<i>Component Equipment Number</i>	<i>System Identification</i>	<i>Name of Manufacturer</i>	<i>Manufacturer Serial Number</i>	<i>National Board Number</i>	<i>Other Identification (Work Order No., Minor Modification, Design Change, etc.)</i>	<i>Year Built</i>	<i>Repaired, Replaced, or Replacement</i>	<i>ASME Code Stamped</i>	<i>Description of Work</i>	<i>Test Conducted</i>
RV-2-71B	NB	Target Rock	Mod. # 67F-000-15 6X10	N/A	WO 00-004720-000	1972	Replaced	N/A	Replaced Relief Valve	System Leakage
RV-2-71C	NB	Target Rock	Mod. # 67F-000-15 6X10	N/A	WO 00-004721-000	1972	Replaced	N/A	Replaced Relief Valve	System Leakage
RV-2-71D	NB	Target Rock	Mod. # 67F-000-15 6X10	N/A	WO 00-004722-000	1972	Replaced	N/A	Replaced Relief Valve	System Leakage
SV-2-70A	NB	Dresser	Mod. # 3707 RA-RT21 S/N BL1137	N/A	WO 00-004230-000	1972	Replaced	N/A	Replaced Safety Relief Valve	System Leakage
SV-2-70B	NB	Dresser	Mod. # 3707 RA-RT21 S/N BL1134	N/A	WO 00-004745-000	1972	Replaced	N/A	Replaced Safety Relief Valve	System Leakage
V70-71C	RBCCW	Honeywell	Mod. # 8105	N/A	WO 00-007152-000	1972	Repaired	N/A	Repaired Plug and Stem	System Leakage
V2-80D	MS	Rockwell	Mod. # 1612JMMY S/N 123	N/A	WO 01-001729-000	1972	Repaired	N/A	Repaired Valve Seat	System Leakage
V14-13A	CS	Rockwell	Mod. # 770 JMMY	N/A	WO 01-001806-000	1972	Repaired	N/A	Repaired Valve Internals	System Leakage
P-18-1B	RBCCW	Byron Jackson	Mod. # DVSS S/N 671-S-1109	N/A	WO 00-001839-000	1972	Repaired/ Replaced	N/A	Repaired/ Replaced Spool on Seal Heat Exchanger Cooling Unit	System Leakage

FORM NIS-2 OWNER'S REPORT FOR REPAIRS OR REPLACEMENTS
As required by the provisions of the ASME Code, Section XI, 1986 Edition, No Addenda

Vermont Yankee Nuclear Power Plant Unit 1
P.O. Box 157, Vernon, VT, 05354

Construction Code B31.1, 1967 Edition, No Addenda, No Code Case

<i>Component Equipment Number</i>	<i>System Identification</i>	<i>Name of Manufacturer</i>	<i>Manufacturer Serial Number</i>	<i>National Board Number</i>	<i>Other Identification (Work Order No., Minor Modification, Design Change, etc.)</i>	<i>Year Built</i>	<i>Repaired, Replaced, or Replacement</i>	<i>ASME Code Stamped</i>	<i>Description of Work</i>	<i>Test Conducted</i>
V16-19-5G	PCAC	Atwood and Morrill	Mod. # 20751H	N/A	WO 00-004108-001	1972	Repaired	N/A	Installed Disc Nut Spacer Shim	Tested in accordance with Operations Procedure OP 4202
V3-114-38-35	HCU	General Electric	N/A	N/A	WO 01-001886-000	1972	Repaired	N/A	Repaired Valve Internals	System Leakage
CV-3-127-38-35	HCU	Hammel-Dahl	Mod. # 2500ASA-999Z1204	N/A	WO 01-001886-001	1972	Repaired	N/A	Replaced Teflon Seat Ring Disc	System Leakage
V13-131	RCIC	Walworth	Mod. # C44099 S/N 5301BSB-WE	N/A	WO 00-006789-000	1972	Repaired	N/A	Repaired Valve Internals	System Leakage
V70-319B	SW	Nibco	Fig. T-134	N/A	WO 01-001934-000	1972	Replaced	N/A	Replaced Valve	System Leakage
V70-319D	SW	Nibco	Fig. T-134	N/A	WO 01-001935-000	1972	Replaced	N/A	Replaced Valve	
V13-6	RCIC	Enertech	Mod. # DRV-2	N/A	WO 01-001732-000	1972	Repaired	N/A	Replaced Valve Spring	System Leakage
V13-7	RCIC	Enertech	Mod. # DRV-2	N/A	WO 01-001733-000	1972	Repaired	N/A	Replaced Valve Spring	System Leakage
V23-3	HPCI	Enertech	Mod. # DRV-B	N/A	WO 01-001740-000	1972	Repaired	N/A	Replaced Valve Spring	System Leakage
V23-4	HPCI	Enertech	Mod. # DRV-B	N/A	WO 01-001748-000	1972	Repaired	N/A	Replaced Valve Spring	System Leakage
RRU-8	HVAC	H. K. Porter	Mod. # 41-523-H S/N M-24442	N/A	WO 00-001039-010	1972	Repaired	N/A	Repaired Leak in Service Water Supply Connection	System Leakage

FORM NIS-2 OWNER'S REPORT FOR REPAIRS OR REPLACEMENTS
 As required by the provisions of the ASME Code, Section XI, 1986 Edition, No Addenda

Vermont Yankee Nuclear Power Plant Unit 1
 P.O. Box 157, Vernon, VT, 05354

Construction Code B31.1, 1967 Edition, No Addenda, No Code Case

<i>Component Equipment Number</i>	<i>System Identification</i>	<i>Name of Manufacturer</i>	<i>Manufacturer Serial Number</i>	<i>National Board Number</i>	<i>Other Identification (Work Order No., Minor Modification, Design Change, etc.)</i>	<i>Year Built</i>	<i>Repaired, Replaced, or Replacement</i>	<i>ASME Code Stamped</i>	<i>Description of Work</i>	<i>Test Conducted</i>
Drywell Seal and Coating	Drywell	CBI	Mod. # General Electric Mark I	N/A	MM 2000-010 WO 00-001840-000	1972	Repaired/ Replaced	N/A	Replaced DW Seal and Protective Coating Repairs	N/A



Entergy

NEC-JH_33

Entergy Nuclear Operations, Inc.
Vermont Yankee
P.O. Box 0250
320 Governor Hunt Road
Vernon, VT 05354
Tel 802 257 7711

February 5, 2008
BVY 08-008

ATTN: Document Control Desk
U.S. Nuclear Regulatory Commission
Washington, DC 20555-0001

- References:
- 1) Letter, Entergy to USNRC, "Vermont Yankee Nuclear Power Station, License No. DPR-28, License Renewal Application," BVY 06-009, dated January 25, 2006
 - 2) Letter, Entergy to USNRC, "Update of Aging Management Program Audit Q&A Database," BVY 07-079, dated November 14, 2007
 - 3) Letter, USNRC to Entergy, "Update on Extension of Schedule for the Conduct of Review of the Vermont Yankee Nuclear Power Station License Renewal Application," NVY 07-157, dated November 27, 2007
 - 4) Letter, Entergy to USNRC, "License Renewal Application, Amendment 33," BVY 07-082, dated December 11, 2007
 - 5) Letter, Entergy to USNRC, "License Renewal Application, Amendment 34," BVY 08-002, dated January 30, 2008

**Subject: Vermont Yankee Nuclear Power Station
License No. DPR-28 (Docket No. 50-271)
License Renewal Application, Amendment 35**

On January 25, 2006, Entergy Nuclear Operations, Inc. and Entergy Nuclear Vermont Yankee, LLC (Entergy) submitted Reference (1), the License Renewal Application (LRA) for the Vermont Yankee Nuclear Power Station (VYNPS).

VYNPS submitted Reference (2) following an NRC audit of the VYNPS Aging Management Program and subsequently received Reference (3), which included an NRC Request for Additional Information. References (4) and (5), respectively, provided the initial response to Reference (3) and later clarifications to that response. Additional clarification and details regarding recirculation nozzle Cumulative Usage Factor (CUF) and water chemistry effects are provided in Attachments 1 and 2 to this letter. VYNPS information meeting the NRC's position on Extended Power Uprate (EPU) operating experience evaluation for Aging Management Programs is also discussed below.

VYNPS had not yet entered operation at EPU levels at the time Reference (1) was submitted. EPU power ascension began in March of 2006. To ensure that operating experience at EPU levels is properly addressed by aging management programs, Entergy will perform an evaluation of operating experience at EPU levels prior to the period of extended operation. In addition to VYNPS operating experience, the evaluation will include operating experience from other BWR plants operating at EPU levels.

*Att
NRR*

This is a new commitment, and has been entered as Commitment #51 on the VYNPS License Renewal Commitment List, Revision 9 (Attachment 3).

Should you have any questions concerning this submittal, please contact Mr. David Mannai at (802) 451-3304.

I declare under penalty of perjury that the foregoing is true and correct.

Executed on February 5, 2008.

Sincerely,



Fred A. Sullivan
Site Vice President
Vermont Yankee Nuclear Power Station

Attachment 1: Additional Information Regarding Recirculation Nozzle CUF
Attachment 2: Additional Information Regarding Water Chemistry Effects
Attachment 3: License Renewal Commitment List, Revision 9

cc: Mr. James Dyer, Director
U.S. Nuclear Regulatory Commission
Office O5E7
Washington, DC 20555-00001

Mr. Samuel J. Collins, Regional Administrator, Region 1
U.S. Nuclear Regulatory Commission
475 Allendale
Road King of Prussia, PA 19406-1415

Mr. Jack Strosnider, Director
U.S. Nuclear Regulatory Commission
Office T8A23
Washington, DC 20555-00001

Mr. Jonathan Rowley, Senior Project Manager
U.S. Nuclear Regulatory Commission
11555 Rockville Pike
MS-O-11F1
Rockville, MD 20853

Mr. Mike Modes
USNRC RI
475 Allendale Road
King of Prussia, PA 19406

Mr. James S. Kim, Project Manager
U.S. Nuclear Regulatory Commission
Mail Stop O-8-C2A
Washington, DC 20555

USNRC Resident Inspector
Entergy Nuclear Vermont Yankee, LLC
P.O. Box 157
Vernon, Vermont 05354

Mr. David O'Brien, Commissioner
VT Department of Public Service
112 State Street – Drawer 20
Montpelier, Vermont 05620-2601

Diane Curran, Esq.
Harmon, Curran, Spielberg & Eisenberg, LLP
1726 M Street, N.W., Suite 600
Washington, DC 20036

BVY 08-008

Attachment 1

Vermont Yankee Nuclear Power Station
License No. DPR-28 (Docket No. 50-271)

License Renewal Application

Amendment 35

Additional Information Regarding Recirculation Nozzle CUF

**VERMONT YANKEE NUCLEAR POWER STATION
LICENSE RENEWAL APPLICATION AMENDMENT 35
ATTACHMENT 1**

Additional Information Regarding Recirculation Nozzle CUF

NRC Request:

Demonstrate why the confirmatory analysis for the feedwater nozzle bounds the geometry of the recirculation outlet nozzle.

Response:

The feedwater nozzle was chosen for the confirmatory analysis since it has the largest number of, and most severe, transients and the highest calculated fatigue usage of the three nozzles which used the VY fatigue analysis approach. The analysis of the feedwater nozzle is bounding for the recirculation outlet nozzle since the calculated usage factors and thermal transient stresses are significantly less than those for the feedwater nozzle.

As pointed out during the January 8, 2008 presentation to the NRC Staff, the recirculation outlet nozzle has a different geometry (i.e., "skewed") as compared to the other nozzles. However, the feedwater nozzle configuration remains conservative and bounding when compared to the recirculation outlet nozzle configuration for the following reasons:

- The previous comparisons of nozzle corner stress factors from BWRVIP-108, which included evaluation of a recirculation outlet nozzle, demonstrate that the recirculation outlet nozzle configuration does not provide results that are significantly different from the other nozzle configurations.
- The transients experienced by the recirculation outlet nozzle are significantly less severe and less numerous than the transients that affect the feedwater nozzle.
- The most significant thermal transient (improper start causing reverse flow) was modeled directly in the Finite Element Model due to its unique characteristics.
- In the nozzle corner, the thermal stresses are small compared to the pressure stresses.
- The previous analyses for all three nozzles for VY yielded significantly lower fatigue usage for the recirculation outlet nozzle compared to the feedwater nozzle.
- Industry experience for the BWR fleet has repeatedly demonstrated that the recirculation outlet nozzle fatigue usage is significantly lower than feedwater nozzle fatigue usage.

BVY 08-008

Attachment 2

Vermont Yankee Nuclear Power Station
License No. DPR-28 (Docket No. 50-271)

License Renewal Application

Amendment 35

Additional Information Regarding Water Chemistry Effects

**VERMONT YANKEE NUCLEAR POWER STATION
LICENSE RENEWAL APPLICATION AMENDMENT 35
ATTACHMENT 2**

Additional Information Regarding Water Chemistry Effects

NRC Request:

Describe how water chemistry effects were accounted for in the evaluation of environmentally assisted fatigue.

Response:

Per Section X.M1 of NUREG 1801 (GALL Report) the environmentally assisted fatigue (EAF) evaluations used appropriate Fatigue Life Correction Factors (F_{en}) calculated using the methodology in NUREG/CR-6583 for carbon and low alloy steels and NUREG/CR-5704 for stainless steels.

For carbon and low alloy steels the F_{en} factor relationships are shown on page 69 of NUREG/CR-6583. As shown on page 60 of NUREG/CR-6583, the input values used to develop the F_{en} factors are sulfur content, strain rate, temperature, and dissolved oxygen content in the fluid. Input values for these parameters were chosen to maximize the F_{en} factors calculated for all components.

The F_{en} factor relationship for stainless steels is shown on page 31 of NUREG/CR-5704. As shown on page 25 of NUREG/CR-5704, the input values used to develop the F_{en} factors are strain rate, temperature, and dissolved oxygen content in the fluid. Similar to the carbon and low alloy steel calculations, the input values were chosen to maximize the F_{en} factors.

The inputs were selected as follows:

- For the carbon and low alloy steel expressions, the transformed sulfur content parameter was set equal to the maximum value of 0.015 to maximize the effects of this parameter.
- For all expressions, the transformed strain rate parameter was set equal to the minimum strain rate (i.e., less than 0.001%/sec) for all transients to maximize the effects of this parameter.
- For all expressions, the transformed temperature parameter was computed using 550°F for all locations. This temperature envelopes normal operating temperatures to maximize the effects of this parameter, and is very conservative for feedwater temperature.
- For the transformed dissolved oxygen parameter, dissolved oxygen (DO) data was taken from recorded plant data for the feedwater line. For all other locations evaluated in the reactor coolant system, the EPRI BWRVIA code was used to determine DO levels. The EPRI BWRVIA model was used to determine DO at component locations at original licensed power (OLP) for both BWR normal water chemistry (NWC) and noble metal water chemistry (NMCA+HWC). Also, current licensed power with NMCA+HWC was evaluated.

**VERMONT YANKEE NUCLEAR POWER STATION
LICENSE RENEWAL APPLICATION AMENDMENT 35
ATTACHMENT 2**

For the purposes of ensuring that the DO effects on F_{en} are conservative and bounding with respect to water chemistry, the F_{en} values used accounted for variations in plant recorded feedwater DO data. It is noted that excursions observed in the plant data used are small in number and are of short duration. Approximately 13 years of recorded feedwater DO measurements, including excursions, were evaluated for input to the EAF analysis. A DO value (50 ppb) was used to calculate bounding F_{en} value for the feedwater piping. This represents the mean of the measured data plus one standard deviation.

For locations in the reactor coolant system, the BWRVIA model was run varying the DO content for the power/water chemistry conditions discussed above. The results of these sensitivity studies showed that the resulting variations in DO at component locations are significantly less than the changes input to the feedwater DO. The variation of feedwater DO (mean plus one standard deviation) was evaluated. This resulted in less than a 2% change in the bounding F_{en} used in the EAF analysis for the low alloy steel components in the beltline and lower sections of the reactor vessel. There is no effect on the bounding F_{en} values from the input feedwater DO variations for the stainless steel components.

The F_{en} factors are determined using several parameters and, collectively, these parameters were chosen to conservatively maximize their contribution. The F_{en} factors are bounding for each location based on all of the input values. The bounding F_{en} factors for each location and material were used for all stress range pairs in the cumulative usage factor calculations.



NEC-JH_34

Entergy Nuclear Operations, Inc.
Vermont Yankee
P.O. Box 0250
320 Governor Hunt Road
Vernon, VT 05354
Tel 802 257 7711

January 30, 2008
BVY 08-002

ATTN: Document Control Desk
U.S. Nuclear Regulatory Commission
Washington, DC 20555-0001

- References:
- 1) Letter, Entergy to USNRC, "Vermont Yankee Nuclear Power Station, License No. DPR-28, License Renewal Application," BVY 06-009, dated January 25, 2006.
 - 2) Letter, Entergy to USNRC, "Update of Aging Management Program Audit Q&A Database," BVY 07-079, dated November 14, 2007.
 - 3) Letter, USNRC to Entergy, "Update on Extension of Schedule for the Conduct of Review of the Vermont Yankee Nuclear Power Station License Renewal Application," NVY 07-157, dated November 27, 2007.
 - 4) Letter, Entergy to USNRC, "License Renewal Application, Amendment 33," BVY 07-082, dated December 11, 2007.
 - 5) Letter, Entergy to USNRC, "License Renewal Application, Amendment 31," BVY 07-066, dated September 17, 2007.

**Subject: Vermont Yankee Nuclear Power Station
License No. DPR-28 (Docket No. 50-271)
License Renewal Application, Amendment 34**

On January 25, 2006, Entergy Nuclear Operations, Inc. and Entergy Nuclear Vermont Yankee, LLC (Entergy) submitted the License Renewal Application (LRA) for the Vermont Yankee Nuclear Power Station (Reference 1).

In Reference (2), Entergy provided an update to the Aging Management Program (AMP) Audit Q&A Database. In Reference (3), the NRC requested additional information relative to audit question number 387. This information was provided in Reference (4).

Subsequent to that submittal and a follow-up meeting with the NRC staff on January 8, 2008, Entergy agreed to perform additional analyses to support the original response. Attachment 1 to this letter provides the results of those analyses. Attachment 2 provides an update to the Cumulative Usage Factor for the Core Spray nozzle forging blend radius that was previously submitted with Reference (5).

This letter contains no new regulatory commitments.

Should you have any questions concerning this submittal, please contact Mr. David Mannai at (802) 451-3304.

A117
NRC

I declare under penalty of perjury that the foregoing is true and correct.

Executed on January 30, 2008.

Sincerely,



Ted A. Sullivan
Site Vice President
Vermont Yankee Nuclear Power Station

Attachments

cc: Mr. James Dyer, Director
U.S. Nuclear Regulatory Commission
Office O5E7
Washington, DC 20555-00001

Mr. Samuel J. Collins, Regional Administrator, Region 1
U.S. Nuclear Regulatory Commission
475 Allendale Road
King of Prussia, PA 19406-1415

Mr. Jack Strosnider, Director
U.S. Nuclear Regulatory Commission
Office T8A23
Washington, DC 20555-00001

Mr. Jonathan Rowley, Senior Project Manager
U.S. Nuclear Regulatory Commission
11555 Rockville Pike
MS-O-11F1
Rockville, MD 20853

Mr. Mike Modes
USNRC RI
475 Allendale Road
King of Prussia, PA 19406

Mr. James S. Kim, Project Manager
U.S. Nuclear Regulatory Commission
Mail Stop O-8-C2A
Washington, DC 20555

USNRC Resident Inspector
Entergy Nuclear Vermont Yankee, LLC
P.O. Box 157
Vernon, Vermont 05354

Mr. David O'Brien, Commissioner
VT Department of Public Service
112 State Street – Drawer 20
Montpelier, Vermont 05620-2601

Diane Curran, Esq.
Harmon, Curran, Spielberg & Eisenberg, LLP
1726 M Street, N.W., Suite 600
Washington, DC 20036

BVY 08-002

Attachment 1

Vermont Yankee Nuclear Power Station
License No. DPR-28 (Docket No. 50-271)

License Renewal Application

Amendment 34

RAI 4.3.3-2 Additional Information

**VERMONT YANKEE NUCLEAR POWER STATION
LICENSE RENEWAL APPLICATION AMENDMENT 34
ATTACHMENT 1**

Vermont Yankee Feedwater Nozzle Confirmatory Analysis Results

On January 8, 2008, the Office of Nuclear Reactor Regulation (NRR) staff and Entergy Vermont Yankee (VY) met in a public meeting to discuss VY's response to RAI 4.3.3-2 on environmentally assisted fatigue (EAF). After a formal presentation and dialogue with NRC staff, VY agreed to perform a confirmatory EAF analysis on the reactor pressure vessel (RPV) feedwater nozzle. This analysis would confirm the VY fatigue analysis approach by performing an alternate confirmatory analysis using ASME Code, Section III, Subsection NB-3200 [1] methodology to demonstrate available nozzle margins and acceptability of the VY approach. Table 1 provides the results of the confirmatory analysis and demonstrates that the existing VY fatigue analysis approach is acceptable.

Discussion

The following items summarize the methods used in the VY confirmatory analysis [2],[3],[4]:

1. The feedwater nozzle was chosen for confirmation since it has the largest number and most complicated and severe transients, and the highest calculated fatigue usage of the three nozzles which used the VY fatigue analysis approach. The analysis of the feedwater nozzle is bounding for the core spray and recirculation outlet nozzles since the calculated usage factors are at least 70% less than those for the feedwater nozzle and the number and severity of thermal transients are less.
2. The confirmatory analysis performed a detailed ASME Code, Section III, Subsection NB-3200 [1] fatigue calculation. The same ANSYS finite element model (FEM) was used as for the current licensing basis fatigue analysis, and was also used in the existing environmental fatigue analysis. The same number and severity of design transients and the same water chemistry inputs were used as had been used in the existing environmental fatigue analysis. Thermal transient stresses were calculated directly using the FEM for all transients.
3. The same transient definitions and cycle counts for 60 years of operation, as defined in Reference [5] and used for the existing analysis [8], were used for computation of cumulative fatigue in the confirmatory analysis.
4. The limiting cross-sections previously evaluated for the feedwater nozzle (nozzle corner and safe end) were evaluated.
5. Primary plus secondary and total stress ranges for all events were calculated and a correction for elastic-plastic analysis (i.e., K_e) was applied, where appropriate. Total stress intensity for each transient pair based on stress component differences was calculated per ASME Code, Section III, Paragraph NB- 3216.2 [1]. Stress ranges for primary plus secondary and primary plus secondary plus peak stress were calculated using all six components of stress (3 direct and 3 shear stresses). When more than one load set was defined for either of the event pair loadings, the stress differences were determined for all of the possible loading combinations, and the pair producing the largest alternating total stress intensity (including the effects of K_e) was used.

**VERMONT YANKEE NUCLEAR POWER STATION
LICENSE RENEWAL APPLICATION AMENDMENT 34
ATTACHMENT 1**

6. For the fatigue usage calculation, stress intensities for the event pairs were re-ordered in order of decreasing primary plus secondary plus peak stress intensity, including a correction for the ratio of modulus of elasticity (E) from the fatigue curve divided by E from the analysis. A fatigue table was created to determine the number of cycles available for each of the events of an event pair, and to determine fatigue usage per ASME Code, Section III, Paragraph NB-3222.4e [1]. For each load set pair in the fatigue table, the allowable number of cycles was determined from the alternating stress, which is half of the corrected total stress intensity range, using the appropriate ASME Code, Section III [1] fatigue curve.
7. Per Section X.M1 of the GALL Report [6], environmental fatigue multipliers were calculated using the F_{en} relationships from NUREG/CR-6583 [7] for carbon and low alloy steels. The F_{en} factors are bounding for all transient pairs based on the highest temperature of each of the transient stress pairs.

The results of the confirmatory analysis and a comparison of the final CUF results from the existing EAF analysis are shown in Table 1 below.

Table 1 - VY Feedwater Nozzle 60 year EAF CUF

Location	Analysis	EAF CUF / Allowable
Safe End	EAF Analysis [8]	0.2560 / 1.0000
	Confirmatory Analysis [4]	0.0994 / 1.0000
Nozzle Corner (Blend Radius)	EAF Analysis [8]	0.6392 / 1.0000
	Confirmatory Analysis [4]	0.3531 / 1.0000

Conclusions:

The existing EAF analysis for the VY feedwater, recirculation outlet, and core spray nozzles used a simplified fatigue analysis approach to calculate CUFs, including bounding F_{en} relationships. The confirmatory analysis used ASME Code, Section III, Subsection NB [1] methods and included more refined but still conservative F_{en} relationships.

For the locations identified above, the EAF results, using either the existing or confirmatory analysis, show that the fatigue usage factors, including environmental effects, are well within allowable values for 60 years of operation.

The confirmatory analysis for the feedwater nozzle, which used ASME Section III [1] code methods, confirms the adequacy of the existing VY fatigue analysis approach for all three nozzles.

**VERMONT YANKEE NUCLEAR POWER STATION
LICENSE RENEWAL APPLICATION AMENDMENT 34
ATTACHMENT 1**

References:

1. American Society of Mechanical Engineers (ASME) Boiler and Pressure Vessel (B&PV) Code, Section III, Rules for Construction of Nuclear Power Plant Components, Division 1-Subsection NB, Class 1 Components, 1998 Edition including 2000 Addenda.
2. Structural Integrity Associates Calculation No. VY-19Q-301, Revision 0, "Design Inputs and Methodology for ASME Code Confirmatory Fatigue Usage Analysis of Reactor Feedwater Nozzle".
3. Structural Integrity Associates Calculation No. VY-19Q-302, Revision 0, "ASME Code Confirmatory Fatigue Evaluation of Reactor Feedwater Nozzle".
4. Structural Integrity Associates Calculation No. VY-19Q-303, Revision 0, "Feedwater Nozzle Environmental Fatigue Evaluation".
5. Entergy Design Input Record (DIR) Rev. 1, EC No. 1773, Rev. 0, "Environmental Fatigue Analysis for Vermont Yankee Nuclear Power Station," 7/26/07.
6. NUREG-1801, Revision 1, "Generic Aging Lessons Learned (GALL) Report," U.S. Nuclear Regulatory Commission, September 2005.
7. NUREG/CR-6583 (ANL-97/18), "Effects of LWR Coolant Environments on Fatigue Design Curves of Carbon and Low-Alloy Steels," March 1998.
8. Structural Integrity Associates Calculation No. VY-16Q-302, Revision 0, "Fatigue Analysis of Feedwater Nozzle".

BVY 08-002

Attachment 2

Vermont Yankee Nuclear Power Station
License No. DPR-28 (Docket No. 50-271)

License Renewal Application

Amendment 34

Update to Core Spray CUF

**VERMONT YANKEE NUCLEAR POWER STATION
LICENSE RENEWAL APPLICATION AMENDMENT 34
ATTACHMENT 2**

Update to Supplemental Information for Environmentally Assisted Fatigue

Vermont Yankee Nuclear Power Station (VYNPS) provided the following information with Amendment 31 in response to License Renewal Commitment 27. The commitment specified addressing environmentally assisted fatigue by refining fatigue analyses to include the effects of reactor water environment to verify that the cumulative usage factors (CUFs) are less than 1. Entergy completed refinement of the fatigue analyses as specified in Commitment 27 in accordance with the clarifying details provided in the letter of July 30, 2007. The results indicated that the CUFs of the most fatigue sensitive locations will be less than 1.0 through the period of extended operation, considering both mechanical and environmental effects. Subsequent to the Amendment 31 submittal, the environmentally-adjusted CUF value for the Core Spray nozzle forging blend radius was updated to reflect new information, as shown in the revised table below. This table supersedes and replaces in its entirety the table submitted as part of Attachment 1 to BVY 07-066, dated September 17, 2007.

The following results of the refined fatigue analyses are the environmentally adjusted CUF values for 60 years of operation for the locations specified in NUREG/CR-6260.

**VYNPS Cumulative Usage Factors for
NUREG/CR-6260 Limiting Locations**

	NUREG-6260 Location	Material	Overall* Environmental Multiplier (F_{en})	Environmentally Adjusted CUF
1	RPV vessel shell/ bottom head	Low alloy steel	9.51	0.08
2	RPV shell at shroud support	Low alloy steel	9.51	0.74
3	Feedwater nozzle forging blend radius	Low alloy steel	10.05	0.64
4	RR Class 1 piping (return tee)	Stainless steel	12.62	0.74
5	RR inlet nozzle forging	Low alloy steel	7.74	0.50
6	RR inlet nozzle safe end	Stainless steel	11.64	0.02
7	RR outlet nozzle forging	Low alloy steel	7.74	0.08
8	Core spray nozzle forging blend radius	Low alloy steel	10.05	0.0432 0.1668
9	Feedwater piping riser to RPV nozzle	Carbon steel	1.74	0.29

* Effective multiplier for past and projected operating history, power level, and water chemistry.



UNITED STATES
NUCLEAR REGULATORY COMMISSION
WASHINGTON, D.C. 20555-0001

NEC-JH_35

SAFETY EVALUATION BY THE OFFICE OF NUCLEAR REACTOR REGULATION
RELATED TO AMENDMENT NO. 229 TO FACILITY OPERATING LICENSE NO. DPR-28

ENERGY NUCLEAR VERMONT YANKEE, LLC
AND ENERGY NUCLEAR OPERATIONS, INC.
VERMONT YANKEE NUCLEAR POWER STATION

DOCKET NO. 50-271

Proprietary information pursuant to
Title 10 of the *Code of Federal Regulations* Section 2.390
has been redacted from this document.
Redacted information is identified by blank space enclosed within double brackets.

implementation of the proposed EPU. Based on this, the NRC staff concludes that spent fuel storage at VYNPS will continue to meet the requirements of draft GDC-40, 42, and 66 following implementation of the proposed EPU. Therefore, the NRC staff finds the proposed EPU acceptable with respect to spent fuel storage.

2.8.7 Additional Review Area - Methods Evaluation

2.8.7.1 Application of NRC-approved Analytical Methods and Codes

The analyses supporting safe operation at EPU conditions are required to be performed using NRC-approved licensing methodology, analytical methods and codes. In general, the analytical methods and codes are assessed and benchmarked against measurement data, comparisons to actual nuclear plant test data and research reactor measurement data. The validation and benchmarking process provides the means to establish the associated biases and uncertainties. The uncertainties associated with the predicted parameters and the correlations modeling the physical phenomena are accounted for in the analyses. NRC-approved licensing methodology, topical reports and codes specify the applicability ranges. The generic licensing topical reports (LTR) covering specific analytical methods or code systems quantify the accuracy of the methods or the code used. The safety evaluation reports approving topical reports include restrictions that delineate the conditions that warrant specific actions, such as obtaining measurement data or obtaining further NRC approval. In general, the use of NRC-approved analytical methods is contingent upon application of these methods and codes within the ranges for which the data were provided and against which the methods were evaluated. Thus, a plant-specific application does not entail review of the NRC-approved analytical methods and codes.

To implement the proposed EPU and maintain the current 18-month cycle, a higher number of maximum powered bundles are loaded into the core and the power of the average bundles is also increased, making the core radial power distribution flatter. Due to an increased two-phase pressure drop and higher coolant voiding, the flow in the maximum powered bundles decreases. This effect leads to a higher bundle power-to-flow ratio and higher exit void fraction. Since the maximum powered bundles set the thermal limits, EPU operation reduces the margins to thermal limits.

Table 2.8.7-1 below shows the predicted operating conditions for the maximum powered bundles for VYNPS as shown in Table 6-2 of Attachment 3 to Reference 25. Figures 2.8.7-1 through 2.8.7-4 show plots for some of these parameters for VYNPS throughout the core cycle.

Table 2.8.7-1 Ranges of Operational Experience

Metric	VYNPS Prediction
[[
]]

As shown, the VYNPS maximum exit void fraction is 87% and the core average bundle exit void fraction is 76%.

2.8.7.2 Applicability of Neutronic Methods

2.8.7.2.1 Methods Review Topics

In Enclosure 3 to a letter dated March 4, 2004, (Reference 69) GE provided its evaluation of the impact of operation at higher void conditions on all of GE's licensing methodologies. The generic evaluation was also based on core thermal-hydraulic conditions that bound the EPU conditions (void fraction 90% or greater). Specifically, operation with a large number of bundles operating at high in-channel void fractions could potentially affect the following topics:

1. Assumptions made in the generation of the lattice physics data that establish the neutronic feedback (see SE Section 2.8.7.2.2).
2. Accuracy of the fuel isotopics generated considering the method employed in the lattice physics (see SE Section 2.8.7.2.2).
3. Assumptions made in the generation of the neutronic parameters in assuming 0% bypass voiding, although voiding is present during some transients (see SE Section 2.8.7.2.2).
4. Applicability of the thermal-hydraulic correlations used to model physical phenomena (see SE Section 2.8.7.3).

- KT - AR

received
10/31/07



UNITED STATES
NUCLEAR REGULATORY COMMISSION
WASHINGTON, D.C. 20555-0001

NEC_JH_62

October 25, 2007

LICENSEE: Entergy Nuclear Operations, Inc.

FACILITY: Vermont Yankee Nuclear Power Station

SUBJECT: SUMMARY OF TELEPHONE CONFERENCE CALL HELD ON AUGUST 20, 2007,
BETWEEN THE U.S. NUCLEAR REGULATORY COMMISSION AND ENTERGY
NUCLEAR OPERATIONS, INC., CONCERNING THE VERMONT YANKEE
NUCLEAR POWER STATION LICENSE RENEWAL APPLICATION

The U.S. Nuclear Regulatory Commission (NRC or the staff) and representatives of Entergy Nuclear Operations, Inc. held a telephone conference call on August 20, 2007, to discuss the regulatory requirements stated in 10 CFR Part 54.21(c)(1) as it relates to the Vermont Yankee Nuclear Power Station license renewal application.

Enclosure 1 provides a listing of the participants and Enclosure 2 contains a summary of the issue discussed with the applicant.

The applicant had an opportunity to comment on this summary.

Jonathan Rowley
Jonathan G. Rowley, Project Manager
License Renewal Branch B
Division of License Renewal
Office of Nuclear Reactor Regulation

Docket No. 50-271

- Enclosures:
1. List of Participants
2. Summary of Discussion

cc w/encls: See next page

Vermont Yankee Nuclear Power Station

cc:

Regional Administrator, Region I
U. S. Nuclear Regulatory Commission
475 Allendale Road
King of Prussia, PA 19406-1415

Mr. David R. Lewis
Pillsbury, Winthrop, Shaw, Pittman, LLP
2300 N Street, N.W.
Washington, DC 20037-1128

Mr. David O'Brien, Commissioner
Vermont Department of Public Service
112 State Street
Montpelier, VT 05620-2601

Mr. James Volz, Chairman
Public Service Board
State of Vermont
112 State Street
Montpelier, VT 05620-2701

Chairman, Board of Selectmen
Town of Vernon
P.O. Box 116
Vernon, VT 05354-0116

Operating Experience Coordinator
Vermont Yankee Nuclear Power Station
320 Governor Hunt Road
Vernon, VT 05354

G. Dana Bisbee, Esq.
Deputy Attorney General
33 Capitol Street
Concord, NH 03301-6937

Chief, Safety Unit
Office of the Attorney General
One Ashburton Place, 19th Floor
Boston, MA 02108

Ms. Carla A. White, RRPT, CHP
Radiological Health
Vermont Department of Health
P.O. Box 70, Drawer #43
108 Cherry Street
Burlington, VT 05402-0070

Mr. David Mannai
Manager, Licensing
Entergy Nuclear Operations
Vermont Yankee Nuclear Power Station
P.O. Box 500
185 Old Ferry Road
Brattleboro, VT 05302-0500

Resident Inspector
Vermont Yankee Nuclear Power Station
U. S. Nuclear Regulatory Commission
P.O. Box 176
Vernon, VT 05354

Director, Massachusetts Emergency
Management Agency
ATTN: James Muckerheide
400 Worcester Road
Framingham, MA 01702-5399

Jonathan M. Block, Esq.
Main Street
P.O. Box 566
Putney, VT 05346-0566

Mr. John F. McCann
Director, Licensing
Entergy Nuclear Operations, Inc.
440 Hamilton Avenue
White Plains, NY 10601

Mr. John T. Herron
Sr. Vice President
Entergy Nuclear Operations, Inc.
1340 Echelon Parkway
Jackson, MS 39213

Vermont Yankee Nuclear Power Station -2-

cc:

Mr. Christopher Schwartz
Vice President, Operations Support
Entergy Nuclear Operations, Inc.
440 Hamilton Avenue
White Plains, NY 10601

Mr. Michael J. Colomb
Director of Oversight
Entergy Nuclear Operations, Inc.
440 Hamilton Avenue
White Plains, NY 10601

Mr. William C. Dennis
Assistant General Counsel
Entergy Nuclear Operations, Inc.
440 Hamilton Avenue
White Plains, NY 10601

Mr. Theodore Sullivan
Site Vice President
Entergy Nuclear Operations, Inc.
Vermont Yankee Nuclear Power Station
P.O. Box 500
185 Old Ferry Road
Brattleboro, VT 05302-0500

Mr. James H. Sniezek
5486 Nithsdale Drive
Salisbury, MD 21801

Mr. Garrett D. Edwards
814 Waverly Road
Kennett Square, PA 19348

Ms. Stacey M. Lousteau
Treasury Department
Entergy Services, Inc.
639 Loyola Avenue
New Orleans, LA 70113

Mr. Norman L. Rademacher
Director, NSA
Vermont Yankee Nuclear Power Station
P.O. Box 0500
185 Old Ferry Road
Brattleboro, VT 05302-0500

Mr. Raymond Shadis
New England Coalition
Post Office Box 98
Edgecomb, ME 04556

Mr. James P. Matteau
Executive Director
Windham Regional Commission
139 Main Street, Suite 505
Brattleboro, VT 05301

Mr. William K. Sherman
Vermont Department of Public Service
112 State Street
Drawer 20
Montpelier, VT 05620-2601

Mr. Michael D. Lyster
5931 Barclay Lane
Naples, FL 34110-7306

Diane Curran, Esq.
Harmon, Curran, Spielberg &
Eisenberg, L.L.P.
1726 M Street, NW, Suite 600
Washington, DC 20036

Ronald A. Shems, Esq.
Shems, Dunkiel, Kassel & Saunders, PLLC
91 College Street
Burlington, VT 05401

Vermont Yankee Nuclear Power Station -3-

cc:

Karen Tyler, Esq.
Shems, Dunkiel, Kassel & Saunders, PLLC
91 College Street
Burlington, VT 05401

Sarah Hofmann, Esq.
Director of Public Advocacy
Department of Public Service
112 State Street - Drawer 20
Montpelier, VT 05620-2601

Jennifer J. Patterson, Esq.
Office of the New Hampshire Attorney
General
33 Capitol Street
Concord, NH 03301

Matias F. Travieso-Diaz, Esq.
Pillsbury, Winthrop, Shaw, Pittman, LLP
2300 N Street, NW
Washington, DC 20037-1128

Matthew Brock, Esq.
Assistant Attorney General
Office of the Massachusetts Attorney
General
Environmental Protection Division
One Ashburton Place, Room 1813
Boston, MA 02108-1598

Anthony Z. Roisman, Esq.
National Legal Scholars Law Firm
84 East Thefford Road
Lyme, NH 03768

Mr. Oscar Limpias
Vice President, Engineering
Entergy Nuclear Operations, Inc.
1340 Echelon Parkway
Jackson, MS 39213

**TELEPHONE CONFERENCE CALL
VERMONT YANKEE NUCLEAR POWER STATION
LICENSE RENEWAL APPLICATION**

**LIST OF PARTICIPANTS
AUGUST 20, 2007**

PARTICIPANTS

Jonathan Rowley
Kenneth Chang
Stephen Hoffman
Michael Metell
Gary Young
Allen Cox
David Lach
David Mannai
Michael Hamer
Brian Ford

AFFILIATIONS

U.S. Nuclear Regulatory Commission (NRC)
NRC
NRC
Entergy Nuclear Operations, Inc. (Entergy)
Entergy
Entergy
Entergy
Entergy
Entergy
Entergy

OPEN ITEMS
VERMONT YANKEE NUCLEAR POWER STATION
LICENSE RENEWAL SAFETY EVALUATION REPORT

AUGUST 20, 2007

The U.S. Nuclear Regulatory Commission (NRC or the staff) and representatives of Entergy Nuclear Operations, Inc. held a telephone conference call on August 20, 2007, to discuss the regulatory requirements stated in 10 CFR 54.21(c)(1) as it relates to the Vermont Yankee Nuclear Power Station (VYNPS) license renewal application (LRA).

Discussion summary: It is the NRC position that in order to meet the requirements of 10 CFR 54.21(c)(1), an applicant for license renewal must demonstrate in the LRA that the evaluation of the time-limited aging analyses (TLAA) has been completed. The NRC does not accept a commitment to complete the evaluation of the TLAA prior to entering the period of extended operation.

Fatigue analyses based on a set of design transients and on the life of the plant are treated as TLAA's. The applicant made a commitment (license renewal Commitment #27) to address environmentally assisted fatigue by refining fatigue analyses to include the effects of reactor water environment to verify that the cumulative usage factors are less than 1.0. The NRC could not accept this commitment.

Based on the discussion, the applicant agreed to amend its LRA to demonstrate that the evaluation of the TLAA has been completed. The NRC's review of this TLAA evaluation will be documented in the final VYNPS safety evaluation report.